Intracellular Processing of Luteinising Hormone and Follicle-stimulating Hormone

James G. Evans
BSc (Hons) Coventry University

Medical Research Council
Reproductive Biology Unit
Centre for Reproductive Biology
37 Chalmers Street
Edinburgh EH3 9EW
United Kingdom

Thesis submitted to the University of Edinburgh
for the degree of Doctor of Philosophy.

December 1998

For Sarah.

Declaration

Except where acknowledgement is made by reference, the experiments detailed in this thesis were the unaided work of the author. No part of this work has previously been accepted for any other degree, nor is any part of it being concurrently submitted in candidature for another degree.

James G. Evans
December 1998

Acknowledgements

During the preparation of this thesis I have been very lucky to receive lots of help from many people within the CRB. I would like to thank Julie Brooks, Wendy Struthers and Pawlina Largue for their patience during my formative months of laboratory destruction. More recently Linda Nicol and Gwen Cowan have provided me with unsurpassed technical assistance for which I am sincerely grateful. I would particularly like to thank Joanne McVerry for holding my hand in dark, cold rooms and Judith McNeilly for receiving blame so lugubriously. Janet Crawford came all the way from somewhere warm to lend me expert advice in thesis-related matters and I appreciate her sacrifice. My thanks also go to Maggie Paterson for her assistance during protein gel electrophoresis.

I would also be foolish not to thank Joseph Gaughan, Martin H. Wilson, Mike Millar, Harden Rahe, Davey Miller and Antti Perheentupa. Without these fine specimens of masculinity I would have had no-one to aspire to. Phil Taylor, Ted Pinner, Tom McFetters and Steve Clarke are equally virile men with enhanced computational and graphical capabilities without whom this thesis would have been just a small forest. Thanks to Ian Swanston and Fiona Pitt for their help in the assay lab.

I would like to thank Pamela Brown for instructing me in the finer details of molecular biology. She has provided me with all the training I will need for a future in molecular biology and I am sincerely thankful.

During the past three years I have been fortunate enough to work with Alan McNeilly. I have remained inspired by his uncompromising enthusiasm and vision to talk in silly accents and enjoy science. I hope to have the chance to work with Alan again as he has always been a friend first and boss second.

I would like to thank all those with whom I have worked for their support and friendship throughout my studies.

Abstract

The pituitary glycoproteins LH and FSH are secreted from gonadotrophs via regulated and constitutive pathways under control of GnRH. Several distinct types of secretory vesicles (granules) have been previously reported to contain gonadotrophins colocalised with Ca^{++}-binding aggregative granin proteins. The putative role of granins in gonadotrophin granulogenesis was investigated in this thesis using recombinant DNA technology. Mammalian expression constructs were transfected into cell lines permitting comparative expression levels for each of the proteins under investigation.

Expression of LH and FSH in transiently transfected JEG3 (human choriocarcinoma) and CHO cells was demonstrated by RT-PCR and confocal microscopy. Although granin expression did not affect the degree of hCG storage in JEG3 cells, chromogranin A (CgA) and secretogranin II (SgII) did exert an enhancement of hCG expression. oLH expression in CHO cells also appeared to be enhanced by CgA. In addition SgII appeared to reduce storage of oLH in cotransfected CHO cells. Like hCG, LH and FSH exhibited dispersed distribution within the cytosol suggesting constitutive secretion. CgA and chromogranin B (CgB) displayed punctate expression within transfected CHO cells. Coexpression of CgB and oLH in CHO cells demonstrated their colocalisation in the ER and TGN but not within CgB-only secretory vesicles. In contrast CgA expression appeared to induce formation of CgA and LH-containing secretory vesicles (310-640nm diameter). Their apparent divergence into oLH- and CgA-only vesicles towards the periphery of the cell suggests that this granin does not have a role in LH exocytosis correlating with *in vivo* data. The suggested role of CgA in pre-exocytotic sorting and retention of LH is strengthened by the observation of reduced LH storage in high passage $L\beta T_2$ cells (mouse gonadotrophs with regulated LH secretion) with undetectable levels of intracellular CgA.

Fusions of oLH and oFSH β-subunits with enhanced green fluorescent protein (EGFP) exhibited granin-independent aggregation in CHO and $L\beta T_2$ cells cotransfected with the gonadotrophin α-subunit. Observation of live CHO cells expressing the α-subunit and an EGFPC-oFSHβ fusion protein

revealed that these aggregates exhibited vesicle-like movement within the cytoplasm and subplasmalemmal areas culminating in exocytosis.

Analysis of whole mouse pituitaries using confocal microscopy demonstrated the prevalence of bihormonal gonadotrophs and their close relationship with capillaries. Gonadotrophs exhibited differential localisation of LH and FSH. Colocalised LH and CgA occurred towards the periphery of the cell whereas FSH remained in more central areas of the cytosol. CgA was absent from areas juxtaposed to capillaries whereas LH immunoreactivity remained. This is in accordance with previously reported data and *in vitro* observations. Pituitaries from transgenic mice expressing stabilised oFSHβ mRNA under control of the LH promoter exhibited an approximate 4-fold increase in FSH expression. Comparison with non-transgenics by confocal microscopy suggests that overexpression of FSH leads to increased colocalisation with LH in the regulated secretory pathway. Unexpectedly a 2-fold increase in SgII expression was also observed in this transgenic model and may represent adaptation of the gonadotroph to increased regulated secretion.

Abbreviations

aa	amino acid
AcCoA	acetyl coenzyme A
ACTH	adrenocorticotrophin
αGSU	alpha gonadotrophin subunit
AMV	avian myeloblastosis virus
ANOVA	analysis of variance
AP-1	activator protein 1 (c-*fos* & c-*jun*)
AP-2	activator protein 2
AS	antisense
ATF-1	activating transcription factor 1
ATP	adenosine triphosphate
bp	base pairs
°C	degrees Celsius
$[Ca^{++}]_i$	intracellular calcium concentration
$[Ca^{++}]_{ex}$	extracellular calcium concentration
cAMP	cyclic 3',5' adenosine monophosphate
CAT	chloramphenicol acetyltransferase
cDMEM	DMEM containing FCS and antibiotics
cDNA	copy DNA
CG	chorionic gonadotrophin
CgA	chromogranin A
CgB	chromogranin B
CHO	Chinese hamster ovary
Ci	Curie
ΔC_m	change in membrane capacitance
CMV	cytomegalovirus
CPE	carboxypeptidase E
cpm	counts per minute
CRE	cAMP-response element
CREB	CRE binding protein
CREM	CRE modulating protein
CSP	cysteine string protein
CTP	carboxy-terminal peptide
DAG	diacylglycerol
DARS	donkey anti-rabbit serum
DEX	dexamethasone
DOPE	L-dioleoyl phosphatidylethanolamine
DOTAP	N-[1-(2,3-Dioleoyloxy)propyl]-N,N,N-trimethyl-ammonium salts
DMEM	Dulbecco's modification of Eagle's medium
DNA	deoxyribonucleic acid
DPBS	Dulbecco's phosphate buffered saline
E_2	oestradiol
EDTA	ethylene diaminetetra-acetic acid
efDMEM	oestrogen-free cDMEM
EGFP	enhanced green fluorescent protein

EM	electron microscopy
ER	endoplasmic reticulum
ERE	oestrogen-response element
FACS	fluorescence-activated cell sorting
FCS	fetal calf serum
PLSD	protected least significant difference
FITC	fluorescein isothiocyanate
FSH	follicle-stimulating hormone
FSK	forskolin
GAPDH	glyceraldehyde 3-phosphate dehydrogenase
GH	growth hormone
GnRH	gonadotrophin releasing hormone
GnRH-R	GnRH receptor
GTP	guanosine triphosphate
GRE	glucocorticoid-response element
HBS	HEPES-buffered saline
HEPES	*N*-[2-hydroxyethyl] piperazine-*N'*-[2-ethane sulfonic acid]
HPD	hypothalamically disconnected
HSV-IE	Herpes simplex virus immediate early region
ICC	Immunocytochemistry
IP_3	inositol 1,4,5-triphosphate
IP_3-R	IP_3 receptor
IRMA	immunoradiometric assay
IU	international units
JRE	junctional regulatory element
Kb	kilobases
K_D	dissociation constant
KDa	Kilodaltons
LB	Luria Bertani
LH	luteinising hormone
oLHβ/oFSHβ	stabilised oFSHβ gene under control of the oLHβ promoter
mA	milli-amperes
MAPK	mitogen-activated protein kinase
MAPKK	MAPK kinase
mRNA	messenger ribonucleic acid
neo^R	neomycin resistance
NRS	normal rabbit serum
NSF	*N*-ethylmaleimide-sensitive factor
OD	optical density
ORF	open reading frame
OVX	ovariectomized
PAGE	polyacrylamide gel electrophoresis

PCR	polymerase chain reaction
PIP_2	phosphatidylinositol 4,5-bisphosphate
PKA	cAMP-dependent protein kinase
PKC	protein kinase C
PM	plasma membrane
PTH	parathyroid hormone
PRL	prolactin
RIA	radioimmunoassay
RNA	ribonucleic acid
RNase	ribonuclease
RPA	RNase protection assay
rpm	revolutions per minute
RT-PCR	reverse transcriptase polymerase chain reaction
SDS	sodium dodecyl sulphate
SEM	standard error of the mean
SgII	secretogranin II
SNAP-25	synaptosome-associated protein of 25 kDa
αSNAP	soluble NSF attachment protein α
SNARE	SNAP receptor
SSC	standard sodium citrate
TAE	tris-acetate EDTA
TBE	tris-borate EDTA
TGN	*trans*-Golgi network
TLC	thin layer chromatography
TPA	12-*O*-tetradecanoylphorbol-13-acetate
TRITC	tetramethyl rhodamine isothiocyanate
TSE	trophoblast-specific element
UT	untranslated
UV	ultra-violet
V	volts
VAMP	vesicle-associated membrane protein
X-gal	5-bromo-4-chloro-3-indolyl-β-D-galactopyranoside

All DNA sequences are shown in the 5'->3' orientation unless stated. All protein sequences are shown in the amino-terminal -> carboxy-terminal orientation unless stated.

Table of Contents

List of Tables, Figures and Movies*

(*movies are stored on the CD inside the front cover of this thesis).

Chapter One

Literature Review

1.1 Introduction

The studies described in this thesis relate to investigations aimed at improving the understanding of posttranslational processes during the differential secretion of the pituitary gonadotrophins luteinising hormone (LH) and follicle-stimulating hormone (FSH). Although this research represents basic science, it will be made clear during the following literature review that LH and FSH are crucial to normal reproductive physiology. Furthermore *in vivo* studies carried out during the past 30 years have revealed significant detail regarding the physiological functions of LH and FSH and their interactions with target organs. More recently the advent of recombinant DNA technology has led to detailed knowledge regarding genetic regulation of the gonadotrophin genes. Although considerable work has been undertaken regarding these areas, a relatively small proportion has focused on the intracellular aspects relating to the most fundamental question of LH and FSH secretion; how are they differentially secreted? The main aim of this thesis is to answer this question.

The remainder of this chapter will review the findings of several key papers related to gonadotrophin secretion, the factors controlling it and the molecular mechanisms by which it occurs. A brief overview of the reproductive physiology of the oestrous cycle in the mouse and the ewe will be followed by more detailed discussion of the molecules involved and their interaction. The cellular organisation of the anterior pituitary and detailed discussion of the genetic organisation and protein structure of key molecules will be covered. A summary of the evidence derived from analyses of secretion in neuroendocrine tissues *in vivo* will be given. Granins, implicated in this section will then be discussed in detail with regard to regulation of expression, protein structure and possible intracellular roles. Evidence gained from patch-clamp and other *in vitro* studies of neuroendocrine secretion will be discussed with regard to protein sorting, granulogenesis and exocytosis. Particular attention will be given to the specific molecules implicated in these processes.

1.2.1 The Oestrous Cycle

The oestrous cycle describes the rhythmic appearance of sexual receptivity known as oestrous. The biological significance of this cycle is that it allows control over the time at which parturition will occur. This is important as it may increase the chance of offspring survival if timed to coincide with favourable environmental conditions. Much of the understanding of the oestrus cycle has been obtained from work carried out on the ewe. Data from ovine models will be related to the more limited findings obtained from work with rodents as the final experimental chapter within this thesis regards studies on murine gonadotrophs.

The oestrous cycle of the ewe lasts for 17 days throughout the breeding season of October to March (Goodman & Karsch, 1980). In the ewe this cycle can be divided into two parts, the luteal phase (day 2 to day 13) and the periovulatory phase (day 14 to day 1) where day 0 of the cycle is the time of ovulation (oestrus) (Baird & McNeilly, 1981). Rodent oestrus cycles are shorter than those of sheep lasting approximately 4 to 5 days (Greenwald & Roy, 1994). A brief description of the main differences between ovine and rodent oestrus cycles will be given after more detailed coverage of the abundant data regarding the ovine oestrus cycle.

1.2.2 The Luteal Phase

Luteolysis, occurring around day 14 in the ewe, is triggered by the luteolysin prostaglandin F2α (PGF2α) which is secreted by the endometrium (Baird & McNeilly, 1981). Positive control of PGF2α has been shown by oestradiol administration which triggers release of PGF2α. Conversely, a prolonged luteal phase occurs after irradiation-induced ablation of oestrogenic follicles (Hixon *et al.*, 1983; Karsch *et al.*, 1970).
The functional corpus luteum which is formed in the ovary produces serum concentrations of progesterone up to 4ng/ml; these characterise the ovine luteal phase. Specifically secretion of progesterone occurs from the luteinized granulosa and theca cells of the recently ruptured follicle (Hauger *et al.*, 1977). Throughout the luteal phase this progesterone, together with oestradiol from the developing waves of follicles, prevents the occurrence of the LH surge. Immunisation against progesterone leads

to ovulation approximately 96 hours later in the ewe (Thomas *et al.*, 1987). Exogenous progesterone given during the follicular phase also prevents the high levels of oestradiol present at the end of the luteal phase from triggering the LH surge and arrests follicle maturation (Baird & McNeilly, 1981).

1.2.3 The Follicular Phase

Following luteolysis, progesterone serum levels fall rapidly resulting in a wave of follicle growth (Smeaton & Robertson, 1971). The growing follicles produce increased serum concentrations of oestradiol which in turn affect pituitary gonadotrophin secretion. LH responds to oestradiol positively (Webb & England, 1982; Karsch *et al.*, 1983) whereas FSH synthesis is negatively regulated (Baird & McNeilly, 1981; Campbell *et al.*, 1990). Inhibin secretion from developing follicles also regulates follicle-stimulating hormone (FSH) expression negatively (Baird *et al.*, 1991). This is particularly important in human reproduction where FSH levels are more tightly controlled. Declining FSH concentrations lead to selection of a dominant follicle which is able to proceed to ovulation (Scaramuzzi *et al.*, 1993). In rodents a secondary rise in FSH serum levels may recruit greater numbers of larger follicles for subsequent ovulation

Mutual positive feedback between LH and oestradiol leads to ever rising serum levels of LH (Currie & McNeilly, 1995). LH released in a pulsatile fashion culminates in the LH surge near the end of the follicular phase (Hauger *et al.*, 1977; Pant *et al.*, 1977) with ovulation occurring approximately 24 hours later (Cumming *et al.*, 1971).

1.2.4 The Periovulatory Period

Behavioural oestrus coincides with a surge-type release of LH and FSH (Baird & McNeilly, 1981). The preovulatory LH surge is mediated by high concentrations of oestradiol which promote increased GnRH pulse frequency (Clarke *et al.*, 1987; Moenter *et al*, 1991) sensitising the gonadotrophs to GnRH (Clarke *et al.*, 1984) and leading in turn to a synchronistic release of massive amounts of LH; a surge.

Serum concentrations of LH greater than 5ng/ml which occur during the surge inhibit follicular aromatase (Moore, 1974; Baird & McNeilly, 1981)

resulting in reduced oestradiol production. The destructive effect of high LH concentrations leads to cessation of the mutual positive feedback loop and a concomitant decrease in LH secretion.

A second period of elevated serum concentrations of FSH occurs 20-30 hours after the LH surge; this is known as the FSH rebound (Baird & McNeilly, 1981; Salmonsen *et al*, 1985). The function of this secondary surge may be to recruit primordial follicles into the next developing wave (Smeaton & Robertson, 1971; Pant *et al.*, 1977; McNatty *et al.*, 1981; Lahlou-Kassi *et al.*, 1984).

1.2.5 The Rodent Oestrus Cycle

Terminology regarding the temporal assembly of the rodent oestrus cycle differs from that of the ovine oestrus cycle and is broken up into oestrus, metestrus, diestrus and proestrus. Essentially the oestrus cycle of rodents is similar to that of sheep except that the luteal phase (diestrus) is much shorter. The relatively large size of follicles in rodents is caused by higher levels of FSH due to reduced circulating inhibin. These larger follicles do not require a prolonged period of growth therefore the luteal phase is much shorter at only 1-2 days (Greenwald & Roy, 1994). The biological significance of this difference is that rodents are capable of producing multiple ova (approximately 10 per rat) in a relatively short time. This strategy of reproduction is in contrast to that of sheep which produce 1-2 offspring per year and reflects the 'boom or bust' approach to colonisation favoured by rodents (Short, 1985).

1.3.1 The Hypothalamo-Pituitary-Gonadal Axis

Development and maintenance of mammalian reproductive function is regulated by the hypothalamus, the pituitary gland and the gonads. Co-ordinated positive and negative feedback between these glands is crucial for reproductive fitness and is carried out by systemic transmission of glycoproteins, peptides and steroids. A simplified schematic representation of the hypothalamo-pituitary-gonadal axis is contained in figure 1.3.1a.

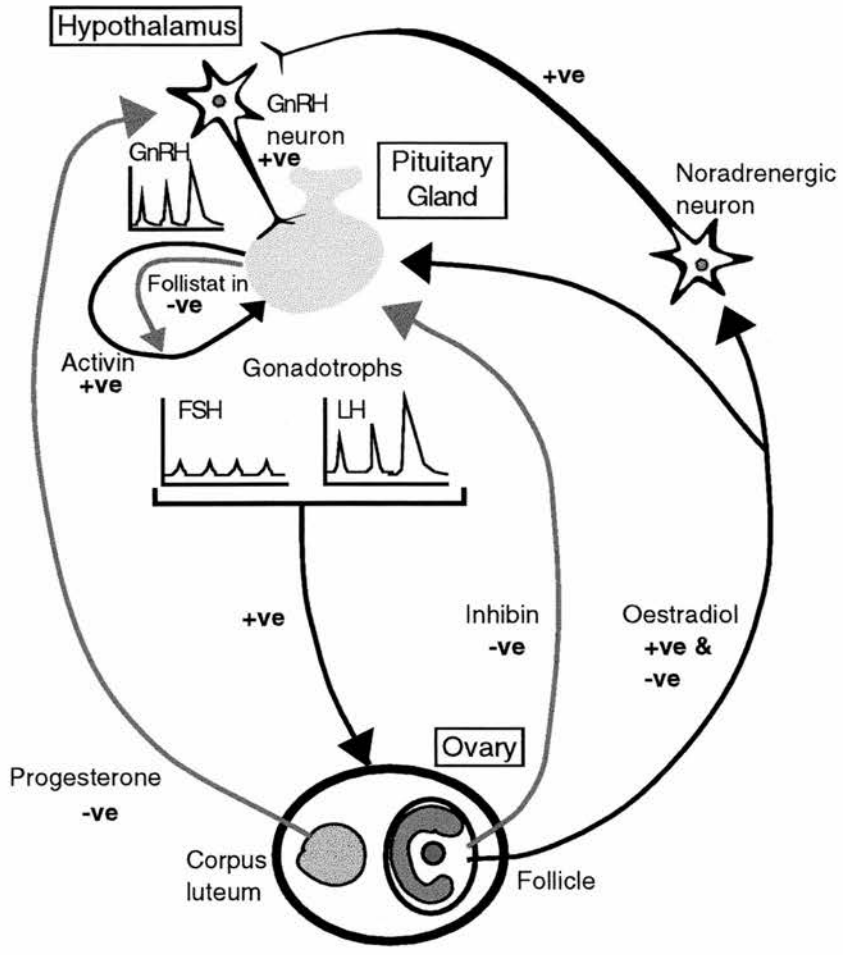

Figure 1.3.1a: Schematic representation of the hypothalamo-pituitary-gonadal axis in the non-primate female.

Hypothalamic stimulation of the pituitary gonadotrophs by GnRH is modulated by the positive oestrogen feedback from the developing wave of follicles. Recently oestradiol has been demonstrated to act on the GnRH neurons via noradrenergic neurons in the caudate region of the brain. Oestradiol also acts directly on the gonadotroph during positive and negative feedback. Progesterone from the corpus luteum negatively regulates GnRH release via stimulation of β-endorphin secretion. Gonadotrophs secrete FSH and LH differentially acting positively on gonadal development and function respectively. Inhibin secreted by the follicles negatively regulates FSHβ expression. Activin is secreted by the pituitary gland increasing FSHβ expression. Follistatin binds and inhibits the positive regulation of FSH expression by activin.

1.3.2 Secretion of Gonadotrophin-Releasing Hormone

Gonadotrophin-releasing hormone (GnRH) is a decapeptide derived from the 56 amino acid (aa) precursor gonadotrophin-releasing hormone-associated peptide (GAP) (Seeburg & Adelman, 1984). Mammalian species exhibit complete conservation of the GnRH sequence whereas the amino acid sequence of GAP is approximately 85% conserved between mouse, rat and human. GAP stimulates prolactin (PRL) secretion at low concentrations but inhibits it at higher concentrations (Seeburg *et al.*, 1987), GAP also stimulates LH secretion although with much lower efficacy than GnRH (Nickolics *et al.*, 1985).

GnRH is released from a population of neurons whose origins are found in several areas of the fore brain (Lehman *et al*, 1986; Sherwood *et al*, 1976; Silverman *et al*, 1987; Witkin *et al*, 1982). In the ovine there are approximately 2500 GnRH neurons (Caldani *et al*, 1988). Anterograde axonal transport of GnRH terminates at the median eminence where the decapeptide is stored until required for release. Transport via the hypophyseal portal blood vessel brings GnRH in contact with the anterior pituitary gland where it stimulates expression of LHβ, FSHβ and the α gonadotrophin subunit (αGSU) genes as well as secretion of the mature hormones (Dierschkle *et al.*, 1970; Schally *et al.*, 1971; Aiyer *et al.*, 1974b; Lincoln & Fraser, 1979; Fraser & McNeilly, 1982). Immunoneutralisation of GnRH abolishes LH secretion in the ewe (Clarke *et al.*, 1978; McNeilly, 1984), ram (Lincoln & Fraser, 1979), ovariectomized rats (Snabels & Kelch, 1979), castrated male rats (Ellis *et al.*, 1983) and stump-tailed macaques (Fraser & McNeilly, 1982). Naturally occurring or steroid-induced LH surges are also inhibited by immunoneutralisation of GnRH in female rats and sheep and gilts (Fraser & McNeilly, 1982; Fraser & McNeilly, 1983; Koch *et al*, 1973; Blake & Kelch, 1981; Esbenshade & Britt, 1985). Pulsatile administration of GnRH to ovariectomized (OVX) and hypothalamically disconnected (HPD) rhesus monkeys restored normal gonadotrophin secretory profiles and menstrual cycles (Knobil *et al.*, 1980).

The 'GnRH pulse generator' located in a region of the arcuate nucleus of the mediobasal hypothalamus controls release of GnRH from the median eminence (Goodman & Karsch, 1981; Knobil, 1981). Secretion by the GnRH-containing GT1 cell line is inhibited by exposure to PRL (Milenkovic *et al.*,

1994) and GnRH release in women can be inhibited by administering an analogue of met-enkephalin (del-Pozo & Martin-Perez, 1985). Hypothalamic stimulation of GnRH release can be increased by opioid antagonist administration which results in greater LH pulse frequency during the luteal phase and greater amplitude during the follicular phase in the ewe (Brooks *et al.*, 1986). Pulsatility of GnRH release is important for maintenance of gonadotrophin serum levels as administration of continuous GnRH to OVX and HPD rhesus monkeys leads to a decline in LH and FSH serum levels. However, this effect is reversible upon provision of a pulsatile GnRH regime (Belchetz *et al*, 1978). Similar studies in ewes (Clarke *et al.*, 1984) and clinical investigations of GnRH deficiency in humans have also shown the need for GnRH pulsatility (Santoro *et al*, 1986; Leyendecker *et al*, 1980; Crowley, 1980; Shoemaker *et al*, 1981).

Continuous sampling to measure the GnRH pulse profiles of a conscious female sheep using the method of Moenter *et al* (1991), revealed profile details while incurring limited tissue damage. During the luteal phase GnRH pulse frequencies of 0.25±0.05 pulses/hr with a mean amplitude of 3.2±1.0 pg/min were reported, the frequency of these pulses rose to over 1 pulse/hr at early follicular phase (Moenter *et al*, 1991). During two periods prior to the GnRH surge (-24 to -28hrs and -8 to -2hrs) pulse amplitude decreased whereas the frequency continued to rise (Evans *et al.*, 1997). This GnRH surge, which triggers the LH surge and continues after it, reaches plasma concentrations of approximately 20pg/ml (Moenter *et al*, 1991). Although studies have reported a direct correlation between GnRH and LH pulses (Clarke & Cummins, 1982; Levine *et al*, 1982; Vugt *et al*, 1983) some GnRH pulses during the onset of the GnRH surge did not result in a release of LH (Moenter *et al*, 1991). The presence of GnRH in cerebrospinal fluid has been postulated to be part of an alternative feedback loop. However, administration of radioactively-labelled GnRH to the third ventricle of cannulated ewes did not result in elevated radioactivity in hypophyseal blood samples. A role for GnRH in the CSF has yet to be determined (Skinner *et al.*, 1998).

1.3.3 The Anterior Pituitary

The anterior pituitary is derived from Rathke's pouch which is identified during foetal development as a slight thickening and invagination of the oral ectoderm. There are five cell types within the anterior pituitary defined by the types of hormone they produce. Differentiation of anterior pituitary cell types occurs during foetal development. Corticotrophs secrete adrenocorticotrophin (ACTH) and are the first cell type to be established within the anterior pituitary. Thyrotrophs secrete thyroid-stimulating hormone (TSH), gonadotrophs secrete follicle-stimulating hormone (FSH) and luteinising hormone (LH) and somatotrophs secrete growth hormone (GH). Lactotrophs, secreting prolactin (PRL) are the last anterior pituitary cell type to differentiate (Simmons *et al.*, 1990). Crucially gonadotrophs express the GnRH receptor (GnRH-R), a G-protein coupled receptor (GPCR) which when activated stimulates gonadotrophin secretion (discussed later) (Conn *et al.*, 1987).

1.3.4 The Gonads

The gonads are the target organs for LH and FSH and each exerts a specific effect. The biological effect of gonadotrophins is mediated through receptor binding on the target cell therefore subtle changes in the structure of the hormone may exert different levels of activation. Indeed this has been shown to be true as deglycosylated (more acidic) forms of the gonadotrophins which are produced as a result of increasing age or removal of testosterone are less effective than more basic forms secreted in response to GnRH stimulation (Reader *et al.*, 1983; Wide & Hobson, 1983). FSH stimulates follicular growth in female mammals (Clark *et al.*, 1979) and promotes spermatogenesis in the Sertoli cells of males (Dorrington *et al.*, 1975). LH acts synergistically with FSH in females (McNeilly *et al.*, 1991a) and later enables selection of dominant follicles during declining FSH concentrations and high frequency, low amplitude LH pulses (Campbell *et al.*, 1995). Ovulation is normally triggered by LH (Cumming *et al.*, 1971) although it can be triggered artificially using CG which has a longer serum half life (Picton *et al.*, 1990). In the male LH binds to and activates LH receptors on Leydig cells promoting androgen secretion which in turn promotes development of secondary sexual characteristics (Sharpe, 1994).

Positive and negative feedback occurs from the gonads in the form of steroids such as oestradiol, progesterone and testosterone and effects the hypothalamus as well as the pituitary gland (Keri *et al.*, 1991; Couzinet & Schaison, 1993). Positive regulation of LH secretion by oestradiol occurs in the absence of progesterone leading to the LH surge. The mechanisms whereby oestradiol exerts its effect are both direct and indirect. Oestradiol may affect LHβ expression by increasing transcription directly via an oestrogen response element (ERE) in the promoter (Shupnik & Rosenzweig, 1991) and indirectly by increasing the expression and number of GnRH-receptors (GnRH-R) present on the gonadotroph (Clarke *et al.*, 1988; Turgeon *et al.*, 1996). The relatively low numbers of oestrogen receptors in GnRH neurons suggests that an alternative mechanism of positive regulation of GnRH secretion by oestrogen may exist (Jennes *et al.*, 1997). Recently a mechanism has been proposed whereby the positive regulation of GnRH secretion by oestrogen occurs via noradrenergic neurons in the caudate region of the brain. This model may also account for the observed 16 hour time-delay between oestrogen administration and the onset of the LH surge (Clarke 1998 - personal communication).

Progesterone acts via stimulation of β-endorphin release to reduce GnRH release from the hypothalamus (Horton *et al.*, 1989; Couzinet & Schaisson, 1993). Although testosterone positively regulates FSHβ expression by increasing its mRNA half-life (Paul *et al.*, 1990; Perheentupa *et al.*, 1993), it may also act indirectly via alterations in GnRH release from the hypothalamus resulting in negative feedback (Shupnik, 1996a).

The gonadal peptides activin and inhibin are secreted from gonadotrophs as well as the gonads and are related to the transforming growth factor-β family (de Krester & Robertson, 1989). These gonadal peptides regulate FSH expression with no effect on that of LH (Shupnik, 1996b). Activin acts both transcriptionally and at the level of mRNA stability to increase FSHβ expression (Attardi & Winters, 1993; Weiss *et al.*, 1995) with inhibin acting antagonistically (Attardi & Winters, 1993; Weiss *et al.*, 1993). Follistatin is a structurally unrelated peptide which is also secreted from extragonadal tissues including folliculo-stellate cells and gonadotrophs in the anterior pituitary. Follistatin acts indirectly to stimulate FSHβ expression by binding inhibin (Carroll *et al.*, 1989). Recently it has been suggested that

the role of gonadal activin and follistatin in FSHβ expression is limited by the low proportion which remains unbound (and therefore active) within the blood (de Krester 1998 - personal communication).
Further detail relating to regulation of specific gonadotrophin subunit genes by steroids and gonadal peptides is discussed in sections 1.4.3-5.

1.4.1 Gonadotrophs

The majority of gonadotrophs are immunopositive for both LH and FSH and comprise approximately 10-15% of the anterior pituitary.
Gonadotrophs often exist as single cells or small clusters and are surrounded by lactotrophs (Allaerts *et al.*, 1991). A paracrine relationship between these closely associated cells has been suggested (Sato, 1980).
Intriguingly, gonadotrophs secrete these two structurally similar glycoproteins differentially through constitutive and regulated secretory pathways demonstrated *in vitro* (Muyan *et al.*, 1994). FSH which is expressed at low levels is secreted through the constitutive pathway in small secretory vesicles ubiquitous among mammalian cells. Basal LH secretion is also secreted via the constitutive pathway (McNeilly *et al.*, 1991b). LH, which for normal reproductive health in females requires large amounts in order to produce an LH surge, is stored in large electron-dense vesicles or granules prior to ligand-stimulated release (Misro & Conn, 1988). The molecular mechanisms which underlie the differential secretion of LH and FSH may involve granins as these molecules colocalise within secretory vesicles (Hillarp, 1958; Fischer-Colbrie *et al.*, 1987; Watanabe *et al.*, 1998b).
Neuroendocrine cells secrete proteins such as hormones and neurotransmitters via a specialised regulated pathway (Orci *et al.*, 1987). This exclusivity of this regulated pathway to cells of neuroendocrine origin has recently been disputed. The Chinese hamster ovary (CHO) cell line has recently been shown to secrete glycosylated proteins via a cryptic regulated pathway (Chavez *et al.*, 1996). Although this has yet to be demonstrated *in vivo*, these findings suggest that the regulated secretion of proteins may occur in a wide variety of cell types. The presence of a regulated pathway in gonadotrophs is visually apparent by the presence

of electron-dense secretory vesicles within the cytoplasm. The 40-fold difference between LH and FSH content within the pituitary gland reflects differential expression and predominate secretion via the regulated and constitutive pathways respectively (McNeilly *et al.*, 1991b).

Granule morphology is complex with many different sizes and densities reported. Large vesicles 500nm in diameter which contain an electron-dense core immunoreactive for LH and a periphery immunoreactive for FSH are present within the cytoplasm. Colocalisation of the granins chromogranin A (CgA) and secretogranin II (SgII) occurs with the LH and FSH in these larger vesicles. Proximal to the plasma membrane (PM), smaller electron-dense vesicles (also referred to as granules) 200nm in diameter exist which are immunoreactive for LH and SgII but not FSH (Watanabe *et al.*, 1991; Watanabe *et al.*, 1998b). Sex-related differences in granule morphology have been reported for vesicles containing CgA but not for those containing SgII. In female rats CgA-containing granules are generally much smaller than their male counterparts and vary throughout the oestrus cycle (Watanabe *et al.*, 1998a).

1.4.2 Gonadotrophins

Gonadotrophins are heterodimeric glycoproteins (Li & Starman, 1964; Ward *et al*, 1966) which comprise a common alpha subunit (αGSU) and a specific beta subunit (Liao & Pierce, 1970; Morgan & Canfield, 1971). They belong to a superfamily of cysteine-knot growth factors which activate GPCRs (Lapthorn *et al.*, 1994). LH, FSH, thyroid-stimulating hormone (TSH) and chorionic gonadotrophin (CG) all share the αGSU in their heterodimeric structure. LH and FSH are secreted from gonadotrophs whereas thyrotrophs secrete TSH which maintains thyroid function by activating the TSH receptor (TSH-R) (Nagayama *et al.*, 1990). CG which is found exclusively in primates and equids is secreted from chorionic trophoblasts. CG binding and activation of the LH receptor maintains pregnancy (Stewart & Allen, 1981).

Molecular detail regarding the genetic organisation of the αGSU and β subunits of FSH and LH will now be discussed. A schematic representation of the genetic organisation for the three gonadotrophin subunits is shown in figure 1.4.2a for reference during the following discussion.

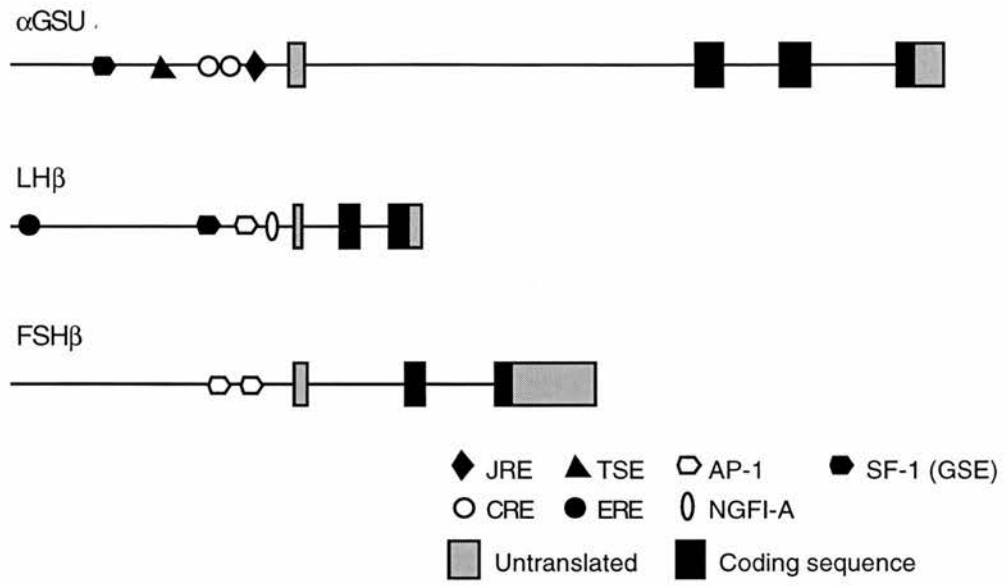

Figure 1.4.2a: The organisation of the αGSU, LHβ and FSHβ genes.

The αGSU gene is by far the largest of the three gonadotrophin genes depicted here. The greater length of this gene is conferred by the large first intron which ranges from 6.5 to 14.7Kb between species. The αGSU promoter details are specific to the human gene as this contains elements necessary for placental expression. The FSHβ gene contains a relatively large 3' untranslated region which is responsible for the short half-life of the mRNA.
JRE (junctional regulatory element), CRE (cAMP-response element), TSE (trophoblast-specific element), ERE (oestrogen- response element), AP-1 (activator protein 1 binding site), SF-1 (steroidogenic factor 1 binding site), GSE (gonadotroph-specific element). The representations are not drawn to scale (modified from Bousfield *et al* 1994).

1.4.3 The Glycoprotein Alpha Subunit

A common alpha subunit in the structure of gonadotrophins may represent an evolutionary economy in biochemical expenditure; functional motifs inherent in receptor activation and binding would not require additional expression for each bioactive heterodimer. Furthermore, an evolutionary advantage may be obtained by the absence of selection pressures for large single chain molecules.

Control of αGSU expression during primate and equid development is limited to the gonadotrophs and thyrotrophs of the pituitary and

trophoblasts in the placenta. In other species no αGSU expression is observed in the placenta. Investigation of the controlling factors may now be aided by the development of the αGSU expressing pituitary-derived cell lines, αT3-1 (Windle *et al.*, 1990) and $L\beta T_2$ (Thomas *et al.*, 1996), which complement studies using the JEG3 choriocarcinoma cell line (Kohler & Bridson, 1971).

The αGSU gene occurs as a single copy in the human genome and is located on chromosome 6 (Fiddes & Talmadge, 1984). The gene contains four exons; exon 1 contains untranslated sequences and is separated from exon 2, which encodes the signal peptide and the first nine amino acids of the mature molecule, by a large intron which varies in size from 6.5 to 14.7 Kb depending on the species. Exons 3 and 4 encode the remaining amino acids of the mature polypeptide, 10 to 71 and 72 to 96 respectively. Exon 4 also contains sequence information for the 3' untranslated region. The coding sequences for the αGSU of several species including murine, ovine and human are highly homologous and range from 730 to 800 nucleotides in length (Bousfield *et al*, 1994). For example, the ovine molecule comprises 72 nucleotides encoding a 24 amino acid signal sequence and 288 nucleotides coding for the mature protein of 96 amino acids, the 5' 70 nucleotides and 3' 287 nucleotides contain untranslated sequences (Bello *et al.*, 1989).

In the rat, mRNA transcripts for the αGSU gene are detected at embryonic day 11.5 which precedes the respective β subunits. In species other than human and equid, expression is confined to a placode of somatic ectoderm which subsequently develops into Rathke's pouch, precursor of the anterior pituitary (Simmons *et al.*, 1990).

αGSU gene expression is regulated by several *trans*-activating proteins acting upstream of the αGSU gene. The human αGSU gene enhancer comprises four distinct types of enhancer elements which include a trophoblast-specific element (TSE) between -159bp and -182bp which binds the placental protein TSEB (Delegeane *et al.*, 1987), a GATA element (-141 to -161bp) which binds α-ACT and two cAMP-responsive elements (CRE). The αGSU CREs are palindromic sequences of TGACGTCA between -146 and -111 which bind the ubiquitous CRE-binding protein (CREB) (Jameson

et al., 1988b; Horn *et al.*, 1992). Placental expression is also enhanced by a unique CCAAT-binding protein located at -93bp (Kennedy *et al*, 1990) and binding to the junctional regulatory element (JRE) immediately downstream of the CREs (Anderson *et al.*, 1990). Species other than human and equine lack the necessary TSE, GATA and CREs to allow placental expression of αGSU gene (Bokar *et al.*, 1989). Gonadotroph-specific expression of the αGSU gene is regulated by the 54kDa transcription factor SF-1 which binds to the gonadotroph-specific element (GSE) located between -219bp and -211bp. The exact sequence to which the 54kDa protein binds is TGACCTTGT with this sequence showing strong conservation in many mammalian species (Horn *et al.*, 1992; Brown *et al.*, 1993; Keri & Nilson, 1996; Halvorson *et al.*, 1996). The first five bases of the GSE shows homology with the nuclear steroid hormone receptor superfamily (Naar *et al.*, 1991).

Regulation of mRNA stability, like that of transcriptional activity, is a key mechanism for control of gene expression. Measurement of mRNA from cultured cells at time-points after administration of a transcriptional inhibitor such as actinomycin D allows evaluation of mRNA stability. The half-life of the αGSU mRNA is 6.5±0.25 hours and by 9 hours of actinomycin D exposure the poly-A tail of remaining αGSU mRNA is reduced by 80-90% (Bouamoud *et al.*, 1992).

Secondary structure of the αGSU is conferred by the formation of 5 disulphide bridges between cysteine residues (Lapthorn *et al.*, 1994), conservation of the nucleotide sequences encoding these key amino acid residues is apparent even between mammals and teleosts (Bousfield *et al*, 1994). Disulphide bond formation within the αGSU structure is undertaken in the rough endoplasmic reticulum (RER) and occurs cotranslationally (Mise & Bahl, 1980). Disulphide bridges form between the cysteine residues at positions 7 and 31, 10 and 60, 28 and 82, 32 and 84 and 59 and 87 in the αGSU (Lapthorn *et al.*, 1994). Mutation of nucleotide sequences responsible for encoding the cysteine residues at either 7, 31, 32, 59 or 87 to alanine did not affect the αGSU conformation and produced bioactive hCG from cotransfected Chinese Hamster ovary (CHO) cells. Similar mutations affecting cysteines at 10, 28, 60, 82 or 84 caused conformational changes which resulted in reduced dimer formation and an increased rate of αGSU

degradation (Furuhashi *et al.*, 1994). Expression of αβ fusions *in vitro* has demonstrated that disruption of the disulphide bridge between residues 10 and 60 reduces heterodimer formation to 5% of wild-type levels but still produces a bioactive single-chain hCGαβ molecule (Sato *et al.*, 1997). Certain sequence deletions between the cysteine residues have been implicated in species specificity of heterodimer formation (Burzawa-Gerard & Fontaine, 1976). Deletion of the P-T-P motif at residues 38-40 in the αGSU abolished hCG dimerisation in transfected CHO cells. Similarly any substitutions of Tyr^{37} or Thr^{39} also prevented hCG dimerisation (Sato *et al.*, 1997). Clearly dimer formation is, at least in part, controlled by structural features of the αGSU. The role played by the respective β-subunits is discussed in the following sections.

Expression of mutated αGSU in CHO cells stably cotransfected with either the human FSHβ or human CGβ allowed evaluation of respective receptor activation on 293 cells stably transfected with the FSH-receptor (FSH-R) or LH-receptor (LH-R) DNA. For FSH activity residues His^{90} and Lys^{91} within the αGSU are crucial. FSH-R binding was improved by the substitution of αGSU valine for Lys^{91} but reduced subsequent cAMP production to undetectable levels. Similar results were obtained when LH-R activation was measured after the same residues were mutated in the hCG αGSU. Mutation of αGSU His^{90} to either arginine or proline reduced FSH binding to the FSH-R but did not alter hCG binding to the LH-R (Zeng *et al.*, 1995).

N-glycosylation occurs at asparagine residues 56 and 82 in the αGSU (52 and 78 in human) with the former being essential for biological activity of hCG (Matzuk *et al.*, 1989). Interactions between the αGSU and either FSH or LH β-subunit have been shown to determine the differential glycosylation of the αGSU within each functionally specific dimer. The asparagine-linked oligosaccharides of the αGSU in bovine LH terminate with a SO_4-4GalNAcβ(1->4)GlcNAcβ(1->2)Manα . However αGSU on FSH terminates with sialic acidα-Galβ(1->4)GlcNAcβ(1->2)Manα . Apparently association of the αGSU with the FSHβ prevents recognition of the dimer by a specific *N*-acetylgalactosamine transferase which is responsible for the differential glycosylation of the αGSU in LH. These observations suggest a possible mechanism whereby differential sorting of LH and FSH may occur as well as allowing functional specificity (Smith & Baenziger, 1988). A recognition

sequence of P-X-R/K has been reported for this enzyme (Smith & Baenziger, 1992).

The αGSU clearly fulfils roles within each glycoprotein dimer and it is not a static structure to which the β subunits adapt. Although the role of bioactivity is clearly suggested and undoubtedly important, the significance of differential glycosylation with regard to intracellular trafficking is of particular relevance to the studies described in this thesis.

Free αGSU displays *O*-glycosylation at Thr^{43} which prevents LH dimerisation *in vitro* (Parsons *et al.*, 1983). Placental free αGSU does not exhibit such *O*-glycosylation and appears to prevent CG dimerisation via *N*-glycosylations (Thotakura & Blithe, 1995). The higher rate of synthesis and resistance to degradation of the αGSU in comparison to the glycoprotein β subunits leads to an excess of free αGSU which is successfully secreted (Kourides *et al.*, 1980). An intracellular role of the excess of degradation-resistant αGSU produced in gonadotrophs has not been determined. However, it seems likely that the abundance of intracellular αGSU may prevent the tightly controlled coexpression of β subunits becoming subjected to less precise control by lysosomal degradation in the absence of sufficient αGSU (Bassetti *et al.*, 1995).

The exact role of free extracellular αGSU is unclear although some studies suggest a role in lactotroph differentiation (Begeot *et al.*, 1984), prolactin secretion from cultured human decidua (Blithe *et al.*, 1991) and perhaps in stimulation of neoplastic growth (Bidart *et al.*, 1997). Transgenic knockouts are not appropriate for determining the role of free αGSU as absence of this subunit prevents formation of the heterodimeric gonadotrophins thus abolishing normal thyroid and gonadal development (Kendall *et al.*, 1995)

1.4.4 Follicle-stimulating Hormone

The human, bovine, pig and rat follicle-stimulating hormone (FSH) β subunits are encoded by a single gene (Jameson *et al.*, 1988a; Kim *et al.*, 1988; Gharib *et al.*, 1989). The human gene is located on chromosome 11 (Naylor *et al.*, 1983). The presence of a putative ovine FSHβ (oFSHβ) pseudogene showing 87% homology to oFSHβ distinguishes it from the other species (Guzman *et al.*, 1991). Further investigation into the

expression characteristics of this putative pseudogene has yet to be reported.

The FSHβ gene spans over 5000bp, the ovine sequence is 5191 bp in length, containing three exons and two introns. The long 3' untranslated sequence contributes greatly to the mRNA which is over twice the length of the αGSU and LHβ mRNAs at approximately 1700 bp in length. The mRNA half-life of FSHβ has been reported as 1.0 ± 0.13 hours in primary cultured rat pituitary cells (Bouamoud *et al.*, 1992) and removal of the 3' untranslated sequence results in significantly increased mRNA expression in transient transfections (Mountford *et al.*, 1992).

Recently, information regarding the presence of two functional activator protein-1 (AP-1) binding sites within the oFSHβ promoter has been reported. These elements present at -120 and -83 are flanked by two non-functional AP-1-like sites at -155 and -10. The functionality of the elements was confirmed by site-directed mutagenesis and activation by 12-*O*-tetradecanoylphorbol-13-acetate (TPA) *in vitro*. *In vivo* evidence that these AP-1 sites are functional is demonstrated by the presence of c-*fos* and c-*jun* within the nucleus of over 75% of FSHβ-containing gonadotrophs (Strahl *et al.*, 1997). The presence of these sites suggests that an FSHβ transcriptional response to GnRH-R activation via the mitogen-activated protein kinase (MAPK) signalling pathway may occur (Naor *et al.*, 1998).

The human FSHβ gene expresses four mRNA species which is in contrast with other species which produce only one (Jameson *et al.*, 1988a). An alternate splicing donor site located in the first exon results in 35% of transcripts with a 33 base 5' untranslated region as opposed to the normal 63 bases. Polyadenylation variants account for the other two mRNA species and 20% of FSHβ mRNA lack the long 3' untranslated sequence due to incorporation of a stop codon at the consensus AATAAA sequence. The conventional FSHβ mRNA molecule of 1700 bases in length arises from polyadenylation at a site homologous to that found in non-human species (Gharib *et al.*, 1990). Regulation of FSHβ expression *in vivo* has been shown to occur both transcriptionally and posttranslationally. Gonadal peptides inhibin and activin appear to act at different stages of FSHβ synthesis with opposing effects and without affecting expression of the

αGSU or LHβ genes. Inhibin has been demonstrated as reducing oFSHβ transcription by 50% (Clarke *et al.*, 1993) whereas activin promotes rFSHβ mRNA abundance by stabilising the mRNA molecule (Carroll *et al.*, 1991) and by increasing transcription (Weiss *et al.*, 1995).

The ovine FSHβ mRNA translates into a polypeptide of 111aa with two sites of *N*-glycosylation at the asparagine residues at positions 6 and 23 (Sairam *et al.*, 1981). Conservation of 12 cysteine residues within all gonadotrophin β-subunits imparts their related structures. In comparison to disulphide bond formation within the αGSU, disulphide bonds within the β-subunits occur between amino- and carboxy-terminal regions and may result in a more rigid structure (Tsunasawa *et al.*, 1977). Due to the relative scarcity of FSH in comparison to CG and LH, the majority of structural studies have not been carried out using FSH. Some detail has been extrapolated from structural comparisons with other gonadotrophin β-subunits and is discussed in the following section. Interestingly, over 50% of the residues in this sequence are required for bioactivity which is nearly twice that of LHβ aa sequences (Bousfield *et al*, 1994). oFSH serum concentrations range between 0.5-6ng/ml and the serum half-life is approximately 160 minutes (Roche, 1996). The presence of sulphated oligosaccharides for which a receptor is expressed in the liver ensures that target organ exposure to FSH is limited (Fiete *et al.*, 1991). The biological significance of this may be that serum concentrations of FSH do not accumulate and that efficient clearance allows the pulsatile secretion profile of FSH in peripheral blood to be maintained.

Transgenic knockouts of the FSHβ gene demonstrate the physiological requirement for the FSH heterodimer in normal reproductive function as males were found to be subfertile and females infertile. Female infertility arose due to the lack of antral follicle formation. Males demonstrated reduced seminiferous tubule volume whereas Leydig cells appeared similar to controls. These data are in accordance with the known roles of FSH *in vivo* (Kumar *et al.*, 1997).

1.4.5 Luteinising Hormone

Luteinising hormone (LH) is the heterodimeric glycoprotein comprised of the αGSU and the specific LHβ subunit. The human LHβ subunit is encoded

by a single gene located on chromosome 19 (Naylor *et al.*, 1983). Activation of the LHβ gene is restricted to cells of the gonadotroph lineage occurring at embryonic day 16.5 (e16.5) in rat development (Simmons *et al.*, 1990).
The related β subunit of chorionic gonadotrophin (CGβ) is encoded by a total of 7 genes or pseudogenes which are transcribed at various levels of efficiency due to altered 5' sequences. All of these genes are expressed within placental trophoblasts (Bo & Boime, 1992). Genetic duplication of an ancestral LHβ gene and subsequent rearrangement may have led to the evolution of this CGβ gene cluster (Talmadge *et al.*, 1984). Homology of the LHβ and CGβ genes is high within the coding regions but 5' untranslated sequences and promoters appear to have a divergent relationship. Using the human choriocarcinoma cell line JEG3 which expresses hCG, it has been demonstrated that the CGβ promoter contains a cAMP-responsive element (CRE) and is functionally distinct from that of the αGSU promoter. Unlike transcription of the αGSU gene, CGβ transcription is inhibited by cycloheximide administration and thus is dependent on *de novo* protein synthesis. Furthermore the CGβ CRE does not bind CREB but does contain binding sites for multiple placentally-expressed transcription factors (Talmadge *et al.*, 1984; Milsted *et al.*, 1987; Jameson & Lindell, 1988) .
Far less has been revealed about the regulation of the LHβ gene than the αGSU due to the protracted development of a cell line expressing the LHβ gene. The $L\beta T_2$ cell line expresses both the LH α and β subunits which are stored in dense-core vesicles and are secreted under control of the GnRH-R (Thomas *et al.*, 1996). Currently no data from $L\beta T_2$ cells regarding LHβ promoter structure have been reported. Previous studies using rat LHβ promoter resections to assay reporter gene transcription in transfected primary rat pituitary cultures has revealed that only a relatively small region of the upstream untranslated sequence is necessary for efficient transcription. Sequences contained between -1700bp and -75bp were not required for reporter gene expression in this system (Kim *et al.*, 1990) and transgenic studies in mice have shown that sequences within -1900bp are sufficient for expression of a reporter gene specifically within the gonadotroph cell lineage (Brown *et al.*, 1993). The primary cell culture of a tissue such as the pituitary gland, which contains a heterogeneous population of cells, may present misleading results due to possible

transfection of multiple cell types and subsequent reporter activity from lineages not normally involved in LH expression *in vivo*. Oestradiol exposure increases LH secretion from gonadotrophs *in vitro* (Turgeon *et al.*, 1996) and *in vivo* (Jackson *et al.*, 1975). Using the GH_3 somatomammotroph cell line an oestrogen response element (ERE) containing the palindromic sequence GGACACCATCTGTCC has been located at -1173bp. Promoter resections containing this sequences exhibited enhanced reporter expression by 1.7 to 3-fold. Furthermore constructs containing two copies of the ERE showed an increase of 2.5 to 4-fold (Shupnik & Rosenzweig, 1991). The presence of an activator protein-1 (AP-1) binding site within the rLHβ promoter (Shupnik, 1996b) may allow a transcriptional response to GnRH-R activation via protein kinase-C (PKC)-dependent stimulation of the MAPK pathway (Naor *et al.*, 1998).

Using the mouse gonadotroph-derived αGSU-expressing αT3-1 cell line, a gonadotroph-specific element (GSE) in the rat LHβ was characterised and found to specifically bind the orphan nuclear receptor steroidogenic factor-1 (SF-1) (Halvorson *et al.*, 1996). LHβ sequences show high homology (>75%) between bovine, human and rat genes. The presence of a SF-1 motif (TGACCTTG) at -124bp is likely to contribute to the tissue specificity of oLHβ transcription. The LHβ gene also contains a TATAA box at -31bp, a short (7bp) 5' untranslated sequence within exon 1 and a polyadenylation site 21bp from the end of the transcriptional unit (Brown *et al.*, 1993).

Disruption of the rat LHβ promoter SF-1 binding site in transgenic mice resulted in almost complete inhibition of expression of the CAT reporter in males and females. Interestingly this reduction could not be compensated for using induction with GnRH after gonadoectomy (Keri & Nilson, 1996). Although SF-1 binding sites are present within the αGSU and LHβ promoters no such binding sites have been located in the corresponding regions of the FSHβ gene. It has been postulated that SF-1 may control tissue-specific expression of the FSHβ gene indirectly (Brown & McNeilly, 1997). Disruption of the gene encoding another transcription factor, NGFI-A, produces infertile female transgenic mice as a consequence of a deficiency in LH. Reduced transcription of other key hormones such as prolactin and FSHβ as well as the GnRH-R appeared unaffected. Although

LH was undetectable (by immunoblotting) in female NGFI-A knockouts, levels were only decreased in males suggesting differences in transcriptional regulation. Parallel cotransfection experiments undertaken *in vitro* using the αT3-1 and CV-1 cell lines determined a synergistic relationship between SF-1 and NGFI-A binding. This effect was inhibited by mutation of the guanosine residues in the canonical NGFI-A binding site located at -50bp (Lee *et al.*, 1996). Similar experiments using the $L\beta T_2$ cell line (male murine gonadotroph) (Thomas *et al.*, 1996) may reveal mechanisms exclusive to the regulation of LHβ transcription in the male.

The oLHβ gene, when transcribed, produces a 1069bp heterologous nuclear RNA (hnRNA) molecule which contains three exons of 22bp, 168bp and 335bp. The mRNA half life for oLHβ is 44 ± 0.5 hours (Bouamoud *et al.*, 1992).

The oLHβ gene encodes a protein 141aa in length which includes a 20aa signal peptide (Brown *et al.*, 1993). The closely related hCGβ gene produces a polypeptide with a high degree of homology to LHβ but differs at the carboxy terminus due to the presence of an additional 31aa sequence. The carboxy-terminal peptide (CTP) is hydrophilic in nature displaying *O*-glycosylation at four serine residues. The CTP is believed to have arisen as a consequence of a frameshift mutation which resulted in a readthrough at nucleotides encoding amino acid 114 (Talmadge *et al.*, 1984).

The conservation among all gonadotrophin β subunits of 12 cysteine residues reveals the location of 6 disulphide bonds (Tsunasawa *et al.*, 1977). These disulphide bonds are largely responsible for the rigid structure of gonadotrophin β subunits. Circular dichrographic spectral analyses of gonadotrophin subunits before and after dimerisation have revealed that whereas the β subunits remain similar the α subunit structure is dynamic (Jirgensons & Ward, 1970). More recent work by Lapthorn *et al* (1994) examined the crystal structure of hCG and although it revealed detailed information regarding the molecular interactions of the αGSU and hCGβ subunit it failed to relate these to free αGSU. The sequence similarity between the CGβ and LHβ genes suggests that the structure of their respective dimer may also be similar. Notably, the interaction of the αGSU and the hCGβ subunits occurs via the C-A-G-Y sequence (hCGβ 34-36) and is

stabilised by a disulphide bridge. The C-A-G-Y sequence appears conserved in mammalian species with some species variation occurring at the alanine residue. Notably oLHβ contains a glycine residue in place of the alanine but maintains the consensus in the corresponding FSH sequence (Bousfield *et al*, 1994). This disulphide bridge formed between cysteine residues at hCGβ 26 and 110 forms a loop which wraps around the αGSU. This unusual motif is also essential for binding to the LH receptor (Lapthorn *et al.*, 1994). The structural dominance of the β subunit presumably reflects the functional specificity that gonadotrophin β subunits impart on the dimeric hormone.

Formation of the hLH dimer has been investigated using CHO cells transfected with αGSU and mutant LHβ or CGβ expression constructs. Comparison of the rate of hLH assembly to that of CG revealed that the former occurs with less efficiency. The main structural differences between the β-subunits are the carboxy-termini and the *N*-linked glycosylations. The LHβ subunit possesses a hydrophobic carboxy-terminus whereas the serine-rich CTP of hCGβ is hydrophilic. Furthermore hLHβ unlike other LHβ subunits is not *N*-glycosylated at residue 13 due to disruption of the recognition sequence. Considerable mutational analysis and expression of chimeric β-subunits has revealed that the interaction of the amino- and carboxy-termini of the hLHβ subunit is responsible for its relative inefficiency of dimer formation. LHβ appears to be unique among the gonadotrophin β-subunits as FSHβ and TSHβ combine with the αGSU at rates comparable to that of hCGβ (Matzuk & Boime, 1989).

LH serum concentrations range from 0.5 to 100ng/ml and the half-life of the 32kDa protein is approximately 20 minutes which reflects rapid clearance by the kidneys (Roche, 1996). Like FSH, LH contains sulphated oligosaccharides whereas hCG does not. The pituitary gonadotrophins including TSH are rapidly cleared by the liver while hCG remains in the serum (Fiete *et al.*, 1991).

Although a direct transgenic knockout of the LHβ gene has yet to be reported, the NGFI-A transcription factor knockout abolished expression of the LHβ gene causing subfertility in males and infertility in females (Lee *et al.*, 1996).

1.4.6 The GnRH Receptor and Intracellular Signalling

Gonadotroph cells express the GnRH-R on the PM and specific high affinity binding of GnRH activates multiple second messenger systems (Conn *et al.*, 1987; Huckle & Conn, 1987; Wooge & Conn, 1987). The GnRH-R is a member of the GPCR family and contains seven transmembrane regions with a truncated intracellular carboxy-terminus. Ligand-receptor binding induces dimerisation and micro-aggregation of GnRH-R molecules (Conn, 1984). A recent review by Naor *et al* describes functional mutations of the GnRH-R structure in great detail (Naor *et al.*, 1998).

The single copy of the human GnRH-R gene located on chromosome 4 contains three exons and spans over 18.9kb. The gene encodes a 327 amino acid protein which is highly homologous to sequences in the sheep, rat, mouse and cow (Kakar *et al.*, 1992; Reinhart *et al*, 1992; Tsutsumi *et al.*, 1992; Eidne *et al.*, 1992; Brooks *et al.*, 1993; Chi *et al.*, 1993; Illing *et al.*, 1993). Control of GnRH-R expression in gonadotrophs is a crucial part of the hypothalamo-pituitary gonadal axis as it provides a means for regulating the amount of signal received by the gonadotroph.

The inhibitory effect of progesterone on GnRH-R mRNA has been demonstrated *in vitro* using ovine pituitary cultures (Sealfon *et al.*, 1990). *In vivo* studies of GnRH-R mRNA regulation throughout the oestrus cycle of sheep investigated the role of GnRH, E_2 and inhibin. In normal ewes GnRH-R mRNA levels appear to coincide with serum E_2 (Brooks *et al.*, 1993), although either GnRH-R antagonists or inhibin decrease mRNA levels in the absence of E_2 (Brooks & McNeilly, 1994). Further regulation of the GnRH signal detected by gonadotrophs occurs via internalisation of the GnRH-R after chronic agonist treatment (Schvartz & Hazum, 1987) and may be mediated by the asparagine-arginine-serine (D-R-S) motif present on the second intracellular domain of the receptor (Arora *et al.*, 1995). Desensitisation of the GnRH-R also occurs which dampens the gonadotrophs response to hypothalamic stimulation (Gorospe & Conn, 1987).

The effects of GnRH-R activation within gonadotrophs include stimulation of gonadotrophin gene transcription and modulation of gonadotrophin exocytosis (McNeilly *et al.*, 1991b) (figure 1.4.6a). The myriad of second

messenger systems allows precise control of the intracellular response to receptor activation. Furthermore, as a result of the amplification inherent in the cascade of protein interactions, a reduced quantity of agonist may be required thus reducing the likelihood of nonspecific interactions. Although the exact signalling pathway involved in GnRH-R stimulation of gonadotrophin subunit transcription has yet to be revealed, GnRH-R activation leads to formation of the transcription factors c-*jun* and c-*fos* via MAPK cascade. AP-1 formation by c-*jun* and c-*fos* could lead to transcription of gonadotrophin subunit genes although this has yet to be demonstrated. As has already been discussed the rLHβ (Shupnik, 1996b) and oFSHβ (Strahl *et al.*, 1997) promoters contain AP-1 binding sites which may facilitate a positive transcriptional response to GnRH-R activation. The rat secretogranin II promoter (see section 1.6.3) also contains multiple AP-1 sequences although with single base deviations from the consensus (Jones *et al.*, 1996). However as yet no clear relationship between SgII transcription and GnRH-R activation has been demonstrated.

GnRH-R activation also controls the release of gonadotrophins via intracellular signalling. Phospholipid metabolism is increased by GnRH-R activation as a result of guanosine triphosphate protein (G protein) activity (Hawes *et al.*, 1992b). G proteins catalyse breakdown of membrane-bound phosphatidylinositol 4,5-bisphosphate (PIP_2) to inositol 1,4,5-trisphosphate (IP_3) and diacylglycerol (DAG) by phospholipase C (PLCβ) (Huckle & Conn, 1988; Keisel, 1993). DAG is also produced as a result of phospholipase D (PLD) activity. Activation of phospholipase A_2 (PLA_2) leads to production of leukotrienes which also stimulate LH release (Anderson, 1996).

IP_3 production initiates a Ca^{++} spike by activating its Ca^{++} channel receptor located on the endoplasmic reticulum (ER) (Shangold *et al*, 1988) and perhaps other intracellular Ca^{++} ($[Ca^{++}]_i$) stores. The exact role of elevated intracellular IP_3 concentrations is unclear as GnRH and sodium-fluoride mediated LH release can both be uncoupled from IP_3 turnover (Hawes *et al.*, 1992b), furthermore GnRH-R desensitisation can also be uncoupled (Hawes *et al.*, 1992a).

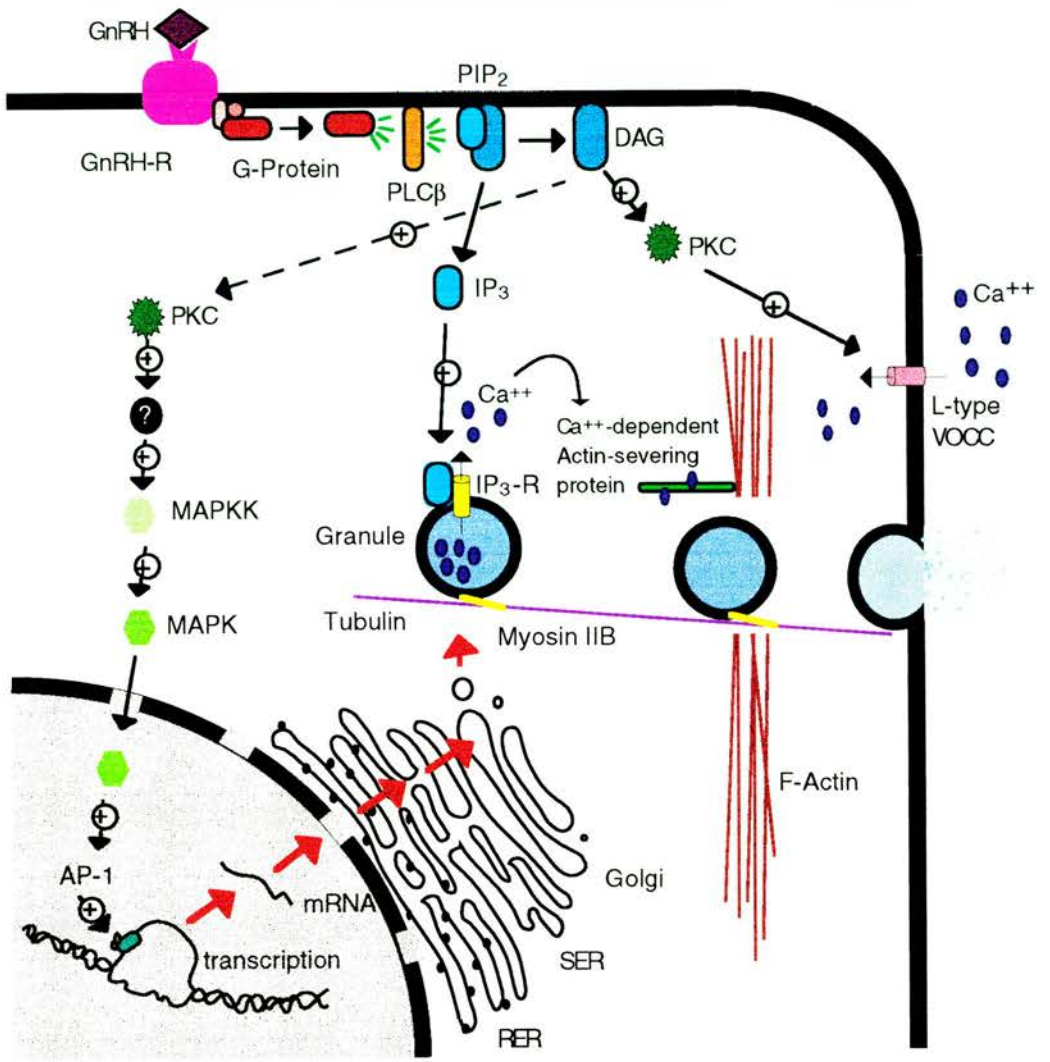

Figure 1.1.6a: Schematic representation of intracellular signalling by the GnRH-R (adapted from Anderson 1996 and Naor *et al* 1998).

This simplified diagram indicates the multiple effects of activation of the GnRH receptor (GnRH-R) within a gonadotroph. Activation of this G protein coupled receptor releases the α subunit of the G protein which activates PLCβ in turn catalysing cleavage of PIP_2. The products of this cleavage DAG and IP_3 are responsible for the subsequent intracellular cascades. The assignment of myosin IIB to movement of gonadotrophin vesicles is putative.

Gonadotrophin releasing hormone (GnRH), GnRH receptor (GnRH-R), phopholipase C (PLC), phosphoinositide 4,5-bisphosphate (PIP_2), inositol 1,4,5-trisphosphate (IP_3), diacylglycerol (DAG), Ca^{++}-dependent protein kinase (PKC), voltage-operated calcium channel (VOCC), IP_3 receptor (IP_3-R), mitogen-activated protein kinase kinase (MAPKK), mitogen-activated protein kinase (MAPK), activator protein 1 (AP-1, contains c-*jun* and c-*fos*), endoplasmic reticulum (ER), rough ER (RER)

DAG activates PKC which mobilises extracellular Ca^{++} ($[Ca^{++}]_{ex}$) (Andrews *et al*, 1990; Izumi *et al*, 1990) Using the reverse haemolytic plaque assay LH exocytosis was measured in response to GnRH treatment in the presence of PKC inhibitors such as retinal and isoquinolone sulphonamide (also known as H7). This demonstrated the role of PKC in mediating LH release after repeated exposure to GnRH lasting in excess of 90 minutes (Lewis *et al.*, 1989) and correlates with the model of GnRH-induced LHβ transcription via PKC stimulation of the MAPK pathway (Naor *et al.*, 1998). PKC isoforms exist within the anterior pituitary (Johnson *et al.*, 1993) and it has been demonstrated using permeabilised cells that although PKCε is not required, PKCα and PKCβ are crucial for ligand-stimulated exocytosis. PKC mediates Ca^{++} influx by activation of L-type voltage-gated Ca^{++} channels (Anderson, 1996). PKC sensitisation to Ca^{++} is increased by DAG (Kishimoto *et al*, 1980) and this process has been implicated in LH release by the application of phorbol esters (Smith *et al.*, 1984). The many isoforms of PKC may be responsible for the wide-ranging effects of GnRH-R activation through specific interaction with a variety of key transcription factors (Cesnjaj *et al.*, 1994).

Using patch-clamped cells with monophasic Ca^{++} fluxes in Ca^{++}-free media it has been demonstrated that LH exocytosis can occur independently of $[Ca^{++}]_{ex}$ (Tse *et al.*, 1993). However, more recent experiments suggest that activation of the GnRH-R results in a biphasic Ca^{++} flux, where an initial peak is followed by a plateau. The biphasic nature of this response has been shown to derive from mobilisation of both $[Ca^{++}]_i$ and $[Ca^{++}]_{ex}$ (McArdle *et al.*, 1996). Modulation of these specific fluxes by the ovarian steroids E_2 and progesterone demonstrated that pretreatment of rat gonadotrophs with 1nM E_2 for 48 hours enhanced the oscillatory response when challenged with GnRH. The effect of progesterone in conjunction with E_2 had different effects depending on the length of exposure prior to GnRH treatment. Short-term (3hrs) exposure to progesterone caused a biphasic Ca^{++} flux in 30% of GnRH-treated cells whereas no control cells exhibited this response. Long-term (48hrs) progesterone exposure reduced the majority of Ca^{++} fluxes to subthreshold levels (Ortmann *et al.*, 1992).

Other agents which result in Ca^{++} oscillations such as ionomycin, Ca^{++} channel activators, Ca^{++} ionophores and Ca^{++}-loaded liposomes stimulate LH

exocytosis with similar efficacy to GnRH (Conn *et al*, 1979; Conn & Rodgers, 1980c; Conn*et al*, 1980b; Conn *et al*, 1980a; Conn *et al*, 1983). Activin has been shown to inhibit the activity of GnRH-R-associated Ca^{++} channels. However, the molecular interactions by which this mechanism may positively regulate FSH exocytosis remains unclear (Katayama & Conn, 1994).

1.5.1 *In vivo* Studies of Neuroendocrine Secretion

Application of GnRH to gonadotrophs can cause different intracellular responses. Priming, in which an enhanced rate of GnRH-stimulated LH release is observed after prior exposure to GnRH was reported as early as 1974 (Aiyer *et al.*, 1974a). Although observations of priming of gonadotrophs in cultured rat and mouse pituitaries were reported soon after (discussed in section 1.7.3) *in vivo* studies relating to intracellular observations were not reported until 20 years later. Transmission electron microscopy (EM) analyses of sheep pituitaries throughout the oestrus cycle demonstrated a priming of gonadotrophs in response to GnRH. The frequency of gonadotrophs exhibiting polarisation of granules towards a local blood vessel increased from 20% in the mid-luteal phase to 90% during the LH surge. Granules participating in the mass-exocytotic episode appeared to be 130-150nm in diameter as after the LH surge only granules of 300nm remained. At 24 hours post-surge gonadotrophs appeared devoid of all granule classes. Although priming appeared restricted to the smaller class of granules, larger granules were obviously released subsequent to the surge. Results from this study did not allow elucidation of the mechanism by which these larger granules were exocytosed. Whether these larger granules condense to form releasable granules or factors governing size exclusion become amenable to release of previously retained LH is not yet clear. Interestingly, replenishment of the degranulated cytoplasm was apparent in the post-surge gonadotrophs by LH-immunoreactivity in rough endoplasmic reticulum (RER) (Currie & McNeilly, 1995). A key point of this paper is the observation that granule polarisation occurs towards local blood vessels which is in contrast to the following *in vivo* study.

Although confocal microscopy of dual-labelled gonadotrophs does not possess the resolution of EM it does allow accurate assessment of colocalisation events. OVX ewes administered 50mg oestradiol benzoate showed a specific mobilisation of LH-only granules to an area adjacent to the PM. Although 17% of control ewes contained mobilised LH granules, 83% of gonadotrophs in oestradiol benzoate-treated ewes exhibited LH granule mobilisation. Thomas (Thomas & Clarke, 1997) suggests that polarisation is not directed in the gonadotrophs of animals around the time of the LH surge. Exact monitoring of the serum levels for the individual animals was not reported thus preventing determination of the individuals proximity to the surge. This may be significant in that post-surge polarised granules may be absent from membrane areas juxtaposed to the blood vessel. Closer examination of images presented in this study clearly shows areas of PM devoid of LH immunoreactivity. It is possible that these areas represent sites of release post-surge. Using this method of microscopy did not permit the localisation of adjacent blood vessels. Interestingly, FSH-containing granules remained dispersed within the cytosol in all gonadotrophs observed (Thomas & Clarke, 1997).

Although FSH is primarily released via the constitutive pathway resulting in tonic secretion profiles as observed in GnRH-antagonist treated animals some episodic secretion has been reported. Continuous sampling of the hypophyseal portal blood vessel which is in close proximity to gonadotrophs and for which peripheral vessels are not a source of blood has allowed accurate measurements of FSH profiles to be made (Padmanabhan *et al.*, 1997). Peripheral blood samples may not reflect the true nature of pulsatile FSH release due to the reduced half-life of isoforms released episodically; 25 minutes versus 3 to 6 hours (Akbar *et al.*, 1974). Close correlation of GnRH profiles and FSH release was reported in conjunction with GnRH-independent pulses and tonic secretion (Padmanabhan *et al.*, 1997). These characteristics contrast with previous measurements of peripheral blood which suggest only tonic secretion (Wallace & McNeilly, 1986). While this study may implicate as yet undetermined FSH-specific secretagogues as well as other possible mechanisms it should be noted that a paper by the same laboratory reported similar episodic, GnRH-independent and basal secretion events

for LH (Midgley *et al.*, 1997). Perhaps the most relevant finding of these papers is the observation that the time-lag between GnRH pulses and FSH pulses is almost indiscernible in comparison to the 1.26 minutes between GnRH and LH (Midgley *et al.*, 1997; Padmanabhan *et al.*, 1997). These results suggest that GnRH-dependent release of a labile FSH isoform is more rapid than that of LH. The rapid exocytosis of FSH may represent a difference between the dynamics of constitutive vesicles in comparison to the much larger LH-containing regulated granules. GnRH-stimulated rearrangement of actin bundles (Anderson, 1996) in non-primed cells may allow more mobile constitutive vesicles to move towards the PM *en masse* thus mimicking an episodic release comparable to that of LH which ensues after slow transit of granules to the PM.

Granins, which will be discussed in the following section, have been implicated in regulated secretion of gonadotrophins (Huttner & Natori, 1995). A recent study demonstrated the correlation between granin regulation and granule morphology in gonadotrophs. The frequency of granules immunoreactive for chromogranin A (CgA) or secretogranin II (SgII) was reported in castrated rats treated with either testosterone or oestradiol. Larger granules (>300nm diameter) present in the cytoplasm of gonadotrophs are immunoreactive for LH, FSH, SgII and CgA whereas smaller granules (<200nm diameter) show immunoreactivity for LH and SgII (Watanabe *et al.*, 1991). A recent study of gonadotrophs in the ewe has demonstrated that LH granules, polarised during oestradiol treatment, also contain SgII and cysteine-string protein (CSP) (Thomas *et al.*, 1998). This data substantiates evidence for a role of SgII during release of small granules in the LH surge (Watanabe *et al.*, 1991; Currie & McNeilly, 1995).

Castrated rats exhibit reduced CgA expression in comparison to controls which is restored by administration of testosterone. The frequency of large granules was markedly reduced in castrated rats but again returned to control levels after treatment with testosterone. Changes in SgII expression and frequency of granule immunoreactivity was not as striking as that of CgA in castrated males (Watanabe *et al.*, 1998b). Studies on female rats also show an absence of large CgA-immunoreactive granules in accordance with the findings in castrated rats (Watanabe *et al.*, 1998a). CgA-dependent aggregation of LH has been reported and is

discussed in section 1.7.2 (Colomer *et al.*, 1995). The effect of reduced LH aggregation was not reported by Watanabe. However, down regulation of GnRH by administration of testosterone causing reduced LH expression did not prevent the appearance of large CgA-immunoreactive granules (Watanabe *et al.*, 1998b). Non-functioning (endocrinologically silent) pituitary adenomas have been demonstrated to contain chromogranin B (CgB) and SgII in electron-dense granules devoid of hormone. CgA expression appeared less robust as 20% (1/5) of the neoplasms did not contain any CgA-immunoreactivity. These data suggest that hormones are not required for granin-containing granule formation (Rosa *et al*, 1992).

CgB has been shown to colocalise with other granins and LH in the bovine anterior pituitary suggesting a co-operative role during regulatory secretion (Bassetti *et al.*, 1990). CgB overexpression under control of the cytomegalovirus (CMV) promoter in transgenic mice led to sorting of the granin to exocrine zymogen granules in pancreatic acinar cells. This suggests that due to the conservation of cellular mechanisms integral to secretion the correct sorting of this granin and presumably others is not restricted to cells of neuroendocrine origin (Natori *et al.*, 1998).

In castrated rats LHβ subunit expression exceeds that of the αGSU which leads to degradation of the excess β-subunits. Degradation of the β-subunits occurs in lysosomal compartments but does not colocalise with immunoreactivity for αGSU, FSHβ or SgII (Bassetti *et al.*, 1995).

Other membrane-associated proteins have been reported as key components to vesicle fusion during exocytosis. Although details regarding the interactions of these proteins have been almost entirely derived from studies using *in vitro* technologies, a recent study by Jacobsson & Meister (1996) at the Karolinska Institute has provided excellent detail regarding protein expression within the pituitary gland of male rats. Interpretation of *in situ* hybridisation analyses has determined an abundance of specific mRNA for synaptotagmin-I, CSP, cellubrevin, vesicle-associated membrane protein (VAMP)-2, munc-18, synaptosome-associated protein of 25kDa (SNAP-25)-a, soluble NSF attachment protein α (αSNAP) and syntaxins 1A, 4, and 5 in the anterior and intermediate lobes. These areas also contained less abundant message for synaptotagmin III,

SNAP-25b and syntaxin 2. mRNA was absent for species of synaptotagmin II, VAMP-1 and syntaxins 1B and 3.

Confocal observations revealed the colocalisation of synaptotagmin I-III immunoreactivities with those of all major pituitary hormones except LH and FSH. However, all hormone-expressing cells within the anterior lobe showed immunoreactivities for VAMP, CSP, *N*-ethylmaleimide soluble factor (NSF), αSNAP, SNAP-25 and syntaxin (Jacobsson & Meister, 1996). In contrast to these results a more recent study of the pituitary in the ewe during oestradiol benzoate treatment revealed that syntaxin was not present in any pituitary cells and synaptotagmin was only detected in gonadotrophs and lactotrophs. The expression of these proteins within the pituitary did not change in response to oestradiol benzoate (Thomas *et al.*, 1998). Surprisingly this study did not investigate changes in either mRNA or protein levels during oestradiol benzoate treatment.

The proposed interaction of these molecules is discussed within section 1.7.3 and represented schematically in figure 1.7.3a. Taken in the context of findings in other systems (see section 1.7.3), these data give compelling evidence that the molecular mechanisms involved in regulated exocytosis are highly conserved throughout neuroendocrine cell lineages.

The following section will centre on the role of granins. Two main reasons have led to their investigation as potential sorting proteins within gonadotrophs. Firstly they are abundantly expressed in a variety of neuroendocrine tissues (O'Connor, 1983; Fischer-Colbrie *et al* 1987) and secondly, they are present within the secretory granules of gonadotrophs (Watanabe *et al.*, 1991).

1.6.1 The Granin Family

Co-storage of acidic water-soluble proteins with catecholamines in bovine adrenal chromaffin cells was first reported as early as 1958 (Hillarp, 1958). Almost ten years later Schneider *et al* named the protein Chromogranin A (Schneider *et al.*, 1967). Granin molecules are acidic (anionic) secretory glycoproteins expressed in all neuronal and endocrine cell lineages (O'Connor, 1983). Members of the family are defined by the presence of a decapeptide motif E-S/N-L-X-A/D-X-D/E-X-E-L and multiple dibasic

cleavage sites from which peptide products are derived (Gerdes *et al.*, 1989).

Table 1.6.1 Current Members of the Granin Family.

	Molecular Weight (kDa) by SDS-PAGE	Features	Reference(s)
Chromogranin A	70	colocalisation with LH & FSH in >300nm granules binds IP_3-R dimer/tetramer	Schneider *et al* 1967 Watanabe *et al* 1991 Yoo & Lewis 1994
Chromogranin B (Secretogranin I)	100	highly aggregative colocalises with other granins	Pohl *et al* 1990 Yoo 1995 Bassetti *et al* 1990
Secretogranin II (Chromogranin C)	86	co-migrates with LH in <200nm granules during oestradiol treatment no C-terminal disulphide bond	Gerdes *et al* 1989 Schimmel *et al* 1992 Watanabe *et al* 1991 Thomas *et al* 1998
Secretogranin III	63	cleavage at unconserved sites	Ottiger *et al* 1990 Holthius *et al* 1996
Secretogranin IV (HISL-19 antigen)	35+32	perinuclear in malignant tissue	Krisch *et al* 1988 Neuhold & Ullrich 1993
Secretogranin V (7B2)	25	regulates activity of PC2 chaperonin homology	Martens 1988 Braks & Martens 1994
NESP55	55	peptide is antagonist for scrotonergic receptor $5\text{-}HT_{1B}$	Ischia *et al* 1997
Golgin-245	245	multiple coiled-coil domains	Fritzler 1995

Several granin-type molecules have been putatively identified and some such as SgII reassigned falsely as a novel protein SIIp (Conn *et al.*, 1992). It is interesting to note from table 1.6.1 that the range of molecular weights for granins is considerable. It may also be noted that exact roles have not been assigned for any granins although some bioactivity has been associated with the many granin-derived peptides (see section 1.6.6). Only the three granin molecules chromogranin A (CgA), chromogranin B (CgB - also known as secretogranin I) and secretogranin II (SgII - also known as chromogranin C) have been studied in detail (Eiden *et al.*, 1987). The following discussion will focus on these three prominent granins.

During the past 15 years the investigation of the role of granins has centred on three main areas; bioactive peptides, disease markers and regulated secretion.

Peptides, formed as a result of proteolytic processing within the secretory granule, exhibit a wide range of roles including secretagogues, antibacterial agents and cell adhesion molecules (Zhang *et al.*, 1994; Drees & Hamilton, 1994; Muller & Tougard, 1995; Strub *et al.*, 1996; Jin *et al.*, 1996; Muller *et al.*, 1997).

Detection of abnormally high serum CgA levels has clinical relevance as a marker for neoplasia in neuroendocrine tissue (Deftos *et al.*, 1987; Secco *et al.*, 1996; Hsiao *et al.*, 1990), the prostate (Deftos & Abrahamsson, 1998) and in cases of hypertension (O'Connor, 1985; Takiyyuddin *et al.*, 1995). Detection of CgA-like immunoreactivity in the cerebrospinal fluid of schizophrenic patients has been used as an indicator of tonic arousal (Vankammen *et al.*, 1991). Radioimmunoassays (RIAs) (O'Connor, 1984; Syversen *et al.*, 1994) and immunohistochemical analyses (Schmid *et al.*, 1991; Schmid *et al.*, 1994) have been used effectively in diagnosis of these conditions.

Colocalisation of granins with other secretory proteins has led to speculation that one of their roles may be in sorting specific types of proteins during regulated secretion in a variety of different tissues (Huttner & Natori, 1995; Watanabe *et al.*, 1998a). The putative role of granins in regulated secretion will be the main focus of this section after

discussion of granin gene structure and regulation. A brief summary of granin-derived peptides will conclude discussion of granins.

1.6.2 Organisation of Granin Genes

CgA, CgB and SgII are each encoded by single copy genes in mammalian genomes. The human CgA gene is located on chromosome 14q32 (Murray *et al.*, 1987) whereas the rat and mouse genes are located on chromosomes 6 and 12 respectively (Simon-Chazottes *et al.*, 1993). The human CgB and SgII gene loci are 20pter-p12 and 2q35-q36 respectively (Mahata *et al.*, 1996). Murine CgB is located on chromosome 2 (Jenkins *et al.*, 1991) whereas SgII is found on mouse chromosome 1 and rat chromosome 9 (Mahata *et al.*, 1996). An evolutionary relationship, perhaps that of gene duplication, between CgA and CgB is suggested by homology at the amino- and carboxy-terminal encoding regions (Pohl *et al.*, 1990).

The CgA gene contains 8 exons in human (Mouland *et al*, 1994), mouse (Wu *et al*, 1991) and bovine genomes (Iacangelo *et al.*, 1991). The bovine and mouse CgA genes span 13.6kb and 11kb respectively (Iacangelo *et al.*, 1991; Wu *et al.*, 1991). Although the organisation of the CgB gene appears similar to that of CgA, it has only five exons of which the third is the largest (Pohl *et al.*, 1990). The structure of the mouse SgII gene is unlike those of CgA and CgB as it consists of only two exons. The second exon encodes the entire protein as the first contains only 5' untranslated (UT) sequences (Schimmel *et al.*, 1992) (figure 1.6.2a).

Exon assignment within the CgA gene corresponds to the function of the transcribed protein and subsequently cleaved peptides which are described in detail below. The signal peptide is encoded by exon 1 with exons 2 - 5 encoding the amino-terminal domain. Exons 6 and 7 contain sequence information for variable domains and exon 8 encodes the second conserved domain, at the carboxy-terminal region (Hendy *et al.*, 1995). CgB exons are similarly organised with regard to assignment for exons 1, 2 and 3. Notably, exon 3 in each gene contains conserved sequences for cysteine residues important for formation of a disulphide loop. Exon 5 in CgB

corresponds to the carboxy-terminal encoding sequences equivalent to those in exon 8 of CgA. The variable domain of CgB is encoded by exon 4.

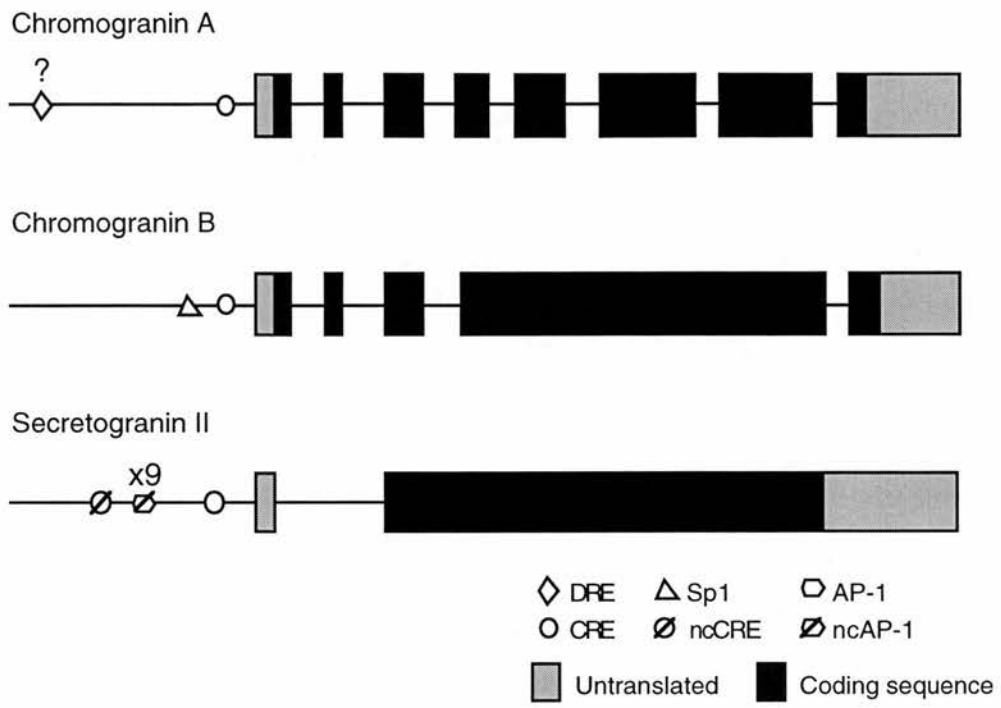

Figure 1.6.2a: Schematic representation of granin gene organisation.

Of the three granins depicted here CgA has the most complex genetic organisation with 8 exons. CgB shows similarity to CgA in the first three exons and last exon. The SgII gene is the simplest in structure with only two exons, the second of which contains the entire coding region. Promoter details are limited as indicated by the putative assignment of the DRE (distal regulatory element) to that of CgA and near consensus (nc) binding sites for AP-1 (activator protein 1) and CRE (cAMP-response element). The introns and promoters are not drawn to scale.

1.6.3 Regulation of Granin Expression

Chromogranin A

Expression of the CgA gene in non-neuroendocrine cells such as enterochromaffin-like cells, which influence gastric acid secretion by parietal cells, has been shown to be affected by nicotine and famotidine (an H_2-receptor antagonist). CgA mRNA and protein levels were both increased in rats fed famotidine and/or nicotine. Administration of both

factors resulted in a rise of the CgA mRNA to 18S rRNA ratio from 0.61±0.04 to 0.96±0.04, CgA protein levels increased from 7.4±1.2 to 14.7±2.01 pmol/gram of tissue (Gomez *et al.*, 1997).

Secretion of CgA from the parathyroid gland has been shown to be positively regulated by 1,25-dihydroxyvitamin D. mRNA levels increased by 1.6, 3.2 and 5.6-fold upon administration of 10, 50 and 250 pmol/100 grams body weight, respectively (Soliman *et al.*, 1997). Primary cultures of porcine parathyroid cells treated with pancreastatin, a CgA-derived peptide (see below), exhibited negative regulation of CgA expression through several mechanisms. Using nuclear run-on assays it has been demonstrated that pancreastatin at 10^{-7}M reduced CgA transcription by 52% after 12 hours. Pancreastatin also affected CgA mRNA stability and reduced the half-life from 33 to 18 hours. The presence of pancreastatin reduced secretion of CgA, as measured by RIA, by 40% after only 4 hours (first time point) and by 80% after 24hrs. The effect on CgA secretion may actually occur far quicker as pancreastatin affects parathyroid secretion within an hour of administration (Zhang *et al.*, 1994).

Glucocorticoid treatment has been shown to positively regulate CgA expression in the rat pituitary (Fischer-Colbrie *et al.*, 1989). In the mouse adrenocorticotroph AtT-20 cell line 48 hour exposure to dexamethasone (DEX) increased CgA mRNA levels by 2.5-fold and CgA secretion by five-fold (Wand *et al.*, 1991).

E_2-treatment of rat pituitary cell aggregates demonstrated a 50% reduction in mRNA levels using 10^{-8}M E_2 with 34% reduction in CgA protein expression. Interestingly, this treatment did not reduce the expression of gonadotrophin subunits emphasising the importance of co-ordinate regulation by pulsatile GnRH regimes (Anouar & Duval, 1992).

Recently the promoter structure for the human CgA (hCgA) gene has been studied with particular regard to regulation of expression in neuroendocrine cells. The location of three upstream domains; a distal positive domain (-4.8 to -2.2kb), a proximal negative domain (-258 to -181bp) and the proximal positive domain (-147 to -61bp) was determined (Canaff *et al.*, 1998).

The proximal positive domain contains the most highly conserved sequences and those which are necessary for basal transcription in

neuroendocrine cells. In rodent, bovine and human CgA proximal domains there are four conserved sequences; a GAGA sequence, a cAMP response element (CRE) (Mouland *et al.*, 1994), a TG box and a TATA box. Deletion of the CRE resulted in background reporter expression levels in all cell lines tested except TT cells (human thyroid) where deletion of the TG box was also required. Furthermore, the relative input of upstream sequences was assessed in promoter constructs containing up to 2300bp of 5' sequence. Reporter expression from these constructs fell by 50-75% (Canaff *et al.*, 1998). This construct however, excludes the majority of the distal positive domain while including the proximal negative domain. The role of the CRE in cAMP-stimulated hCgA expression was demonstrated to be cAMP-dependent protein kinase (PKA)-dependent as administration of a PKA inhibitor, H89, prevented stimulation while also reducing basal transcription by 85% (Canaff *et al.*, 1998). In this system cAMP binds to PKA allowing its dissociation from the holoenzyme which permits entry of PKA subunits into the nucleus to activate CREB by phosphorylation (Spaulding, 1993).

Other studies have suggested that a distal regulatory element (DRE) between-570 and -555 may increase reporter expression in BEN cells by five-fold (Nolan *et al.*, 1994). Further investigation suggested that DRE activity is dependent on a unique DRE-binding factor (DBF), expressed specifically in neuroendocrine cells, which mediates assembly of a functional transcription complex (Nolan *et al.*, 1996). However, the more recent study by Canaff *et al* where several cell lines of neuroendocrine and non-neuroendocrine origin were used, suggests that BEN cells may be exceptional with regard to enhancement of reporter expression by this sequence (Canaff *et al.*, 1998). Screening of DBF expression in a range of cell lines and *in vivo* may demonstrate its role more clearly.

The significance of an ERE and a glucocorticoid-response element (GRE)-like sequence (Iacangelo *et al.*, 1991) were not investigated in any of the three studies discussed in the previous paragraph. However, the presence of these elements within the bovine CgA promoter suggests that the observations of positive and negative regulation by DEX and E_2 respectively, may also occur through similar sequences in conserved rodent CgA promoters (Fischer-Colbrie *et al.*, 1989; Wand *et al.*, 1991;

Anouar & Duval, 1992). Recent observations of changes in CgA-immunoreactive granule sizes throughout the rat oestrus cycle and the prevalence of larger CgA-immunoreactive granules in males provides clear *in vivo* evidence for the regulatory role of E_2 presumably through the ERE (Watanabe *et al.*, 1998b; Watanabe *et al.*, 1998a). However the mechanism by which testosterone has been demonstrated to exert a positive effect on CgA expression in rats has yet to be reported (Watanabe *et al.*, 1998b)

The exact mechanisms whereby CgA expression is controlled in widespread tissues remain unclear. The presence of a CRE within the proximal positive domain does however substantiate evidence of positive regulation by factors increasing intracellular cAMP levels. Ligand binding to the G protein coupled GnRH-R leads to an intracellular cascade which via diacylglycerol (DAG) activation of PKC generates cAMP (Anderson, 1996). Although yet to be demonstrated *in vivo* it is likely that GnRH would have a stimulatory role on CgA transcription.

Chromogranin B

The promoter structure for CgB has not been studied in as much detail as that of CgA. However certain motifs and characteristics have been characterised. The murine CgB promoter is very GC-rich with the 5' proximal 215bp exhibiting 75% GC. The TATA box is present at -31bp and a CRE further upstream at position -102. An Sp1 binding site, also present in the parathyroid hormone promoter, is located at -134bp. The CRE may allow response to external factors such as GnRH whereas the high GC content of the promoter may restrict expression of the gene to specific tissues (Pohl *et al.*, 1990).

In PC-12 cells treated with the adenylate cyclase activator forskolin (FSK) the rise in intracellular cAMP concentrations led to increased accumulation of CgB mRNA. This required PKA activation but occurred independently of *de novo* protein synthesis. Furthermore the positive regulatory effect of FSK on CgB transcription reached 601±87% of control 2 hours post-treatment with accumulated mRNA rising 2.5-fold and protein concentrations increasing by more than 3-fold (Thompson *et al.*, 1994).

Accumulation of CgB mRNA is stimulated in GH_3B6 cells by 1nM E_2 treatment and occurs maximally after 48-72 hours exposure (Laverriere *et al.*, 1991). If this effect is a result of transcriptional induction it contrasts with effects observed for CgA and SgII (Anouar & Duval, 1992).

A 3-fold reduction of CgB expression by DEX administration in studies using a transgenic murine somatomammotroph-derived cell line has been reported (Thiny *et al.*, 1994). This observation correlates with previous *in vitro* evidence using the rat somatomammotroph GH3B6 cell line where DEX was shown to reduce CgB mRNA accumulation to 23% of control levels (Laverriere *et al.*, 1991). In the PC-12 cell line treatment with either FSK or cycloheximide did not reduce the CgB half-life of 19±6 hours (Thompson *et al.*, 1994).

Secretogranin II

The regulation of SgII expression by administration of secretagogues or the PKC activator 12-*O*-tetradecanoylphorbol-13-acetate (TPA) has been investigated by two laboratories using primary cultures of bovine chromaffin cells. Fischer-Colbrie *et al* (1990) reported no change in SgII mRNA levels after treatment with nicotine, however Soszynski *et al* (1993) observed a considerable (150±27%) increase in SgII protein levels. Both groups reported that administration of TPA led to mRNA abundance increasing 3.2-fold and protein by 97±7%. Combination of forskolin and TPA treatment produced a rise in SgII levels comparable with those observed by Soszynski *et al* (1993) after nicotinergic stimulation (Fischer-Colbrie *et al.*, 1990; Soszynski *et al.*, 1993). The findings from these groups suggest that, in chromaffin cells, SgII expression is positively regulated by the action of PKC and cAMP-dependent mechanisms. The disparity between SgII mRNA and protein abundance after nicotinic stimulation may arise through a reduction in the level of RNA degradation induced by undetermined effectors of nicotinergic receptors. Further research is required to clarify this point as is equivalent secretagogue-based work using pituitary-derived cells.

A study using rat pituitary cultures demonstrated a 30% decrease in SgII mRNA levels after a 72 hour exposure to 10^{-8} M oestradiol (E_2) (Anouar & Duval, 1992). The negative regulation of SgII by E_2 contrasts with findings

in a transgenic mouse somatomammotroph-derived cell line (Thiny *et al.*, 1994) and *in vivo* observations of both male and female rat gonadotrophs where no change in response to E_2 was reported (Fischer-Colbrie *et al.*, 1989; Watanabe *et al.*, 1998a). The effect of E_2 during a controlled pulsatile GnRH regime has yet to be reported but may reflect the effects of co-ordinate regulation of gene expression not exerted during *in vitro* studies. This may be particularly relevant in light of the putative role of AP-1 production by activated GnRH-R and the presence of near-consensus AP-1 sequences within the rat SgII promoter discussed below (Jones *et al.*, 1996). DEX treatment of a cell line derived from transgenic murine somatomammotrophs demonstrated a 1.5-fold increase in SgII mRNA levels (Thiny *et al.*, 1994). Despite this more recent analysis of the rat SgII promoter failed to find a glucocorticoid response element (see below) (Jones *et al.*, 1996).

Studies on SgII promoter regulation in PC-12 cells demonstrated a down-regulation of mRNA levels in response to FSK treatment. FSK administration required at least 48 hours to exert its negative effect upon mRNA levels eventually reducing them to 22% of control levels. The opposite effect of FSK on the rate of SgII transcription was observed when the protein synthesis inhibitor cycloheximide was administered in conjunction leading to a rise of 1290±96% of control levels. The relatively low endogenous rate of transcription appeared unaffected by FSK treatment which suggests that cAMP production (induced by FSK) may affect SgII mRNA stability. Alternatively, due to the marked rise in SgII mRNA accumulation during combined administration of FSK and cycloheximide it has been postulated that expression of labile regulatory proteins is halted leading to unrestricted stimulation of SgII transcription by cAMP (Thompson *et al.*, 1994). Specific labile regulatory proteins which interact with the SgII promoter have yet to be characterised.

Promoter detail relating to the rat SgII gene has recently been revealed using resections of a 2.6Kb 5' untranslated region upstream of a luciferase reporter gene. The location of proximal elements and distal enhancer sequences were determined by reporter assays after transfection of neuroendocrine or non-neuroendocrine cell lines. Sequence analysis revealed the presence of a consensus TATA box at -27 to -31bp, a CRE at -65

to -72 and a CAAT box sequence at -158bp. Furthermore the proximal 450bp 5' regions of mouse and rat SgII genes exhibit over 90% homology. Distal elements for binding of known transcription factors were also revealed by sequence analysis. Two Pit-1 sites are located at -2537 to -2529bp and -1254 to 1246bp as well as 15 E boxes (bind helix-loop-helix transcription factors) which span the region between -2531 and -173bp. Binding elements differing by only one base from the consensus were found for activator protein-1 (AP-1) 9 times within the -2639 to -304bp region. Four activator protein-2 (AP-2; binding induced by cAMP) sites were also found between -2602 and -69bp and a one base consensus deviation was found for CRE at -1786 to 1779bp. Notably, sequences permitting oestrogen receptor or glucocorticoid receptor binding are absent from the sequences of rat SgII promoter investigated in this study (Jones *et al.*, 1996). More recently a 19bp element (at -80 to -62) responsible for the transcriptional effects of cycloheximide treatment has been demonstrated to bind a complex containing CREB and CRE-modulator (CREM) or activating transcription factor-1 (ATF-1). Although FSK increases the response to cycloheximide from 3.8- to between 8- and 12-fold, no change in formation of this protein complex was observed. The authors suggest that FSK may enhance the transcriptional response to cycloheximide by aiding interaction with general transcription machinery (Jones & Scammel, 1998).

The absence of an ERE within the SgII promoter correlates well with the lack of SgII modulation during the oestrus cycle of rats (Watanabe *et al.*, 1998a) and in males (Fischer-Colbrie *et al.*, 1989). The reduction in SgII mRNA levels *in vitro* during E_2 treatment (Anouar & Duval, 1992) and the presence of near-consensus AP-1 binding sites (Jones *et al.*, 1996) may suggest a positive regulatory role for GnRH which counteracts that of E_2 *in vivo* maintaining levels of SgII expression (see section 1.4.6).

Pit-1 binding sites within the SgII promoter may allow specific expression within lactotrophs and thyrotrophs. However as yet SgII appears limited to relatively low expression in somatomammotroph cells (Hashimoto *et al.*, 1987).

The presence of a consensus CRE and a distal one-base deviation CRE within the rat SgII promoter correlate well with these findings from studies using PC-12 cells (Jones *et al.*, 1996).

It is possible that elements responsible for negative regulation by E_2, such as the ERE observed in bovine CgA promoter sequences, are located distal to the -2612bp analysed by Jones *et al.* Positively regulating sequences such as GRE which may explain induction of SgII expression in murine somatomammotrophs may also be located upstream of the -2612bp used in reporter constructs (Jones *et al.*, 1996; Thiny *et al.*, 1994).

Overall it is apparent from these studies that a number of molecular signalling pathways are used to regulate granin gene expression. This is consistent with their diverse tissue expression. However it is not clear whether granin genes are regulated by similar means in a variety of tissues or whether their regulation is specifically controlled to meet the secretory requirements of the cell type in question. It is likely that these three prominent granins CgA, CgB and SgII are regulated within the gonadotroph in line with the large fluctuations reported for the gonadotrophins LH and FSH. As yet no studies have been carried out to determine the regulation of granin genes across the oestrus cycle.

1.6.4 Protein Structure of Granins

Prior to discussing putative roles for members of the granin family some detailed structural characteristics and interactions will be described.

The anionic nature of these glycoproteins derives from the high content of glutamic acid and proline residues, typically 25% and 10% respectively, pI values range between 4.5 and 5.5 (Fischer-Colbrie & Schober, 1987). The murine CgA gene contains a unique poly-glutamine insertion in exon 5 (Iacangelo & Eiden, 1995) the significance of which remains to be determined. The high degree of posttranslational modification within granins includes *N*- and *O*-glycosylation, phosphorylation, sulphation, pyroglutamylation, carboxymethylation, α-amylation and disulphide bond formation. Although posttranslational modifications may determine rates and specificities of proteolytic processing, the significance of these modifications in terms of intracellular interactions has not been reported. However a brief summary of posttranslational modifications found on granins will now be given. Glycosylation of CgA and CgB is similar as both contain approximately 5% sugar residues. CgA and CgB may differ as CgB

contains more fucose and mannose. CgB contains *N*-glycosylation sites whereas *O*-glycosylation may be predominant in bovine CgA. Chromaffin granule CgA and CgB are both phosphorylated at serine and threonine residues with a maximum of five phosphoserine residues per molecule. CgB shows sulphated tyrosine residues and sulphation of carbohydrate side chains whereas CgA shows only the latter. However, CgA labelled in PC-12 cells exhibits a proteoglycan form but the amount *in vivo* may be limited and no proteoglycan forms of CgB exist in bovine tissue. Pyroglutamylation in which glutamic acid residues are converted to pyroglutamyl residues by glutamic cyclase occurs for CgB-derived peptides in the adrenal medulla. Carboxymethylation of CgA may occur cotranslationally as carboxymethylase is a cytosolic enzyme. α-Amidation of the carboxy-terminal glycine residue of the CgA-derived peptide pancreastatin has been reported although the significance of this modification has not been determined. For more detailed discussion of posttranslational modifications in granins refer to Winkler & Fischer-Colbrie 1992 (Winkler & Fischer-Colbrie, 1992). Single disulphide bonds are present within the amino-terminal regions of both CgA and CgB but are absent from the structure of SgII and it has been suggested that these represent a type of conformational sorting signal (Gerdes *et al.*, 1989). A putative receptor for this conformational signal had been suggested as carboxypeptidase E (CPE) after initial studies demonstrated an interaction (Cool *et al.*, 1997). However cells expressing antisense (AS)-CPE do not exhibit misrouting of CgA suggesting redundancy in this mechanism (Normant & Loh, 1998).

Human and bovine CgA contain 439 and 431aa respectively with an 18aa signal peptide located at the amino-terminus. The predicted molecular mass of CgA is 48kDa whereas analysis by SDS-PAGE determines a mass of 70kDa (Iacangelo *et al.*, 1986).

The CgB polypeptide is longer than either CgA or SgII, the human form is 657aa and the bovine 626aa, both of which have a 20aa signal sequence (Bauer & Fischer-Colbrie, 1991). The predicted molecular mass of bovine CgB is 71.5kDa (Bauer & Fischer-Colbrie, 1991) although its migration by SDS-PAGE corresponds to a protein of 100kDa (Gill *et al.*, 1991). The bovine SgII polypeptide is 586aa long, with a predicted molecular mass is 67.5kDa

but with migration by SDS-PAGE corresponding to a mass of 86kDa (Fischer-Colbrie *et al.*, 1990).

Predicted and apparent molecular weights for granins are often dissimilar due to the high level of posttranslational modification and the abundance of acidic residues which retard the protein in the presence of SDS.

Granins are low affinity, high capacity Ca^{++}-binding molecules. For example each molecule of CgA binds 32 and 55 Ca^{++} molecules at pH 7.5 and 5.5 respectively with a K_D of 2-4mM (Yoo & Albanesi, 1991). Clearly pH has a striking effect on granin structure.

Effects of changes in intracellular calcium concentrations ($[Ca^{++}]_i$) and pH on the structure and functional behaviour of granins will now be covered. pH values decrease with passage through the regulated secretory pathway from pH 7.5 within the ER decreasing to about pH 6.3 in the *trans*-Golgi network (TGN) with a further decrease to between pH5.0 and 5.5 in mature secretory granules. Changes in $[Ca^{++}]_i$ inversely correlate with the decrease in pH with basal levels in the ER rising to 40nM within mature granules. It may be possible that microdomains of even higher $[Ca^{++}]_i$ within discrete areas of the cell (Thorn, 1996) may facilitate extreme conformational interactions between granins and components of the secretory pathway.

The oligomerisation of CgA at pH5.5 and 35mM Ca^{++} is entropic which results in nearly all secretory vesicle CgA being tetrameric. 96% of CgA is dimeric at pH 7.5 with no Ca^{++} which corresponds to conditions within the ER and *cis*-Golgi (Yoo & Lewis, 1992). A specific region including residues 407 to 431aa has been demonstrated as a crucial for entropic dimerisation and tetramerisation of CgA independently of $[Ca^{++}]_i$ (Yoo & Lewis, 1993).

Although CgA clearly forms oligomeric structures SgII and CgB may remain monomeric throughout the regulated secretory pathway (Yoo & Albanesi, 1991; Yoo, 1995).

Changes in pH and $[Ca^{++}]_i$ also play a role in determining the aggregation of CgA and CgB *in vitro*. Furthermore, increases in $[Ca^{++}]_i$ also determine, through conformational changes, the hydrophobicity of CgA and CgB thus influencing their affinity for membrane interactions. Using the fluorescent hydrophobic region-specific probe 4,4'-*bis*(1-anilinonapthalene 8-sulphonate) (Rosen & Weber, 1969), increases in

fluorescence were observed in samples containing CgA after addition of Ca^{++}. The high sensitivity of CgB to $[Ca^{++}]_i$ (discussed below) caused aggregation and prevented observation of increases in hydrophobicity (Yoo, 1995).

pH and Ca^{++} induced conformational changes in CgA and CgB have also been studied using CD spectroscopy (Yoo & Albanesi, 1991; Yoo, 1995). Shifts from pH 7.5 to 5.5 caused CgB α-helicity to rise from 15 to 20%, addition of 0.2mM Ca^{++} increased α-helicity further to 25% and reduced random coil from 70 to 65%. For comparable conformational change in CgA Ca^{++} concentrations in excess of 10mM were required (Yoo & Albanesi, 1990a). Ca^{++} concentrations greater than 2mM induced aggregation of CgB as determined by turbidity assays. Aggregation characteristics of CgA and CgB in the presence of different $[Ca^{++}]_i$ at pH 5.5 and 7.5 have been compared using turbidity assays which measure absorbance at 320nm. The comparison shows that maximal CgA aggregation requires 40mM Ca^{++} whereas maximal CgB aggregation, which is six-fold higher than that of CgA, occurs at only 4mM Ca^{++}. In order to obtain a level of aggregation giving an A_{320nm} of 0.2, CgB requires 0.2mM Ca^{++} whereas for CgA a concentration of 33mM is needed (Yoo, 1995). These analyses indicate a 165-fold greater sensitivity of CgB than CgA to Ca^{++}. Possible reasons for the difference in aggregation dynamics for CgA and CgB proposed by Yoo *et al* (1995) include the greater propensity for CgB to reveal hydrophobic domains and maintained monomeric status which may allow greater mobility for molecular interactions (Yoo, 1995).

Co-aggregation of CgA and CgB using mixtures of the two granins showed aggregation at Ca^{++} concentrations intermediate to the maximal values normally required. Co-aggregation at 13mM Ca^{++} was obtained most effectively with a CgA:CgB ratio of nearly 3:1 (0.4mg/ml:0.15mg/ml). In chromaffin granules CgB concentrations are approximately 10-fold less than CgA. At this ratio co-aggregation occurred with 30mM Ca^{++} which is 2.5 fold higher than that required for similar concentrations of CgB alone but 30% lower than needed for CgA (Yoo, 1995).

Aggregation of SgII in PC-12 cells has been demonstrated at pH5.2 in the presence of 10mM Ca^{++}. Absence of Ca^{++} or an increase in pH to 7.4 reduced the aggregative behaviour of SgII. Secretion of SgII was limited to

approximately 3.5% of total SgII expression in normal PC-12 cells. However, cells treated with ammonium chloride which prevents formation of low pH environments intracellularly exhibited an increase in SgII release to 45% of total SgII expressed. This suggests that disruption of SgII aggregation prevents retention of SgII within the cell. Most importantly, SgII aggregates formed under permissive conditions excluded IgG suggesting a sorting mechanism specific for proteins secreted by the regulated pathway (Gerdes *et al.*, 1989). Treatment of gonadotrophin-secreting cultures with ammonium chloride or similar agents has not been reported but this may elucidate an aggregative role of SgII in retention of LH.

CgA and CgB have also been shown to interact with secretory membranes (Kang & Yoo, 1997; Yoo & Kang, 1997) and CgA more specifically with the membrane-bound 1,4,5-trisphosphate receptor (IP_3-R) (Yoo & Lewis, 1994) and CPE (Cool *et al.*, 1997). Truncated forms of CgA and CgB as well as specific peptides were used to determine key regions in the granin structure involved in membrane interactions. Truncated CgA proteins lacking the N-terminal region 1-39aa which contains the conserved sequence IVEVISDTLSKPSPMPVSKE (18-37aa) failed to bind membrane-containing columns at pH5.5 (Kang & Yoo, 1997). Membrane-binding by CgB was stronger than that of CgA as increasing the pH from 5.5 to 7.5 in conjunction with 1M KCl was required for elution. Although truncated proteins lacking the conserved 1-48aa failed to bind the membrane-coated column, proteins lacking the C-terminal residues at 450-626aa exhibited only 50% of the binding shown by the intact molecule. It was suggested that the carboxy-terminal region of CgB may be involved in intramolecular interactions determining amino-terminal conformations integral in membrane binding (Yoo & Kang, 1997)

The intramolecular disulphide bond of CgB between residues 16 and 37, which although critical for sorting to the regulated pathway (see below), is not crucial for aggregation under *in vitro* conditions equivalent to those found in the TGN (Chanat *et al.*, 1994). The lack of sorting to a regulated pathway in PC-12 cells suggests that conformational integrity imparted by the disulphide bond facilitates binding to an as yet uncharacterised receptor involved in protein sorting (Chanat *et al.*, 1994). These results are

not to be confused with those published in the paper by Yoo and Kang which demonstrate that the N-terminal peptide corresponding to residues 16 to 37 bind the vesicle membrane at pH5.5 (Yoo & Kang, 1997). This pH is equivalent to values within the secretory vesicle, as opposed to pH6.4 and 10mM $[Ca^{++}]_i$ which is equivalent to the TGN.

The IP_3-R is a 260kDa eight transmembrane region receptor/Ca++ channel located on secretory granules (Furuichi *et al.*, 1989). CgA binding is specific to four residues on the second intraluminal loop of the IP_3-R and may bind via an amino-terminal motif leaving more dynamic regions free to interact with other granins, secretory proteins and Ca^{++} (Yoo & Lewis, 1994).

A conserved region at 40-55aa within CgA corresponds to a calmodulin-binding region and shows complete conservation between all CgA molecules. The binding to calmodulin is Ca^{++} dependent with a dissociation constant of 17nM which is comparable with other calmodulin-binding proteins (Yoo, 1992).

The functional implications of these structural characteristics and interactions within the regulated secretory pathway will be discussed in the following section.

1.6.5 Intracellular Roles

The two main putative intracellular roles for granins are protein sorting and granulogenesis (Iacangelo & Eiden, 1995). A third role relating to granule structure is that of $[Ca^{++}]_i$ mobilisation during exocytosis (Yoo & Lewis, 1994). This final role may be particularly significant in light of *in vivo* evidence for the absence of conventional calcium sensors such as synaptotagmin in rat gonadotrophs (Jacobsson & Meister, 1996).

Functional studies of CgA and CgB using *in vitro* aggregation and conformational analyses by Yoo *et al* (1995) have led to the suggestion that the two granins work in concert during granulogenesis. The high Ca^{++} sensitivity of CgB may predispose it to form aggregates before CgA prior to entering the TGN. Furthermore the greater affinity of CgB, in comparison with CgA, for membranes suggests that it may bind the lipid envelope before CgA. Membrane interactions have not been reported for SgII

although, like CgA and CgB, it does exhibit pH- and Ca^{++}-dependent aggregation (Gerdes *et al.*, 1989).

Co-aggregation of CgA and CgB when mixed in permissive conditions may not be surprising. Co-aggregation of otherwise non-aggregative proteins of physiological relevance such as LH suggests a clear role for granins. Adrenal extracts containing CgA induced aggregation of pituitary samples containing LH in the presence of 25mM Ca^{++} at pH5.8. PRL aggregation appears to occur spontaneously in the same conditions whereas aggregation of processing enzymes such as dopamine β-hydroxylase and peptidyl glycine α-amidating monooxygenase is CgA-dependent (Colomer *et al.*, 1995). The specific nature of the coaggregative qualities of granins is illustrated by the observation that neither CgA or SgII induce aggregation of proteins such as IgG which are normally secreted via the constitutive pathway (Colomer *et al.*, 1995; Gerdes *et al.*, 1989).

A sequential and co-operative aggregation of secretory proteins may occur, CgB the first to undergo conformational change in response to increased pH and Ca^{++} binds the *cis*-Golgi membrane and aggregates with itself and subsequently CgA. CgA aggregation and tetramerisation may allow interaction with a large number of secretory proteins within the TGN lumen. Binding of Ca^{++} by CgA exposes hydrophobic regions increasing the likelihood of membrane interactions. 40mM $[Ca^{++}]_i$ within the secretory vesicle causes CgA binding to the second intraluminal loop of the second messenger receptor IP_3-R. Conformational changes induced by IP_3 binding to the IP_3-R may be transmitted to CgA. IP_3-R and CgA interactions may facilitate mobilisation of Ca^{++} from the vesicle lumen in turn causing conformational changes in CgB which may aid vesicle collapse during the exocytotic event (Yoo & Albanesi, 1990b). Although the putative role of CPE as a sorting receptor for CgA has recently been disproven (Normant & Loh, 1998) it is possible that a similar granin-specific mechanism may exist. This is suggested by the misrouting of CgB in which the putative conformational sorting signal had been disrupted (Kromer *et al.*, 1998). Interestingly this study also demonstrated correct sorting of CgB when the intact molecule was coexpressed suggesting co-operative sorting presumably mediated by aggregation. The colocalisation of SgII in the smallest category of gonadotrophin granules (Watanabe *et*

al., 1991) which appear to be preferentially released during the LH surge (Currie & McNeilly, 1995; Thomas *et al.*, 1998) may indicate a role during the final stages of membrane fusion.

How this proposed scenario fits into the popular model of exocytotic tethering, docking and fusion (Burgoyne & Morgan, 1993) (see figure 1.7.4a) is unclear but may be addressed during the course of this thesis.

1.6.6 Granin-derived Peptides

Although a considerable number of studies have been undertaken elucidating the numerous cleavage products of granins and their various wide-ranging roles (for a recent review see Fischer-Colbrie, 1996), only a brief summary of the current understanding will be given in the following section. Figure 1.6.1a summarises the diversity of peptides produced from CgA, CgB and SgII.

CgA has the greatest number of derived peptides within the granin family. In the adrenal medulla 50% of CgA molecules undergo proteolysis whereas in the anterior pituitary a lower percentage is processed. The reasons for this difference remain unclear (Barbosa *et al.*, 1991), but may relate to post-translational processing. Pancreastatin corresponds to residues 240-288 in the carboxy-terminal region of porcine CgA (Tatemoto *et al.*, 1986; Iacangelo *et al.*, 1988). Pancreastatin was initially demonstrated as inhibiting glucose-stimulated insulin release (Tatemoto *et al.*, 1986), and subsequently for amylase release from the exocrine pancreas (Funakoshi *et al.*, 1988) and gastric acid from parietal cells (Lewis *et al.*, 1988). Stimulatory effects of pancreastatin have been reported for glucagon and L-arginine-stimulated insulin release (Ishizuka *et al.*, 1991). Further detail concerning inhibition of parathyroid hormone (PTH) and CgA secretion from the parathyroid gland (Fasciotto *et al.*, 1989) has been elucidated with regard to transcriptional inactivation and decrease of mRNA stability. Pancreastatin at concentrations of 10^{-9} to 10^{-7}M decreased CgA and PTH secretion by 75% and 93% after only four hours and mRNA abundance decreased after 12 hours by 87% and 80%. Half-lives of CgA and PTH mRNAs were reduced from 33hrs to 18hrs and from 38hrs to 20hrs, respectively (Zhang *et al.*, 1994). Other peptides with similar roles include parastatin

(347-419aa) and β-granin (1-113aa with phosphorylated Ser^{81}) (Strub *et al.*, 1997).

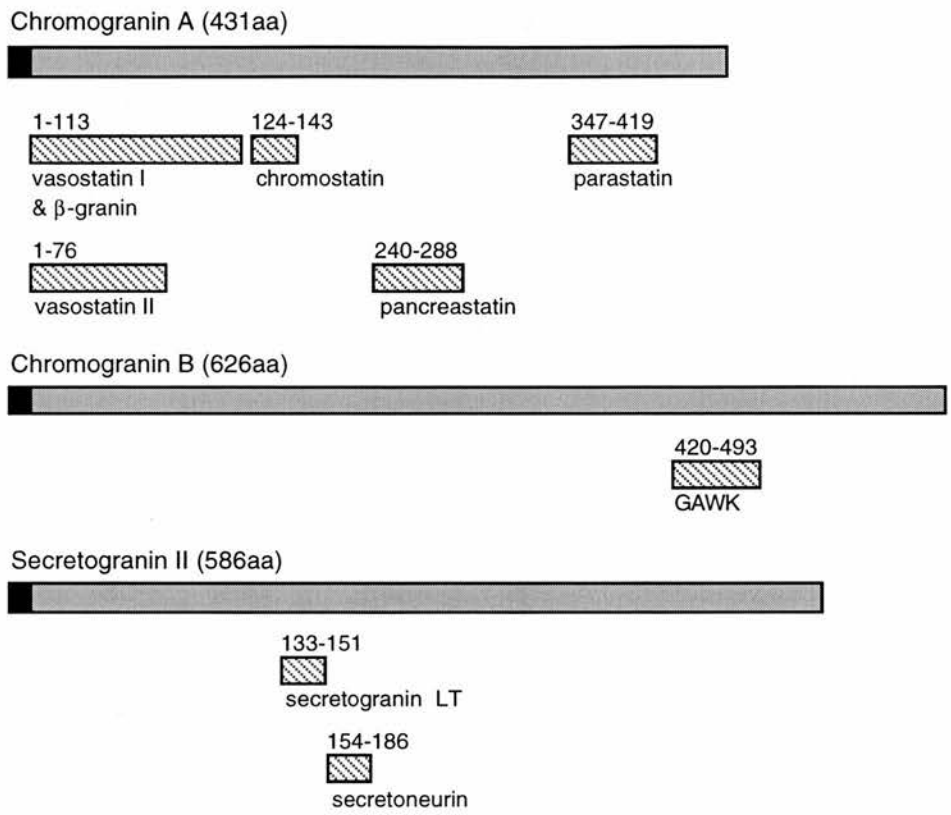

Figure 1.6.6a: Naturally occurring granin-derived peptides.

Although CgA is the shortest of the granins shown here, it has the greatest number of derived peptides. The vasostatins (I & II) have been shown to inhibit endothelin-1. Chromostatin inhibits catecholamine release whereas pancreastatin, parastatin and β-granin reduce parathyroid and CgA secretion. β-granin is similar to vasostatin except that it is phosphorylated at Ser^{81}. GAWK is the only peptide derived from CgB and has yet to be assigned a role. Secretogranin LT and secretoneurin are both secretagogues for dopamine, dynorphin B and gamma-aminobutyric acid. The lengths of the undigested granins shown refer to bovine forms (aa=amino acids). The peptide sequences are shown amino-terminus to carboxy-terminus with the filled (black) area corresponding to the signal peptide.

Other naturally occurring CgA-derived peptides include chromostatin (124-143aa) which may inhibit the secretion of catecholamines from chromaffin cells (Galindo *et al.*, 1991) and vasostatins I (1-76aa) and II (1-113aa) which inhibits the action of endothelin-1 preventing vascular tension (Aardal & Helle, 1992). Other CgA fragments have been investigated for roles which range from pro-adhesion (Gasparri *et al.*, 1997) to antibacterial activity (Strub *et al.*, 1996).
An intracellular role of CgA proteolysis as a competitive inhibitor of the prohormone convertase PC2 has been suggested (Seidah *et al.*, 1987), and it is conceivable that a similar role exists for other granins. Indeed SgV (7B2) has been shown to specifically interact with PC2 in a regulatory manner (Braks & Martens, 1994).

The main peptide derived from CgB is GAWK (420-493aa) and although its role has yet to be determined it is used as a marker for pancreatic islet tumours and pheochromocytoma (Sekiya *et al.*, 1989). Similarly use of the monoclonal antisera HISL-19 which detects SgIV has been used in diagnosis of medullary thyroid carcinoma (Neuhold & Ullrich, 1993).

Secretoneurin is a 33aa peptide derived from SgII (154-186aa) which has been show to stimulate dopamine release from rat striatal slices (Saria *et al.*, 1993). Effects of secretoneurin and secretogranin LT (133-151aa) on secretion of dynorphin B, dopamine, gamma-aminobutyric acid, glutamate and aspartate from the rat *substantia nigra* and *neostriatum* has revealed specificities and dose-dependent relationships of these peptides (You *et al.*, 1996). Other SgII-derived peptides have yet to be assigned biological functions although their presence within secretory granules provides a useful marker for enzymatic activity within the dynamic granule lumen (Muller & Tougard, 1995; Urbe *et al.*, 1997).

Granin processing within the distinct secretory pathways of gonadotrophs has yet to be investigated in detail. The interaction of granin-derived peptides with other granule contents may have distinct regulatory consequences taken in light of the compelling evidence for inhibition of secretion in a variety of cell lines.

1.7.1 *In vitro* Studies of Neuroendocrine Secretion

Studies using the recently isolated $L\beta T_2$ cell line have focused on exocytosis (see later) and hormonal priming. This second area of gonadotrophin research has not been possible until development of this novel cell line and thus stands alone within this section of the literature review. $L\beta T_2$ cells treated with four 10nM GnRH pulses per day over four days secreted progressively more LH each day. The greatest rise in LH release was apparent after the first GnRH pulse each day with the subsequent pulses eliciting a much smaller response. This observation suggests that LH abundance intracellularly is depleted after the first pulse each day and requires an extended period of non-stimulation to replenish stores. GnRH-R and LHβ gene expression were also altered by GnRH treatment. GnRH-R mRNA abundance was significantly raised after 3 days of treatment with 0.2nM E_2 and 20nM DEX in the absence of GnRH pulses and further increased by a daily GnRH regime. LHβ mRNA was unchanged by steroids alone but rose significantly in response to GnRH treatment. αGSU mRNA exhibited no significant change after 3 days of treatment with either steroids alone or in conjunction with GnRH (Turgeon *et al.*, 1996).

The remainder of this section will be divided into three stages; sorting, granulogenesis and exocytosis.

1.7.2 Protein Sorting

Sorting is believed to occur within the ER and Golgi apparatus prior to transport towards the cell surface although definitive proof for pituitary gonadotrophins has yet to be reported. Using CHO and HepG2 cells Weiland *et al* demonstrated that the constitutive pathway is the default route for protein traffic and requires no specialised signal (Weiland *et al.*, 1987). Expression of both LH subunits in transfected CHO cells similarly did not lead to storage via a regulated pathway expressing only unglycosylated hormone (Bielinska *et al.*, 1994). This is despite recent evidence which suggests that CHO cells are capable of regulated secretion (Chavez *et al.*, 1996). Expression of the same constructs in the rat somatomammotroph-derived GH_3 cell line led to storage of LH in an intracellular pool which was releasable by stimulation with FSK or KCl. Similar expression of hCG led to storage within the same pool although with less efficiency. The αGSU

expressed alone was released via the constitutive pathway (Bielinska *et al.*, 1994). Comparison of LH and FSH secretion from transfected GH_3 cells revealed differential sorting of the two hormones *in vitro*. Basal secretion of LH was undetectable by SDS-PAGE whereas FSH was readily observed. Stimulation of the transfected cells with either KCl or FSK caused release of both hormones. However the magnitude of secretagogue-stimulated release of FSH was far smaller than that of LH indicating more efficient storage of LH than FSH (Muyan *et al.*, 1994). It may be noted that GH_3 cells express SgII (Janovick *et al.*, 1995) although the expression of other proteins involved in the regulated pathway is assumed by the appearance of storage granules. Nevertheless the presence of at least SgII further implicates the granin in storage and release of LH.

The aggregative properties of granins and their colocalisation with regulated secretory proteins has led to speculation that they are sorting factors. However, differential sorting of PRL and GH in bovine somatomammotrophs may occur by preferential self-aggregation (Hashimoto *et al.*, 1987) whereas LH only aggregates in the presence of granins *in vitro* (Colomer *et al.*, 1995). The aggregative characteristics of LH in the presence of granins and its storage in granin-expressing GH_3 cells is compelling evidence for a role of granins in sorting of gonadotrophins to a regulated pathway.

1.7.3 Granulogenesis

Movement of vesicles by tubulin after release from the TGN was initially suggested by their interaction in a cell-free system (Sherline *et al.*, 1977) More recently use of nocodazole which inhibits tubulin polymerisation has demonstrated the relationship during granule maturation in PC-12 cells (Tooze *et al.*, 1991). Secretion of CgB expressed as a fusion protein with the green fluorescent protein (GFP) has been shown to occur via a constitutive pathway in stably transfected Vero cells. Inhibition of microtubule polymerisation using nocodazole reduced the rate of secretion for the fusion protein by approximately 50%. Furthermore real-time visualisation of nocodazole-treated cells showed a significantly reduced motility of secretory vesicles in comparison to untreated cells (Wacker *et al.*, 1997).

The proteolytic processing of SgII in PC-12 cells transfected with PC2 expressing plasmids, has been used as an indicator for intragranular pH. The acidity of granules was shown to increase from pH6.3 in immature secretory granules (ISGs) which is equivalent to that of the TGN, to pH5.0-5.5 in mature granules (Urbe *et al.*, 1997). In bovine primary cultures of chromaffin cells, granules have been observed to swell when stimulated by nicotine or extracellular K^+. Granule diameters of 234nm prior to stimulation increase to approximately 275nm and this increase occurs prior to fusion with the plasma membrane. Ammonium chloride, which raises intragranular pH, inhibits 50% of catecholamine secretion by preventing granule swelling. Ammonium chloride treated chromaffin cells contain large granules which juxtapose to the PM but do not fuse efficiently (Ornberg *et al.*, 1995). The observation of granule swelling prior to exocytosis from gonadotrophs has not been reported, indeed a trend appears of smaller granules being proximal to the PM (Watanabe *et al.*, 1991; Currie & McNeilly, 1995). However granule swelling during regulated secretion of gonadotrophins may now be investigated by similar ammonium chloride treatment of the $L\beta T_2$ cell line.

Total granules in a single chromaffin cell number approximately 20000 and out of this population only about 1000 are within 10nm of the PM (Steyer *et al.*, 1997). The role of actin as a barrier between the stored granules and the PM has been investigated in cultured lactotrophs from normal female rats. F-actin which is localised at the periphery of the lactotroph becomes disassembled at foci after treatment with secretagogues such as forskolin (FSK) or TRH. Inhibition of this disassembly by exposure to as little as 50nM dopamine reduces PRL secretion (Carbajal & Vitale, 1997). The myosin motor and Rho GTPase activating protein Myr5 has been shown to interact directly with actin filaments (Mooseker & Cheney, 1995). Scinderin contains two actin- and two PIP_2-binding sites and causes rearrangement of peripheral actin filaments in chromaffin cells. Peptides designed to bind these sites blocked Ca^{++}-induced noradrenaline exocytosis in a dose-dependent manner (Zhang *et al.*, 1996). Myr5 and scinderin may represent an excellent candidates for co-ordination of different second messenger signalling

pathways with actin rearrangements. Following disassembly of a region of the cortical actin network, the recruited granules move towards the PM. F-actin barriers and disassembly may play important roles in control of regulated gonadotrophin release. Evidence for the role of myosin motors in the movement of granules towards the PM has recently been reported by the inhibition of LH release in wortmannin-treated rat gonadotrophs. Both cultured rat pituitary gonadotrophs and αT3-1 cells were found to contain the 20kDa phosphorylation-dependent protein non-muscle myosin IIB light chain. These results strongly suggest that this myosin motor plays a role in granule movement during the stages immediately prior to exocytosis (Rao *et al.*, 1997).

1.7.4 Exocytosis

Much of the work on neuroendocrine exocytosis has involved the use of primary cultures of bovine chromaffin cells and the adrenal medulla-derived PC-12 cell line. Three types of experimental approach have been used to study proteins involved in exocytosis. Microinjection of proteins into cells during patch-clamp analyses where membrane capacitance readings may be made which relate to individual fusion events (Burgoyne & Handel, 1994). Selectively porated cells may be studied by addition of neurotoxins and implicated proteins prior to stimulation of exocytosis with Ca^{++} (Baker & Knight, 1978). Transfection of a marker either transiently or stably allows the effects of treatments with specific neurotoxins such as tetanus toxin or secretion of co-transfected gene products to be quantified (Chung *et al.*, 1995).

Detailed knowledge concerning the temporal assembly of a fusion complex has been gained using selectively porated chromaffin cells (Baker & Knight, 1978). Leakage of factors involved in Ca^{++}-triggered exocytosis prevents repeated assays but allows reconstitution of the necessary factors individually and dissection of exocytotic processes (Sarafian *et al.*, 1987). In chromaffin cells several key molecules have been identified which have a role in intracellular membrane interactions. Soluble proteins include *N*-ethylmaleimide sensitive fusion protein (NSF) (Block *et al.*, 1988) and the soluble NSF attachment proteins (SNAPs), α-SNAP and β-SNAP (Clary *et al.*, 1990). SNAP receptors (SNAREs) are normally

membrane-bound and include vesicle-associated membrane protein (VAMP), synaptosome-associated protein of 25kDa (SNAP-25) and syntaxin 1 (Sollner *et al.*, 1993). Burgoyne and Morgan (1998) have proposed a model for exocytosis based on use of porated chromaffin cells (figure 1.7.4a). The key element in this model is that it allows for the separation of proximal granules into primed and ATP-dependent pools. Primed granules are not only in close proximity with the PM but are also docked requiring only a Ca^{++} flux to trigger ATP-independent fusion (Holz *et al.*, 1989).

Future studies, particularly using mammalian and yeast two-hybrid systems, may reveal key motifs involved in fusion complex formation. More traditional biophysical studies measure changes in membrane capacitance (ΔC_m). Increases in ΔC_m reflect an increase in cell surface area as a consequence of lipid incorporation into the PM during vesicle fusion. Reductions in ΔC_m indicate endocytotic episodes reducing the cell surface area to its pre-exocytotic value. Applying this patch-clamp methodology Tse *et al* (1993) have investigated exocytosis from cultured gonadotrophs. The male rat gonadotroph contains approximately 10 000 granules with a 200nm diameter of which 600 to 1000 are located within 200nm of the PM. Each granule contributes 1.3 femtoFerands (fF) to the PM capacitance, a 10 second exposure of GnRH caused a ΔC_m of approximately 700fF which relates to an increase in cell surface area of 10% and the release of 540 granules. The involvement of $[Ca^{++}]_i$ during exocytosis was demonstrated by the absence of ΔC_m in the presence of the calcium chelator EGTA. The source of calcium involved in triggering exocytotic fusion was demonstrated as being intracellular by the observation of increased $[Ca^{++}]_i$ after GnRH stimulation in calcium-free media and secondly the lack of a comparable increase in cumulative ΔC_m in the presence of extracellular calcium (Tse *et al.*, 1993). Recent studies using αT3-1 cells and video imaging of $[Ca^{++}]_i$ using calcium fluorophores has demonstrated the importance of the biphasic $[Ca^{++}]_i$ flux. In accordance with previous findings by Tse *et al* (1993) the first spike of $[Ca^{++}]_i$ from intracellular stores was shown to cause exocytosis. Replenishment of these stores was shown to require the action of voltage-gated channels and extracellular calcium (McArdle *et al.*, 1996). Voltage-gated release of

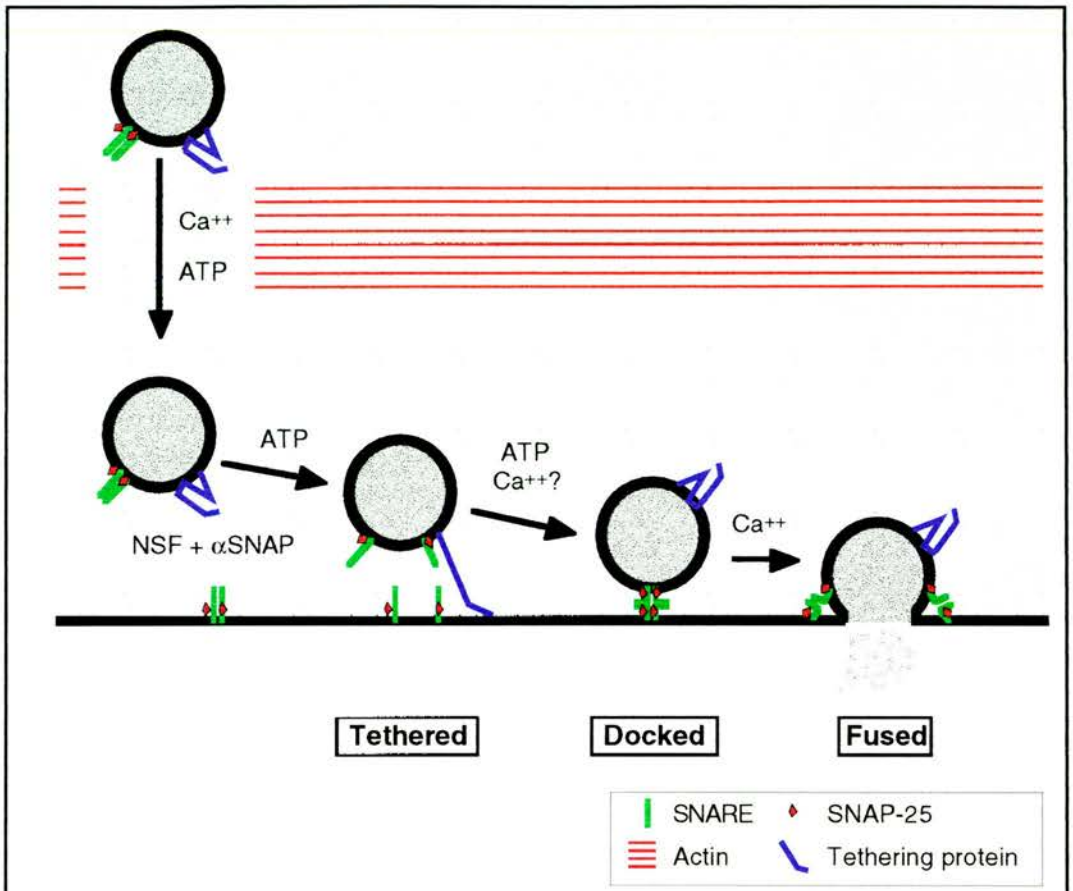

Figure 1.7.4a: A model for neuroendocrine exocytosis (adapted from Burgoyne & Morgan 1998 and Robinson & Martin 1998).

Initial segregation of the vesicles from the plasma membrane is achieved by the actin barrier which may be dissolved in a calcium and ATP-dependent manner by as yet undetermined proteins. This stage may be referred to as a recruitment of secretory vesicles. *N*-ethylmaleimide-sensitive factor (NSF) complexed with soluble NSF attachment protein α (αSNAP) may facilitate changes in SNAP receptor (SNARE eg. syntaxin) structure in an ATP-dependent process which permits subsequent membrane interactions. The first stage of the exocytotic event in this model is tethering which may be mediated by as yet undetermined cytoskeletal elements. Docking of vesicles involves interaction of SNAREs on each membrane and may induce conformational change. In this fully docked state fusion of the primed vesicles is independent of ATP requiring only a calcium flux. A further role of NSF and αSNAP may also exist after exocytosis in the recycling of vesicle membrane proteins to the ER and TGN.

calcium failed to trigger exocytosis despite a rise in $[Ca^{++}]_i$ equivalent to that which causes exocytosis in chromaffin cells (Augustine & Neher, 1992). Speculation that calcium released from voltage-gated stores may not be in close proximity or is segregated from the area at which vesicle fusion occurs in gonadotrophs explaining the lack of response exhibited by the pituitary cell (Tse *et al.*, 1993). Another possibility may be that chromaffin granules have voltage-gated channels whereas gonadotroph granules do not.

Certainly chromaffin granules have been demonstrated to contain the IP_3-R/Ca++ channel which interacts with CgA (Yoo & Lewis, 1994) but as yet the same has not been demonstrated in gonadotrophs.

GnRH-stimulated exocytosis has been demonstrated to be dependent on the GTP-binding Rab3B protein in cultured rat gonadotrophs. Antisense oligonucleotides (AS) directed against Rab3B reduced the percentage of cells expressing the protein from 94.6±1.7 to 70.8±2.8%. In Rab3B-negative cells exocytosis (measured using the fluorophore TMA-DPH) was reduced to less than 20% of control cells without adversely affecting LH expression or $[Ca^{++}]_i$. RIA of secreted LH and FSH from AS-treated populations demonstrated an approximate 20% decrease in basal and GnRH-stimulated release of both gonadotrophins (Tasaka *et al.*, 1998). Although the exact mechanism by which Rab3B mediates GnRH-induced and basal exocytotic events has yet to be determined, these data clearly shows that Rab3B is crucial for secretion of each pituitary gonadotrophin via constitutive and regulated pathways.

Exocytosis in the $L\beta T_2$ cell line has been limited so far to a single report. In this study the exocytotic response of single cells was measured using ΔC_m . The effect of E_2 and DEX on LH release was found to be critical. Although cells treated with GnRH in the absence of 0.2nM E_2 and 20nM DEX did elicit a rise in $[Ca^{++}]_i$, a significantly smaller ΔC_m was observed than in E_2/DEX-treated cells. The authors suggest that this data represents mediation of the exocytotic response by E_2 through sensitisation of the fusion machinery (Thomas *et al.*, 1996). Future studies using this cell line may elucidate the role of actin, exocytotic machinery and granins within this model.

1.8 Summary

This chapter has described the oestrus cycle of the ewe and described the major differences to those of rodents illustrating the physiological importance of gonadotrophins in reproduction. Clearly LH and FSH fulfil specific but related roles which is reflected in their relative abundancies. Control of their expression in gonadotrophs is complex and represents co-ordinate regulation by the hypothalamic decapeptide GnRH, steroids and gonadal peptides within the hypothalamo-pituitary-gonadal axis. Posttranslational control of LH and FSH expression also influences bioactivity and release. Intracellularly this is manifest by the appearance of small (<200nm) electron-dense secretory vesicles containing LH and SgII. These represent the regulated secretory pathway in which LH is stored until release in massive quantities during the LH surge through which its biological role of inducing ovulation may be achieved. The growth and selection of follicles does not require large releases of FSH from the pituitary therefore secretion occurs predominantly via the constitutive pathway. Posttranslational sorting of gonadotrophins to the different secretory pathways may be mediated by Ca^{++}-binding aggregative proteins known as granins. Colocalisation of specific granins during distinct stages of gonadotrophin granulogenesis as well as induction of LH aggregation *in vitro* implicates them in this process. CgA and CgB appear to be involved in the aggregation and sorting of gonadotrophins with SgII perhaps fulfilling a role during the latter stages of secretion. A specific role for the abundant granin-derived peptides has yet to be assigned within the gonadotroph. Regulation of granin expression may involve several intracellular signalling pathways as suggested by the multiple transcription factor binding elements within their promoters. CgA in particular appears to be upregulated in response to testosterone. Other biologically relevant responses of granin expression have yet to be determined *in vivo*. Exocytosis from gonadotrophs is triggered by $[Ca^{++}]_i$ fluxes and appears to involve conserved molecular machinery expressed in other neuroendocrine tissues. SNAREs have been implicated by their presence in gonadotrophs *in vivo* yet unlike Rab3B, their functionality remains to be demonstrated.

Clearly studies of gonadotrophin secretion have, and continue to be undertaken, using widely different approaches both *in vivo* and *in vitro*. It is also apparent that through these diverse studies physiologically relevant molecular data regarding the enigma of differential gonadotrophin secretion is being obtained.

1.9 Scope of this Thesis

These studies aim to investigate the mechanisms involved in the intracellular processing of pituitary gonadotrophins with particular focus on the putative roles of CgA, CgB and SgII in gonadotrophin sorting and aggregation. In order to carry out these investigations a predominantly *in vitro* approach will be complemented by *in vivo* studies using normal and transgenic mice.

Gonadotrophin-secreting cell lines are limited with only the placentally-derived JEG3 and recently characterised pituitary-derived $L\beta T_2$ cell line currently available. The human JEG3 cell line secretes CG presumably via a constitutive pathway (Kohler & Bridson, 1971) whereas murine $L\beta T_2$ cells store and secrete LH under control of GnRH (Thomas *et al.*, 1996). Use of these relatively complex cell lines will be balanced by studies using the CHO cell line (Puck *et al.*, 1958) which is of non-neuroendocrine origin. An immediate aim of this thesis is to develop an *in vitro* expression system that will permit the study of gonadotrophins and granins within these three cell lines. Assessment of the effects of granins on gonadotrophin overexpression in each of these cell lines will be carried out using conventional biochemical techniques in conjunction with indirect immunofluorescence and fluorophore-fusion protein expression.

1.10 Layout of this Thesis

The following chapter will detail materials used and general methodology employed throughout this thesis. Appendices I and II contain details regarding buffers and suppliers respectively.

The five main experimental chapters follow chapter two. The first of these details design and isolation of specific mammalian expression constructs used in the subsequent three chapters. Chapters four, five and six contain studies carried out using the JEG3, CHO and $L\beta T_2$ cell lines respectively. The

final experimental chapter focuses on investigations carried out on normal and transgenic murine gonadotrophs *in vivo*. After the experimental chapters a general discussion will follow in which the main findings of this thesis will be developed into a model of gonadotrophin secretion. Questions raised by this model will be used to propose possible approaches for future studies of gonadotrophin secretion.

Chapter Two

General Materials and Methods

2.1 Introduction

This chapter details routine methods used to manipulate DNA, culture various mammalian cell lines as well as more general laboratory procedures. The composition of routinely used buffers can be found in Appendix I and a complete list of suppliers is contained in Appendix II.

Control of substances hazardous to health (COSHH) safety guidelines for the handling of hazardous chemicals and biohazardous materials were followed. Where indicated this required the use of fume hoods, sharps bins, special areas for use of radioisotopes and a Level II biocontainment cabinet. Operator protection often required the use of one or more of the following; laboratory coats, latex gloves, protective eyewear and a lead apron.

2.2 General Materials

General chemicals were purchased from Merck-BDH (UK) and were AnalaR grade for use in molecular biology techniques. Water was double distilled and deionised prior to autoclaving for use in molecular biology techniques. Autoclaving of solutions was not carried out for less stringent methods such as immunocytochemistry.

The tables below contain details of specialised materials used and are grouped into general areas of methodology.

Table 2.2a: Bacterial strains and culture materials.

Bacterial Strains & Materials	**Genotype**	**Supplier**
Subcloning and MAX Efficiency™ Competent *E.coli* DH5α cells	$F^- \lambda^- \phi 80d$*lacZ*Δ*M15* Δ(*lacZYA*-*argF*)U169 *deoR recA1 endA1 hsdR17* (r_K^-, m_K^+) *phoA supE44 thi-1 gyrA96 relA1*	Gibco BRL [UK]

JM109 cells	*endA1 recA1 gyrA96 thi hsdR17* (r_K^-, m_K^+) *relA1 supE44* Δ(*lac-proAB*) [F' *proAB lacI*^{q} *ZΔM15*]	Promega [UK]
Epicurian Coli SURE2™ *E.coli* cells	F^- λ$^-$ e14$^-$(McrA$^-$) Δ(*mcrCB*$^-$ *hsdSMR*$^-$*mrr*)*171 endA1 supE44 thi-1 gyrA96 relA1 lac recB recJ sbcC umuC*: : Tn*5*(Kan^R) *uvrC* [F' *proAB lacI*^{q} *ZΔM15* Tn*10*(Tet^R) Amy Cam^R]	Stratagene [UK]
Luria Bertani (LB) Broth & Agar		Anachem [UK]
Kanamycin		Sigma-Aldrich [UK]
Ampicillin		Sigma-Aldrich [UK]

Table 2.2b: Sources of Clones and Vectors.

Genetic Material	**Size of Plasmid (insert)**	**Source**
pcDNA3.1/His/lacZ	8.6kb	Invitrogen[NL]
pBluescript KS+	2.96kb	Stratagene [USA]
pcDNA3	5.45kb	Clontech [UK]
pEGFP-C1 & pEGFP-C3 carboxy-terminal fusion vectors	4.7kb	Clontech [UK]
full length ovine αGSU cDNA in pSP72	3.18kb (717bp)	T.E.Adams [Aus]
poLHβ (pGEM3 with oLHβ cDNA)	2.87kb (520bp)	B.Miller [USA]
poLHβg	7.23kb (1.78kb)	P.Brown [MRC, UK]

full-length oFSHβ cDNA in pSP72	4.05kb (1.59kb)	T.E.Adams [Aus]
oFSHβ genomic clone with HSV-IE polyA in pBluescript KS+	5.81kb (2.85kb)	P.Brown [MRC, UK]
pHCGA-4 (pGEM3 with full length human chromogranin A cDNA)	4.6kb (1.8kb)	ATCC [USA]
pbChrB73 (pcDV-1 with full length bovine chromogranin B cDNA)	5.58kb (2.36kb)	R.Fischer-Colbrie [A]
pbSgII61 (pcDV-1 with full length bovine secretogranin II cDNA)	5.58kb (2.36kb)	R.Fischer-Colbrie [A]

Table 2.2c: Molecular Biology Kits

Kits	**Supplier**
Hybaid Recovery (DNA purification kit II)	Hybaid [UK]
MoBio UltraCleanTM MiniPrep Kit	CamBio [UK]
Qiagen Endofree™ Plasmid Kit	Qiagen [UK]
Qiagen Gel Purification Kit	Qiagen [UK]
Titan™ RT-PCR kit	Boehringer Mannheim [UK]
Wizard Plus™ MiniPrep Kit	Promega [UK]
Ready-to-Go™ ligase tubes	Pharmacia [UK]
Spin-X tubes	CoStar [UK]
MAIAclone hCG immunoradiometric (IRMA) assay	Serono [F]
ECL/ECF Western blotting kits	Amersham [UK]
*redi*PRIME™ DNA labelling system	Amersham Life Sciences [UK]

Table 2.2d: Mammalian Cell lines and Materials.

Mammalian Cell Culture	**Source**
Chinese Hamster Ovary (CHO) cell line (ECACC number 85050302)	ECACC [UK]
CHO-K1 cell line (ECACC number 85051005)	ECACC [UK]

JEG3 human choriocarcinoma cell line (ECACC number 92120308)	ECACC [UK]
$L\beta T_2$ cell line	P.Mellon [USA]
Dulbecco's Phosphate Buffered Saline (DPBS)	Sigma-Aldrich [UK]
Dulbecco's Modification of Eagle's Medium (DMEM)	Sigma-Aldrich [UK]
Pipette pump	Jencons [UK]
Inverted Light Microscope	Olympus [UK]
Soldering Iron	Merck (BDH) [UK]
Opti-MEM	Gibco BRL [UK]
Penicillin/Streptomycin Solution (stabilised)	Sigma-Aldrich [UK]
G418 solution	Sigma-Aldrich [UK]
Trypsin solution	Gibco BRL [UK]
Gonadotrophin Releasing Hormone (GnRH)	Sigma-Aldrich [UK]
Heat inactivated Fetal Calf Serum (FCS)	Sigma-Aldrich [UK] and HyClone [USA]
DOTAP	Boehringer Mannheim [UK]
Clonfectin™	Clontech [USA]
PerFect™ lipid system	Invitrogen [NL]
Tfx10	Promega [UK]
Multiwell tissue culture plates (48, 24, 12 & 6 well varieties)	CoStar [UK]
NUNC 1.8ml Cryotubes	Gibco BRL [UK]
Tissue Culture Flasks ($162cm^2$, $75cm^2$ & $25cm^2$ sizes)	CoStar [UK]

Table 2.2e: Primary Antisera; Targets and Source.

Primary Antisera Target/Designation	**Raised in**	**Source**
αGSU (R20)	rabbit	A.S. McNeilly [MRC, CRB]

human Chorionic Gonadotrophin β-subunit (clone PC-2)	mouse	Sigma-Aldrich [UK]
human Chromogranin A (clone LK2H10)	mouse	Serotec [UK]
bovine Chromogranin A	rabbit	R. Fischer-Colbrie [Austria]
bovine Chromogranin B	rabbit	R. Fischer-Colbrie [Austria]
human FSH (M91)	rabbit	A.S. McNeilly [MRC, CRB]
bovine LH (clone 518B7)	mouse	J. Roser [USA]
human Secretogranin II (clone C-19)	mouse	Santa Cruz Biotechnology [D]
α-Tubulin-FITC conjugate (clone DM 1A)	mouse	Sigma-Aldrich [UK]

Table 2.2f: Immunocytochemistry

Immunocytochemistry	**Supplier**
Bodipy 630/650	Molecular Probes [NL]
Citifluor	UKC [UK]
Goat anti-rabbit FITC conjugate	Sigma-Aldrich [UK]
Goat anti-rabbit TRITC conjugate	Sigma-Aldrich [UK]
Goat anti-mouse FITC conjugate	Sigma-Aldrich [UK]
Goat anti-mouse TRITC conjugate	Sigma-Aldrich [UK]
Propidium Iodide	Sigma-Aldrich [UK]
Normal Rabbit Serum	SAPU [UK]
Donkey anti-Rabbit Serum	SAPU [UK]

Table 2.2g: Specialised Computer Software.

Specialised Computer Software	**Source**
AssayZap	P.Taylor [MRC, CRB]
Adobe Photoshop 5	MacWarehouse [UK]
LSM 510	Zeiss [UK]

GCG	MRC Human Genome Mapping Project (HGMP) Internet Resource
GeneJockeyII	P.Taylor [MRC, UK]
ImageQuant	Molecular Dynamics [UK]
Microsoft Excel version 4.0	MacWarehouse [UK]
GB-Stat version 6.5	Dynamic Microsystems [USA]
StatView version 4.02	MacWarehouse [UK]

2.3 Molecular Biology

2.3.1 Restriction Endonuclease Digestion

Restriction enzymes and buffers were obtained from Boehringer Mannheim (UK), MBI Fermentas (UK) or Promega (UK) and were used in accordance with the manufacturers guidelines. Enzyme reactions contained 2-3 units of enzyme per µg of DNA, the volume of enzyme added did not exceed 10% of the total reaction volume and the reaction was mixed by gentle flicking before incubation.

2.3.2 Agarose Gel Electrophoresis

Separation of DNA molecules on agarose (Agarose MP; Boehringer Mannheim, UK) gels allowed visual confirmation of DNA size and concentration. Gel concentrations varied from 0.8% to 2% depending on the size of the molecules to be separated. Low concentration gels, used for separating plasmid DNA, were buffered in TAE (40mM Tris acetate, 1mM EDTA pH8) whereas TBE buffer (45mM Tris borate, 1mM EDTA pH8) was used for high resolution of DNA fragments typically less than 500bp in length. Ethidium bromide (Sigma-Aldrich, UK) was added to both the gel and the running buffer at a final concentration of 0.5µg/ml. When using TAE buffered gels, samples were loaded with 10x Blue loading buffer (see Appendix I). 6x OJ loading buffer (see Appendix I) was used for higher concentration TBE buffered gels. *Hin*dIII or *Hin*dIII/*Eco*RI restricted Lambda bacteriophage genome was used as molecular size markers for comparison with restriction digests. Estimation of DNA concentration was also carried out by comparison with these markers. Products from reverse

transcriptase polymerase chain reactions (RT-PCRs) were compared with 100bp molecular size markers (Promega, UK). Voltage applied to the gel varied from 1.5-2.0mV/cm for overnight applications to 8-10mV/cm for 30-90 minutes dependent on the size of fragments to be resolved. Visualisation of DNA in the presence of the fluorescent intercalating agent ethidium bromide was undertaken using an ultraviolet transilluminator (302nm wavelength). Photographs were taken using a Polaroid 667 camera.

2.3.3 Extraction of DNA from Agarose Gel

Removal of contaminating polysaccharides and ethidium bromide from DNA separated in agarose gels was necessary because these components inhibit the activity of enzymes used in downstream applications. Three methods were used to extract DNA fragments separated by agarose gel electrophoresis; Spin-X tubes (CoStar, UK) Hybaid Recovery II (Hybaid, UK) and Qiagen Gel Purification kit (Qiagen, UK). All kits were used in accordance with the manufacturers guidelines.

2.3.4 Phenol Chloroform Extraction

Phenol chloroform extraction separates nucleic acids from proteins and was used for purification of DNA after enzymatic treatment. Low volume samples were increased to 500µl with TE buffer (10mM TrisHCl 1mM EDTA, pH8) to minimise sample loss in subsequent manipulations. During all transfers of the aqueous phase careful attention was made to avoid contact with the interphase to prevent protein contamination. It should also be noted that handling of phenol, like all hazardous chemicals, was in accordance with COSHH guidelines.

An equal volume of TE-saturated phenol was added, then the sample was vigorously vortexed followed by centrifugation at 13000 rpm for 5 minutes in an Heraeus Sepatech Biofuge 13. The upper aqueous phase was then transferred to a separate microcentrifuge tube. Subsequently a half volume of phenol was applied to the transferred aqueous phase and again vortexed. A half volume of chloroform was then added to the mixture and vortexed to remove phenol from the nucleic acid fraction. Centrifugation was repeated and the aqueous phase transferred. To completely remove

phenol from the nucleic acid fraction chloroform was added in an equal volume. After a 2 minute centrifugation and transfer of the supernatant the purified DNA-containing solution was returned to ice where precipitation and concentration followed as detailed below.

2.3.5 Precipitation of Nucleic Acids

Precipitation of nucleic acids followed the method of Shapiro (Shapiro, 1981). For this application 2 volumes of absolute ethanol and 0.3M sodium acetate pH 5.2 were used. The precipitating sample was incubated at -20°C for at least 30 minutes before it was centrifuged for 15 minutes at 13000rpm and 4°C in an Heraeus Sepatech Biofuge 22R with HFA 22.2 rotor. The pellet was then washed to remove any residual salts. This was achieved by vortexing in 70% ethanol followed by centrifugation for 5 minutes. This step was repeated before the pellet was air-dried and resuspended in an appropriate volume of TE buffer. Preparations were stored at -20°C.

2.3.6 Dephosphorylation of Linear DNA

In order to form a phosphodiester bond between two bases of the same DNA strand DNA ligase requires adenosine triphosphate (ATP) and a 5'-PO_4^- and a 3'-OH group on each DNA strand (Legerski & Robberson, 1985). Removal of the 5'-PO_4^- groups from linearised plasmids prevents religation and formation of a circular DNA structure. Linear DNA strands are poorly transformed into competent bacteria in comparison to covalently-closed circular DNA structures. These factors are exploited in ligation of DNA sequences with compatible 5' and 3' ends.

Removal of 5'-PO_4^- groups was initially undertaken using calf intestinal phosphatase (CIP; Boehringer Mannheim, UK) however the recently available shrimp alkaline phosphatase (SAP; Boehringer Mannheim, UK) was subsequently used. Both enzymes are efficient dephosphorylation enzymes but SAP has the advantage of being more easily heat inactivated. Residual CIP activity is often present after incubation at 65°C thus preventing insert ligation due to continued dephosphorylation.

Use of CIP and SAP was in accordance with manufacturers guidelines except ten times more enzyme was used per reaction to ensure complete removal of 5'-PO_4^- groups.

Inactivation of CIP was achieved by incubation at 56°C for 30 minutes in the presence of 0.5% SDS, 100mg/ml Proteinase K (Sigma-Aldrich, UK) and 5mM EDTA.

2.3.7 DNA Ligation

Ligation of DNA fragments with cohesive or 'sticky' ends is more efficient than blunt-ended ligations of DNA. Sticky-ended fragments are characterised by overhanging 5' or 3' single-stranded DNA (ssDNA). T4 DNA ligase catalyses ligation of both types of DNA fragments. For all ligations Ready-to-Go™ ligase tubes (Pharmacia, UK) containing 6 Weiss units of lyophilised T4 DNA ligase were used in accordance with the manufacturers guidelines unless stated. These tubes also contain polyethylene glycol so as to promote interactions of DNA termini by macromolecular crowding.

Calculation of the amount of vector and insert DNA to be included in the reaction was determined by a ratio of 3:1 for the insert to vector termini. The amount of insert DNA to be added to the 50ng (100ng for blunt-ended ligations) of vector was estimated as a function of their relative lengths. For example, ligation of an 600bp insert into a 5400bp vector would require nine times more vector than insert (i.e. 50ng:5.6ng) in order to give a ratio of 1:1 DNA termini as the vector is nine times the length of the insert. However, for a 3:1 ratio of insert to vector required to give optimal recombinant formation 16.7ng of the insert is required. These approximations were based on studies by Legerski & Robberson (Legerski & Robberson, 1985).

Either two or three control reactions were performed during ligations dependent on the ligation being attempted. Linearised vector in the absence of the insert fragment and without T4 DNA ligase was incubated under normal ligation conditions. Linearised DNA is poorly transformed into competent bacteria so any colonies formed indicate the presence of undigested vector within the ligation. During ligation of phosphatase-treated linearised DNA a similar reaction was performed under the same conditions in the presence of T4 DNA ligase. This second control was essential for determining the efficiency of 5' dephosphorylation which

when low leads to a high background of self-ligated vectors. The final control reaction contains linearised plasmid with compatible ends which is incubated in the presence of T4 DNA ligase. This reaction demonstrates the efficiency of the ligase reaction.

2.3.8 Bacterial Transformation

Bacterial transformation requires that the cells be competent. Competency relates to the propensity of the bacteria for DNA uptake and may be induced by chemical means.

An overnight culture of an appropriate *E.coli* strain in LB broth was grown at 37°C with vigorous incubation. 200µl of this culture was then used to inoculate 50mls of fresh LB broth. This culture was incubated until the optical density (OD) at a wavelength of 600nm reached 0.3-0.5. Cells at this OD were in the logarithmic stage of growth critical for the preparation of competent cells. The cultures were centrifuged in an Heraeus Sepatech Megafuge 1.0 with swing-out rotor at 3000rpm for 10 minutes at 4°C. The bacterial pellet was resuspended in 5ml of solution CM1 (10mM NaAc pH5.6 , 5mM NaCl & 50mM $MnCl_2$) and incubated on ice for 20 minutes. Centrifugation was repeated and the bacterial pellet resuspended in solution CM2 (10mM NaAc pH5.6, 5% glycerol, 70mM $CaCl_2$ & 5mM $MnCl_2$) before incubation on ice.

Transformation of these cells was undertaken immediately using 1-3µl of a ligation reaction. The DNA and bacteria mixture was incubated on ice for 30 minutes prior to heat shock at 42°C for 90 seconds which promotes DNA uptake. The cells were then returned to ice for 2 minutes, 1ml of room temperature LB broth was added and the cells were then incubated for 1 hour. 50-200µl of this culture was spread on LB agar plates containing the appropriate antibiotic, left to dry for 10 minutes at room temperature before overnight incubation at 37°C.

Competent cells of various *Escherichia coli* K12 strains including JM109 (GibcoBRL, UK) (Yanisch-Perron *et al.*, 1985), DH5α (GibcoBRL, UK) (Hanahan, 1983) and Epicurian Coli SURE2 (Stratagene, USA) were used in accordance with manufacturers guidelines. Transformation of these strains was undertaken by essentially similar means involving incubation on ice and heat-shock.

All competent cells used were deficient in the *recA* recombination enzyme. In addition to this, SURE2 competent cells were also deficient in an enzyme pathway involved in recombination of DNA cruciform structures (formed by inverted repeats) and Z-DNA sequences (formed by alternating sequences of purines and pyrimidines) (Gough & Murray, 1983). If no transformants were obtained with JM109 or DH5α competent cells, possibly due to formation of DNA cruciforms and Z-DNA, then SURE2 cells were used.

A control transformation was always undertaken to assess the competency of prepared or supplied cells. 1ng of pGEM3 plasmid was added to the transformation mixture as described above. For certain high competency cells such as the SURE2 strain only 10pg of pUC18 was added in accordance with manufacturers guidelines.

2.3.9 Preparation of Bacterial Glycerol stocks

Long-term storage of bacterial stocks was undertaken at -70°C by addition of a solution containing 40% glycerol, 10mM $MgSO_4$ and 0.5% NaCl to an equal volume of a fresh overnight stationary phase bacterial culture.

2.3.10 Isolation of Plasmid DNA

Plasmid DNA was isolated from bacterial cultures of 3-5 ml (minipreps) and 500ml (megapreps) volumes. All cultures contained the appropriate antibiotic for the plasmid used and were incubated at 37°C for approximately 16 hours with vigorous agitation. Either ampicillin (Sigma-Aldrich, UK) at 100μg/ml or kanamycin (Sigma-Aldrich, UK) at 30μg/ml were used depending on the selection marker present within the vector.

a) Minipreps

For isolation of limited quantities of plasmid DNA (<50μg), small 3-5 ml cultures were harvested using the MoBio UltraClean™ (CamBio, UK) miniprep kit. The following modifications were made to the manufacturers guidelines. All centrifugation steps were performed for a minimum of 2 minutes. Furthermore, despite using only 1.5ml of culture, centrifugation after addition of the binding buffer (solution 3) required extension to 10 minutes to prevent the appearance of a flocculant solution.

b) Megapreps

Two methods were used when large-scale isolation of plasmid DNA was required for application in transfection procedures (see section 2.4.8). The Qiagen Endofree Megaprep kit was used in accordance with the manufacturers guidelines.

The use of caesium chloride-ethidium bromide density gradient centrifugation was also carried out for preparation of high purity DNA (Sambrook *et al.*, 1989).

500ml of LB broth was inoculated with 1ml of a preculture inoculated approximately 24 hours earlier. Cultures were transferred to 250ml Nalgene centrifuge tubes and centrifuged at 6 000 rpm for 10 min at 4°C using a JA-14 fixed angle rotor in a J2-21 Beckman centrifuge. The bacterial pellets were gently resuspended in a total of 36ml of buffer P1 (100µg/ml RNase A, 50mM TrisHCl pH8, 10mM Na_2EDTA pH 8) to prevent complete rupturing of the cell membrane which may allow release of genomic material. 36ml of buffer P2 (0.2N NaOH, 1% SDS) was then added to the suspension and incubated for exactly 5 minutes at room temperature. This alkali buffer partially lyses the cell membrane allowing release of the relatively small plasmid DNA while retaining the larger unwanted genomic material. Addition of 36ml of chilled buffer P3 (3M KAc pH5.5) and incubation for 15 minutes on ice neutralises the alkali lysis reaction and reduces the viscosity of the lysate. Centrifugation for 20 minutes at 7000 rpm and 4°C followed. The supernatant was carefully filtered through Miracloth (20-25µm pore size; CamBio, UK) to produce a transparent solution containing the plasmid DNA. This DNA was transferred to 14ml Falcon centrifuge tubes and precipitated by addition of 0.6 volumes of isopropanol. After gentle mixing the samples were centrifuged using a JA-20.1 aluminium fixed angle rotor in the same centrifuge for 20 minutes at 10 000 rpm. The pellet was then resuspended in TE buffer and phenol extracted. Plasmid DNA was precipitated at -20°C for at least 15 minutes in the presence of 10% volume of 3M NaAc pH5 and 2 volumes of 100% ethanol. At this stage samples were accumulated and processed when sufficient numbers existed to fill the ultracentrifuge rotor (see later). The precipitated sample was then centrifuged for 5 minutes at 10 000 rpm and

4°C before repeated washing with 70% ethanol. The translucent pellet was resuspended in 2ml of TE buffer and stored on ice during the following preparatory stages.

Preparation of the caesium chloride (Boehringer Mannheim, UK) gradient was carried out as follows. Exactly 11.2ml of sterile water was added to a 14ml screw-cap centrifuge tube and the meniscus carefully marked on the side of the tube then the water was discarded. CsCl (9.46g) was weighed into the tube then the DNA sample, 500µl ethidium bromide (10mg/ml; Sigma-Aldrich, UK) and TE buffer were added until the solution reached the 11.2ml mark made previously. The plasmid solution was then added to duplicate 6ml ultracentrifuge tubes (model 03945-7K04; Sorvall, UK) so that the volume reached the neck of the tube. Crimped tubes were then weighed and balanced against each other with each having a weight of approximately 10.8g. The balanced ultracentrifuge tubes were loaded into a TV-1665 titanium rotor which was then sealed with 200lbs per square inch of torque. The samples were then centrifuged in a Sorvall UltraPro 80 ultracentrifuge at 225000 g for 16 hours at 20°C. The ultracentrifuge was programmed in accordance with the manufacturers guidelines so that the rotor decelerated slowly allowing gradual reorientation of the DNA band. This step ensured that a distinct band was formed which allowed easy visualisation and removal under ultraviolet light.

Using a low wavelength ultraviolet light source (254nm) to minimise DNA crosslinking the plasmid DNA band was located and removed using an 18-gauge needle attached to a 5ml syringe. The plasmid DNA band was always below any contaminating genomic material. RNA molecules and proteins which had formed a pellet on the side of the tube were avoided during the removal process. Isolated plasmid DNA was transferred to a 14ml screw-cap centrifuge tube to which an equal volume of CsCl-saturated isopropanol was added. Vigorous shaking and removal of the upper phase was repeated until the red coloration of ethidium bromide was no longer visible. The lower phase was transferred to a 14ml screw-cap centrifuge tube which was subsequently filled with 70% ethanol, mixed and precipitated at -70°C for 20 minutes. Prior to centrifugation for 10 minutes at 7000rpm and 4°C, the sample was warmed by hand for 2-3 minutes to resolubilise any coprecipitated salts. The pellets were then transferred to microcentrifuge

tubes and washed twice in 70% ethanol before air drying of the DNA pellet and resuspension in 1ml of TE buffer. After a final phenol extraction the DNA was again precipitated in 300mM NaAc pH5 and 100% ethanol before two washes in 70% ethanol and resuspension in 1ml of TE buffer. 1µl of the purified plasmid was analysed after electrophoresis on a 0.8% agarose gel and by spectrophotometrical analysis at 260 and 280nm.

2.3.11 Spectrophotometrical Analysis of Nucleic Acids

The amount and quality of purified nucleic acids was assessed by analysis of optical density (OD) at two ultraviolet wavelengths, 260 and 280nm. At 260 nm nucleic acids are detected where an OD equal to 1 is equivalent to 50µg/ml of double-stranded DNA or 40µg/ml of ssDNA or RNA. OD readings at 280nm indicate the presence of other high molecular weight molecules including proteins and carbohydrates. High quality preparations should possess a 260:280 ratio of approximately 1.8 for DNA and 2 for RNA. For transfection procedures only purified DNA with a 260:280 ratio between 1.7 and 1.8 was used.

2.3.12 Guidelines for use of RNA

RNA molecules are subject to nuclease digestion by RNases. A variety of RNases are present on skin therefore vigilant use of gloves during RNA application was carried out at all times. RNases are particularly resistant to heat inactivation thus autoclaving alone is not sufficient to ensure their destruction. RNase-free pipette tips containing filters (Promega, UK) were used for all transfers of liquids. Solutions for use in RNA applications were treated with 0.1% of the RNase inhibitor diethyl pyrocarbonate (DEPC) (Fedorcsak & Ehrenberg, 1966) and left to evaporate overnight in a fume hood prior to autoclaving. RNA preparations were kept on ice while in use and were stored at -70°C.

2.3.13 Extraction of RNA

RNA is comprised of three subtypes; messenger RNA (mRNA), transfer RNA (tRNA) and ribosomal RNA (rRNA). RNA was extracted from cell lines using Tri-reagent (Sigma-Aldrich, UK) in accordance with the manufacturers guidelines.

Media was removed from the cultures followed by washing with Dulbecco's phosphate buffered saline (DPBS). 1ml of Tri-reagent was added per cm^2 of culture surface immediately lysing the cells. The lysate was then transferred into microcentrifuge tubes and incubated at room temperature for 5 minutes. 200µl of chloroform was added per ml of lysate and the tubes were then vigorously shaken for 15 seconds. After incubation at room temperature for a further 10 minutes, the tubes were centrifuged for 15 minutes at 4°C and 13000rpm in an Heraeus Sepatech Biofuge 22R with HFA 22.2 rotor. The aqueous phase was then transferred and an equal volume of isopropanol added before mixing and incubation at room temperature for 10 minutes. Following further centrifugation the pellets were washed twice in 75% ethanol, air-dried and resuspended in DEPC-treated sterile water. The purity of the RNA preparation was assessed by spectrophotometrical analysis as described in section 2.3.11.

2.3.14 Reverse Transcriptase Polymerase Chain Reaction

This modification (Mocharla *et al.*, 1990) of the polymerase chain reaction (PCR) (Mullis *et al.*, 1986) utilises the viral enzyme reverse transcriptase (RT) to produce template DNA for amplification by PCR. During these studies the Titan™ kit (Boehringer Mannheim, UK) was used in accordance with the manufacturers guidelines with the following modifications. Elongation steps were performed at 72°C which is 4°C higher than the recommended temperature. This modification aimed to reduce amplification of non-specific fragments. The Titan™ kit contains a mix of three enzymes; the avian myeloblastosis virus (AMV) RT, *Taq* DNA polymerase and the high fidelity DNA polymerase *Pwo*. *Pwo* DNA polymerase has a proof-reading capability which compensates for the relatively high error rate of *Taq* polymerase which is one base approximately every 1000 bases.

2.3.15 Oligonucleotide Primer Design

Oligonucleotides were designed specifically for use in RT-PCR using a combination of the GCG (MRC HGMP resource) and GeneJockeyII computer software programs (P.Taylor, MRC CRB). When designing the requisite pair of specific oligonucleotides several guidelines were observed.

Firstly the length of the molecules was constrained to between 18 and 22 bases. The melting temperature (T_m) of the oligonucleotide dimer was designed to be between 55 and 65°C where possible and was estimated using the calculation below.

$$T_m = (G+C \times 4^oC) + (A+T \times 2^oC)$$

The T_m for each primer in a pair was manipulated by changes in oligonucleotide length so that the difference in T_m did not exceed 3°C.

A site for hybridisation on the target molecule was chosen where the presence of two guanosine monophosphate or cytidine monophosphate bases at the 3' end of the oligonucleotide would allow secure attachment of the oligonucleotide. This was particularly important for the 3' end as it was from this terminus that polymerisation occurred.

Using the GCG software, intramolecular annealing was assessed for each primer. The formation of hairpin loops as depicted in figure 2.3.15a below, provided a 3' end from which primer extension could be initiated. Primers with this design fault did not efficiently amplify target sequences due to preferential self-annealing.

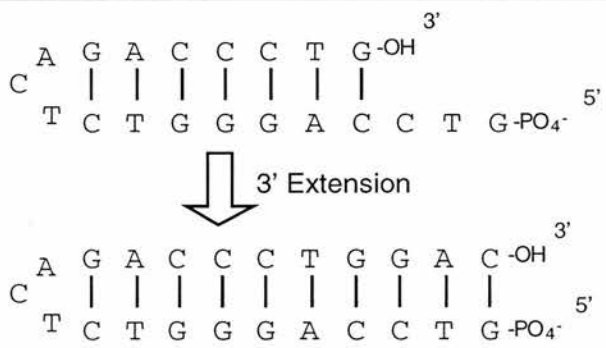

Figure 2.3.15a: Hairpin formation by oligonucleotide primers.

Primers with internal sequence homology may 'self-anneal' allowing polymerisation without binding to the target sequence. These hairpin structures were unable to bind the target sequence and were therefore effectively 'removed' from subsequent rounds of polymerisation reducing the efficiency of the reaction.

Annealing between pairs of primers was also minimised to avoid formation of primer-dimers (figure 2.3.15b). Reactions in which this occurred were characterised by the presence of very short DNA sequences and reduced amplification of the target.

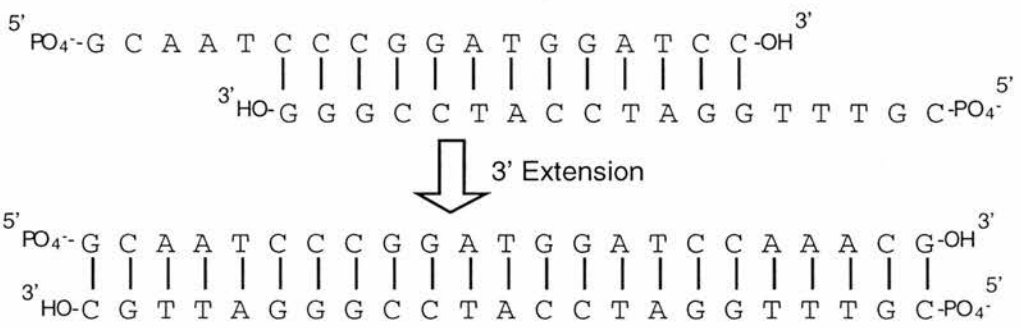

Figure 2.3.15b: Primer-dimer formation by oligonucleotide primers.

Pairs of primers with sequence homology may preferentially anneal to each other allowing polymerisation without binding to the target sequence. Formation of these short DNA structures prevented primer binding to the target sequence effectively 'removing' the primers from subsequent rounds of polymerisation and reducing the efficiency of the reaction.

By designing primers to target sequences which did not contain more than three base stretches of the same nucleotide both hairpin-loops and primer-dimers were reduced.

Although these guidelines were always used, for some target sequences the high GC content prevented complete compliance.

All oligonucleotides were supplied by Genosys (UK).

2.3.16 Agarose Gel Electrophoresis under Denaturing Conditions

RNA molecules were separated by denaturing agarose gel electrophoresis. A 1% agarose gel containing 3-(*N*-morpholino)propanesulfonic acid (MOPS; Sigma-Aldrich, UK) buffer (see Appendix I) and 2.2M formaldehyde were prepared in a fume hood.

RNA in final volume of 12µl was mixed with 25µl deionised formamide, 5µl 10x MOPS buffer (see Appendix I) and 8µl 40% formaldehyde. This mixture was then heated at 65°C for 5 minutes and cooled on ice before addition of 5µl blue loading dye (Appendix I). Denatured RNA samples were loaded onto the gel and electrophoresed for approximately 16 hours.

2.3.17 Transfer Of Nucleic Acids to Nylon Membranes

Transfer of DNA to nylon membranes followed the method described by Southern (Southern, 1975) and was as follows.

As high molecular weight DNA transfers inefficiently from agarose gels, the genomic DNA was hydrolysed to fragments of approximately 1kb in length. This was achieved by incubation of the gel at room temperature for 15 minutes in weak HCl (22ml/litre) which depurinated residues within the DNA structure. Two 15 minute exposures to 0.5N NaOH denatured the DNA after which the gel was neutralised in 3M NaCl 500mM TrisHCl pH7.4 for 1 hour.

RNA gels required no pretreatment before transfer and both RNA and DNA from agarose gels were transferred to membranes in similar ways.

Transfer of DNA or RNA molecules separated by agarose gel electrophoresis as previously described was mediated by construction of the apparatus shown in figure 2.3.17d.

A concentration gradient was established using SSC buffer (see Appendix I). Both RNA and DNA transfer methods used a reservoir of 20x SSC. 3MM paper directly above the nylon membrane was soaked in either 2x SSC for DNA transfer or 3x SSC for RNA transfer. Paper towels were changed frequently and the presence of cling-film ensured that the buffer did not circumvent the agarose gel during the transfer process. The weight on top of the paper towels ensured that the apparatus was compact facilitating efficient buffer migration. The transfer process was carried out for approximately 16 hours at room temperature. Crosslinking of the transferred nucleic acid to the nylon membrane was achieved by exposure to ultraviolet light in a Spectrolinker XL-1000 (Stratagene, USA) set to 'optimal crosslinking'.

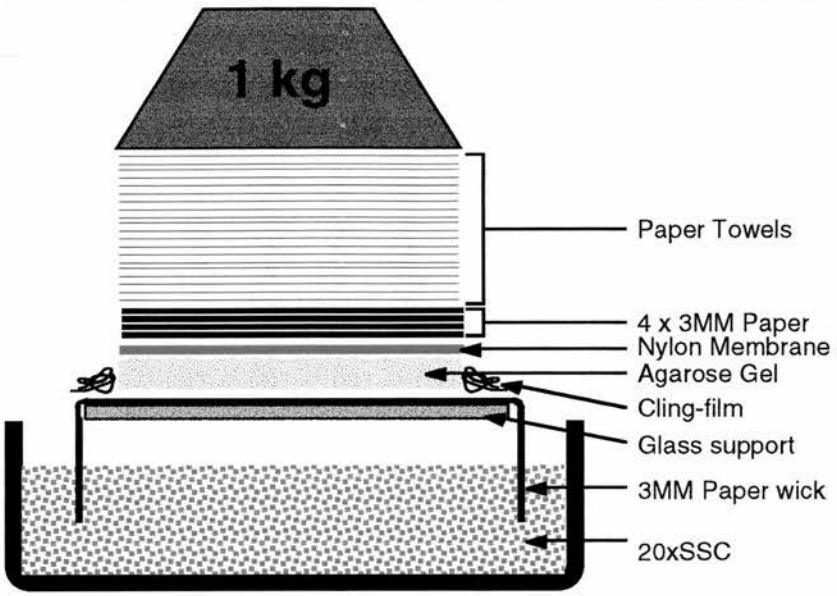

Figure 2.3.17a: Apparatus used for transfer of nucleic acids to nylon membranes.

After agarose gel electrophoresis the separated nucleic acids in the gel were transferred to the nylon membrane using a diffusion gradient. The lower reservoir contained 20xSSC whereas the 3MM paper was soaked in either 2xSSC or 3xSSC. Cling-film surrounding the gel prevented the 20xSSC bypassing it. Paper towels were changed regularly during the transfer process so as to prevent premature equilibration. An appropriate weight was placed on top of the apparatus to ensure efficient liquid transfer.

2.3.18 Radioactive Labelling of DNA probes

Specific cDNA molecules were used as probes to detect RNA or DNA fragments transferred to nylon membranes. The *redi*PRIME™ kit (Amersham, UK) was used in accordance with manufacturers guidelines to incorporate [α^{32}P]-deoxycytidine triphosphate (dCTP; DuPont NEN, UK) with a specific activity of 3000Ci/mmol. This system is based in the method devised by Feinberg & Vogelstein (Feinberg & Vogelstein, 1983) except that random nonomeric primers were used in place of the original hexamers. Verification of the labelling procedure was undertaken by addition of 1µl of the reaction to glass filter paper which was left to dry before removal of unincorporated nucleotides by washing in 5% trichloroacetic acid (TCA)

20mM sodium pyrophosphate solution. The sample was then washed in 70% ethanol and dried before detection of incorporated [^{32}P]-deoxycytidine monophosphate residues by Cerenkov counting. It should be noted that detection of disintegrations per minute (dpm) in dry filters containing ^{32}P is only 25% efficient using the [^{3}H] channel of the scintillation counter. Hence dpm/µg DNA were calculated by multiplying the total counts per minute (cpm) by four. All probes were radiolabelled in excess of $1x10^{9}$ dpm/µg DNA.

2.3.19 Hybridisation of DNA probes

Nylon membranes were washed in 3X SSC to remove residual agarose prior to a prehybridisation in Church & Gilbert hybridisation buffer (see Appendix I) (Church & Gilbert, 1984) at 65°C for 2 hours using a Hybaid Midi dual 14 oven (Hybaid, UK). The specific DNA probes labelled with [^{32}P]-dCTP were denatured in 0.2M NaOH at 4°C for 5-10 minutes before addition to the hybridisation mix. Hybridisation of the probes was carried out in Church & Gilbert hybridisation buffer at 65°C for approximately 16 hours. To remove excess unhybridised probe, the membranes were given a preliminary vigorous 30 second wash in 2X SSC and 0.1% SDS at 65°C followed by three 20 minute washes. The membranes were air-dried at room temperature before exposure in a PhosphorImager cassette for 24-72 hours followed by scanning on a Molecular Dynamics STORM™ PhosphorImager and quantitation using Molecular Dynamics ImageQuant™ software (Molecular Dynamics, UK).

2.4 Mammalian Cell Culture

2.4.1 Established Cell lines

Culture of various established cell lines was undertaken. These included the human choriocarcinoma JEG3 cell line (Kohler & Bridson, 1971), the mouse adrenocorticotroph AtT-20 cell line (Gumbiner & Kelly, 1982), the mouse gonadotroph αT3-1 cell line (Windle *et al.*, 1990), the Chinese hamster ovary (CHO) cell line and the CHO-derived CHO-K1 cell line (Puck *et al.*, 1958) the rat somatomammotroph GH_3 cell line (Tashjian *et al.*, 1968)

and the recently described mouse gonadotroph $L\beta T_2$ cell line (Thomas *et al.*, 1996).

2.4.2 Cell Culture Suite Design

A small self-contained cell culture suite was designed for exclusive use of established cell lines. Class 2 microbiological air flow cabinets, CO_2 incubators, a bench-top swing-out rotor centrifuge, a -20°C freezer and a refrigerator were to be contained in this suite. Control of air-flow was the major consideration in the layout of the suite. Previous experience from culture work undertaken elsewhere had shown that air currents were often the cause of serious contamination of incubators and an example scenario is depicted in figure 2.4.2ai. For this reason incubators were situated facing away from the suite door. Furthermore the door to the suite was constructed in a sliding format so as to minimise generation of air currents during entry and exit of the suite. The layout of the cell culture facility used during these studies is depicted in figure 2.4.2aii.

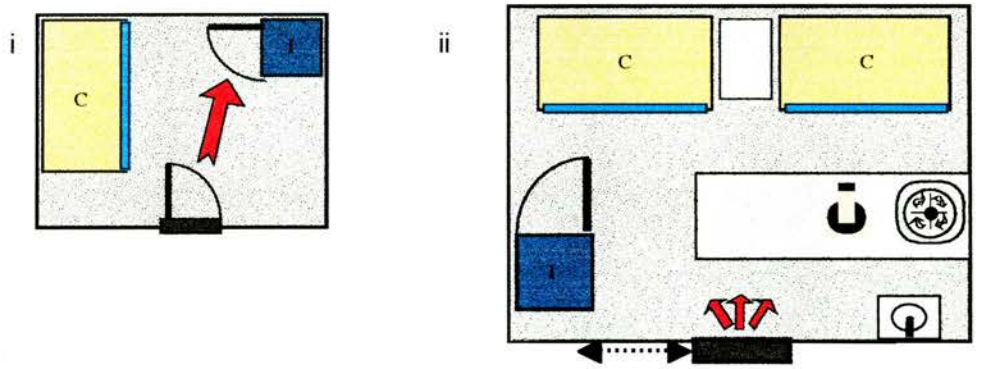

Figure 2.4.2a: Floorplans of two cell culture facilities demonstrating the significance of airflow from exterior sources.

i) Airflow (arrow) within the cell culture suite is generated by the external door which directs potentially contaminating air towards the incubator (I). ii) The cell culture suite used during these studies has a sliding door which generates less airflow into the facility. In addition the incubator is positioned facing away from the external door to minimise airborne contamination. Airflow cabinet (C), CO_2 incubator (I).

2.4.3 General Aseptic Technique

Specific laboratory coats were used for cell culture and were changed weekly. Long latex gloves were used to fully cover wrists when arms were extended. Isopropanol diluted to 70% in double-distilled water was used to sterilise all surfaces, bottles and instruments during use. A Class II Microbiological Safety cabinet was used for all manipulations of living mammalian cell cultures. The safety cabinet was cleaned with the antiseptic solution Tisept and sprayed with 70% isopropanol prior to and after use. Routine cleaning of the safety cabinet was undertaken using bleach solution which was rinsed off all surfaces using 70% isopropanol.

The HEPA-filtered air-flow within the cabinet prevents airborne transmission of particles between the cabinet and the external environment in both directions (see figure 2.4.3a). This characteristic protects the operator from harmful airborne effects of biohazardous materials while also preventing airborne contamination of cultures.

The Sanyo CO_2 incubator used to culture cells was humidified using a pan containing double-distilled and autoclaved water saturated with copper sulphate. The incubator door was never left open for more time than necessary so as to prevent non-sterile air-flow contaminating the water pan or surfaces.

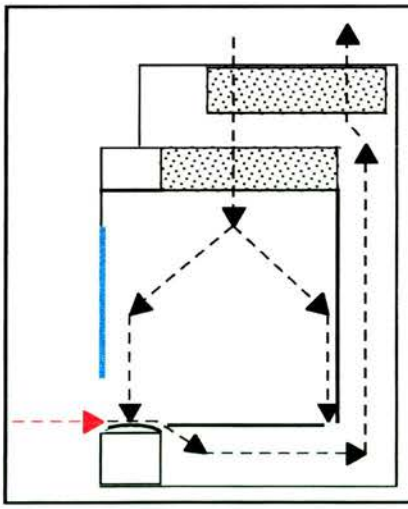

Figure 2.4.3a: Schematic representation of a Class II Microbiological Airflow Saftey cabinet.

Airflow (dashed arrows) is HEPA-filtered prior to entering the sterile cabinet. Airborne contamination (red dashed arrow) via the operator access hatch is prevented by a 'curtain' of air which directs the external airflow away from the working area. This airflow is then directed out of the cabinet via another HEPA filter.
▨ = HEPA filter

2.4.4 Resuscitation of Cell lines

Frozen ampoules were removed from dry ice and left at room temperature for 1 minute followed by thawing at 37°C for 2-3 minutes. Thawed suspensions were washed in Dulbecco's Modification of Eagle's Medium with 10% fetal calf serum (FCS) and 100 units/ml penicillin and 0.1 mg/ml streptomycin (this mix will be referred to as cDMEM) and then centrifuged for 5 minutes at 1000 rpm in a Sorvall Econospin centrifuge with swing-out rotor (DuPont, UK). Removal of supernatant was followed by resuspension in 5ml cDMEM and culture in the following conditions.

2.4.5 Routine Passaging of Cell lines

All cell lines were maintained in tissue culture flasks with 25cm^2 culture area. The flasks containing 5ml cDMEM were incubated at 37°C with 5% CO_2 in a humidified incubator. Occasionally, for cell lines in which growth rate appeared adversely affected HyClone fetal calf serum was used in place of that supplied by Sigma-Aldrich. This had the effect of recovering individual cell line proliferation to acceptable levels and proved especially effective for culture of LβT$_2$ cells. All FCS was batch-tested for optimum growth of cell lines used in these studies.

Culture medium was removed from confluent cultures by aspiration with a sterile Pasteur pipette attached to a vacuum pump. After each use of the aspiration apparatus bleach solution was used to rinse the tubing for future applications in order to prevent possible cross-contamination. cDMEM was replaced with Dulbecco's phosphate buffered saline (DPBS) in order to dilute inhibitory serum concentrations for subsequent application of trypsin. DPBS was removed by aspiration prior to addition of 500µl 1x trypsin-EDTA solution (0.05% trypsin, 0.02% EDTA) per 25cm^2 culture surface. The degree of trypsinisation was controlled by concentration of the trypsin-EDTA solution, duration of application and incubation temperature. These parameters varied for each cell line used and is summarised in table 2.4.5a below.

Table 2.4.5a: Trypsinisation of Cell lines.

Cell Line	Trypsin-EDTA Solution	Incubation Temperature	Duration of Incubation (secs)
CHO	1x	37°C	30
CHO-K1	1x	37°C	45
JEG3	1x	37°C	120
$L\beta T_2$	0.1x	room temp.	10

Trypsin is inhibited by FCS therefore addition of cDMEM was undertaken when cells were observed to detach from the culture surface. The cells were resuspended using a sterile plastic Pasteur pipette with an aperture of approximately 1mm. This suspension was then diluted in cDMEM and applied to sterile culture vessels. The dilution used depended on the rate of proliferation of the cell line and the time at which achievement of confluency was desired. Cell suspensions were not over-diluted as this often reduced the viability of the culture.

2.4.6 Estimation of Cell Number

100µl of a cell suspension was mixed with 900µl DPBS prior to addition to a haemocytometer with coverslip attached. The loaded haemocytometer was viewed using an inverted microscope. Cells were counted within the four corner squares of the counting chamber. Each square corresponds to a volume of $0.1mm^3$ or $10^{-4}\ cm^3$. In order to calculate the number of cells per ml of the original suspension the mean figure from four squares was multiplied by 10^5.

2.4.7 Long-term Storage of Cell lines

Stocks of cell lines were maintained in the liquid phase of a nitrogen storage vessel (Merck BDH, UK). Cultures maintained as previously described were used when confluency was estimated as between 60-80%. Cells were trypsinised as previously described and resuspended in 5ml cDMEM prior to centrifugation for 5 minutes at 1000 rpm in a Sorvall Econospin centrifuge with swing-out rotor (DuPont, UK). Removal of the supernatant by aspiration and resuspension of the pellet in 500µl FCS chilled to 4°C followed. This suspension was transferred to 1.8ml NUNC cryotubes. Addition of 500µl 20% dimethyl sulphoxide (DMSO) in FCS chilled

to 4°C was followed by overnight (approximately 16 hours) incubation at -70°C in a Nalgene container which contained a 250ml reservoir of isopropanol. Use of this specialised apparatus controlled the temperature descent of the cell suspension to approximately 1°C per minute and improved cell viability. Following overnight incubation at -70°C frozen ampoules were transferred to liquid nitrogen for long-term storage.

2.4.8 Transient Transfections

Cell lines were transiently transfected with DNA constructs so as to assess the characteristics of their expression. Various methods exist for introduction of exogenous nucleic acids into mammalian cells including microinjection, electroporation, viral transfection, calcium chloride-based and lipid-based methods. During these studies calcium chloride- and lipid-based methods were used. For all transfections cells were plated in the appropriate vessels (flasks, dishes or chamber slides) at a density which produced 50-80% confluency 16-24 hours later. Assessment of the transient gene expression was undertaken by various means 24-72 hours later. All constructs used in transfections were purified by CsCl density gradient centrifugation or the Endofree Megaprep kit (Qiagen, UK) so as to reduce toxicity caused by contaminating bacterial endotoxins.

2.4.9 β-Galactosidase Staining

Transfection of the pcDNA3.1/His/lacZ plasmid (Invitrogen, NL) which contains the β-galactosidase gene allowed relatively simple assessment of transfection efficiency through colorimetric staining and counting of positive (blue) cells.

Cells were fixed for 5 minutes at room temperature in DPBS containing 2% formaldehyde and 0.2% gluteraldehyde. After washing with DPBS the cells were incubated overnight at 37°C in DPBS containing 5mM $K_3Fe(CN)_6$, 5mM $K_4Fe(CN)_6$, 2mM $MgCl_2$ with 1mg/ml 5-bromo-4-chloro-3-indolyl-β-D-galactopyranoside (X-gal). Cells were washed with DPBS and the number of blue-stained cells established. Cells were viewed at 100x magnification using an inverted microscope and representative photomicrographs were taken using a Labovert inverted microscope with a Ricoh KR-10M camera and Leitz Periplan LT 160mm lens. For high transfection efficiencies 4

counts of 250 cells per field of view were undertaken using a multichannel counter and the positive proportion represented as a percentage.

2.5 Protein Analysis

2.5.1 Protein Extraction

Proteins were extracted from cell lines in 100mM sodium carbonate as this has been previously determined to be the optimal buffer for isolation of gonadotrophins [A.S.McNeilly - personal communication]. After resuspension in the buffer the cells were incubated at room temperature for an hour. To ensure complete release of proteins from intracellular compartments the samples were exposed to three alternating cycles of 5 minutes incubation in a dry ice ethanol bath and 5 minutes at 37°C followed by vigorous vortexing. Lysates were then centrifuged at 13000rpm for 5 minutes in an Heraeus Sepatech Biofuge 13 at room temperature to remove cell debris and the supernatant transferred and stored at -20°C.

2.5.2 Total Protein Quantification

Following the method of Bradford (Bradford, 1976) total protein concentrations in cell lysates were determined. 200-fold dilution of the lysate in a total of 1ml sterile water was followed by brief vortexing. 200µl of protein dye (Bio-Rad, UK) was subsequently added to the diluted sample and mixed by inverting 6 times. Protein standards containing 25, 12.5, 6.25, 3.125, 1.56 and 0.78µg/ml bovine serum albumin (BSA; Sigma-Aldrich, UK) were similarly treated. Mixing of the samples and standards was undertaken without formation of excessive bubbles as these cause aberrant OD readings. OD at 595nm was measured after incubation of the samples at room temperature for 5 minutes.

2.5.3 Assessment of Chloramphenicol acetyltransferase Activity

Chloramphenicol acetyltransferase (CAT) is a tetrameric cytosolic molecule comprised of 23kDa subunits. CAT activity in the presence of acetyl coenzyme A (AcCoA) inhibits binding of the antibiotic

chloramphenicol to the 50S subunit of ribosomes. Chloramphenicol is converted to hydroxy acetoxy derivatives by CAT which are unable to bind the ribosomal component and therefore unable to inhibit protein synthesis at the translation stage. It is the production of these derivatives which is detected in the CAT assay using radioactively-labelled chloramphenicol separated by thin layer chromatography (TLC).

CAT activity was assessed using the method of Gorman *et al* (Gorman *et al.*, 1982) as follows. A volume of cell lysate containing 2µg of protein as determined by Bradford assay was added to 0.25M TrisHCl pH7.8 giving a final volume of 193µl. Inactivation of CAT inhibitors was achieved by incubation at 65°C for 10 minutes. 2µl ^{14}C-chloramphenicol (50 Ci/mmol) and 5µl 50mM acetyl coenzyme A (Boehringer Mannheim, UK) were subsequently added to the reaction and mixed before incubation at 37°C for 5-30 minutes. Extraction of the ^{14}C-chloramphenicol was achieved by addition of 600µl ethyl acetate and vortexing for 10 seconds 3 times. The sample was then centrifuged at room temperature for 30 seconds at 13000rpm in an Heraeus Sepatech Biofuge 13 before careful transfer of the organic phase to a new microcentrifuge tube. The transferred sample was then vacuum-dried before resuspension in 20µl ethyl acetate and separation by TLC in a solvent containing a 95:5 ratio of chloroform to methanol. The dry TLC plate was exposed for at least 48 hours in a PhosphorImager cassette before scanning on a STORM™ PhosphorImager and quantification using ImageQuant™ software (Molecular Dynamics, UK].

The increased mobility of the mono- and diacetate forms of ^{14}C-chloramphenicol allowed their separation from unconverted ^{14}C-chloramphenicol. The amount of CAT activity was determined as the percentage of acetylated ^{14}C-chloramphenicol per sample (Gorman *et al.*, 1982).

2.5.4 Iodination of Antigens

Antigens were iodinated using the chloramine-T method. 500µCi ^{125}I was added to 10µl chloramine-T (2mg/ml in 0.25M PBS) and 5µg of antigen and vortexed for 15 seconds. 10µl sodium metabisulphate (2mg/ml in 0.25M PBS) was then added prior to vortexing for a further 20 seconds. 1ml 1%

BSA in 0.05M PBS was added to the reaction and vortexed for 30 seconds halting the iodination reaction. Total counts were established prior to application of the sample to a 30cm Sephadex G100 column (1cm diameter) coated with 1% BSA in 0.05M PBS. After adding the sample to the column, residual ^{125}I in the reaction tube was counted. This allowed calculation of the total radioactivity applied to the column. Forty 30-drop fractions were collected using a Gilson model 201 fraction collector and radioactivity plotted to assess labelling of the antigen. Peak fractions were pooled and stored in a lead-lined container at -20°C.

2.5.5 Radioimmunoassays

Various radioimmunoassays (RIAs) were performed during these studies however the general methodology employed for all RIAs will be described here.

Unless otherwise stated 100µl of appropriately diluted sample was added to 10x75mm plastic test tubes containing 200µl 0.1% bovine serum albumin (BSA; Sigma-Aldrich, UK) in 0.075M PBS using a Microlab automatic pipettor. 100µl of primary antisera was subsequently added to each tube, mixed and incubated for at least 16 hours at 4°C. The appropriate tracer was diluted to approximately 15000 cpm per 100µl in 0.1% BSA 0.075M PBS. Following addition of 100µl of the diluted tracer to each tube and mixing, they were incubated at 4°C for at least 16 hours. 100µl each of secondary antisera and normal antisera were added to the tubes, mixed and incubated for a further 16 hours at 4°C. All assays used normal rabbit serum (NRS; SAPU, UK) and donkey anti-rabbit serum (DARS; SAPU, UK). Following this final incubation the immunocomplexes were separated by addition of 1ml 0.9% saline, 4% PEG 6000 and 0.2% Triton X-100 and centrifugation at 3000rpm in a Sorvall Omnispin R centrifuge (DuPont, UK) for 25 minutes at 4°C. Supernatants were removed and tubes were left to dry at room temperature. Radioactivity was measured using a 1261 Multigamma counter (Wallac, UK) and data analysed using AssayZap (P.Taylor, MRC CRB).

The sensitivity of the LH RIAs was 0.2ng/ml and 0.08ng/ml for the FSH RIA. The intra- and inter-assay coefficients of variation were <7% and <10% respectively over the concentration range of the samples in all RIAs.

Table 2.5.5a: RIA components; Sera and Dilutions

Assay	Primary Antisera and [Source]	Final Dilution of Primary Antisera	Tracer material and [Source]	Secondary Antisera dilutions	
				NRS	DARS
oLH	R29 [A.S. McNeilly]	1:120000	LER-1056-C2 [NIDDK, USA]	1:800	1:64
oLH (hCG -ve)	R29 (hCG -ve) [A.S. McNeilly]	1:12000	LER-1056-C2 [NIDDK, USA]	1:800	1:64
oFSH	anti-oFSH-1 [NIDDK, USA]	1:12000	oFSH-19 [NIDDK, USA]	1:400	1:32
rLH	anti rLH-S-11 [NIDDK, USA]	1:150000	rLH-RP-3 [NIDDK, USA]	1:400	1:16

2.5.6 Gel Electrophoresis of Proteins under Denaturing Conditions

Separation of denatured protein subunits was undertaken by polyacrylamide gel electrophoresis (PAGE) in the presence of the anionic detergent sodium dodecyl sulphate (SDS; Boehringer Mannheim, UK) (Laemmli, 1970). Polyacrylamide crosslinked by *N,N'*-methylenebisacrylamide in the presence of ammonium persulfate and *N,N,N',N'*-tetramethylethylenediamine (TEMED; Sigma-Aldrich, UK) provided the matrix in which the proteins were separated. High resolution of the protein bands was achieved by using a discontinuous gel containing stacking and resolving components. The stacking gel at 5% acrylamide was less dense than the resolving gel which varied between 6% and 15% depending on the range of protein sizes at which resolution required. The pH of the stacking gel was 6.8 whereas the resolving gel and running buffer were at pH8.8. These two differences caused migrating proteins to be concentrated at the interface between the two gel types prior to separation within the resolving gel producing distinct bands.

Protean II xi vertical gel apparatus (Bio-Rad, UK) were used to pour and run all SDS-PAGE gels. Acrylamide solutions (10% acrylamide in 375mM TrisHCl pH8.8 and 1% SDS) were degassed before 1mm thick resolving gels were poured and covered with a 1:1 mixture of butanol and water ensuring that a level upper margin was produced. The gel was left to polymerise at

room temperature for 30-60 minutes then the butanol:water mixture was removed and replaced with 250mM TrisHCl pH8.8 and stored at 4°C overnight. The 5% stacking gel containing 125mM TrisHCl pH6.8 and 1% SDS was similarly degassed prior to pouring and addition of an appropriate comb. Polymerisation was left to occur at room temperature while samples were prepared for loading. Denaturation of a known amount of protein between 20 and 50µg was subjected to denaturation by boiling for 5 minutes in the SDS-PAGE loading buffer (see Appendix I). Both reducing and non-reducing loading buffers were used. The reducing buffer contained 0.2% β-mercaptoethanol (Sigma-Aldrich, UK) to prevent oxidation of the protein. The samples were left to cool at room temperature before addition to the gel. A constant current of 20mA was applied through the stacking gel and 30mA through the resolving gel in SDS-PAGE running buffer (see Appendix I) for 3-4 hours. The gel apparatus was assembled following the manufacturers guidelines.

2.5.7 Gel Electrophoresis of Proteins under Non-denaturing Conditions

Assessment of multimeric protein abundance was undertaken by PAGE under non-denaturing conditions as follows.

Gels and buffers were identical to those used during SDS-PAGE except that no SDS was added (see Appendix I). The Bio-Rad Protean II xi vertical gel tank (Bio-Rad, UK) was used in accordance with manufacturers guidelines. Samples were loaded using buffer which contained no SDS or β-mercaptoethanol. In addition the samples were not boiled prior to electrophoresis. A constant current of 20mA was applied through the stacking gel and 30mA through the resolving gel in native-PAGE running buffer (see Appendix I) for 3-4 hours.

2.5.8 Transfer of Proteins to Nitrocellulose Membranes

Proteins separated under both denaturing and native conditions were attached to a solid phase prior to immunological assay. A Bio-Rad Transblot™ wet transfer tank (Bio-Rad, UK) was used for both transfer methods in accordance with manufacturers guidelines. The apparatus used is shown in figure 2.5.8a. There were two differences between transfer of

denatured and native proteins. For transfer of denatured proteins wet-blot buffer (25mM Tris, 192mM glycine and 20% methanol) was used whereas native proteins were transferred in 0.7% acetic acid. The differences in these buffers imparted different behaviour on the proteins. Denatured proteins continued to exhibit anionic migration due to the continued binding of SDS and the presence of Tris and glycine in the transfer buffer. Native proteins in the continued absence of SDS and the removal of the electrophoresis buffer migrated towards the cathode. In both cases the apparatus was run for approximately 16 hours at 25V.

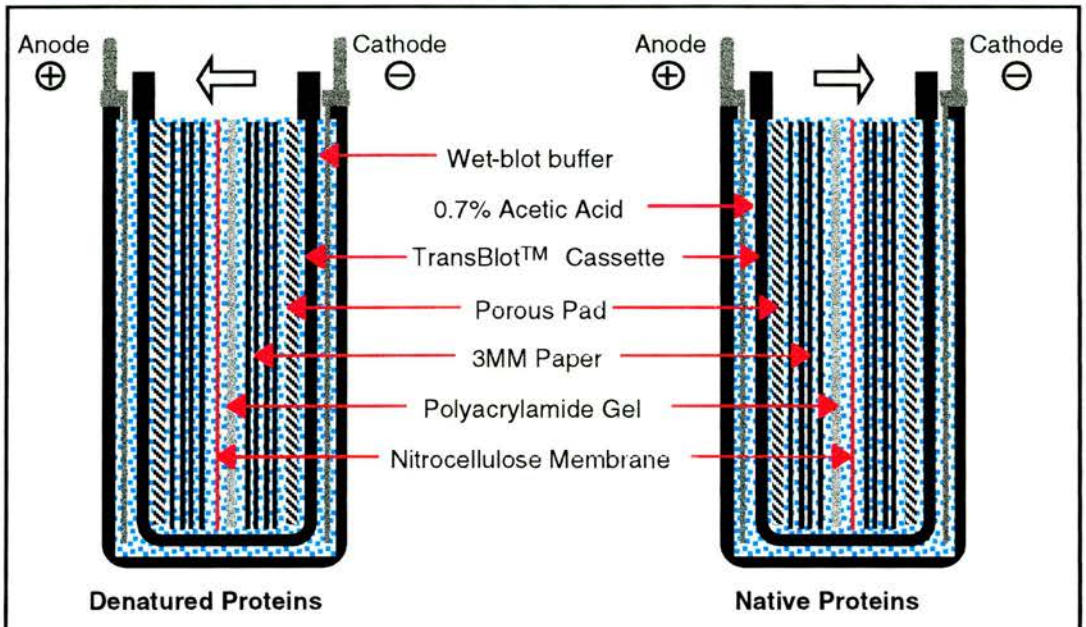

Figure 2.5.8a: Apparatus used for transfer of denatured and native proteins to nitrocellulose membranes.

Wet-blot buffer used for transfer of denatured proteins contained 25mM Tris, 192mM glycine and 20% methanol. Transfer was undertaken for approximately 16 hours at 25V. The buffer was cooled throughout operation by a pipe passing cold water through the apparatus.

2.5.9 Slot-blotting

Initial optimisation of primary antisera concentrations required for analysis of proteins attached to nitrocellulose membranes (Millipore, UK) was carried out by slot-blotting. Purified antigen was applied to the

membrane with a vacuum using a Bio-Dot SF apparatus and filter papers (Bio-Rad, UK). Proteins attached to the membrane were then detected by either ECL or ECF detection methods (Amersham, UK) described below.

2.5.10 Immunodetection of Immobilised Proteins

Two similar methods were employed to detect proteins transferred to nitrocellulose membranes. The ECL kit (Amersham, UK) required exposure to light-sensitive film whereas visualisation of fluorescence produced using the ECF kit (Amersham, UK) was undertaken using the STORM™ PhosphorImager on the blue fluorescence mode. Quantification of protein abundance within samples was more easily achieved using the ECF kit. Use of the ECL and ECF kits and the STORM™ PhosphorImager was in accordance with manufacturers guidelines.

2.6 Fluorescence

2.6.1 Indirect Immunofluorescence in Mammalian Cells

Transiently transfected cell lines cultured in glass chamber slides under normal conditions as described in 2.4.5 were washed with phosphate-buffered saline (PBS) before being fixed in Bouins fixative (Appendix I) for 5 minutes at room temperature. With the plastic chamber still attached to the glass slide the Bouins fixative was removed and replaced with PBS. Washing in PBS for 5 minutes with gentle agitation at room temperature was repeated three times to remove the fixative. The cells were permeabilised by adding PBS containing 1% bovine serum albumin (BSA), 10% normal goat serum and 0.2% Non Idet P-40 for 20 minutes with gentle agitation at room temperature. Washing in PBS for 5 minutes with gentle agitation at room temperature was repeated three times to remove the detergent. The cells were incubated in blocking solution (PBS containing 1% BSA and 10% normal goat serum) for two hours at room temperature with gentle agitation to reduce non-specific antibody binding. Primary antisera was subsequently added and incubated for at least 16 hours at 4°C. Excess primary antisera was removed by washing in PBS for 5 minutes with gentle agitation at room temperature; this was repeated three times. Fluorescent conjugates of appropriate secondary antisera were diluted 1:30

in blocking solution and incubated for two hours in the dark at room temperature with gentle agitation. Prolonged PBS washes of 10 minutes at room temperature with gentle agitation were repeated at least three times. After removal of the plastic chambers, coverslips were mounted using Citifluor (UKC, UK) and sealed using clear nail varnish. Slides were then viewed by confocal microscopy or stored in the dark at 4°C.

2.6.2 Direct fluorescence in Mammalian Cells

Cells transiently transfected with constructs encoding the enhanced green fluorescent protein (EGFP; Clontech, UK) were viewed after fixing or live as described below.

a) Fixed Cells: Removal of the culture media was followed by washing in PBS for 5 minutes at room temperature with gentle agitation. Subsequently the cells were fixed by incubation for 5 minutes in Bouins (Appendix I) at room temperature. Three washes of 5 minutes in PBS at room temperature preceded removal of the plastic chamber slide and mounting as previously described.

b) Live Cells: In the absence of a specialised perfusion chamber allowing observation of living cells cultured on circular glass coverslips at 37°C an alternative method was employed. Chamber slides containing EGFP-expressing cells were maintained at 37°C using an OmniSlide thermocycler (Hybaid, UK). Removal of the chamber was followed by mounting in DPBS using rubber adhesive and glass coverslips. The use of rubber adhesive followed Clontech's guidelines which suggest that nail varnish may adversely affect EGFP fluorescence. Viewing of the live sample was limited to approximately 5 minutes to avoid the adverse effects of temperature reductions.

2.6.3 Confocal Microscopy

Analysis of indirect immunofluorescence on cells and tissues was undertaken using a Zeiss Axiovert 100M microscope and LSM510 scanning module with oil immersion x40, x63 and x100 objectives (Zeiss, UK). Scans were performed at either 1024x1024 or 2048x2048 pixels resolution. Data analysis was undertaken using a Dell Optiplex Gxi computer (Zeiss, UK). Confocal microscopy allows analysis of specimens whist reducing

background fluorescence from out of focus objects. A schematic representation of the principle of confocal microscopy is depicted in figure 2.6.3a.

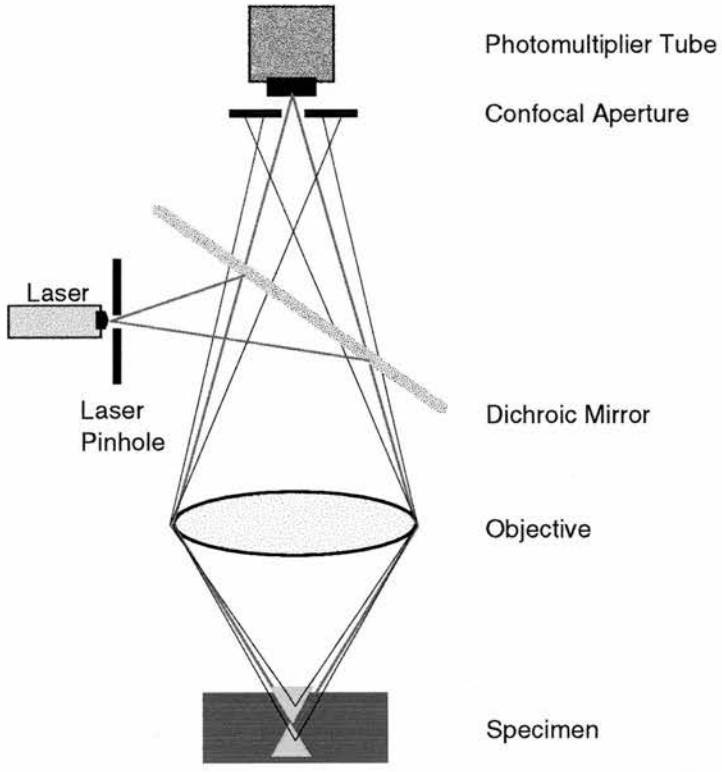

Figure 2.6.3a: A schematic representation of confocal microscopy.

Fluorescence is excited by an appropriate wavelength of light provided by the laser source. The laser beam is focussed onto the sample using one or more specific dichroic mirrors and an objective. Fluorescence emitted from the sample is focused through the confocal aperture so that emissions from voxels outside the plane of focus (shown in yellow) are omitted from the image collected by the photomultiplier tube (PMT). Data collected by the PMT can be transferred to computer for immediate analysis. Multiple lasers and fluorophores may be used at one time through the specific nature of the dichroic mirrors and by using filters.

Immunocytochemistry (ICC) using secondary antisera conjugated with fluorophores such as fluorescein isothiocyanate (FITC) or Tetramethyl rhodamine isothiocyanate (TRITC) allows simultaneous visualisation of antigen binding. The excitation and emission spectra for FITC and TRITC

are distinct (figure 2.6.3b) which allows colocalisation studies to be carried out. The excitation of FITC and EGFP was undertaken with a 488nm argon laser set at between 8 and 15% of maximum power. Detection of light emitted from FITC was carried out with a 505-535nm bandpass filter. TRITC excitation was achieved using a 543nm HeNe laser set at 40 to 100% of maximum power which was detected using a longpass 585nm filter. Visualisation of EGFP was undertaken as described for FITC-conjugated antisera as their excitation and emission spectra are similar.

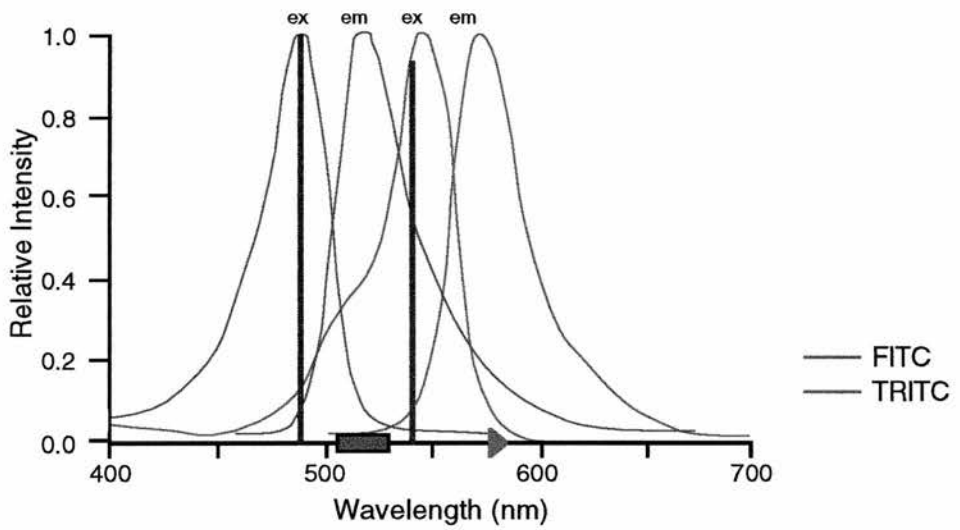

Figure 2.6.3b: Excitation and emission spectra for fluorescein isothiocyanate (FITC) and tetramethyl rhodamine isothiocyanate (TRITC).

The maximal excitation wavelengths for FITC and TRITC are distinct which allowed use of specific lasers for each fluorophore conjugate. FITC excitation was undertaken using an argon laser at 488nm (vertical green line) whereas TRITC excitation was achieved using a HeNe laser at 543nm (vertical red line). FITC emissions were detected using a bandpass filter between 505 and 535nm (green box) with those of TRITC detected using a 585nm longpass filter (red arrow). Although the longer emission spectra overlap, the relative intensity is low thus interference between the two dyes was not significant. Excitation spectra (ex), emission spectra (em).

When using FITC conjugates in the absence of TRITC conjugated secondary antisera the nuclear stain propidium iodide (Sigma-Aldrich, UK) was

sometimes used by addition to Citifluor at a final concentration of 10µg/ml. The emission spectra for this dye coincided with those of TRITC and hence they were never used together. Phase contrast images collected at the same time as fluorescence were overlaid allowing three sets of data to be viewed in a single two-dimensional image. Furthermore due to the focused nature of the excitatory laser beam (figure 2.6.3b), confocal microscopy permits visualisation of tissue as a series of optical slices. This feature reduces the need for serial sectioning and allows representation of data as a three-dimensional image useful in observing stereological relationships.

2.7.1 Data Analysis

Raw data was manipulated in Microsoft Excel 4.0 (MacWarehouse, UK), standard errors were calculated using GB-Stat 6 (Dynamic Microsystems, USA) and statistical analyses carried out using StatView 4.02 (MacWarehouse, UK). One-way analysis of variance (ANOVA) was calculated using Fisher's protected least significant difference (PLSD).

Chapter Three

Mammalian Expression Constructs

3.1 Introduction

This chapter will focus on the building of mammalian expression constructs used throughout the *in vitro* studies in this thesis.

Whereas the expression of the gene of interest in a comparatively physiological context is the end point of most studies, the genetic material often requires manipulation prior to this. In order to generate sufficient DNA for subsequent studies, bacterial cultures are used to propagate DNA as part of a plasmid. Mammalian expression vectors such as pcDNA3 (Invitrogen, NL) have sequences that allow their propagation in both prokaryotes and eukaryotes and for this reason they are often referred to as shuttle vectors. The shuttle vector pcDNA3 contains origins of replication from the *Escherichia coli* plasmid ColE1 and the filamentous bacteriophage f1 which enable propagation at a high copy number in transformed bacteria for propagation. In mammalian cells a different origin is recognised which derives from the simian virus SV40. The enhanced green fluorescent protein (EGFP) C-terminal fusion vectors are also capable of propagation in bacteria using the origin of replication from f1 and the pBR322 backbone. Like pcDNA3, the EGFP C-terminal (EGFP-C) fusion vectors rely on the SV40 origin to maintain their propagation in mammalian cells.

Selection of pcDNA3 and pBluescript KS+ (Stratagene, USA) in *E.coli* is undertaken by resistance to the β-lactam antibiotic ampicillin. Resistance is encoded by a β-lactamase gene the product of which cleaves the β-lactam ring preventing its entry into the bacterium. Ampicillin like other penicillin-derived antibiotics inhibits growth of gram-negative bacteria such as *E.coli* by inhibiting synthesis of the cell wall component peptidoglycan. Ampicillin inhibits peptidoglycan crosslinking in two ways; by acting as an analogue of D-alanine-D-alanine and by binding to and inhibiting the transglycosylase/transpeptidase activity of the essential penicillin binding proteins (PBPs) 1A, 2 and 3. The reduced crosslinking of this net-like structure within the periplasmic space reduces its strength eventually leading to lysis.

Two key characteristics of pcDNA3 made it a suitable candidate for these studies. pcDNA3 contains a neomycin resistance gene (neo^R) which encodes an aminoglycoside 3'-phosphotransferase. Neomycin and its analogue G418 are aminoglycoside antibiotics which are effective against mammalian cells as well as bacteria. Protein synthesis is inhibited by G418 binding to the ribosome at multiple sites which may also lead to misreading of mRNA. The presence of neo^R allows selection of stably transfected cells by application of G418 over a period of 4 to 6 weeks.

The pEGFP-C vectors encode a neo^R protein which also confers resistance to the related antibiotic kanamycin in *E.coli*. By employing a single antibiotic resistance gene these fusion vectors maintain a relatively small size which increases their structural durability.

High expression of the inserted gene in mammalian cells is a desirable characteristic for most studies. This is mainly conferred by upstream promoter and enhancer sequences in the vector which recruit RNA polymerase II producing large numbers of transcripts from which an amino acid sequence may be translated. In pcDNA3 the human cytomegalovirus (CMV) promoter from the immediate early genes is used. The CMV promoter is a strong constitutive promoter and like the SV40 immediate early promoter present in the cDNA cloning vector pcD produces large quantities of RNA transcripts from the insert. Both pcDNA3 and pcD contain poly-A addition site sequences 3' of the inserted gene. This feature provides the mRNA molecule produced with a degree of protection from RNase degradation as this is another factor which can limit final levels of protein expressed.

Essentially the vectors used for mammalian expression constructs contain the necessary sequences for propagation and selection in both *E.coli* and a variety of mammalian cells. Furthermore the presence of a strong constitutive promoter may provide high expression in a comparatively physiological context.

3.2 Methods

This section will cover the strategies used in the engineering of constructs for expression of various genes and cDNA sequences within mammalian cells. Many of the basic molecular biology protocols such as restriction endonuclease digestion, agarose gel electrophoresis and ligation are described in detail within chapter 2.

These constructs include those encoding the key gonadotrophin subunits and granins as well as genes such as chloramphenicol acetyltransferase (CAT) used to assay transfection efficiency. The pcDNA3 shuttle vector (Invitrogen, NL) was used for all constructs described in this chapter with the exception of the enhanced green fluorescent protein (EGFP) fusion constructs derived from the pEGFP-C vectors (Clontech, UK).

3.2.1 The Ovine αGSU Expression Construct

The ovine gonadotrophin alpha subunit (αGSU) cDNA in pSP72 was a kind gift from T.E.Adams (Aus). Subcloning of the αGSU was relatively straightforward and a simplified schematic representation of the cloning strategy used is shown in figure 3.2.1a.

The original plasmid containing the αGSU cDNA was digested with *Eco*RI to excise the 716bp full-length cDNA. After verifying that the DNA sample was completely digested, the remaining reaction volume was electrophoresed overnight in a 0.8% agarose gel and extracted as described in sections 2.3.2 & 3 . pcDNA3 was similarly digested with *Eco*RI and due to the presence of compatible cohesive termini (both *Eco*RI) on the linearised vector, phosphatase treatment was undertaken to reduce the likelihood of the plasmid self-ligating. Calf intestinal phosphatase (CIP; Boehringer Mannheim, UK) was used at 10x the recommended concentration to ensure complete removal of the 5' phosphate groups as described in section 2.3.6 . Ligation of the oαGSU cDNA and pcDNA3 was undertaken using Ready-to-Go™ ligase tubes as described in section 2.3.7. Subcloning efficiency competent *E.coli* DH5α cells (Gibco BRL, UK) were transformed with the ligation products in accordance with manufacturer's guidelines using 2μl of the ligation reactions. Plasmid preparations were assessed by restriction digests with two objectives; to ascertain the presence of the αGSU cDNA and to determine its orientation. Analysis of the predicted construct sequence

determined that *Pst*I digestion would produce different size fragments depending on the orientation of the insert as depicted in figure 3.2.1b.

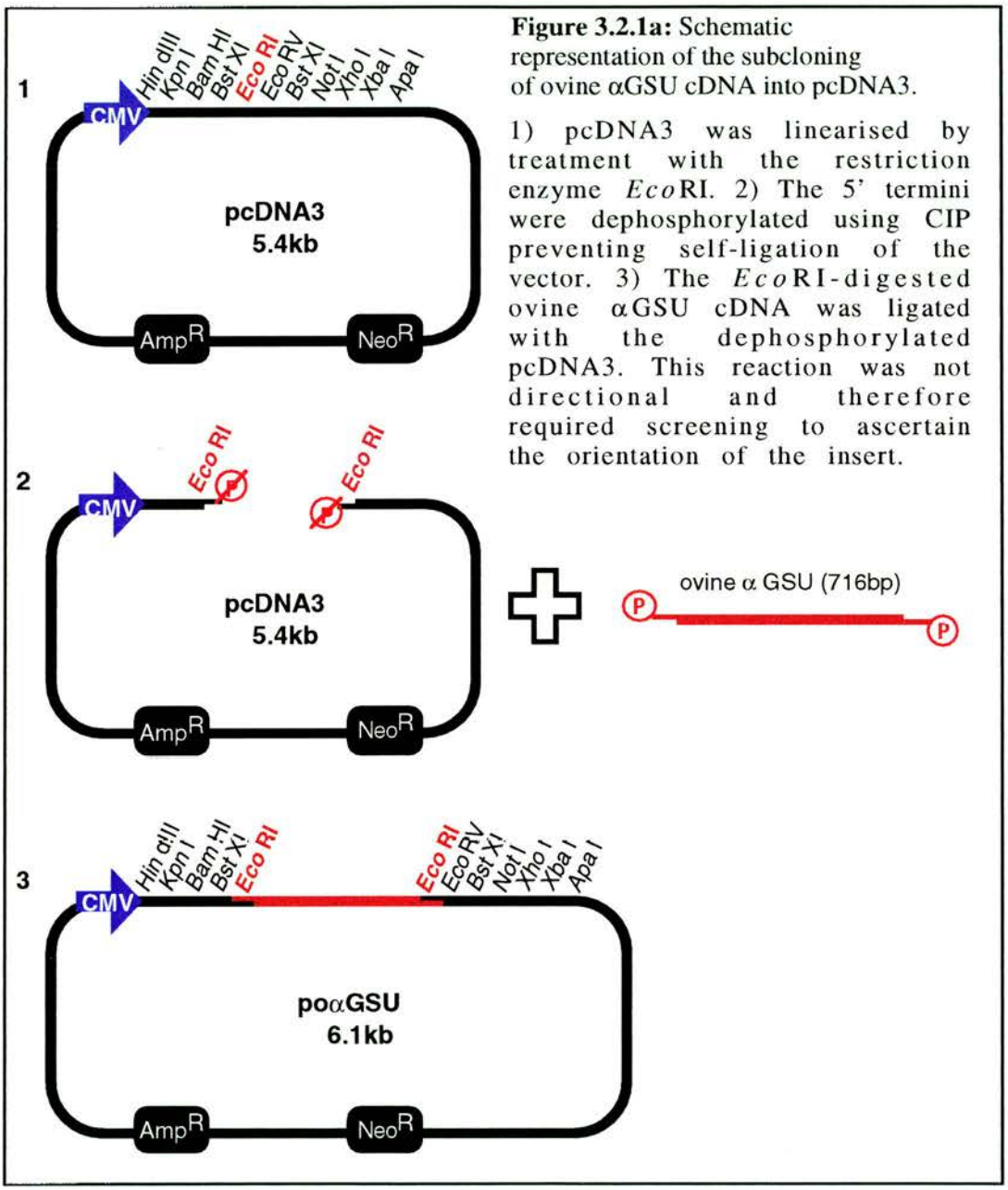

Figure 3.2.1a: Schematic representation of the subcloning of ovine αGSU cDNA into pcDNA3.

1) pcDNA3 was linearised by treatment with the restriction enzyme *Eco*RI. 2) The 5' termini were dephosphorylated using CIP preventing self-ligation of the vector. 3) The *Eco*RI-digested ovine αGSU cDNA was ligated with the dephosphorylated pcDNA3. This reaction was not directional and therefore required screening to ascertain the orientation of the insert.

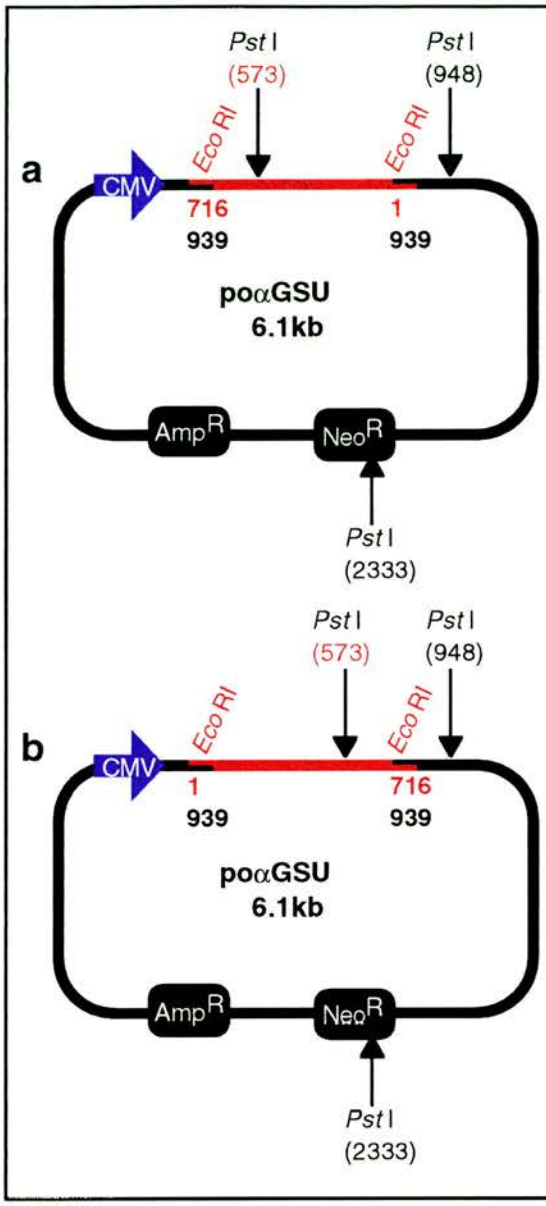

Figure 3.2.1b: Schematic representation of the screening strategy employed to determine orientation of the ovine αGSU cDNA after subcloning into pcDNA3.

a) *Pst* I digestion of the pcDNA3 vector containing the ovine αGSU in the reverse orientation in regard to the CMV promoter should yield fragments of 4196, 1385 and 581 bp. b) *Pst* I digestion of the pcDNA3 vector containing the ovine αGSU in the same orientation as the CMV promoter should yield fragments of 4625, 1385 and 153 bp.
Figures shown in red refer to the ovine αGSU sequence.

Positive recombinants were also digested with *Eco*RI to ascertain whether treatment with excess concentrations of CIP had degraded the 3' overhangs produced by linearisation of the vector. Large-scale preparation of this plasmid construct was undertaken as described in section 2.3.10 . The predicted size of this construct was 6162bp.

3.2.2 The Ovine FSHβ cDNA Expression Construct

Both the cDNA and genomic oFSHβ constructs were engineered so that the native FSHβ 3' UT region was absent. This was carried out to obtain levels of

expression unaffected by the low mRNA stability caused by the long 3' UT of oFSHβ *in vitro* (Mountford *et al.*, 1992).

The full-length cDNA for oFSHβ in pSP72 was a kind gift from T.E.Adams (Aus). A simplified schematic representation of the cloning strategy used to subclone this cDNA into pcDNA3 is depicted in figure 3.2.2a.

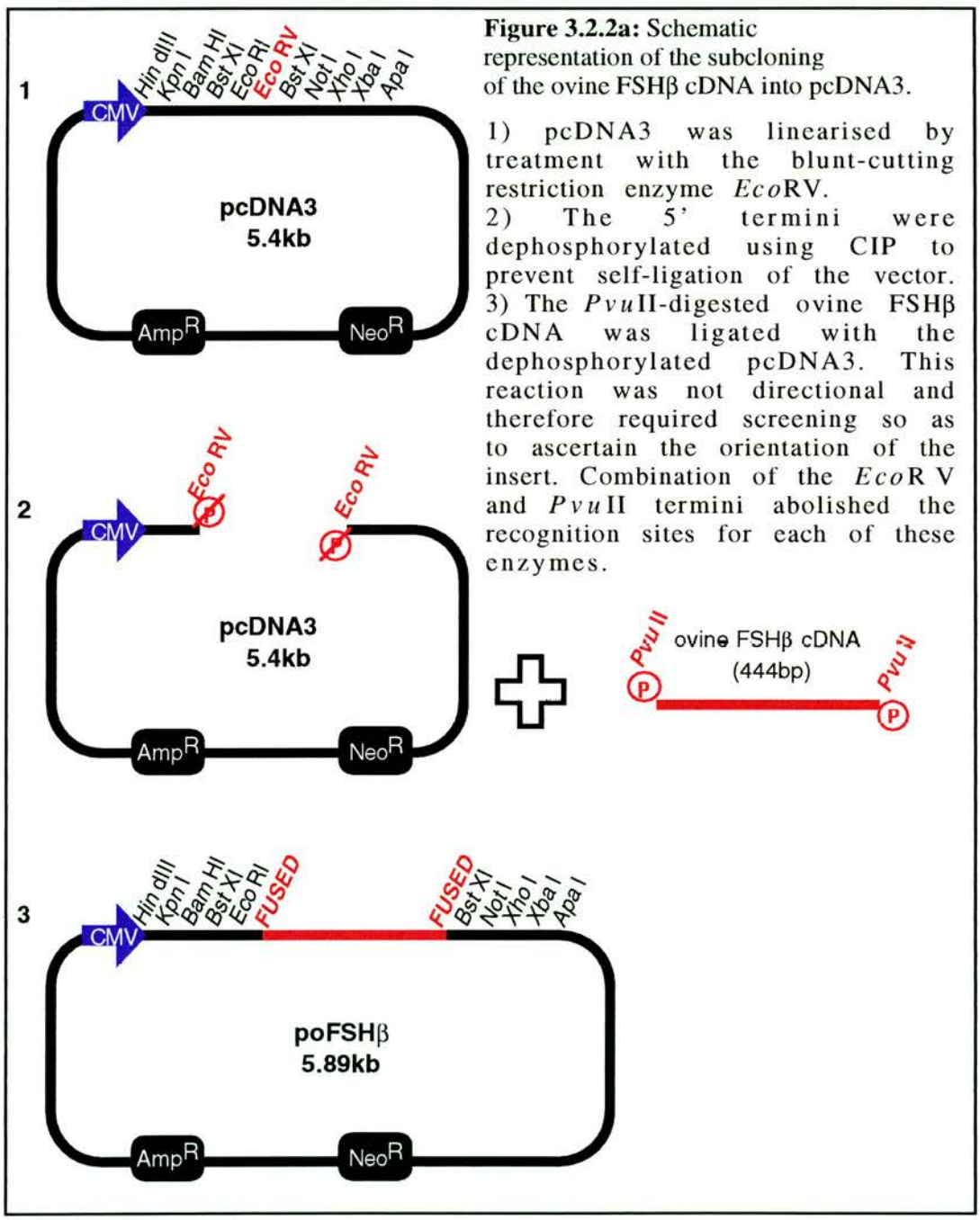

Figure 3.2.2a: Schematic representation of the subcloning of the ovine FSHβ cDNA into pcDNA3.

1) pcDNA3 was linearised by treatment with the blunt-cutting restriction enzyme *Eco*RV.
2) The 5' termini were dephosphorylated using CIP to prevent self-ligation of the vector.
3) The *Pvu*II-digested ovine FSHβ cDNA was ligated with the dephosphorylated pcDNA3. This reaction was not directional and therefore required screening so as to ascertain the orientation of the insert. Combination of the *Eco*R V and *Pvu*II termini abolished the recognition sites for each of these enzymes.

The oFSHβ cDNA was excised from pSP72 by *Pvu*II digestion cutting at +10 and +454bp which included the entire coding region. The mRNA polyadenylation signal was provided by the bovine growth hormone sequence located at 1018-1249bp 3' to the pcDNA3 polylinker. The digest was verified prior to overnight agarose gel electrophoresis and gel extraction of the fragment. *Eco*RV is the only blunt-cutting restriction enzyme site within the pcDNA3 polylinker. Following linearisation of the vector, dephosphorylation was carried out using Shrimp alkaline phosphatase (SAP; Boehringer Mannheim, UK) as described in section 2.3.6 . The 444bp oFSHβ insert and dephosphorylated vector were ligated using Ready-to-Go™ ligase tubes (Pharmacia, UK) in accordance with the manufacturer's guidelines. Subcloning efficiency *E.coli* DH5α cells were transformed with the ligation reaction.

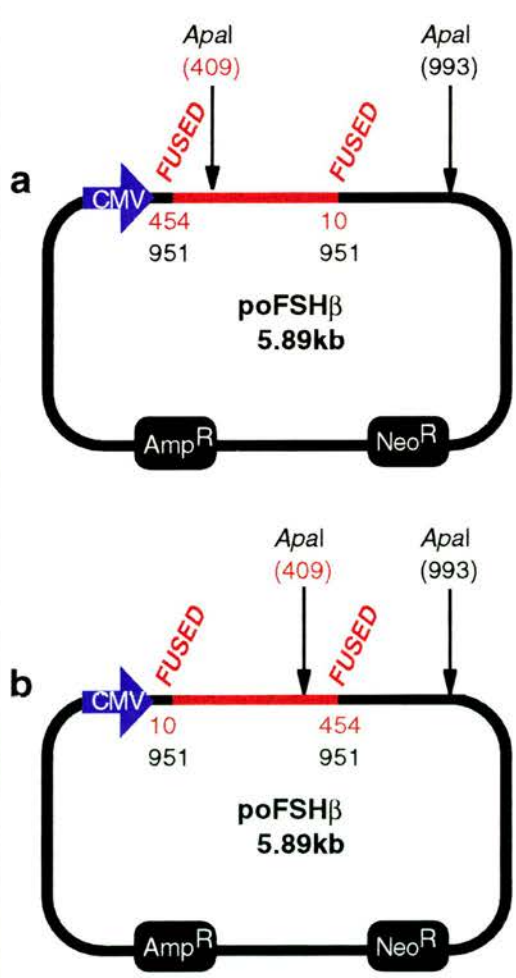

Figure 3.2.2b: Schematic representation of the screening strategy employed to determine orientation of the ovine FSHβ cDNA after subcloning into pcDNA3.

a) *Apa*I digestion of the pcDNA3 vector containing the ovine FSHβ in the reverse orientation in regard to the CMV promoter should yield fragments of 5449 and 441 bp. b) *Apa*I digestion of the pcDNA3 vector containing the ovine FSHβ in the same orientation as the CMV promoter should yield fragments of 5803 and 87bp.
Figures shown in red refer to the ovine FSHβ sequence.

Screening of miniprep DNA required digestion with *Apa*I to determine the presence and orientation of the oFSHβ cDNA insert (figure 3.2.2b). Large-scale preparation of a positive clone was undertaken as described in section 2.3.10.

3.2.3 oFSHβ Genomic DNA Expression Construct

The oFSHβ genomic clone in pBluescript KS+ (Stratagene, USA) was a kind gift from P.Brown (MRC, CRB). However this clone did not contain the transcriptional initiation site as it was spliced downstream of the oLHβ promoter for use in a transgenic model (oLHβ/oFSHβ, see chapter 7). This construct also had the poly-A addition site from Herpes simplex virus (HSV), and had the original 3' UT removed. This feature was engineered in order to provide oFSHβ expression levels that were unaffected by this mRNA species inherent instability.

A schematic representation of the manipulations undertaken during the reconstruction of the full-length oFSHβ genomic clone is shown in figure 3.2.3a. The pGEM4 clone containing the 5' region of the oFSHβ gene was digested with *Hin*dIII and *Pst*I producing a 866bp fragment containing exons 1 and 2. The transcriptional initiation site was located 106bp from the 5' end of this fragment. The 866bp fragment was extracted after overnight agarose gel electrophoresis. Subcloning of this *Hin*dIII-*Pst*I fragment directly into the 5' truncated clone was not possible due to the presence of similar restriction sites. The presence of a unique *Xho*I site 95bp downstream from the transcriptional initiation site prompted the use of this enzyme for the splicing process. An upstream *Xho*I site is not present in either the pGEM4 vector or the oFSHβ gene. However pBluescript KS+ (Stratagene, USA) does contain the site within its polylinker upstream of the *Hin*dIII site. Ligation of the insert and the *Hin*dIII/*Pst*I-linearised pBluescript KS+ was carried out using Ready-to-Go™ ligase tubes (Pharmacia, UK). Miniprep plasmid DNA was isolated from cultures transformed with the ligation. The presence of the insert was determined by retarded migration during agarose gel electrophoresis. Recombinant plasmids were digested with *Xho*I after which the 226bp fragment was extracted from an agarose gel run overnight. This fragment was then ligated with the *Xho*I-digested pBluescript KS+ containing the 5' truncated oFSHβ gene after dephosphorylation with SAP (Boehringer Mannheim, UK).

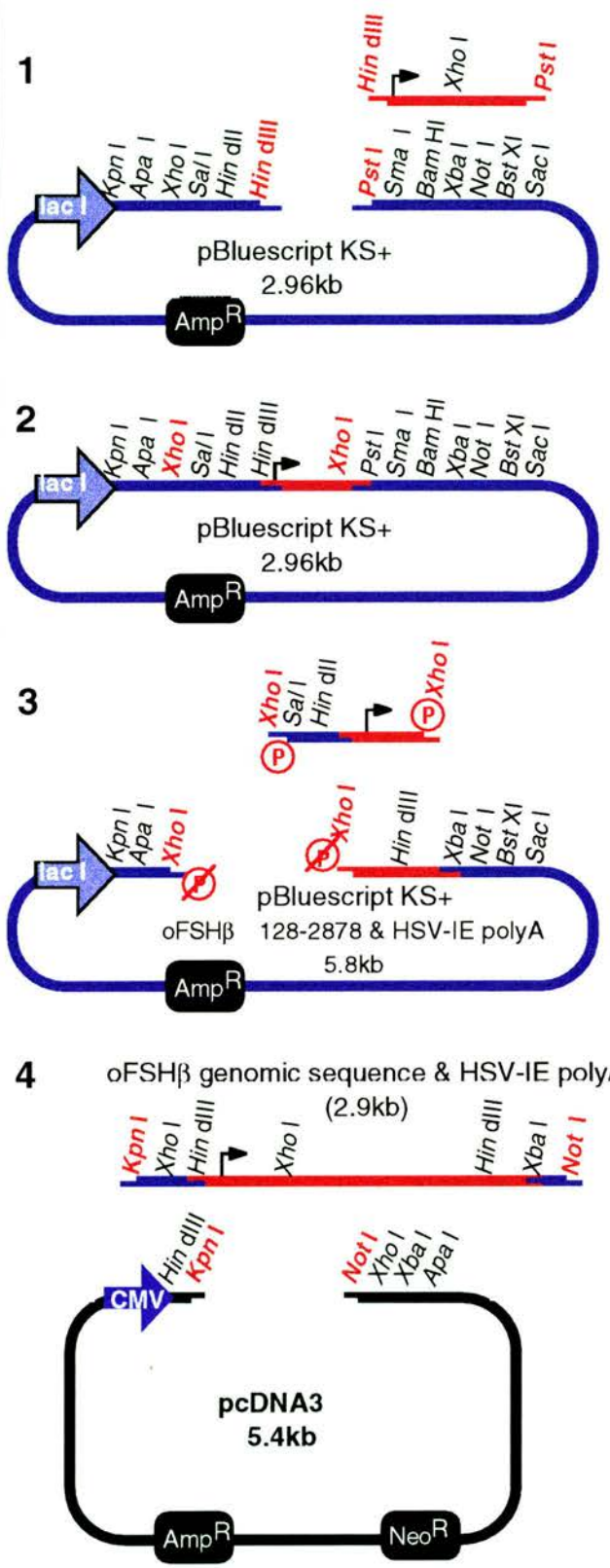

Figure 3.2.3a: Schematic representation of the strategy used to reconstruct the oFSHβ genomic clone.

1) Directional ligation of the 866bp fragment containing the transcriptional start site for oFSHβ into pBluescript KS+.
2) *Xho*I digestion of the ligated plasmid excising the smaller 226bp fragment containing the oFSHβ transcriptional start site.
3) Ligation of the *Xho*I fragment with a plasmid containing the downstream oFSHβ sequences (exons 1-3) and a poly-A addition site from Herpes simplex virus (HSV). The *Xho*I digested plasmid was dephosphorylated prior to ligation.
4) The reconstructed oFSHβ gene was excised from pBluescript KS+ and directionally ligated into the mammalian expression vector pcDNA3 yielding a plasmid 8.35kb in length.

Subcloning efficiency *E.coli* DH5α cells were transformed with this ligation and plasmid DNA isolated. Determining the orientation of the ligated *Xho*I fragment was undertaken using a *Hin*dIII digestion as shown in figure 3.2.3b.

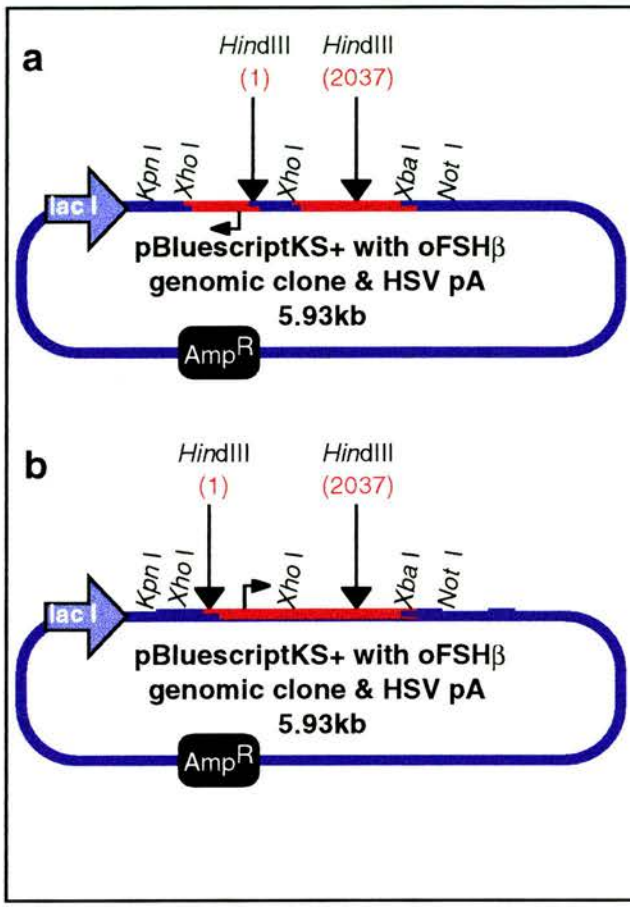

Figure 3.2.3b: Schematic representation of the strategy used to screen recombinants for the orientation of the *Xho*I fragment containing the transcriptional start site for the genomic clone of oFSHβ.

a) *Hin*dIII digestion of the pBluescript KS+/oFSHβ 205-2878 & HSV-IE 3' UT construct containing the 266 bp *Xho*I transcriptional start site fragment in the reverse orientation in regard to the CMV promoter should yield fragments of 4076 and 1855bp.
b) Similar digestion of the construct containing the fragment in the correct orientation should yield fragments of 3894 and 2037bp. Figures shown in red refer to the oFSHβ sequence.

A positive plasmid was digested with *Xho*I to verify that the sites were intact. Extraction of the reconstructed oFSHβ gene from pBluescript KS+ was undertaken in two stages due to conflicts in restriction enzyme buffering requirements. *Kpn*I digestion linearised the construct. Dual digestion with *Not* and *Sca*I excised the oFSHβ gene and cleaved the vector ('suicide-cutting') to allow their resolution by agarose gel electrophoresis and prevent vector contamination of the extracted fragment. The 3049bp oFSHβ *Kpn*I-*Not*I fragment was ligated with a similar digestion of pcDNA3 and transformed into subcloning efficiency *E.coli* DH5α cells. Preparations of plasmid DNA were screened for insertion of the 3049bp oFSHβ *Kpn*I-*Not*I fragment by digestion with *Hin*dIII. The predicted fragments produced by this screening strategy should include the 2037bp band as detailed in figure

3.2.3b and a larger pcDNA3-derived fragment of 6458bp. Large-scale preparation of this construct was undertaken as described in section 2.3.10 .

3.2.4 The Human Chromogranin A Expression Construct

A 1811bp full-length human chromogranin A (hCgA) cDNA in pGEM3-3 (Helman *et al.*, 1988) was obtained from the American-type culture collection (ATCC). *Hin*dIII and *Eco*RI restriction sites within the pGEM3-3 plasmid polylinker permitted excision of the complete hCgA cDNA. Direct subcloning of this fragment into pcDNA3 was carried out as depicted schematically in figure 2.3.4a.

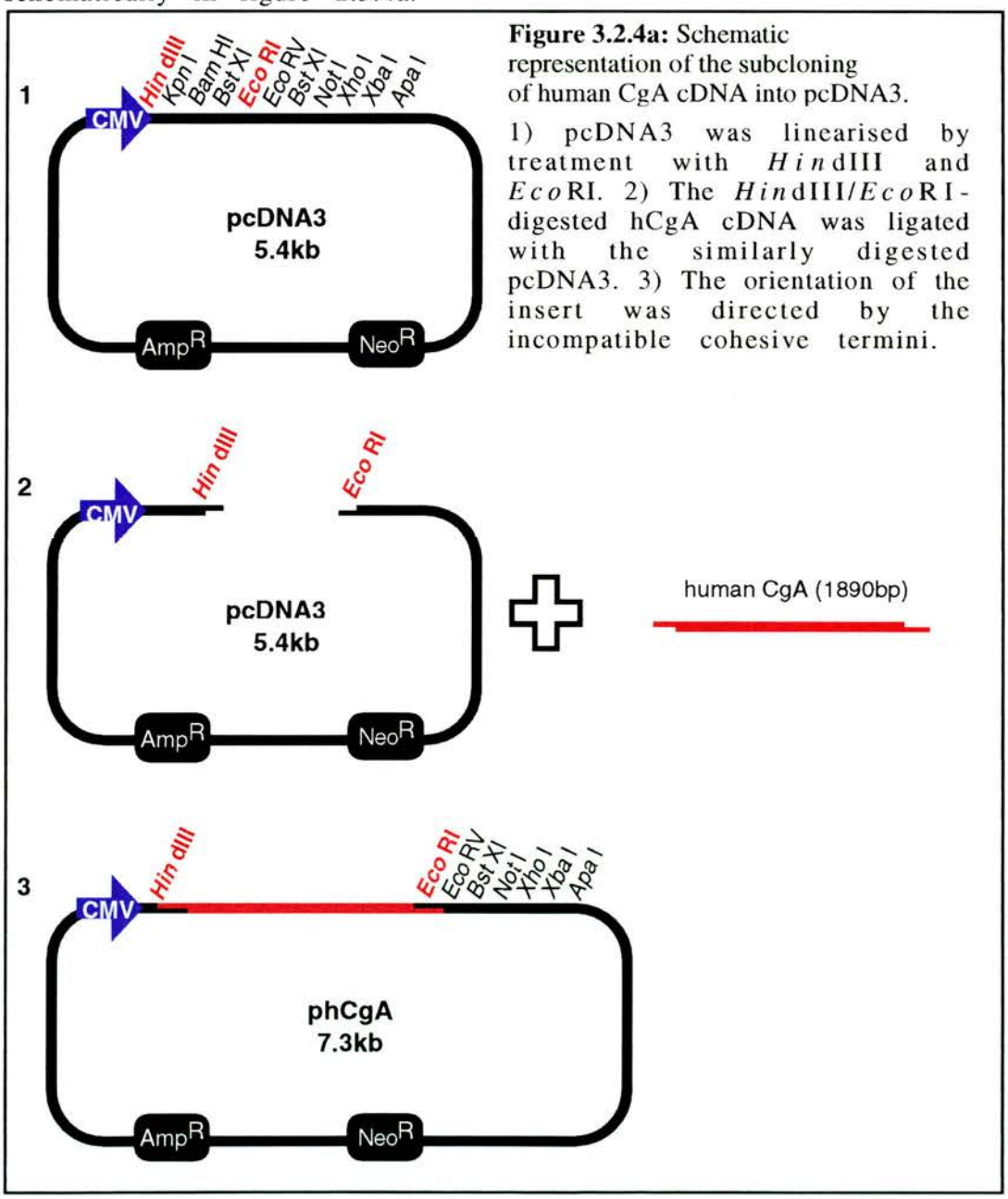

Figure 3.2.4a: Schematic representation of the subcloning of human CgA cDNA into pcDNA3.

1) pcDNA3 was linearised by treatment with *Hin*dIII and *Eco*RI. 2) The *Hin*dIII/*Eco*RI-digested hCgA cDNA was ligated with the similarly digested pcDNA3. 3) The orientation of the insert was directed by the incompatible cohesive termini.

*Hin*dIII and *Eco*RI digestion of the hCgA plasmid and pcDNA3 was followed by ligation and transformation of subcloning efficiency *E.coli* DH5α. Preparations of plasmid DNA were screened for insertion of the hCgA cDNA by simultaneous digestion with *Hin*dIII and *Bam*HI. A schematic representation of the predicted fragments produced is shown in figure 3.2.4b. DNA from a positive clone was isolated on a large-scale as described in section 2.3.10.

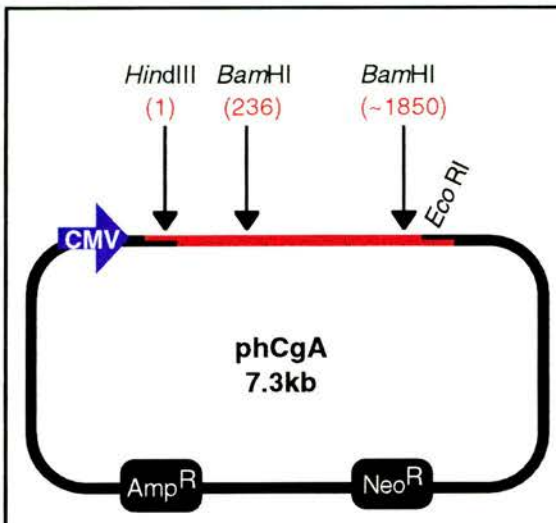

Figure 3.2.4b: Diagnostic restriction digest for the hCgA expression construct phCgA.

The correctly formed construct should produce 3 fragments of 5446, ~1615 and 236bp upon digestion with *Hin*dIII and *Bam*HI.

3.2.5 The EGFPC-oLHβ fusion Construct

The oLHβ subunit cDNA in pGEM3 was a kind gift from B.Miller (USA). Fusion of the protein expressed by this cDNA and the enhanced GFP (EGFP) required that the two sequences be ligated in frame.

The oLHβ cDNA was excised with *Pst*I. The EGFP carboxy-terminal fusion vectors are supplied with the polylinker in three different reading frames; pEGFP-C1, -C2 and -C3 (Clontech, UK). Using GeneJockeyII (P.Taylor, MRC UK), the vector producing an open reading frame (ORF) from the upstream EGFP gene through the oLHβ cDNA was determined to be pEGFP-C3. The preservation of the ORF through the polylinker is shown in figure 3.2.5a.

The strategy used to construct the EGFP-oLHβ fusion plasmid is depicted schematically in figure 3.2.5b.

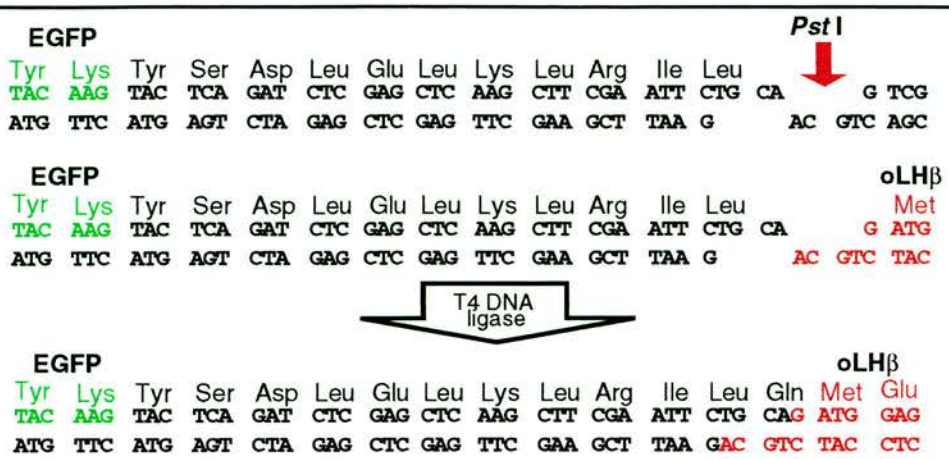

Figure 3.2.5a: Formation of the open reading frame between the enhanced green fluorescent protein (EGFP) gene and the 5' terminus of the ovine LHβ cDNA in the polylinker of pEGFP-C3.

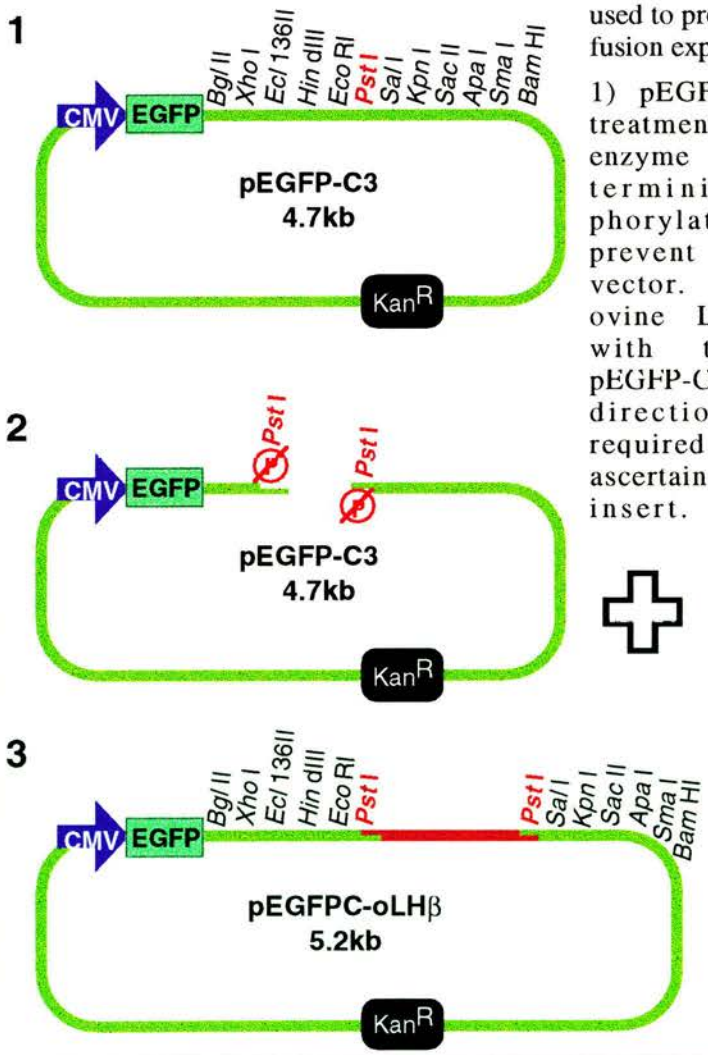

Figure 3.2.5b: Schematic representation of the strategy used to produce an EGFPC-oLHβ fusion expression construct.

1) pEGFP-C3 was linearised by treatment with the restriction enzyme *Pst*I. 2) The recessed 5' termini were dephosphorylated using SAP to prevent self-ligation of the vector. 3) The *Pst*I-digested ovine LHβ cDNA was ligated with the dephosphorylated pEGFP-C3. This reaction was not directional and therefore required screening so as to ascertain the orientation of the insert.

pEGFP-C3 and pGEM3/oLHβ cDNA were digested with *Pst*I. The vector was subsequently dephosphorylated using SAP (Boehringer Mannheim, UK). Ligation reactions were carried out using Ready-to-Go™ ligase tubes in accordance with the manufacturers guidelines. The ligation was used to transform *E.coli* SURE2 competent cells (Stratagene, USA). Plasmids were screened by restriction with *Apa*I at the recommended temperature of 30°C (figure 3.2.5c). Large-scale preparation of this construct was undertaken as described in section 2.3.10.

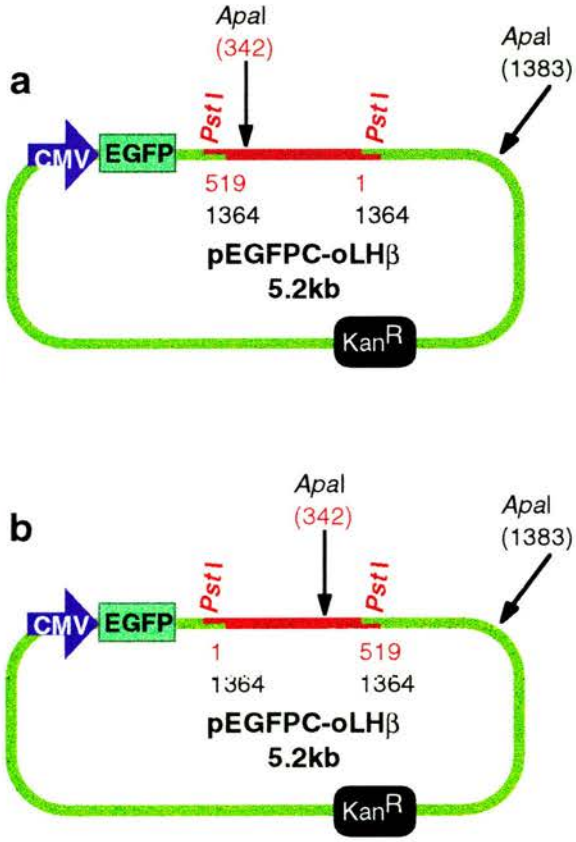

Figure 3.2.5c: Schematic representation of the screening strategy employed to determine orientation of the ovine LHβ cDNA after ligation with pEGFP-C3.

a) *Apa*I digestion of the pEGFP-C3 vector containing the ovine LHβ cDNA in the reverse orientation in regard to the CMV promoter should yield fragments of 4884 and 362bp. b) Similar digestion of a construct containing the ovine LHβ cDNA in the same orientation as the CMV promoter should yield fragments of 5226 and 197bp. Figures shown in red refer to the oLHβ cDNA sequence.

3.2.6 The EGFPC-oFSHβ fusion Construct

The oFSHβ subunit cDNA in pSP72 was a kind gift from T.E.Adams (Aus). Excision of the oFSHβ cDNA required digestion with *Pvu*II. Using GeneJockeyII (P.Taylor, MRC CRB) pEGFPC-3 was determined to be the vector which would produce an ORF between EGFP and the oFSHβ cDNA after ligation of the *Pvu*II and *Ecl*136II termini as depicted below (figure 3.2.6a). The strategy used to construct the EGFP-oFSHβ fusion plasmid is depicted schematically in figure 3.2.6b.

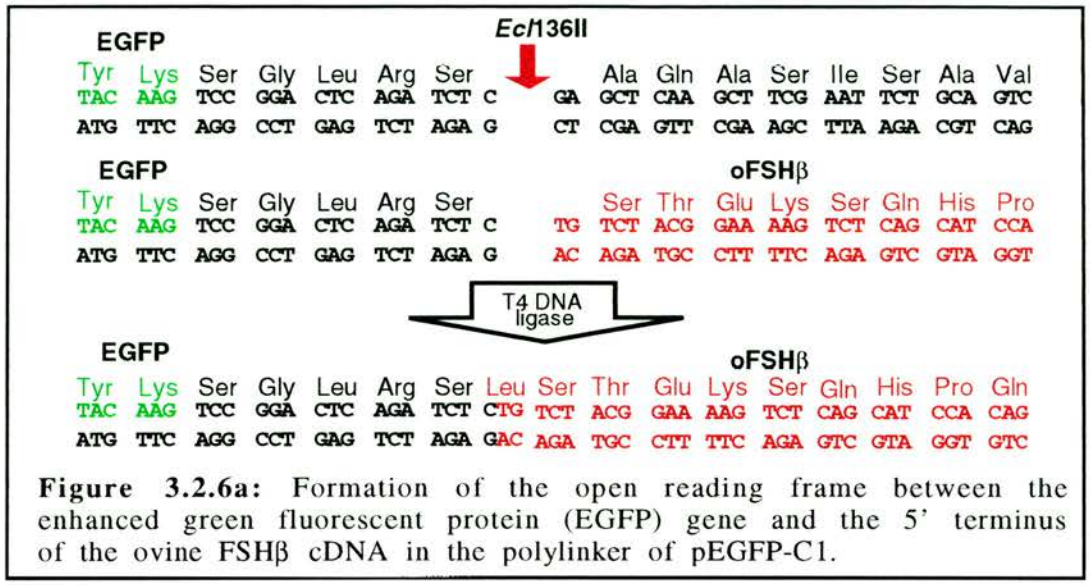

Figure 3.2.6a: Formation of the open reading frame between the enhanced green fluorescent protein (EGFP) gene and the 5' terminus of the ovine FSHβ cDNA in the polylinker of pEGFP-C1.

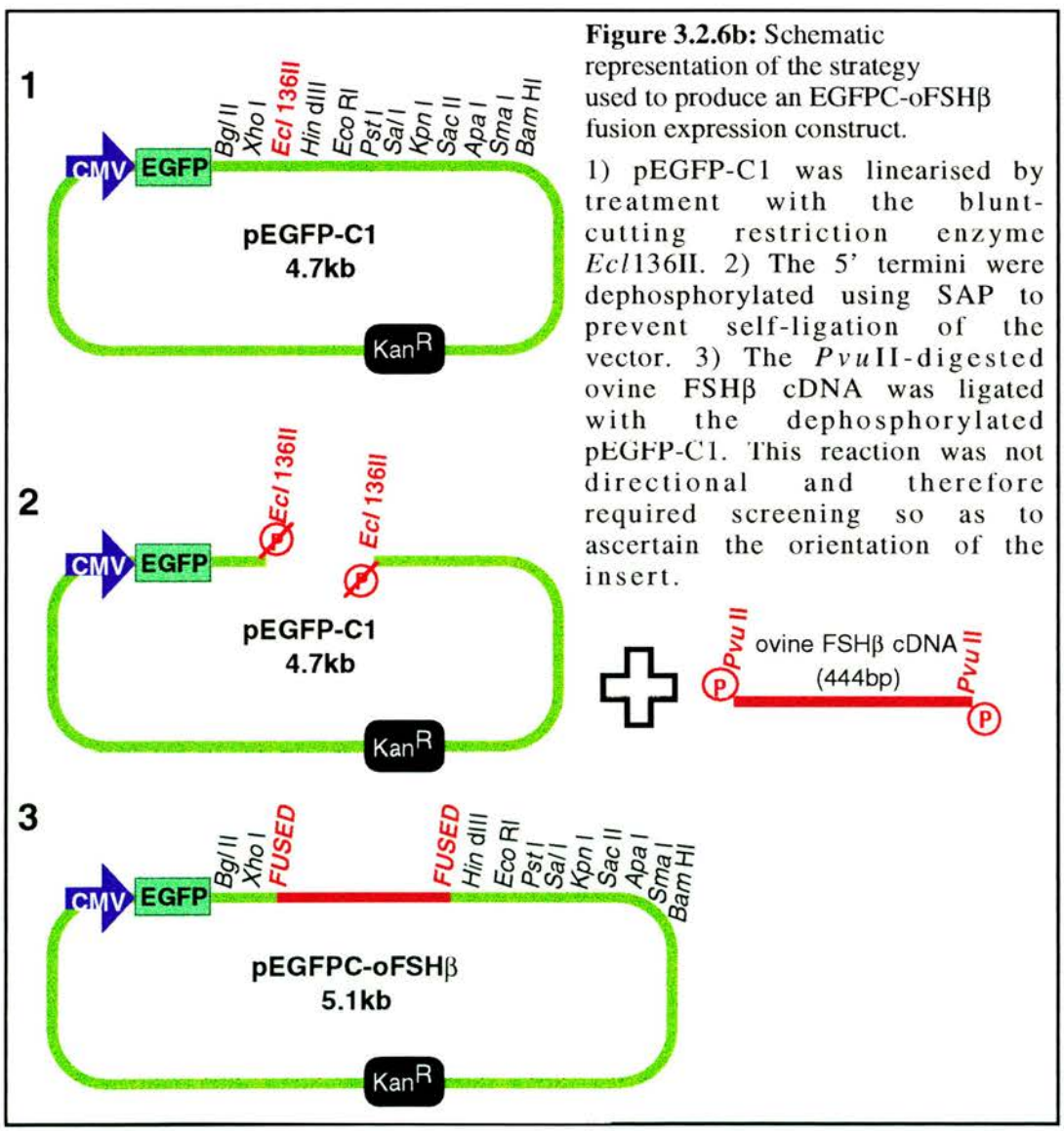

Figure 3.2.6b: Schematic representation of the strategy used to produce an EGFPC-oFSHβ fusion expression construct.

1) pEGFP-C1 was linearised by treatment with the blunt-cutting restriction enzyme *Ecl*136II. 2) The 5' termini were dephosphorylated using SAP to prevent self-ligation of the vector. 3) The *Pvu*II-digested ovine FSHβ cDNA was ligated with the dephosphorylated pEGFP-C1. This reaction was not directional and therefore required screening so as to ascertain the orientation of the insert.

pSP72/oFSHβ cDNA was digested with *Pvu*II and the insert extracted after agarose gel electrophoresis. The pEGFP-C1 vector was similarly digested with *Ecl*136II prior to dephosphorylation with SAP. The ligation reactions using Ready-to-Go™ ligase tubes were carried out in accordance with the manufacturers guidelines with the exception that incubation at the recommended temperature of 16°C was extended to approximately 16 hours. 2µl of each ligation was used to transform MAXefficiency *E.coli* DH5α competent cells (GibcoBRL, UK). Determination of the insert orientation in isolated clones was undertaken by restriction digest using *Pst*I (see figure 3.2.6c). Large-scale preparation of plasmid DNA from a positive clone was undertaken as described in section 2.3.10.

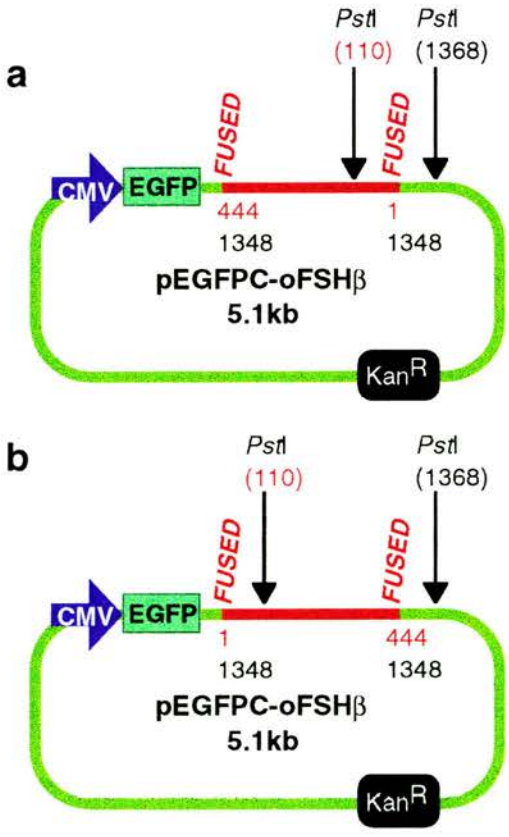

Figure 3.2.6c: Schematic representation of the screening strategy employed to determine orientation of the ovine FSHβ cDNA after ligation with pEGFP-C1.

a) *Pst*I digestion of the pEGFP-C1 vector containing the ovine FSHβ cDNA in the reverse orientation in regard to the CMV promoter should yield fragments of 5047 and 130bp. b) Similar digestion of a construct containing the ovine FSHβ cDNA in the same orientation as the CMV promoter should yield fragments of 4821 and 356bp. Figures shown in red refer to the oFSHβ cDNA sequence.

3.2.7 The CAT Reporter Construct

Chloramphenicol acetyltransferase (CAT) activity can be measured accurately by the method described in section 2.5.3. Use of a reporter construct which expresses an easily measured exogenous protein allows standardisation of protein assay results between individual samples with

regard to transfection efficiency. Using the same mammalian expression vector pcDNA3, a CAT cDNA in pB9 (P.Brown, MRC CRB) was subcloned using the strategy represented schematically in figure 3.2.7a.

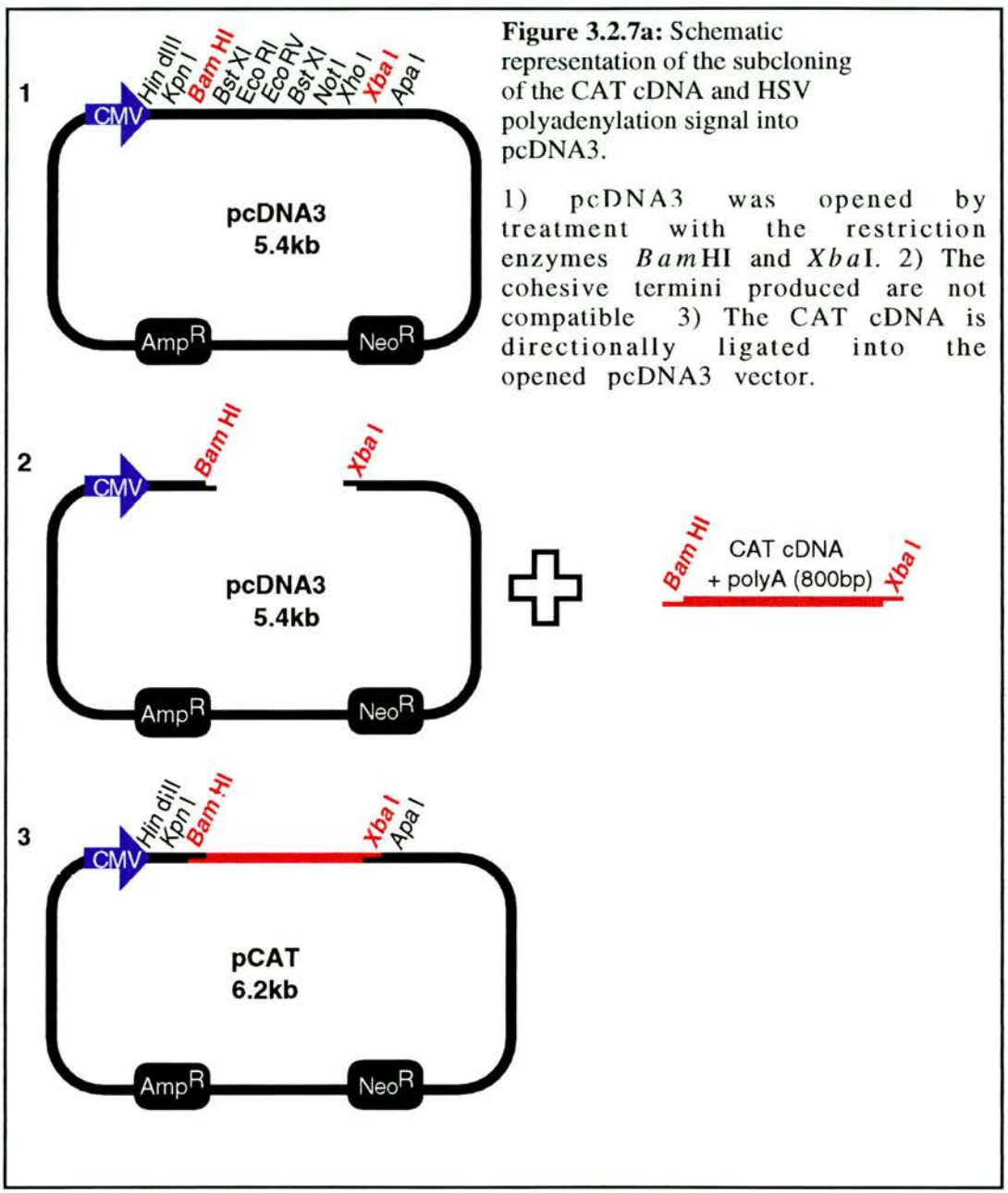

Figure 3.2.7a: Schematic representation of the subcloning of the CAT cDNA and HSV polyadenylation signal into pcDNA3.

1) pcDNA3 was opened by treatment with the restriction enzymes *Bam*HI and *Xba*I. 2) The cohesive termini produced are not compatible 3) The CAT cDNA is directionally ligated into the opened pcDNA3 vector.

Excision of the 800bp CAT cDNA and polyadenylation signal (polyA) was undertaken using *Bam*HI and *Xba*I. pcDNA3 was similarly subjected to *Bam*HI and *Xba*I digestion. Gel extraction of the ~800bp CAT/polyA and 5370bp pcDNA3 fragments was undertaken as described in section 2.3.3. The CAT cDNA and vector were ligated by methods described previously (2.3.7)

and transformed into subcloning efficiency *E.coli* DH5α cells. Screening of plasmid DNA was carried out by digestion with *Bam*HI and *Xba*I. Further verification of the plasmid structure was achieved by *Pst*I digestion as shown in figure 3.2.7b. Large-scale preparation of the positive clone was undertaken as described in section 2.3.10.

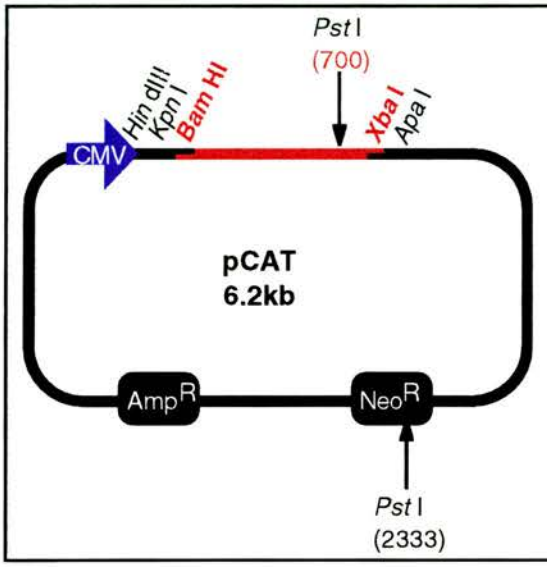

Figure 3.2.7b: Diagnostic restriction digest of pcDNA3 containing the CAT cDNA and HSV polyadenylation signal.

*Pst*I digestion of pcDNA3 containing the CAT cDNA and HSV polyadenylation signal should produce 2 fragments of 4721 and 1449bp.

3.3 Results

3.3.1 The Ovine αGSU Expression Construct

CIP-treatment of the *Eco*RI-linearised pcDNA3 produced a fragment with migration by agarose gel electrophoresis equivalent to approximately 5.4kb (figure 3.3.1ai). The corresponding *Eco*RI digestion of pGEM3 successfully excised the ovine αGSU cDNA which was visualised by agarose gel electrophoresis (figure 3.3.1aii). Miniprep DNA was initially screened by an increase in size versus the empty pcDNA3 vector. *Pst*I screening of these constructs distinguished plasmids containing the insert in the correct orientation by the absence of a 581bp fragment (figure 3.3.1bi). Positive clones were further analysed by digestion with *Eco*RI to excise the insert (3.3.1bii). This gel confirmed that CIP treatment had not damaged the *Eco*RI termini.

After large-scale preparation of the pcDNA3 vector containing the ovine αGSU cDNA, an aliquot of the plasmid was linearised by digestion with *Hin*dIII cutting within the polylinker. The resulting fragment was visualised by agarose gel electrophoresis and corresponded to the predicted

size of the construct of 6162bp (figure 3.3.1biii). This construct was designated poαGSU.

3.3.2 The Ovine FSHβ cDNA Expression Construct

*Pvu*II digestion of pSP72/oFSHβ cDNA successfully excised the insert apparent by the 444bp fragment visualised by agarose gel electrophoresis (figure 3.3.2ai). Gel extraction of this fragment yielded only 37.5ng as estimated by agarose gel electrophoresis which was sufficient for a single ligation reaction (figure 3.3.2aii). Preparation of pcDNA3 by digestion with *Eco*RV linearised the vector (figure 3.3.2aiii) prior to treatment with SAP. Ligation controls containing no insert produced no transformants indicating the high efficiency of SAP treatment in preventing self-ligation of the vector. Screening of eight clones by *Apa*I digestion demonstrated an absence of the 441bp fragment in one sample (figure 3.3.2bi). Although the 87bp fragment was not visible the subsequent *Pst*I digestion clearly showed the 4061, 1726 and 105bp fragments indicating the structural integrity of the plasmid (figure 3.3.2bii). This construct was designated poFSHβ.

3.3.3 oFSHβ Genomic DNA Expression Construct

The 900bp *Hin*dIII-*Pst*I fragment containing 5' UT sequences of the oFSHβ genomic sequence was successfully excised from pGEM3 (figure 3.3.3ai). The pBluescript KS+ was similarly digested and is also shown in figure 3.3.3ai . Both fragments were successfully extracted from the agarose gel (figure 3.3.3aii). pBluescript KS+ DNA containing the 900bp fragment was isolated from transformants and digested with *Xho*I excising the 226bp sequence containing the transcriptional start. This fragment was subsequently extracted from the agarose gel (figure 3.3.3bi).

The pBluescript KS+ vector containing the remaining oFSHβ sequences but with the HSV-IE 3' UT in place of the oFSHβ 3' UT was digested with *Xho*I and extracted from the agarose gel. Following CIP treatment, the 5931bp dephosphorylated plasmid (figure 3.3.3bii) was ligated with the 226bp *Xho*I fragment. Miniprep DNA was screened by *Hin*dIII digestion with the production of three band patterns (figure 3.3.3ci). The single band produced by linearisation of empty vector is apparent in samples 1, 2 and 5. Ligation of the 226bp fragment in the reverse orientation produced 4076 and 1855bp fragments as predicted by the screening strategy. Positive samples produced a 3894bp fragment with similar migration to the 4076bp fragment present in reverse samples. The difference between the 1885bp fragment in the negative samples and the larger 2037bp fragment

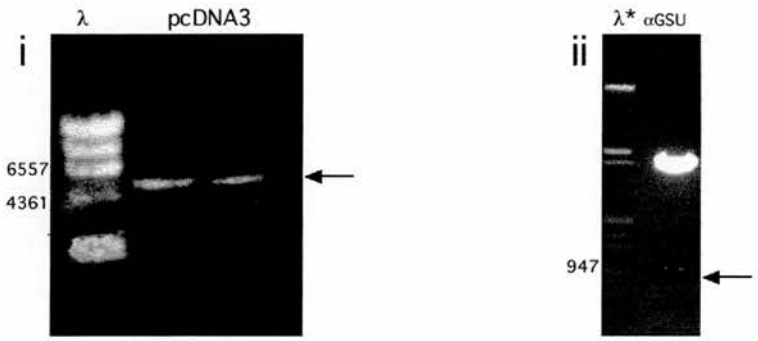

Figure 3.3.1a: Preparation of pcDNA3 and the ovine αGSU cDNA for ligation.

i) pcDNA3 was linearised by *Eco*RI digestion and treated with CIP. The band in both lanes corresponds to approximately 5.47kb. 'λ' denotes 1μg of the λ*Hin*dIII size marker. ii) The pGEM3 clone containing the ovine αGSU cDNA was digested with *Eco*RI. The photograph shows the position of the fragment excised from the gel prior to extraction. The position of this fragment corresponds to the 716bp cDNA. 'λ*' denotes 1μg of the λ*Hin*dIII/*Eco*RI size marker . Both gels contained 0.8% agarose and were run in TAE buffer.

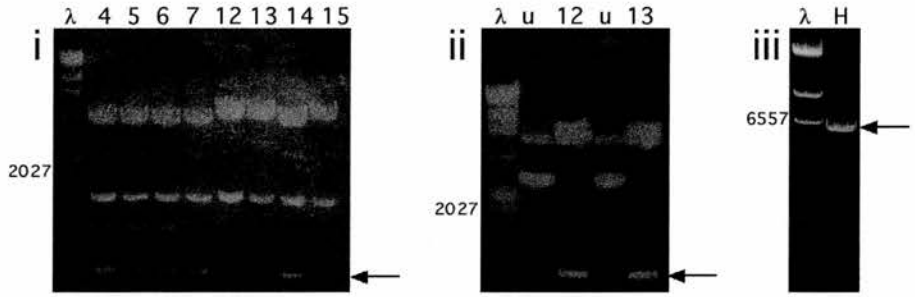

Figure 3.3.1b: Screening pcDNA3 for insertion of the ovine αGSU cDNA.

i) *Apa*I digestion of pcDNA3 constructs containing the ovine αGSU cDNA. The absence of a 581bp fragment (arrow) indicated insertion in the correct orientation for samples 12, 13 and 15. ii) *Eco*RI digestion of samples 12 and 13 produced the 716bp ovine αGSU cDNA. 'u' denotes uncut plasmids. iii) The *Hin*dIII-linearised construct exhibits the correct size of approximately 6162bp. All gels contained 0.8% agarose and were run in TAE buffer. 'λ' denotes 1μg of the λ*Hin*dIII size marker.

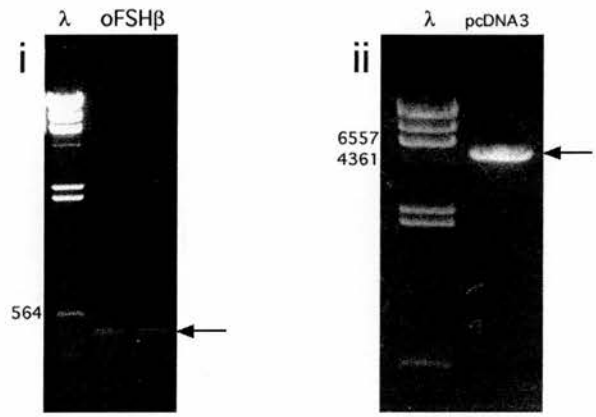

Figure 3.3.2a: Preparation of pcDNA3 and the ovine FSHβ cDNA for ligation.

i) The gel shows the extracted 444bp cDNA from *Pvu*II digestion of pGEM3/oFSHβ cDNA (arrow). ii) The *Eco*RV-linearised and SAP-treated pcDNA3 exhibits the correct size of approximately 5.47kb (arrow). Both gels contained 0.8% agarose and were run in TAE buffer. 'λ' denotes 1μg of the λ*Hin*dIII size marker.

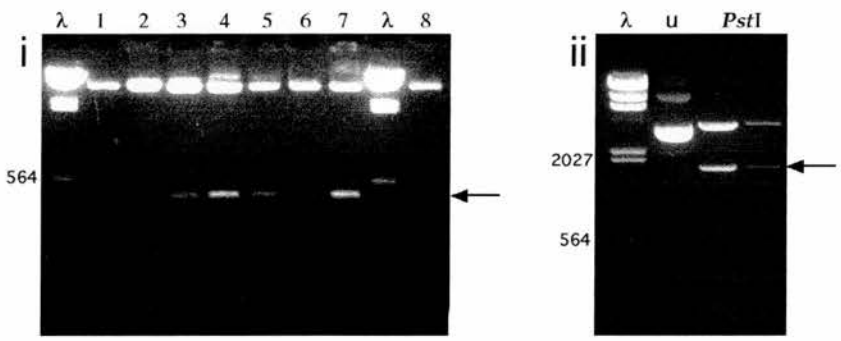

Figure 3.3.2b: Screening pcDNA3 for insertion of the ovine FSHβ cDNA.

i) *Apa*I digestion of miniprep DNA demonstrated the absence of the 441bp fragment (arrow) in sample 2 indicating the presence of the oFSHβ cDNA in the correct orientation. The 87bp fragment was not resolved in this positive sample. ii) *Pst*I digestion of sample 2 after large-scale DNA preparation. Both dilutions of the restriction digest contain the predicted 4061 and 1726bp fragments although the 105bp fragment was not resolved. 'u' denotes uncut construct. Both gels contained 0.8% agarose and were run in TAE buffer. 'λ' denotes 1μg λ*Hin*dIII marker.

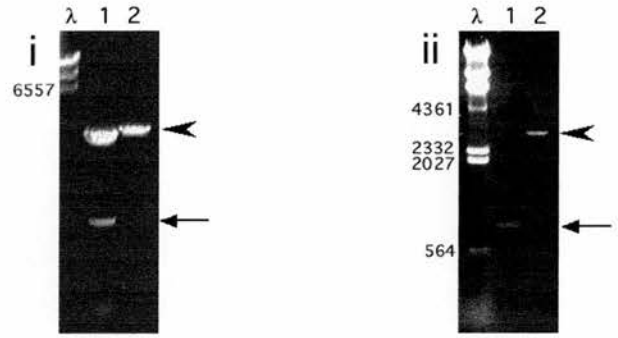

Figure 3.3.3a: Preparation of pBluescript KS+ and the 900bp fragment containing the ovine FSHβ transcriptional start site for ligation.

i) Both plasmids were digested with *Hin*dIII and *Pst*I. The 900bp fragment is present in lane 1 (arrow). The approximate 3kb band in lane 2 represents the linearised pBluescript KS+ vector (arrowhead). ii) The extracted fragments appear free of contamination and correspond to the original digestion. Both gels contained 0.8% agarose and were run in TAE buffer. 'λ' denotes 1μg of λ*Hin*dIII marker.

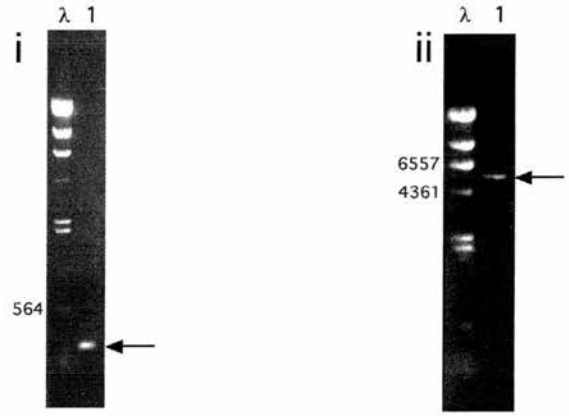

Figure 3.3.3b: Preparation of the 226bp *Xho*I fragment containing the ovine FSHβ transcriptional start and the pBluescript KS+ construct containing the 5'-truncated ovine FSHβ gene and HSV-IE polyA for ligation.

i) pBluescript KS+ containing the 900bp *Hin*dIII/*Pst*I fragment of the ovine FSHβ gene was digested with *Xho*I producing a 226bp fragment (arrow). The gel (lane 1) shows this fragment after extraction from the larger vector sequences. ii) The extracted *Xho*I digestion of pBluescript KS+ construct containing the 5'-truncated ovine FSHβ gene and HSV-IE polyA is shown in lane 1 after CIP treatment. The construct appears at approximately 5.9kb as expected. Both gels contained 0.8% agarose and were run in TAE buffer. 'λ' denotes 1μg of λ*Hin*dIII marker.

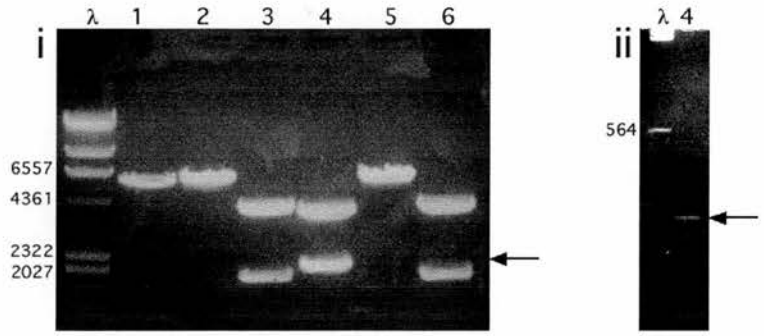

Figure 3.3.3c: Screening the pBluescript KS+ construct containing the 5'-truncated ovine FSHβ gene and HSV-IE polyA for insertion of the 226bp *Xho*I fragment containing the ovine FSHβ transcriptional start.

i) *Hin*dIII digestion of miniprep DNA produced three bands patterns. A single band demonstrated the absence of the insert (lanes 1, 2 & 5). Two bands corresponding to 4076 and 1855bp indicate that the construct contains the insert in the incorrect orientation (lanes 3 & 6). Lane 4 shows the 2037bp fragment (arrow) which indicates the correct orientation of the 226bp *Xho*I insert containing the ovine FSHβ transcriptional start. This gel contained 0.8% agarose and was run in TAE buffer. ii) Digestion of the positive sample (4) with *Xho*I excised the 226bp fragment (arrow) demonstrating the integrity of the restriction sites at which it was ligated. This gel contained 2% agarose and was run in TBE buffer. 'λ' denotes 1μg of λ*Hin*dIII marker.

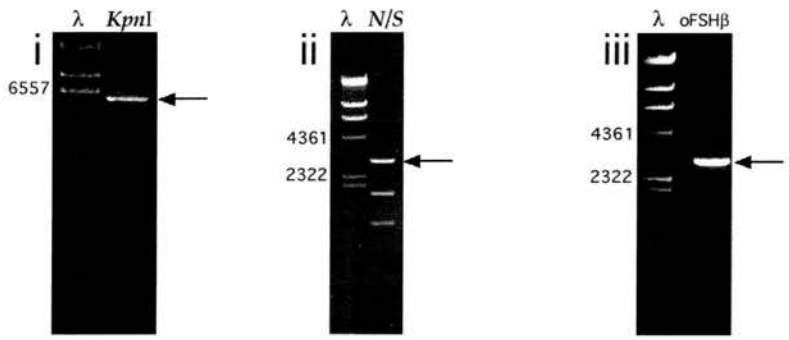

Figure 3.3.3d: Excision of the ovine FSHβ gene and HSV-IE polyA from pBluescript KS+.

i) *Kpn*I digestion linearised the plasmid construct (arrow) with its size corresponding to approximately 5.8kb as expected. ii) Double digestion with *Not*I and *Sca*I excised the modified oFSHβ gene and cut the vector respectively. The 3049bp *Kpn*I-*Not*I fragment (arrow) represents the oFSHβ gene with the smaller bands being derived from the vector. iii) The extracted 3049bp *Kpn*I-*Not*I fragment (arrow) is shown at the correct size and free of contaminating pBluescript KS+ vector fragments. These gels contained 0.8% agarose and were run in TAE buffer. 'λ' denotes 1μg of λ*Hin*dIII marker.

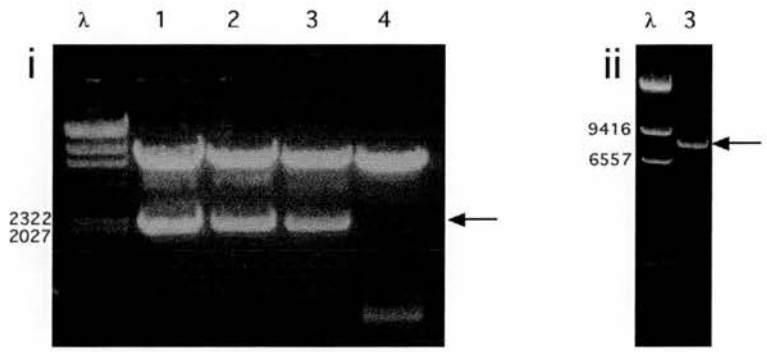

Figure 3.3.3e: Screening of the pcDNA3 for insertion of the ovine FSHβ gene and HSV-IE polyA.

i) *Hin*dIII digestion produced the 2037bp fragment (arrow) in minipreps 1-3 indicating correct insertion of the oFSHβ gene and HSV-IE polyA . ii) Linearisation with *Sca*I produced the expected 8429bp band (arrow). These gels contained 0.8% agarose and were run in TAE buffer. 'λ' denotes 1μg of λ*Hin*dIII marker.

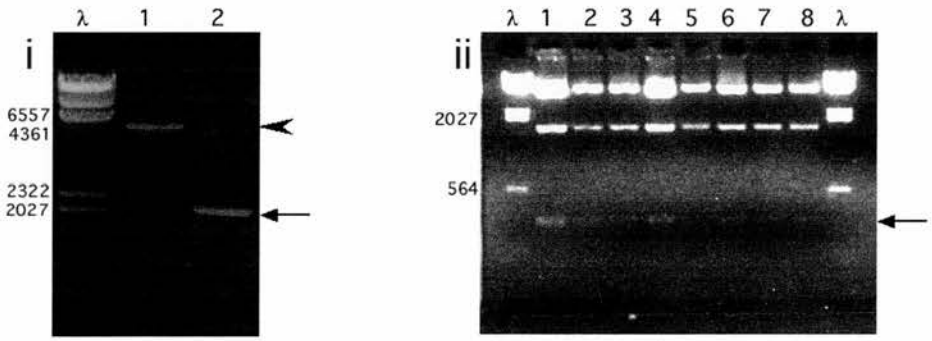

Figure 3.3.4a: Subcloning the human CgA cDNA into pcDNA3.

i) The pcDNA3 (lane 1) and hCgA cDNA (lane 2) fragments were extracted after *Hin*dIII and *Eco*RI digestion. The pcDNA fragment corresponds to approximately 5.47kb (arrowhead) and the hCgA cDNA corresponds to approximately 1890bp (arrow). ii) Screening of recombinant plasmids by *Bam*HI and *Hin*dIII digestion produced the 236bp fragment (arrow) and indicated correct ligation of the cDNA. Both gels contained 0.8% agarose and were run in TAE buffer. 'λ' denotes 1μg of λ*Hin*dIII marker.

produced by digestion of positive samples such as sample 5 is clearly resolved on this gel. Digestion of a positive sample with *Xho*I excised the 226bp fragment verifying its presence in the intact construct (figure 3.3.3cii). After successful linearisation of the construct with *Kpn*I (figure 3.3.3di) digestion with *Not*I and *Sca*I was undertaken. The activity of *Not*I excised the 3049bp fragment containing the oFSHβ-HSV sequence and *Sca*I digested the vector producing two smaller fragments of 1767bp (*Kpn*I-*Sca*I) and 1103bp (*Sca*I-*Not*I) (figure 3.3.3dii). The gel extracted 3049bp fragment (figure 3.3.3diii) was ligated with pcDNA3 *Kpn*I-*Not*I. Plasmids isolated from several recombinant colonies produced the 2037bp fragment after digestion with *Hin*dIII (figure 3.3.3ei). Furthermore the *Sca*I-linearised construct appeared equivalent to 8429bp by agarose gel electrophoresis (figure 3.3.3eii). This construct was designated poFSHβg.

3.3.4 The Human Chromogranin A Expression Construct

Both pGEM3 containing the hCgA cDNA and pcDNA3 were successfully digested with *Hin*dIII and *Eco*RI prior to extraction from the agarose gel (figure 3.3.4ai & aii). The directional cloning of the hCgA cDNA into pcDNA3 was assessed by *Bam*HI and *Hin*dIII. This dual digestion of plasmid DNA isolated from minicultures produced the 236bp fragment corresponding to the 5' region of the hCgA cDNA (figure 3.3.4b). This construct was designated phCgA.

3.3.5 The EGFPC-oLHβ fusion Construct

*Pst*I digestion of pGEM3 containing the ovine LHβ cDNA excised the 519bp fragment (figure 3.3.5ai). The pEGFP-C3 vector linearised by *Pst*I was dephosphorylated using SAP (figure 3.3.5ai).

A single clone exhibited the 197bp fragment after *Apa*I digestion (figure 3.3.5aii). This construct was designated pEGFPC-oLHβ.

3.3.6 The EGFPC-oFSHβ fusion Construct

The oFSHβ cDNA was excised with *Pvu*II and gel-extracted as described for the poFSHβ construct (section 3.3.2). pEGFP-C1 was linearised successfully with *Ecl*136II (figure 3.3.6a). Of the six colonies screened three contained the oFSHβ cDNA in the correct orientation as determined by the presence of a 356bp fragment after *Pst*I digestion (figure 3.3.6b). According to the suppliers of pEGFP-C1 (Clontech, UK) the 500bp fragment is non-clonable ssDNA which is produced under some culture conditions by *E.coli* strains

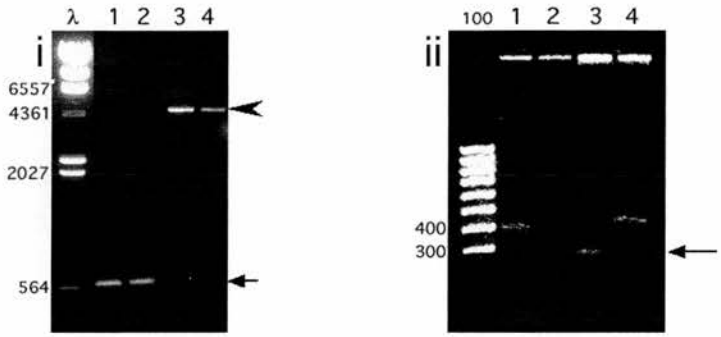

Figure 3.3.5a: Subcloning the ovine LHβ cDNA into pEGFP-C3.

i) The ovine LHβ cDNA (lanes 1&2) and pEGFP-C3 (lanes 3&4) fragments were extracted after *Pst*I digestion. The oLHβ cDNA fragment (arrow) migrates at a position larger than the 564bp marker due to a high GC content which retards its migration. The actual size of the fragment is 519bp. The SAP-treated pEGFP-C3 corresponds to approximately 4.7kb (arrowhead). The gel contained 0.8% agarose and was run in TAE buffer. 'λ' denotes 1μg of the λ*Hin*dIII marker. ii) Screening of recombinant plasmids by *Apa*I digestion produced the 137bp (also retarded due to high GC content) shown by the arrow which indicated correct ligation of the insert. This gel contained 2% agarose and was run in TBE buffer. '100' denotes the 100bp ladder used for size comparison.

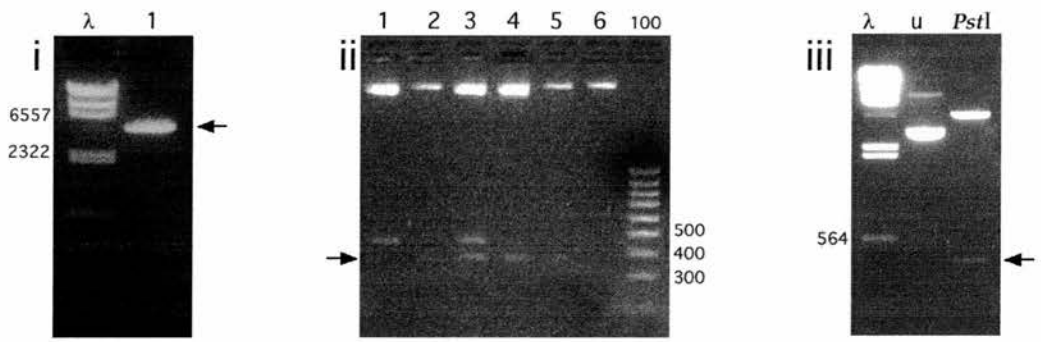

Figure 3.3.6a: Subcloning the ovine FSHβ cDNA into pEGFP-C1.

i) The pEGFP-C1 (lane 1) fragment was extracted after *Ec*l36II digestion. The SAP-treated vector corresponds to approximately 4.7kb (arrow). The gel contained 0.8% agarose and was run in TAE buffer. ii) Screening of recombinant plasmids by *Pst*I digestion produced the 356bp fragment (arrow) in samples 3 and 4 indicating correct ligation of the cDNA. A larger band (400-500 approx.) was also present in lanes 2 and 3. According to the manufacturer of the vector (Clontech) this fragment is single-stranded DNA produced under some culture conditions and is not clonable. This gel contained 2% agarose and was run in TBE buffer. '100' denotes the 100bp ladder used for size comparison. iii) After large-scale preparation of a positive clone *Pst*I digestion was repeated and again produced the 356bp fragment. 'u' denotes uncut construct. 'λ' denotes 1μg of λ*Hin*dIII marker. The gel contained 1% agarose and was run in TBE buffer.

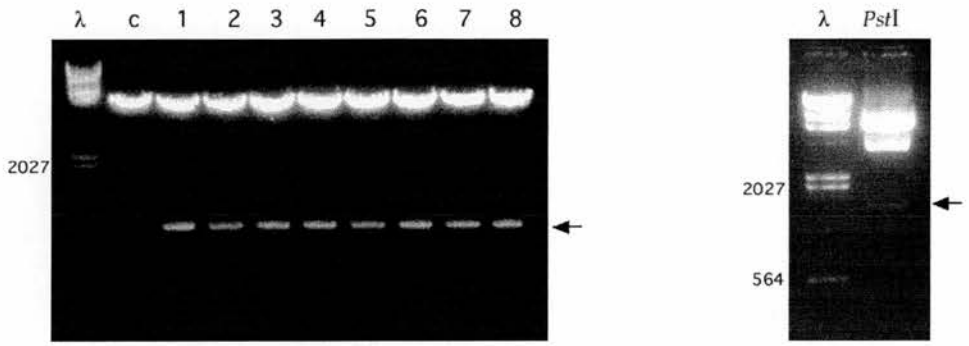

Figure 3.3.7a: Screening pcDNA3 for insertion of the CAT cDNA.

i) Miniprep DNA from samples 1-8 produced the 800bp CAT insert (arrow) after *Bam*HI/*Xba*I digestion. The 'empty' pcDNA3 vector produced no insert (lane c). ii) The *Pst*I digestion was not complete as indicated by the presence of additional bands. However the diagnostic 1449bp fragment is present (arrow) indicating the structural integrity of the construct. These gels contained 0.8% agarose and were run in TAE buffer. 'λ' denotes 1μg of λ*Hin*dIII marker.

harbouring this plasmid. Agarose gel electrophoresis of the construct demonstrated its supercoiled state when intact and production of a 356bp fragment after *Pst*I digestion (figure 3.3.6c). This construct was designated pEGFPC1-oFSHβ.

3.3.7 The CAT Reporter Construct

Excision of the CAT gene and polyA fragment from pB9 produced a fragment of approximately 800bp. Similar digestion of pcDNA3 produced a 5428bp fragment. Recombinant plasmids were screened by *Bam*HI and *Xba*I digestion with all eight clones producing the 800bp fragment indicating the presence of the CAT-polyA sequence (figure 3.3.7a). Digestion of the final plasmid construct with *Pst*I produced the diagnostic 1449bp fragment (figure 3.3.7b). This reporter construct was designated pCAT.

3.4 Discussion

The majority of inserts used to engineer the constructs described in this chapter were cDNAs. However both oFSHβ and oLHβ were also engineered as genomic constructs (poFSHβg and poLHβg - P.Brown). This was undertaken for two main reasons. Firstly work carried out by Irving Boime's group established that genomic constructs for the gonadotrophin β-subunits were expressed efficiently in cell culture (Keene *et al.*, 1989). Introns have been postulated to enhance expression levels *in vitro*. In addition, the presence of introns would facilitate further cloning procedures such as 'exon shuffling' and generation of oLHβ/oFSHβ hybrid molecules. Exclusive use of cDNAs could rule out certain manipulations due to a paucity of suitable restriction sites. The similar 3 exon arrangement of the β-subunit genes may allow relatively straightforward shuffling experiments to be carried out in cell culture initially and then in transgenics and allow elucidation of putative sorting motifs located within the specific β-subunit exons.

The approaches used for subcloning the cDNA and genomic sequences into pcDNA3 or pEGFP-C1/3 relied mainly on traditional enzymatic cleavage and ligation techniques. The structural integrity of the constructs described during this chapter has been analysed by carefully designed restriction mapping. However this by itself does not guarantee expression of the gene inserted into the polylinker of the expression vector. Sequence data could reveal structural anomalies in the event of expression problems. Sequencing was not undertaken as expression of all constructs including those provided from other sources (i.e. poLHβg, pbChrB73, pbSgII61) was

confirmed by RT-PCR, RIA and indirect immunofluorescence in transiently transfected mammalian cells (see chapters 4, 5 and 6).

The pcDNA3 vector has recently been superseded by the development of pcDNA6 (Invitrogen, NL). This vector is based on the design of pcDNA3 but contains a selective marker which confers resistance to the potent antibiotic Blasticidin and contains a poly-histidine sequence downstream of the polylinker (Invitrogen, NL). Future expression studies based on selection of stable clones would benefit from the reduced selection time required when using this vector. In addition the histidine tag may allow immunocytochemical detection of antigens for which antisera are limited or inefficient.

Further modifications or possible enhancements to *in vitro* expression could be facilitated by using EGFP fusion vectors that allow fusion to the amino-terminus of the fluorescent protein gene (Invitrogen, NL). The expression of a fused protein from a construct of this type requires removal of the stop codon from the 3' region of the inserted gene. However engineering these constructs for oLHβ would be further complicated by the necessary removal of the sequence encoding the 7aa hydrophilic tail which is cleaved during secretion (Bousfield *et al*, 1994), thus EGFP carboxy-terminal fusion vectors were used during these studies. Without removal of this sequence the fusion protein would be cleaved. Other fluorescent proteins in which the EGFP gene has been mutated specifically to alter its excitation and emission spectra are currently being developed. Blue- and yellow-shifted variants are only available as part of fusion vectors within limited reading frames and require specialised confocal microscopy equipment such as an ultraviolet laser source and specific filters but may be used in the future.

Other approaches for expression construct production include PCR amplification of the insert. This allows engineering of specific restriction sites onto the termini of the insert facilitating directional cloning into the vector of choice. This approach may be necessary for subcloning of pbChrB73 and pbSgII61 into shuttle vectors as these constructs do not contain suitable restriction sites for excision of the inserts. Due to the contamination-prone nature of PCR, the insert would require verification by sequencing.

The following three chapters will describe the application of the constructs produced during this chapter.

Chapter Four

Gonadotrophin Secretion from a Human Choriocarcinoma Cell line

4.1 Introduction

The JEG3 choriocarcinoma cell line is of human origin. This cell line expresses the α and β subunits of human chorionic gonadotrophin (hCG) which combine to produce the active hormone that is then secreted via the constitutive pathway (Kohler & Bridson, 1971). Alpha subunit gene expression is positively regulated by cyclic AMP (cAMP) leading to a ten-fold increase in expression. The cAMP response element (CRE) found upstream of the alpha subunit gene consists of two 18-bp repeats containing the palindrome TGACGTCA. This CRE resembles those found in other mammalian systems such as the rat somatostatin and human proenkephalin gene (Delegeane & Mellon, 1987).

Until recently no cell line existed which secreted pituitary gonadotrophins through a regulated pathway. At this time the JEG3 cell line provided the only model for studying gonadotrophin secretion. CG is similar in structure to LH and FSH showing 85% and 36% amino acid sequence homology, respectively (Lapthorn *et al.*, 1994). The hCGβ subunit is the largest of the gonadotrophin β subunits at 145 amino acids due to the presence of a 31 amino acid hydrophilic carboxy-terminal peptide which increases the rate of gonadotrophin secretion (Muyan *et al.*, 1996).

The apparent lack of a regulated pathway in the JEG3 cell line allows positive measures to be taken towards inducing formation of such a pathway. As granins have been widely implicated in the regulated pathway of neuroendocrine cells (see 1.6.5) their role may be determined by expression in a non-regulated secretory cell line. Formation of a regulated pathway leading to storage and ligand-stimulated release of hCG would implicate granin expression as a key factor in the differential sorting of pituitary gonadotrophins.

There are two approaches with which to study the expression of exogenous genes within mammalian cells; transient and stable transfections.

4.1.1 Transient transfections

Methods to induce uptake of DNA by mammalian cell lines include those mediated by calcium phosphate (Chen & Okayama, 1987), cationic lipids, DEAE dextran, microinjection or electroporation (for a review see (Gorman, 1986)). Calcium phosphate and lipid-mediated methods used within this study rely on forming complexes with the plasmid DNA that interact more efficiently with the plasma membranes of mammalian cells. The transient nature of this type of transfection relates to the duration of exogenous gene expression which persists for up to 80 hours. Transfected DNA constructs may penetrate the nuclear envelope or remain cytosolic. Transcription of transfected genes is often driven by the cytomegalovirus (CMV) or SV40 promoters and requires the host's transcription machinery. Transfection of cell lines is carried out during their exponential growth phase. Cells within this highly mitotic population will obviously exhibit significant membrane breakdown and reconstitution. Although the role of mitotic cell division may be crucial to the initial uptake of DNA, the concomitant nuclear membrane breakdown may permit further entry of the exogenous plasmid DNA. It is possible to conceive that leakage of RNA polymerase II and transcription factors during mitosis may permit some expression of cytosolic plasmids. However it may be more likely that plasmids which gain entry into the nucleus provide the majority of exogenous gene expression due to the higher concentration of the necessary transcription proteins and cofactors.

Due to the high number of plasmid molecules used during transfection it is likely that mixtures of two or more different plasmids may result in expression relative to the proportion of the plasmid in the original mixture. This hypothesis allows cotransfection of multiple constructs at various ratios to each other in an attempt to alter their relative expression rates assuming that the toxicity of the plasmids and the promoters are similar in all constructs cotransfected.

4.1.2 Stable transfections

Stable transfections are initially undertaken in a similar way to the transient variety however for stable transfections all plasmids must contain a selectable marker gene. In pcDNA3 resistance to the neomycin analogue G418 is conferred by the neo^R gene which encodes an

aminoglycoside phosphotransferase (for more detail refer to the previous chapter). Stable transfection requires a selectable marker to exert a metabolic pressure upon the transfected cell which over time may lead to integration of the plasmid containing the marker as well as the inserted gene into the genome. Although the rate at which DNA integrates may be significantly lower than the rate of DNA uptake, stably transfected cell populations have the advantage of long-term exogenous gene expression therefore obviating the need for repeated transient transfection. Furthermore the clonal selection of colonies surviving exposure to the antibiotic in theory produces populations of genetically identical mammalian cells that express the transfected gene or genes at identical levels. This second factor underlies the main disadvantage of transients in that exogenous gene expression varies considerably between individuals. Induction of high level gene expression by treatment of stably transfected Vero cells with sodium butyrate has been reported (Wacker *et al.*, 1997) although the exact mechanism of action for this agent remains to be determined. Although previously unsuccessful when applied to JEG3 cells (A.Howe - personal communication) sodium butyrate and butyric acid have been used in various cell lines to increase transfection efficiency (Sambrook *et al.*, 1989).

4.2 Materials and Methods

4.2.1 Calcium Phosphate-based transfection

Optimisation of this technique originally described by Graham & Van der Eb (Graham & Van der Eb, 1973) for use with the JEG3 cell line was carried out previously (Howe, 1995). Cells at approximately 60% confluency were washed twice in DPBS before being replaced with cDMEM and incubated for 2 hours under normal conditions. The transfection mix containing the DNA and $CaPO_4^-$ complex was prepared as follows. For duplicate transfections in 6cm diameter dishes 20µg DNA was added to the bottom of a 6ml polypropylene centrifuge tube containing sterile water so that the diluted DNA solution was 450µl in total. 50µl 2.5M $CaCl_2$ was gently added to

the bottom of the tube after which 500µl *N*-[2-hydroxyethyl] piperazine-*N'*-[2-ethane sulfonic acid] (HEPES)-buffered saline pH7 (HBS - see Appendix I) was added in a similar manner. A 500µl volume of air was then slowly released at the bottom of the tube so as to mix the constituent parts of the transfection solution. This mixture was then incubated at room temperature for 30 minutes. 500µl of the transfection mix was overlaid on each of the dishes and incubated under normal culture conditions for 16 hours. Two DPBS washes were carried out prior to replacement of the media. Culture of the transfected cells was then carried out under normal conditions for 24 to 72 hours after which analysis of the cells and media was carried out by methods described elsewhere in this chapter (Howe, 1995).

4.2.2 Optimisation of Lipid-based transfection

All transfection procedures are toxic towards mammalian cells. Toxicity may be caused by small amounts of bacterial endotoxins within preparations of DNA or adverse effects of the transfection agent used. These toxic effects may be reduced if exposure is limited however this requires an efficient transfection agent.

The β-galactosidase-expressing plasmid pcDNA3.1/His/lacZ was transfected into JEG3 cells by the various methods under assessment. Colorimetric staining of fixed cells allowed expression of β-galactosidase to be detected in transfected individuals (see section 2.4.9).

Existing calcium phosphate-based transfection of JEG3 cells required overnight incubation of the transfection mix and cells. Furthermore despite thorough optimisation of this technique, transfection efficiency was relatively low (Howe, 1995). In order to achieve transfection of JEG3 cells with higher efficiency, shorter incubation time and less labour intensity, alternative lipid-based methods were evaluated.

Approximately $4x10^4$ cells were plated 16-20 hours prior to the transfection. For the optimisation process 12-well cell culture plates were routinely used. The three remaining parameters which were varied included the amount of DNA added per well, the ratio of lipid:DNA and duration of transfection. Clonfectin™ (Clontech, USA) and N-[1-(2,3-Dioleoyloxy)propyl]-*N,N,N*-trimethylammonium methylsulphate (DOTAP;

Boehringer Mannheim, UK) were used in accordance with manufacturers guidelines. The PerFect™ lipid system (Invitrogen, NL) which contains eight different lipid mixes for evaluation was also used in accordance with manufacturers guidelines. DMEM (containing no antibiotics or FCS) was used for preparation of the transfection mixture and the subsequent incubation. cDMEM was used for the post-transfection incubation. Expression was assessed for each transfection procedure 48 hours posttransfection by β-galactosidase staining (section 2.4.9).

4.2.3 Optimised JEG3 Transfection

JEG3 cells were seeded in an appropriate culture vessel at approximately 4 x 10^5 cells/cm^2 16-20 hours prior to transfection. A ratio of 6:1 for PerFect™ lipid 4 (Pfx4) to DNA was used. The actual amount of DNA transfected was proportional to the size of culture vessel used. For example 2.5μg of DNA was applied to each chamber of a 12-well plate which therefore required 15μg of Pfx4. The lipid and DNA mixes were prepared according to the manufacturers guidelines and mixed gently prior to addition to the DPBS-washed cells. Incubation of the transfection mix at 37°C and 5% CO_2 for 3-4 hours was followed by a single DPBS wash and replacement of cDMEM. All liquid manipulations were undertaken with extreme care not to detach the cells. This was achieved by tilting the culture vessel and applying the liquid to the vessel wall as opposed to addition directly to the cell monolayer. Further incubation of the cells at 37°C and 5% CO_2 was undertaken for 24-72 hours to allow expression of transfected genes.

4.2.4 Upregulation of hCG Expression

αGSU and hCGβ expression were upregulated by exposure to 1mM dibutyryl 3',5'-cyclic adenosine monophosphate (cAMP; Sigma-Aldrich, UK) (Jameson *et al.*, 1987; Howe, 1995). A working dilution of 100mM dibutyryl cAMP was prepared on the day of use. Incubation of JEG3 cells under normal culture conditions was carried out for 24 hours in the presence of 1mM dibutyryl cAMP.

4.2.5 Immunoradiometric Assay (IRMA) of hCG

This assay supplied by Serono (France) was performed by following the manufacturers guidelines for the quantitative method with the following modifications. The volumes of standard and sample used were 25µl and the volume of ^{125}I-anti-hCG reagent was also reduced by half to 250µl.

4.2.6 Granins and hCG Secretion

Plasmid constructs containing the full-length cDNAs for bovine CgB (pbChrB73) and bovine SgII (pbSgII61) were kind gifts from R. Fischer-Colbrie (University of Innsbruck, Austria). These vectors contain the SV40 promoter whereas the hCgA expression construct (phCgA) contains the CMV promoter.

In order to verify that the SV40 promoter could drive expression of the bCgB cDNA in transfected JEG3 cells Northern analysis was carried out. 10µg of total RNA extracted from the cell lysate was separated on a 1% agarose gel by electrophoresis under denaturing conditions. The RNA transferred to the nylon membrane was crosslinked by application of UV light and subsequently probed with 30ng of the gel extracted and ^{32}P-labelled bCgB cDNA sequence. Visualisation and analysis of the blot was carried out using a STORM™ PhosphorImager (Molecular Dynamics, UK).

All three constructs were transfected into JEG3 cells using the $CaPO_4$ method. An initial study was carried out in which each of the constructs was transfected into 3 separate 35mm diameter dishes seeded with approximately $3.5x10^5$ JEG3 cells 24 hours previously. In addition some cells were transfected with all three constructs in equal proportions. All DNA mixes contained 10% pCAT vector with which comparative transfection efficiencies could be determined. Mock-transfected JEG3 were exposed to the transfection mixture containing no DNA. 24 hours post-transfection all the cells were washed with DPBS twice and the cDMEM replaced. All dishes except 3 of the 6 containing mock-transfected cells received 1mM dibutyryl cAMP. Exposure to dibutyryl cAMP lasted 24 hours after which the media and lysates were harvested for hCG assay. Lysis of the cells was carried out as described in section 2.5.1 using 200µl 100mM

sodium carbonate per dish. Bradford assay of the lysate was undertaken to determine the total protein content of each sample. A volume of lysate determined to contain 1µg of total protein was subjected to CAT assay and quantified using the STORM™ PhosphorImager. 25µl of the lysate and media was assayed for hCG content using the MAIAclone kit (Serono, France).

4.2.7 Detection of oLHβ and oFSHβ mRNA by RT-PCR

Sheep luteal pituitary RNA and mouse kidney RNA were kind gifts from P.Brown (MRC, CRB). Several primers were designed in order to detect expression of oLHβ and oFSHβ following the guidelines described in 2.3.15 . The sequence details, predicted optimal annealing temperatures and product sizes for each of these primers are listed in table 4.2.7a. Primers designed to amplify human glyceraldehyde 3-phosphate dehydrogenase (GAPDH) mRNA are also detailed in table 4.2.7a and were obtained from Clontech (UK).

All RT-PCR was carried out using the Titan™ kit (Boehringer Mannheim, UK) in accordance with manufacturers guidelines. The oFSHβ reactions were assessed at annealing temperature of 56, 60 and 64°C. Annealing temperatures of 62, 66 and 70°C were assessed for the oLHβ RT-PCR. Each of the oLHβ primer combinations were also assessed for their ability to amplify products from mouse kidney RNA.

microscope and LSM510 scanning module (Zeiss, UK) as described in section 2.6.3.

4.2.9 Stable transfection of JEG3 cells

Stable integration of transfected genes requires selection with an antibiotic to which resistance is encoded on the transfected construct. In these studies resistance to G418 was conferred by the neo^R gene within pcDNA3. For the selection process to be effective untransfected cells must be efficiently killed.

In order to determine the G418 concentration required to carry out this selection process G418 was titrated and applied to confluent JEG3 cultures in duplicate wells of a 12-well plate. G418 obtained from Sigma was batch-tested to avoid interbatch variation. cDMEM containing either 0, 31.25, 62.5, 125, 200 or 250µg/ml G418 was added to the wells and changed every 3 days. After one week the cells were trypsinised and counted using a haemocytometer. Three samples were counted for each duplicate well.

JEG3 cells were transfected with either genomic gonadotrophin β-subunit expressing construct only or in combination with poαGSU. 24 hours after transfection using Pfx4 the cells were seeded in large culture vessels with $162cm^2$ growth surface. Approximately $1x10^3$-$1x10^4$ cells were added to each flask so as to achieve sufficient dispersal of individual cells from which discrete colonies may be isolated. 200µg/ml G418 was applied to the transfected cell population upon addition to the large flask. Selection was maintained by regular replenishment of fresh cDMEM containing 200µg/ml G418. After 4-6 weeks of selection discrete colonies were isolated as follows. The location of colonies was determined using an inverted microscope and marked on the underside of the flask using a marker pen. The media was removed and washed twice with DPBS. While still covered in DPBS the upper surface of the flask was removed using a hot soldering iron. 8mm diameter cloning rings supplied with sealant on one end were placed over the marked colonies using sterile forceps after removal of the DPBS. Approximately 25µl trypsin was added to each cloning ring using a sterile fine-tipped plastic Pasteur pipette. Due to the breached structure of the flask incubation at 37°C was not possible. Incubation at room

temperature required optimisation and was varied between 30, 60, 180 and 240 seconds. Approximately 150µl cDMEM was added to each cloning ring to halt the trypsinisation. Complete removal of the limited number of cells was attempted by repeated pipetting of the media within the cloning ring. This was also varied between a single removal of the media up to 20 removals and re-additions to the cloning ring. The media from the cloning ring was transferred to a 96-well tissue culture plate and cultured under normal conditions in the presence of a maintenance dose of 125µg/ml G418. Isolated colonies were maintained in well sizes appropriate to the number of cells. Clones were stored in liquid nitrogen by the method described in section 2.4.7.

4.2.10 Genomic Analysis of Stable Transfections

Analysis of genomic DNA isolated from resuscitated clones was undertaken so as to determine the copy number of inserted genes.

Approximately 5 x10^6 cells were scraped from the flask surface into 1ml DPBS and centrifuged for 5 minutes at 13000rpm and 4°C in an Heraeus Sepatech Biofuge 22R with HFA 22.2 rotor. The pellet containing the intact cells was lysed in 500µl solution containing 1% SDS, 500µg/ml Proteinase K, 10mM TrisHCl pH7.9, 0.15M NaCl and 10mM EDTA pH8. Incubation of the samples for 4 hours at 37°C with occasional gentle agitation ensured digestion of the cellular proteins. The sample was then phenol extracted before precipitation by 1.5 volumes of 100% ethanol. The precipitated DNA was then isolated from the solution using a siliconised glass Pasteur pipette (prepared as described in Appendix I). The DNA was then allowed to air-dry before being resuspended by incubation at 4°C in 1ml of sterile water. Restriction endonucleases were chosen which would excise the oLHβ or oFSHβ genomic sequences. In addition *Bsm*I which cut within the pcDNA3 vector sequence was used to allow reprobing of the membrane to assess integration of the neo^R gene. *Bsm*I and *Xho*I were incubated with 100µl of genomic material from wild-type and poLHβg stably-transfected JEG3 cells. Similarly *Bsm*I and *Xba*I were used to digest wild-type and poFSHβg stably-transfected JEG3 cells. In order to estimate the number of integrated copies copy number controls were prepared from the CsCl-purified stocks of the poLHβ and poFSHβ constructs. 10µg of poLHβ was digested with *Xho*I

whereas poFSHβ was digested with *Xba*I. Digestions of the plasmid and genomic DNA was undertaken according to manufacturers guidelines for 2 hours. Midway through the genomic digest 40 additional units of *Xho*I and *Xba*I were added to the oLHβ– and oFSHβ-containing reactions respectively. Following digestion of the genomic material the DNA content was measured by spectrophotometrical analysis at 260nm. 5µl of a fresh aliquot of DNA loading dye (see Appendix I) was added to 15µg of each genomic digest. This mixture was heated at 65°C for 5 minutes to remove secondary structures prior to loading on a 0.8% agarose gel. Meanwhile copy number controls were prepared by calculating the proportion that each gonadotrophin β–subunit encoding fragment comprised of the human genome.

2µl of each plasmid restriction digest was separated by agarose gel electrophoresis and the concentration of the fragment containing the insert sequences estimated. The proportion that each fragment size comprised of the human genome was then calculated. This figure was then used to determine the amount of the fragment required to represent a similar size sequence in 15µg of the human genome as shown for each gene below.

$$\frac{6\times10^{6}\text{kb}}{2\text{kb}} = 3\times10^{6}$$

$$\frac{15\mu\text{g}}{3\times10^{6}} = 5\times10^{-6}\mu\text{g}$$

1 copy of oLHβ = 5pg of the 2kb poLHβg *Xho*I fragment

$$\frac{6\times10^{6}\text{kb}}{2.4\text{kb}} = 2.5\times10^{6}$$

$$\frac{15\mu\text{g}}{2.5\times10^{6}} = 6\times10^{-6}\mu\text{g}$$

1 copy of oFSHβ = 6pg of the 2.4kb poFSHβg *Xba*I fragment

Copy number controls were loaded on each 20cm 0.8% agarose gel which was electrophoresed at 40V overnight.

Prior to transfer of the DNA a photograph of the gels next to a fluorescent ruler was taken so as to orientate hybridised bands with the Lambda *Hin*dIII marker also run on the gel. DNA transfer, labelling of probes and hybridisation were carried out as described in sections 2.3.17-19. The respective full-length cDNAs provided by B.Miller (USA) and T.E.Adams (Aus) were used as probes.

4.2.11 Analysis of Gene Expression in Stable Transfections

The presence of specific mRNA expression from integrated oLHβ genes was assessed by RT-PCR. RNA was extracted from confluent cultures of JEG3 cells stably transfected with the either the oLHβ gene or both the αGSU cDNA and oLHβ gene using Tri-reagent (Sigma-Aldrich, UK) as described previously for transiently transfected cells. Two different oLHβ RT-PCR reactions were carried out using the Titan™ kit (Boehringer Mannheim, UK) at the annealing temperature of 70°C. Primer lh33 targets the 3' UT of the oLHβ gene and was used in both RT-PCR reactions. Two different 5' primers were used; lh53 and lh52. The former anneals to exon 2 whereas lh52 anneals to the junction region between exons 1 and 2 of the oLHβ gene. Application of lh52 primer allowed detection of aberrant oLHβ splicing.

Detection of oLH in JEG3 cells stably transfected with the oLHβ gene was undertaken by RIA using hCG-stripped R29 antisera. Media and lysates from confluent cultures were harvested as described in section 2.5.1.

4.2.12 Induction of Gene Expression using Butyric Acid

JEG3 cultures stably transfected with the αGSU cDNA and either the oLHβ or the oFSHβ genes were assessed to determine the effect of butyric acid treatment on expression of exogenous genes. Cultures were seeded in 12-well plates at approximately 3.5 x 10^5 cells per well. Cells were maintained in the presence of 125μg/ml G418 to prevent loss of the integrated genes. Media from the first 48 hours of growth was removed and stored at -20°C. Similar cDMEM containing either 0,1, 2, 4, 8, 16mM butyric acid pH8 was added to the wells in duplicate and incubated for 22 hours. After this period

the media was again removed and stored at -20°C. Normal cDMEM was added to the wells and incubated for a further 48 hours. After removal and storage of this media sample the lysates were harvested in 100mM sodium carbonate. RIAs were carried out to measure both intracellular and secreted oLH and oFSH.

Duplicate wells in 6-well plates were seeded with JEG3 cells and once confluent were treated with 16mM butyric acid for 24 hours. RNA was harvested from these cells and RT-PCR carried out using lh52 and lh33 as described previously.

4.3 Results

4.3.1 Lipid-based Transfection of JEG3 cells

Transfection of JEG3 cells using the lipid agent Clonfectin™ produced only 1-2 blue cells per confluent 35mm diameter well when β-galactosidase staining was carried out. Further trials with this lipid were abandoned due to the obvious lack of efficiency for JEG3 cell transfection.

β-Galactosidase staining of DOTAP-mediated transfections demonstrated an optimum incubation time of approximately 6 hours (figure 4.3.1a). Both 3 hour and 24 hour incubations exhibited less than 50% the number of transfected cells achieved with a 6 hour incubation. The ratio of lipid to DNA also appeared to affect transfection efficiency with a ratio of 10:1 producing the greatest number of transfected JEG3 cells. Attempts to increase the transfection efficiency by using more lipid were unsuccessful as shown by the drastically reduced number of blue cells after incubation at a ratio of 30:1. A ratio of 30:1 using only 0.5μg DNA (15:0.5 in figure 4.3.1a) was also assessed with no improvement over previous transfection conditions.

Initial screening of the eight PerFect™ lipids provided clear evidence that lipids Pfx4, Pfx5 and Pfx8 were most suited to transfection of JEG3 cells (figure 4.3.1b). Further optimisation of the conditions as recommended by the manufacturer did not provide an increase in the observed transfection

efficiency. Notably, prolonged exposure to Pfx4 was extremely toxic towards JEG3 cells and resulted in almost all the cells detaching from the culture surface. Increases in lipid concentration were assessed as previously for DOTAP transfections and similarly a reduction in transfection efficiency was observed.

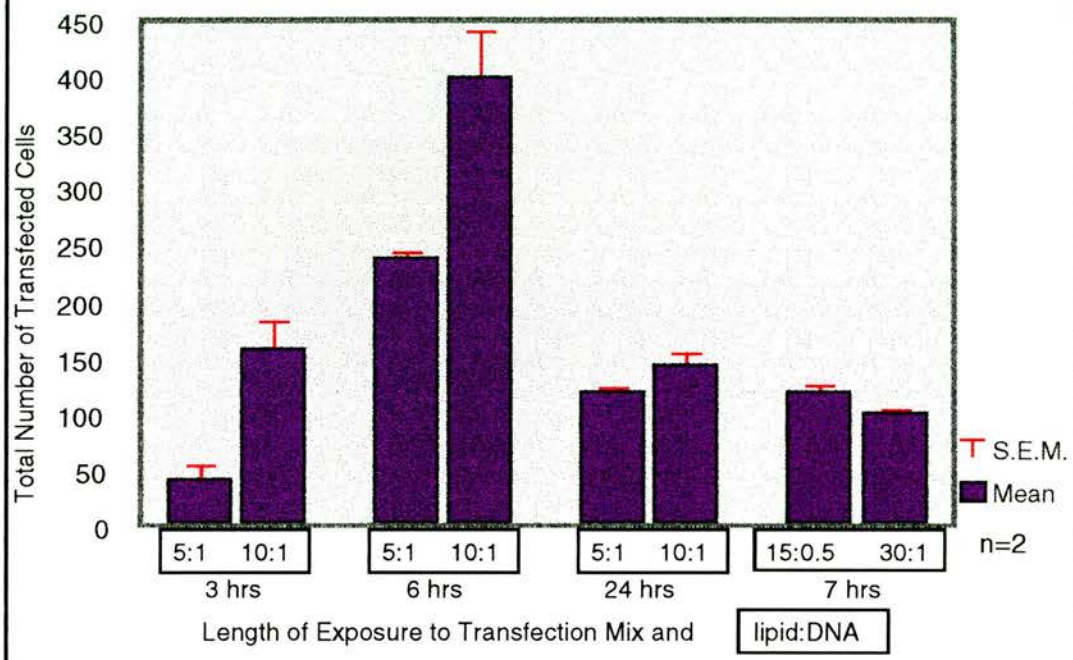

Figure 4.3.1a: JEG3 transfection efficiencies using DOTAP.

Bar chart showing the number of transfected cells produced by different ratios of DOTAP to DNA and lengths of incubation. Transfections were performed in 12 well dishes on JEG3 cells at 60-80% confluency and left for 48 hours post-transfection prior to β-galactosidase staining of confluent wells. Total blue cells per well were used to compare transfection efficiencies.

The 10:1 ratio of DOTAP to DNA incubated for 6 hours provided the highest transfection efficiency using this lipid but transfection mediated by Pfx4 under optimal conditions increased the number of transfected cells 3-fold. Although the optimal transfection conditions produced a relatively high number of transfected cells, the overall transfection efficiency remained low. For comparison with other cell lines transfection efficiency is often expressed as the percentage of transfected cells in the total population of cells. Since approximately $1x10^6$ cells were present within each well of a

12-well plate the optimal transfection efficiency obtained with Pfx4 represents only 1.4%. A representative photograph of JEG3 cells transfected using Pfx4 and stained for β-galactosidase is shown in figure 4.3.1c.

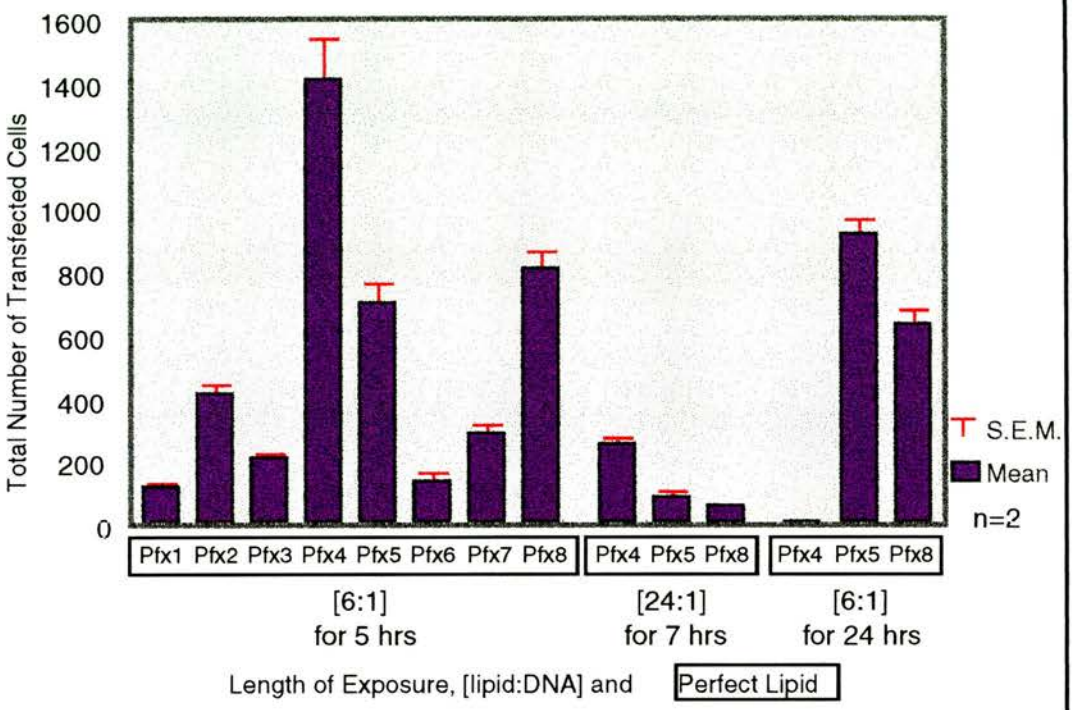

Figure 4.3.1b: JEG3 transfection efficiencies using different PerFect lipids

Bar chart showing the number of transfected cells produced by different PerFect lipids, ratios of lipid to DNA and lengths of incubation. Transfections were performed in 12 well dishes on JEG3 cells at 60-80% confluency and left for 48 hours post-transfection prior to β-galactosidase staining of confluent wells. Total blue cells per well were used to compare transfection efficiencies.

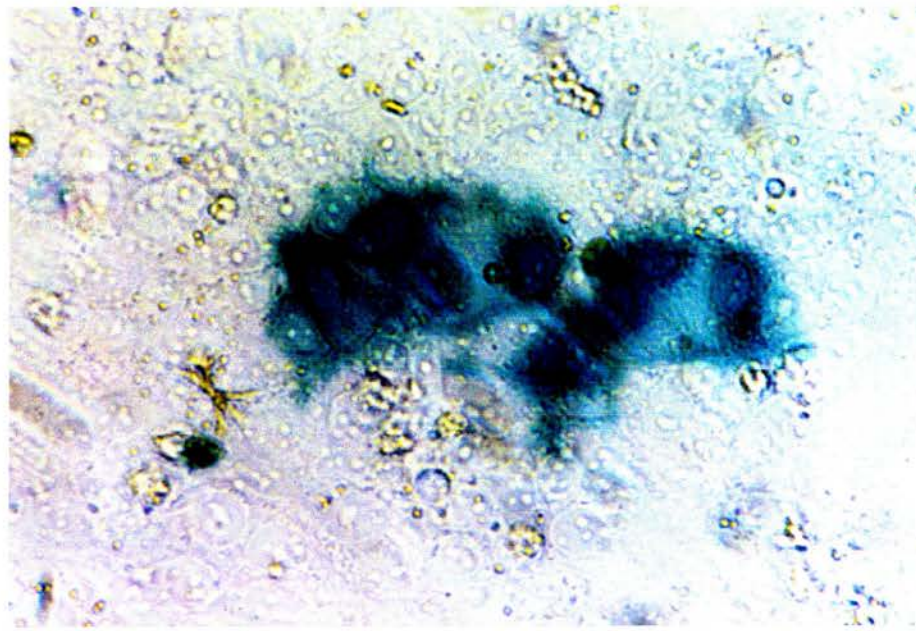

Figure 4.3.1c: JEG3 cells transiently transfected with pcDNA3.1/His/lacZ.

JEG3 cells were transiently transfected with pcDNA3.1/His/lacZ using PerFect lipids. 48 hours posttransfection the cells were fixed and stained for β-galactosidase activity.

4.3.2 Transient granin expression and hCG secretion

Northern analysis of bCgB expression from transiently transfected JEG3 cells provided evidence for production of mRNA transcripts comparable to those expressed in ovine pituitary tissue (figure 4.3.2a). Three bands are present within the transiently transfected JEG3 RNA samples. The smallest band appears slightly larger than the corresponding band produced by hybridisation with ovine pituitary RNA. This analysis confirmed that specific mRNA for bCgB was expressed by JEG3 cells transfected with the pbChrB73 construct. The two larger bands appear less abundant than the smallest band and may represent non-specific hybridisation.

Bradford assay of cell lysates provided the protein concentration of each sample which ranged between 20 and 105ng/µl. Total protein concentration represented variations in cell number which appeared reduced in transfected samples reflecting the toxicity of the procedure. IRMA of hCG in the lysate and media from the transfected and control samples provided concentrations in IU/ml. This figure was adjusted to account for variations in cell number using the Bradford assay results. A comparison of the total hCG expressed by control and transiently transfected JEG3 cells is shown in figure 4.3.2b. Unstimulated cells produced undetectable levels of hCG. Total hCG expression appeared unchanged in cells transfected with the bCgB construct alone whereas transfection of either hCgA or bSgII constructs caused a significant rise in total expression levels. Cells transfected with equal amounts of all three expression constructs exhibited hCG expression levels similar to that of cells transfected with the bCgB construct alone and the untransfected but stimulated cells.

Volumes of lysate containing 1µg of protein were subjected to CAT assay and the activity visualised by exposure of the TLC plate within a PhosphorImager cassette. A representative image obtained after a 48 hour exposure is shown in figure 4.3.2c. All pCAT-transfected samples exhibit CAT activity whereas samples from mock-transfected cells exhibited only background levels. Standardisation of the CAT assay results provided a range of figures between 0 and 1 which were applied to the Bradford-

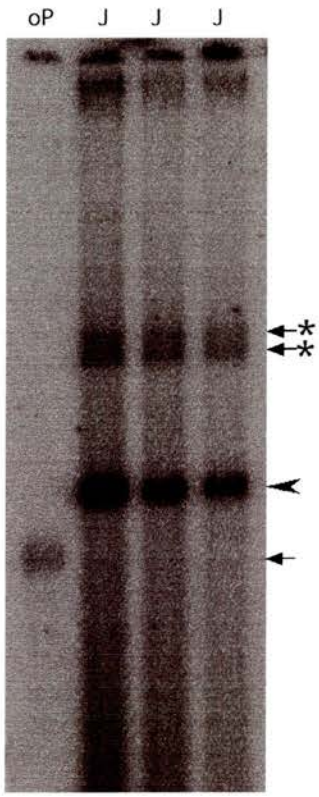

Figure 4.3.2a: Northern analysis of CgB in the ovine pituitary and transiently transfected JEG3 cells.

RNA was extracted from transiently transfected JEG3 cells 48 hours posttransfection using Tri-reagent. Either 10μg of total JEG3 RNA (J) or 5μg of total sheep pituitary (oP) RNA was loaded per lane. The membrane was hybridised with the full-length bCgB cDNA. Transcripts from transfected JEG3 cells (arrow) appeared larger than those detected in the ovine sample. In addition, two much larger transcripts were detected in the transfected JEG3 cells (asterisked arrows).

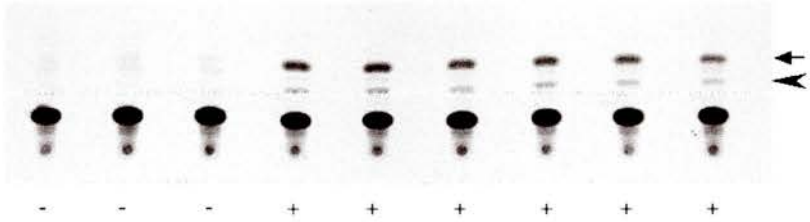

Figure 4.3.2c: Thin layer chromatography of CAT assay reactions.

Lysates were prepared from untransfected cells (-) or from cells 48 hours posttransfection (+). Reactions containing acetyl coenzyme A and $^{[14]}$C-chloramphenicol were incubated at 37°C with 1mg of lysate. The percentage of total chloramphenicol which was mono-acetylated (arrowhead) and di-acetylated (arrow) was determined using a STORM PhosphorImager. Reactions containing lysates from untransfected cells displayed background levels of acetylation.

corrected hCG IRMA results giving figures which take into account variations in transfection efficiency between samples. In order to relate any differences observed in hCG storage between transfected and control JEG3 cells the mean intracellular hCG concentration was expressed as a percentage of the total hCG expressed as shown in figure 4.3.2d.

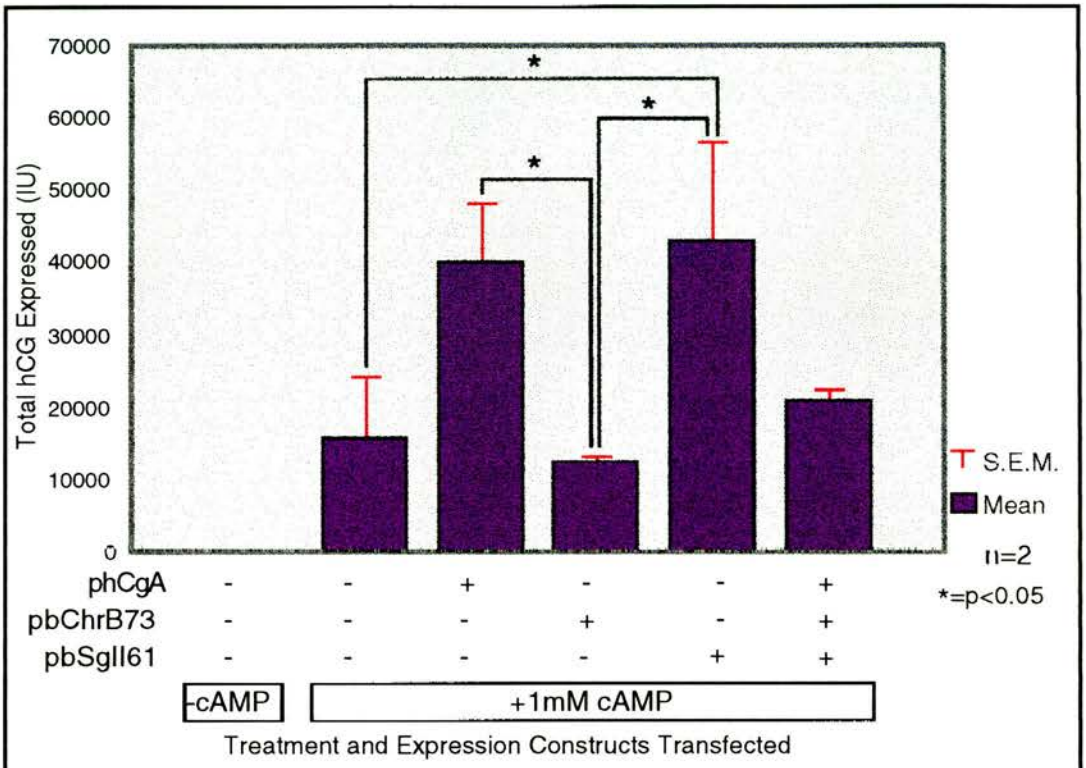

Figure 4.3.2b: Total hCG expression from JEG3 cells transfected with granin expression vectors.

Bar chart showing the relative amounts of hCG in IU expressed by unstimulated JEG3 cells and cells exposed to 1mM cAMP for 24 hours. hCgA and bSgII both cause significantly more expression of hCG in comparison to cells transfected with the bCgB expression plasmid. bSgII expression also causes a significant rise in hCG expression in comparison to untransfected cells. All cells transfected with the bCgB expression construct either alone or in conjunction with the hCgA and bSgII constructs exhibit similar total hCG expression to untransfected cells. hCG expression from unstimulated cells was undetectable.

This representation allows comparison of hCG storage profiles and accounts for both variation in cell number and transfection efficiency.

The bar chart indicates that transfected and control JEG3 cells treated with 1mM dibutyryl cAMP exhibit similar proportions of intracellular hCG. Furthermore cells transfected with a single granin-expression construct or a mixture containing all three constructs failed to exhibit significantly different proportions of intracellular hCG in comparison to the mock-transfected cells.

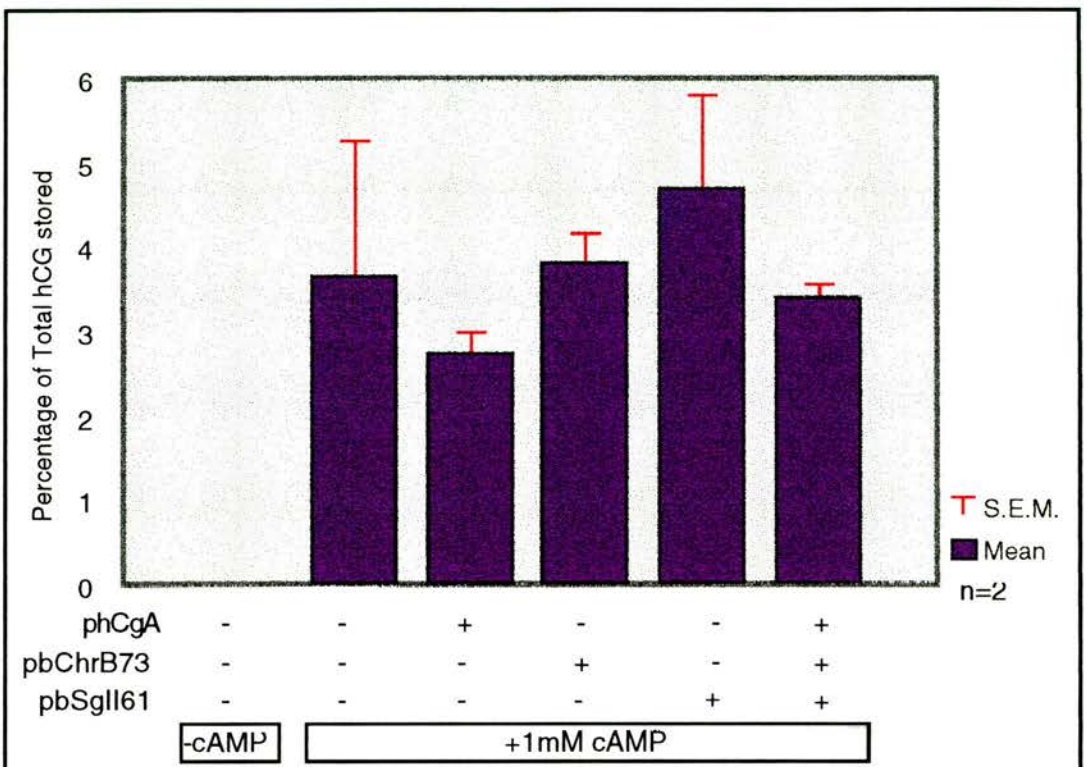

Figure 4.3.2d: Comparison of hCG storage in cAMP-stimulated JEG3 cells transiently transfected with granin expression vectors.

Variations in transfection efficiency were corrected for by application of figures from CAT assays performed on cell lysates. The percentage of CAT-adjusted hCG expressed which remains intracellular after 48 hours of expression does not differ significantly between untransfected cells and cells expressing granins.

4.3.3 Transient Pituitary Gonadotrophin Expression

Transient expression of transfected pituitary gonadotrophin expression construct was initially assessed by RT-PCR.

The integrity of RNA extracted from JEG3 cells and ovine pituitary was confirmed by RT-PCR using GAPDH primers (figure 4.3.3a). Amplification of a fragment corresponding to approximately 450bp is in accordance with the predicted product size for this reaction.

Optimisation of the oFSHβ RT-PCR demonstrated that all combinations of primers produced an amplified DNA product of the predicted size as detailed in figure 4.3.3b. The highest annealing temperature of 64°C reduced the efficiency of the reaction carried out using fsh51 and fsh32 whereas other reactions containing fsh51 appeared unaffected by this annealing temperature. Efficient amplification of the 450bp fragment using fsh51 and fsh33 did not occur at the lowest annealing temperature of 54°C.

Temperature optimisation of the oLHβ RT-PCR showed that at all annealing temperatures the predicted product sizes were exhibited as shown in figure 4.3.3cii. No products were detected in the control reactions containing no RNA. Verification that these reactions were specific for amplification of oLHβ sequences was demonstrated by the lack of products in reactions containing mouse kidney RNA (figure 4.3.3ciii).

oFSHβ expression from poFSHβg was confirmed by the appearance of an amplified DNA fragment which migrated between 400 and 500bp during agarose gel electrophoresis (figure 4.3.3d). The amplification of this fragment coincides with that observed in the reaction containing ovine pituitary RNA and is in accordance with the predicted product size of approximately 490bp for fsh51 and fsh33. The specificity of the RT-PCR was confirmed by the complete absence of amplification in samples containing RNA from untransfected JEG3 cells.

RT-PCR in common with all polymerase-dependent nucleic acid amplifications requires specific annealing of primer sequences. hCGβ and oLHβ sequences show significant homology and non-specific amplification of hCGβ sequences using lh52, lh53 or lh33 could occur due to limited primer mismatches. However despite the sequence similarity of oLHβ and hCGβ it is apparent from the lack of amplicons in reactions containing normal JEG3 RNA that the high annealing temperature of 70°C prevented nonspecific priming. RT-PCR using primers lh52 and lh33 directed towards

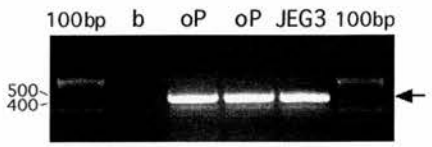

Figure 4.3.3a: GAPDH RT-PCR.

GAPDH mRNA was detected (450bp product) using human primers in RNA from sheep pituitaries (oP) and JEG3 cells (arrow). No products were produced by the reaction containing no RNA (b). The annealing temperature for these reactions was 54°C. The gel contained 2% agarose and was run TBE buffer. 100bp ladders were used as size markers.

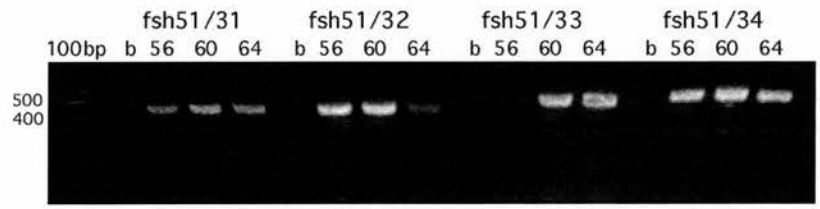

Figure 4.3.3b: Temperature optimisation for the oFSHβ RT-PCR with four sets of primers.

No products were produced from the control reactions containing no RNA (b). All primer combinations produced the predicted product size in the presence of sheep pituitary RNA (fsh51/31=412bp, fsh51/32=412bp, fsh51/33=449bp, fsh51/34=490bp). The primer combination of fsh51 and 33 was used at the annealing temperature of 64°C for subsequent reactions as this produced a relatively high amount of product with no background. The gel contained 2% agarose and was run in TBE buffer. A 100bp ladder was used for size comparison.

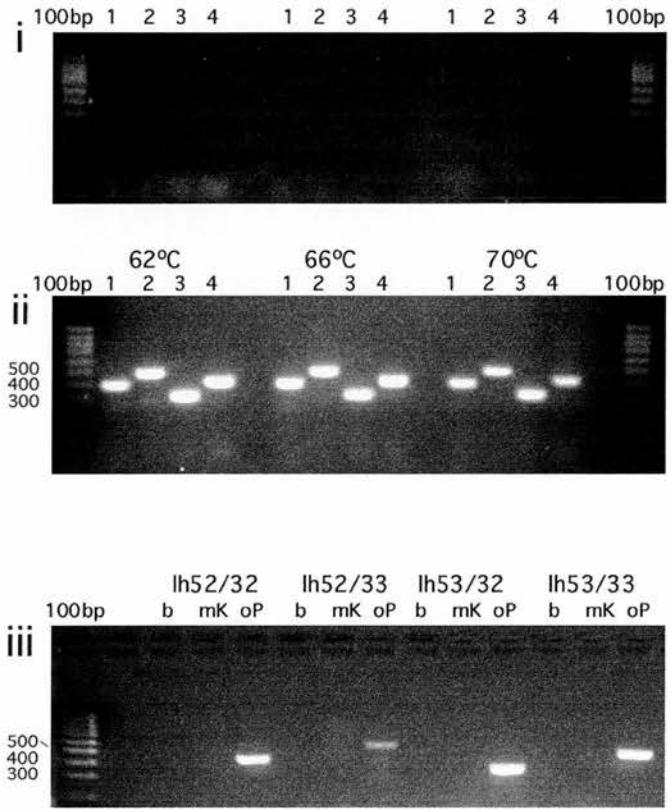

Figure 4.3.3c: Temperature optimisation and specificity of oLHβ RT-PCR primers.

i) Control reactions containing no RNA produced no bands. ii) All bands were in accordance with the predicted product sizes for each primer pair. Annealing temperatures of 62, 66 and 70°C were assessed. Some non-specific products were produced at the lowest annealing temperature but were abolished as the temperature was raised. Where 1=lh52&32 (385bp), 2=lh52&33 (480bp), 3=lh53&32 (311bp), 4=lh53&33 (406bp). iii) The specificity of each primer pair was also verified by RT-PCR of mouse kidney RNA (mK) in comparison to sheep pituitary RNA (oP). These reactions were carried out at the annealing temperature of 70°C. All gels contained 2% agarose and were run in TBE buffer. 100bp ladders were used as markers.

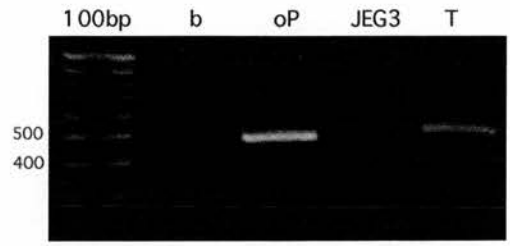

Figure 4.3.3d: Expression of oFSHβ in transiently transfected JEG3 cells as determined by RT-PCR.

No amplified products are visible in the control reaction containing no RNA (b) or the reaction containing untransfected JEG3 RNA (JEG3). Similar size products are present in reactions containing sheep pituitary RNA (oP) and RNA from JEG3 cells transiently transfected with poαGSU and poFSHβg (T). RNA was harvested using Tri-reagent 48 hours posttransfection. Primers fsh51 and fsh33 were used at an annealing temperature of 66ºC.

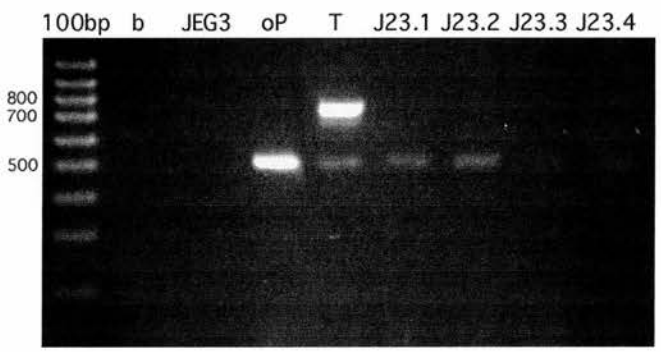

Figure 4.3.3e: Expression of oLHβ in transfected JEG3 cells as determined by RT-PCR.

No amplified products are visible in the control reaction containing no RNA (b) or the reaction containing untransfected JEG3 RNA (JEG3). Similar size products (500bp) are present in reactions containing sheep pituitary RNA (oP) and RNA from JEG3 cells transiently (T) or stably (J23.1-4 clones) transfected with poαGSU and poLHβg. A larger and more abundant product (possibly two products) of approximately 800bp is present in the reaction containing RNA from transiently transfected JEG3 cells. This product is absent from all other reactions. RNA was harvested using Tri-reagent 48 hours posttransfection for RNA from transients or from confluent cultures of the stable clones. Primers fsh51 and fsh33 were used at an annealing temperature of 66ºC. The gel contained 2% agarose and was run in TBE buffer. A 100bp ladder was used for size comparison.

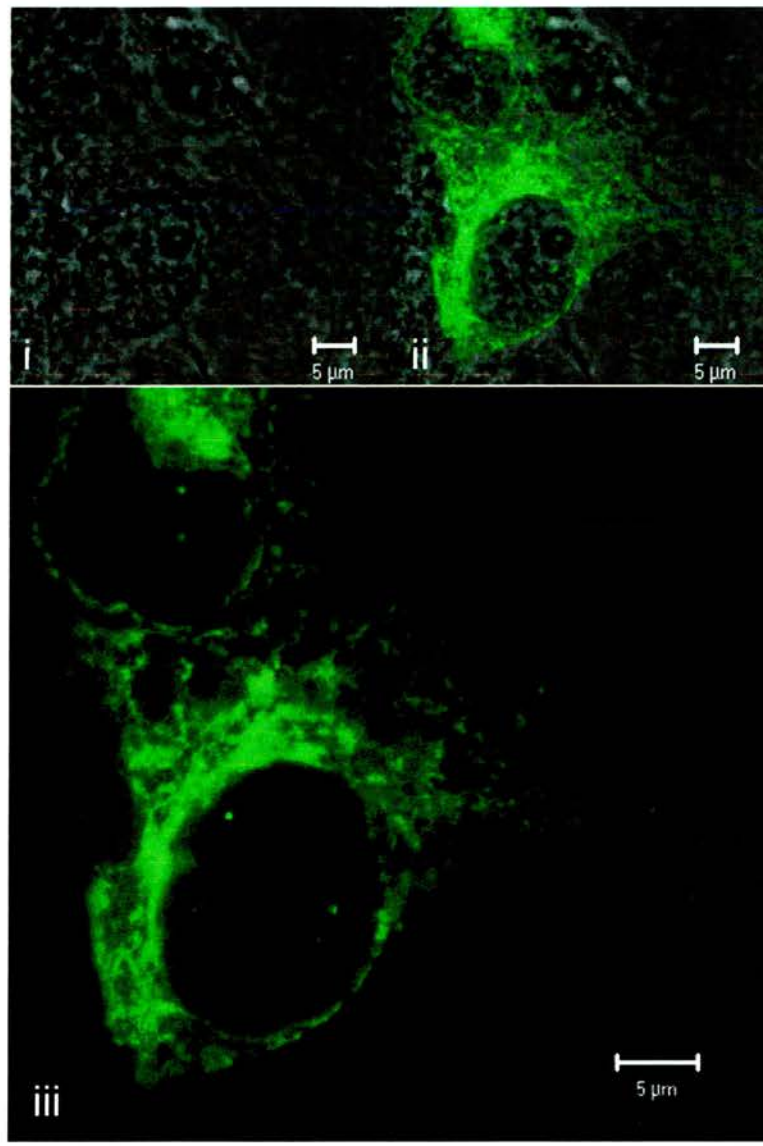

Figure 4.3.3f: Subcellular distribution of oFSH in transiently transfected JEG3 cells.

i) Phase-contrast image. ii) Overlay of fluorescence and phase contrast images. iii) FITC fluorescence. FSH-immunoreactivity appears 'mesh-like' within the cytoplasm of the transfected JEG3 cells. JEG3 cells were transfected with poαGSU and poFSHβg and fixed 48 hours later. FSH primary antisera (M91) was diluted 1:500 and FITC-conjugated goat anti-rabbit secondary antisera diluted 1:40.

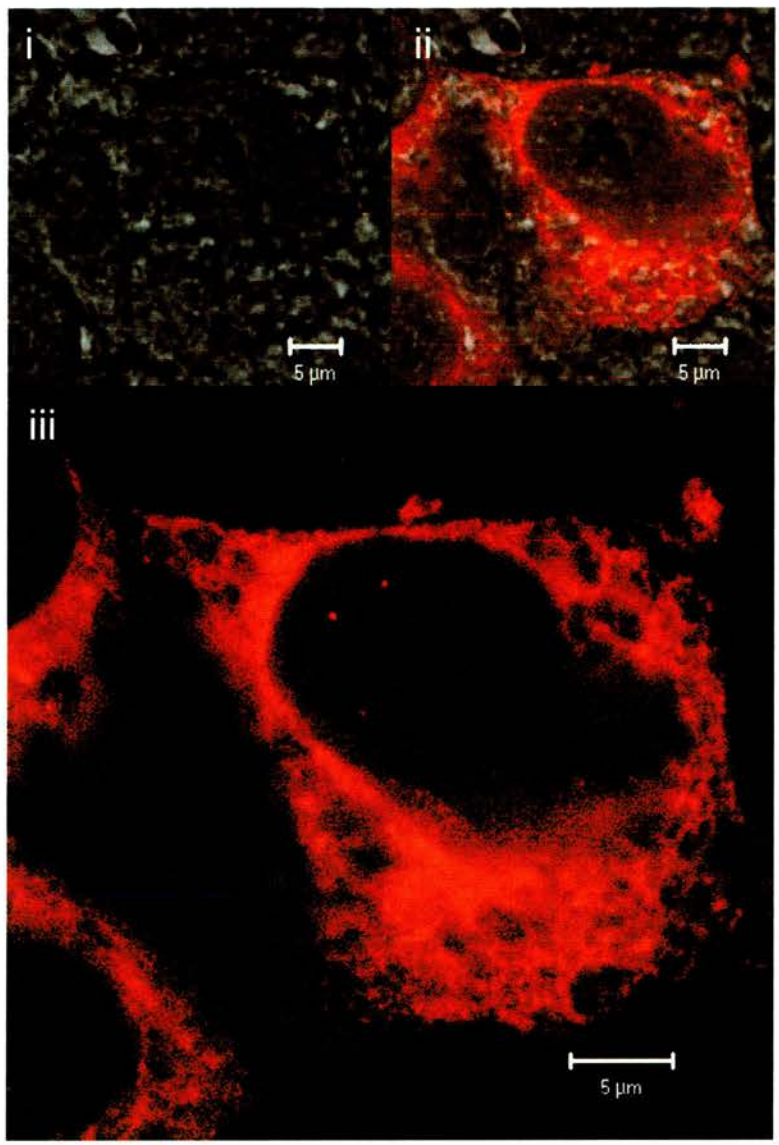

Figure 4.3.3g: Subcellular distribution of oLH in transiently transfected JEG3 cells.

i) Phase-contrast image. ii) Overlay of fluorescence and phase contrast images. iii) TRITC fluorescence. LH-immunoreactivity appears 'mesh-like' within the cytoplasm of the transfected JEG3 cells. JEG3 cells were transfected with poαGSU and poLHβg and fixed 48 hours later. LH primary antisera (518B7) was diluted to 2µg/ml and TRITC-conjugated goat anti-rabbit secondary antisera diluted 1:40.

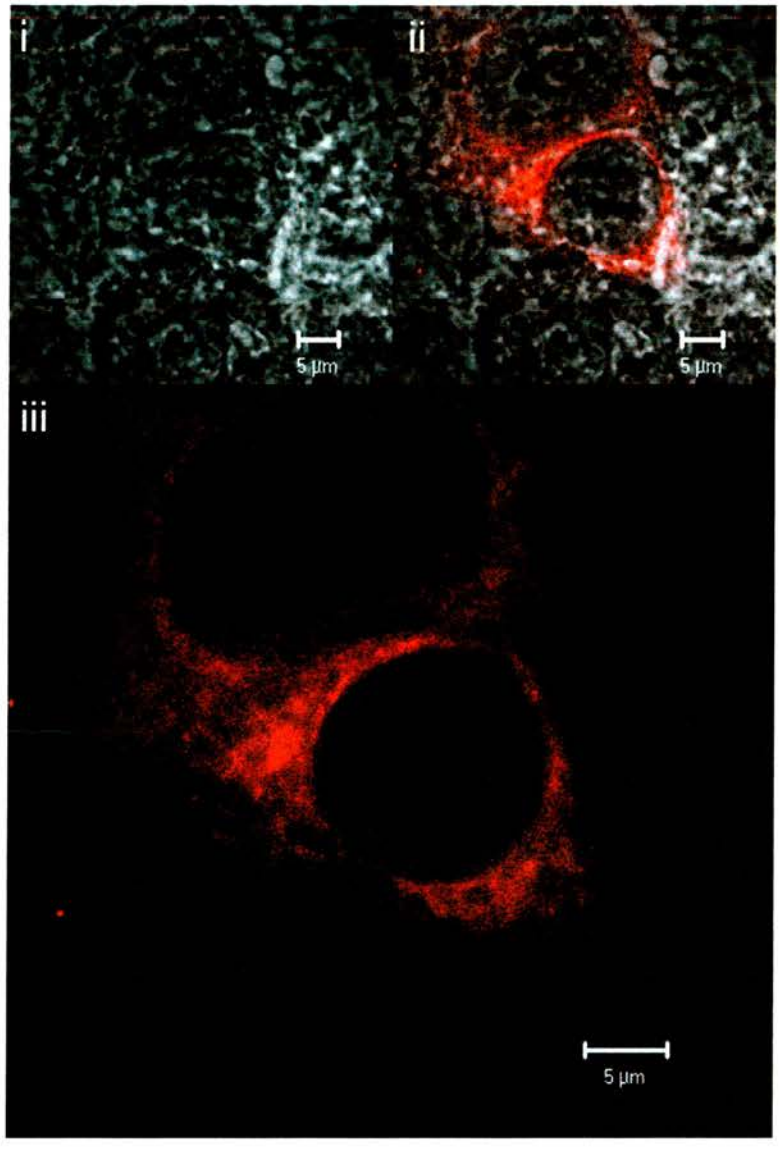

Figure 4.3.3h: Subcellular distribution of hCG in JEG3 cells treated with 1mM dibutyryl cAMP for 24 hours.

i) Phase-contrast image. ii) Overlay of fluorescence and phase contrast images. iii) TRITC fluorescence. The hCG-immunoreactivity appears dispersed throughout the cytoplasm in a 'mesh-like' pattern. JEG3 cells were treated with 1mM dibutyryl cAMP for 24 hours prior to fixing. hCG antisera (PC-2) was diluted 1:250 and goat anti-mouse TRITC conjugate diluted 1:40.

the exon 1-2 junction and 3'UT respectively confirmed oLHβ expression from the poLHβg construct (figure 4.3.3e). RT-PCR of RNA from transiently transfected JEG3 cells produced an amplified DNA product of approximately 480bp which coincides with that produced by the reaction containing ovine pituitary RNA. This fragment is in accordance with the predicted size of the amplicon for this RT-PCR. The transfected JEG3 sample also contains two larger fragments of approximately 750-800bp with the largest of these appearing most abundant.

Protein expression and subcellular localisation of oFSH and oLH was observed by confocal microscopy. JEG3 cells transiently transfected with either the poFSHβg or poLHβg in combination with the poαGSU construct produced cytoplasmic immunoreactivity for FSH and LH respectively (figure 4.3.3f & g). The mesh-like pattern of immunoreactivity coincided with an absence of aggregates or large vesicles. Furthermore this pattern of pituitary gonadotrophin expression was similar to that observed for hCG in untransfected dibutyryl cAMP-stimulated JEG3 cells (figure 4.3.3h).

These results confirm expression of the oLHβ and oFSHβ genes in transiently transfected JEG3 cells. Furthermore the subcellular localisation of the pituitary gonadotrophins appears similar to that of hCG.

4.3.4 Stable Pituitary Gonadotrophin Expression

Cell counts performed on JEG3 cultures after one week of G418 exposure indicated the toxic effect of the aminoglycoside antibiotic with all doses of G418 inducing JEG3 cell death (figure 4.3.4.a) Although all additions of G418 caused cell death, some concentrations caused a disproportionate amount. For example addition of 31.25, 62.5 and 125μg/ml G418 caused additional increases in cell death of 39%, 44% and 19%. This represents a small amount of additional selection pressure caused by the increase of G418 from 62.5 to 125μg/ml. Addition of G418 quantities greater than 125μg/ml reduced the cell number at a much more efficient rate. 200μg/ml G418 reduced the cell number by a further 69% and 250μg/ml by a further 54%. These data demonstrate a threshold effect of G418 action against JEG3 cell survival. Disproportionate increases in cell death occur with incremental additions of G418 above the threshold level of 125μg/ml.

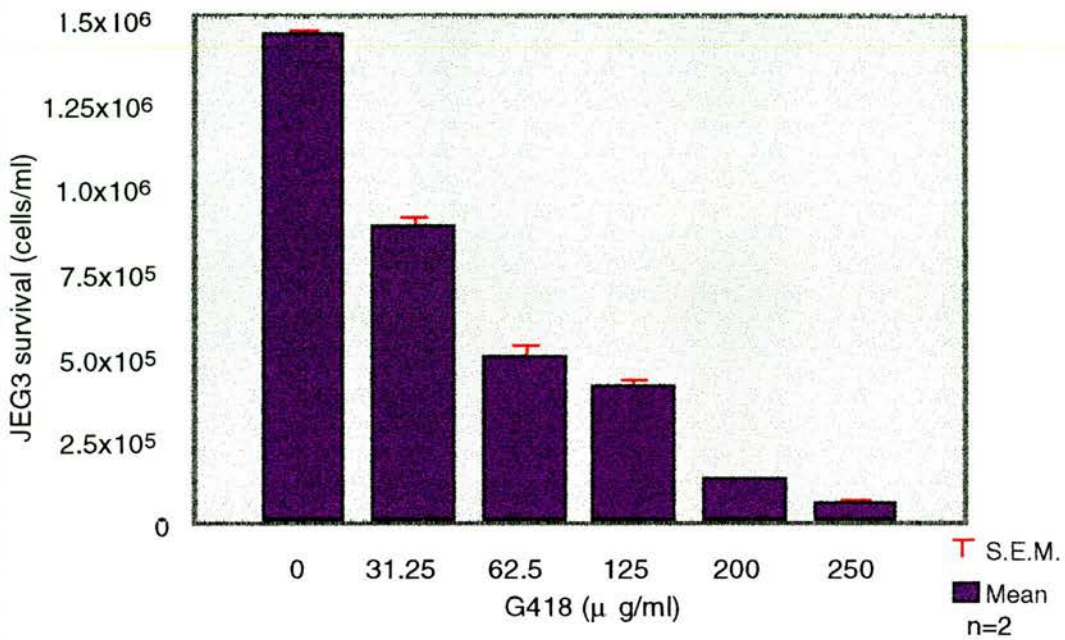

Figure 4.3.4a: Survival of JEG3 cells at different concentrations of G418.

Bar chart showing the number of surviving cells after one week incubation in the presence of G418 at different final concentrations. Cells plated in 12 well dishes were grown to 75% confluency before addition of G418. Media was changed every 2 days and dead cells washed off during this process. After one week the number of attached cells was estimated by counting suspensions in a haemocytometer.

After optimisation of the transfection and isolation methodology several JEG3 colonies containing 1 of 4 construct combinations were isolated. The J21 Pfx4 transfection mixture contained only the poFSHβg construct whereas J22 transfections contained both the poFSHβg and poαGSU constructs. Sixteen J21 clones and ten J22 clones were isolated. J23 transfections were carried out using only the poLHβg construct whereas the J24 transfection mixture contained both the poLHβg and poαGSU constructs. Fourteen colonies were isolated from the J23 transfection and twenty-one from the J24 transfection. Surprisingly the rates of proliferation for stably transfected JEG3 cells appeared unchanged in comparison to untransfected cells.

Representative J22 and J23 clones were resuscitated for screening by Southern hybridisation. Ten J22 clones (J22.1-9 & J22.12) were screened

for integration of the oFSHβ gene however only weak hybridisation at a position corresponding to that of a larger fragment was observed with no detectable oFSHβ sequences (figure 4.3.4b). Seven J23 clones (J23.1-7) were screened for integration of the oLHβ gene. Hybridised bands equivalent in size to the copy number controls were present in samples J23.1-5 (figure 4.3.4c). Samples J23.6 and 7 were not digested fully due to insufficient *Bsm*I enzyme. Other bands present in the sample appear larger than the expected size but show far weaker hybridisation. The copy number controls prepared for the hybridisation were used to quantify the signal produced by the hybridisation in the J23 samples. The copy number controls were added at 50% greater volume than desired so that they correspond to 1.5, 7.5 and 15 copies instead of 1, 5 and 10 copies. However this error did not prevent accurate quantitation of the signal detected in the J23 samples using the standard curve shown below.

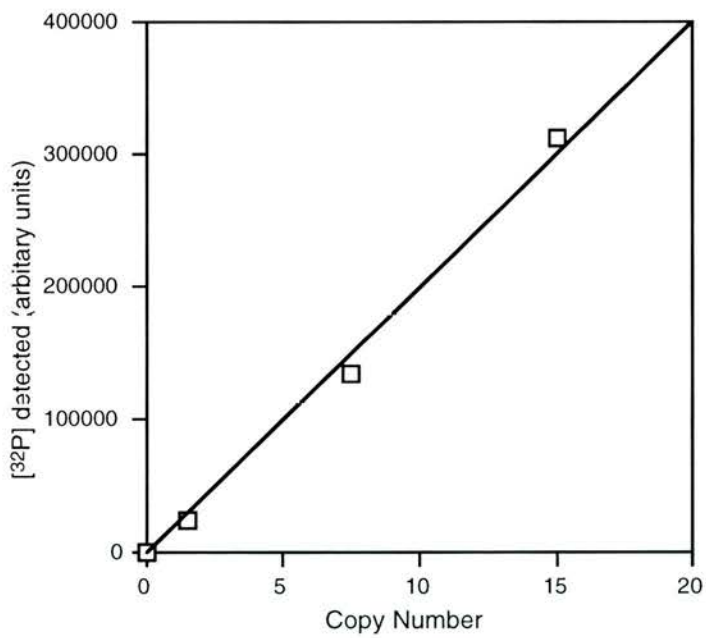

Figure 4.3.4d: Standard Curve for determining the number of integrated copies of the oLHβ gene in stably transfected JEG3 cells.

Copy number controls corresponding to 1.5, 7.5 and 15 copies were probed by Southern hybridisation and quantified using a STORM™ PhosphorImager.

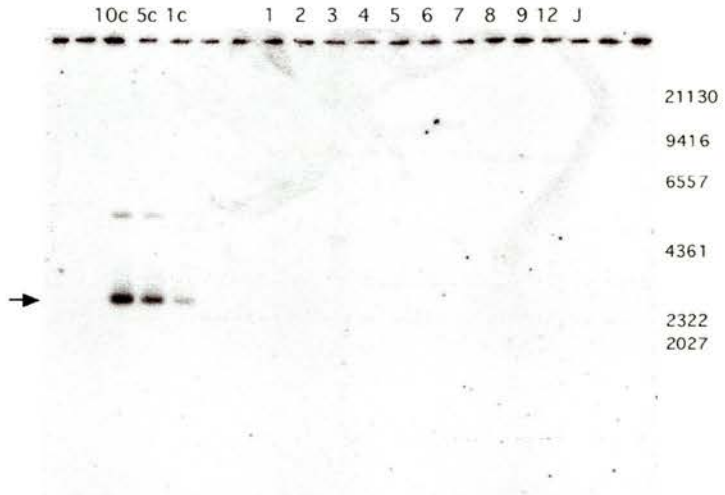

Figure 4.3.4b: Southern analysis of JEG3 cells stably transfected with the oFSHβ gene.

Genomic DNA was extracted from JEG3 clones (J22.1-9, 12 = 1-9, 12) and untransfected JEG3 cells (J) with 15μg DNA loaded per lane. Copy number controls prepared from the poFSHβg construct used in the transfections corresponded to 10 (10c), 5 (5c) and 1(1c) integrated copies of the oFSHβ gene (arrow). No corresponding bands were detected in the samples containing DNA from J22 clones or untransfected JEG3 cells. Fragments sizes from the λ*Hin*dIII marker are shown on the right of the gel.

Figure 4.3.4c: Southern analysis of JEG3 cells stably transfected with the oLHβ gene.

Genomic DNA was extracted from JEG3 clones (J23.1-7 = 1-7) and untransfected JEG3 cells (J) with 15μg DNA loaded per lane. Copy number controls prepared from the poLHβg construct used in the transfections corresponded to 15 (15c), 7.5 (7.5c) and 1.5 (1.5c) integrated copies of the oLHβ gene (arrow). Corresponding bands were detected in the samples containing DNA from J23 clones but not untransfected JEG3 cells. The abundance of integrated copies of the oLHβ gene appeared similar to the signal from the 1.5 copy number control. Additional larger bands were present in both untransfected and stably transfected JEG3 samples. These bands appeared larger in lanes containing DNA from clones J23.6 and J23.7 as these were not subjected to digestion with *Bsm*I. Fragments sizes from the λ*Hin*dIII marker are shown on the right of the gel.

The hybridisation detected in JEG3 clones J23.1-7 corresponded to the size of the copy number controls indicating that the integrated genes were intact. However the level of signal detected required quantification against the copy number controls in order to establish the amount of integration achieved. As depicted in figure 4.3.4e, 4 out of the 7 clones (J23.2-4 and J23.7) exhibited signal equivalent to integration of 1-2 copies of the oLHβ gene. Background detected in untransfected JEG3 cells appeared low and corresponded to the level of signal detected in DNA from J23.5 and J23.6 . The level of integration observed for J23.1 appears to correspond to approximately half a copy of the oLHβ gene.

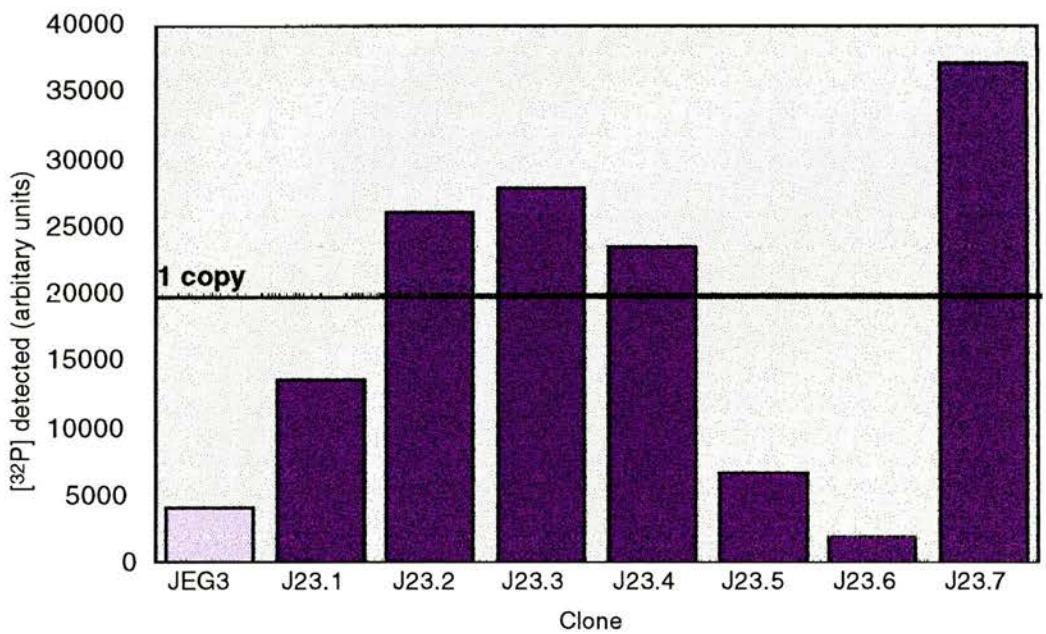

Figure 4.3.4e: Representation of oLHβ signal detected in J23 clones by Southern hybridisation.

Southern hybridisation of the *Xho*I and *Bsm*I digested genomic samples was undertaken using the oLHβ cDNA. The horizontal line on the figure corresponds to the signal equivalent to 1 copy of the oLHβ gene. No clones exhibited levels of hybridisation which exactly corresponded to this standard however J23.2, J23.3 and J23.4 appear most similar. Signal equivalent to that observed for the untransfected JEG3 DNA was detected in samples from clones J23.5 and J23.6. Intermediate levels of signal were detected for J23.1 and J23.7.

The media and lysates from cultures of J23.1-7 were analysed by oLH RIA using the hCG-stripped R29 antisera to assess the level of protein expression obtained after integration of 1-2 copies of the oLHβ gene. The data represented in figure 4.3.3f indicates that oLH formed from the integrated β-subunit and the endogenously expressed hCGα subunit gene was not significantly greater in the lysates of J23 clones compared to untransfected JEG3 cells. However media from the control cells did not produce detectable oLH whereas all J23 exhibited detectable oLH secretion. Although J23.3 and J23.5 media contained considerably more oLH than the other clones, the actual level of secretion was nevertheless low at below 2ng/ml.

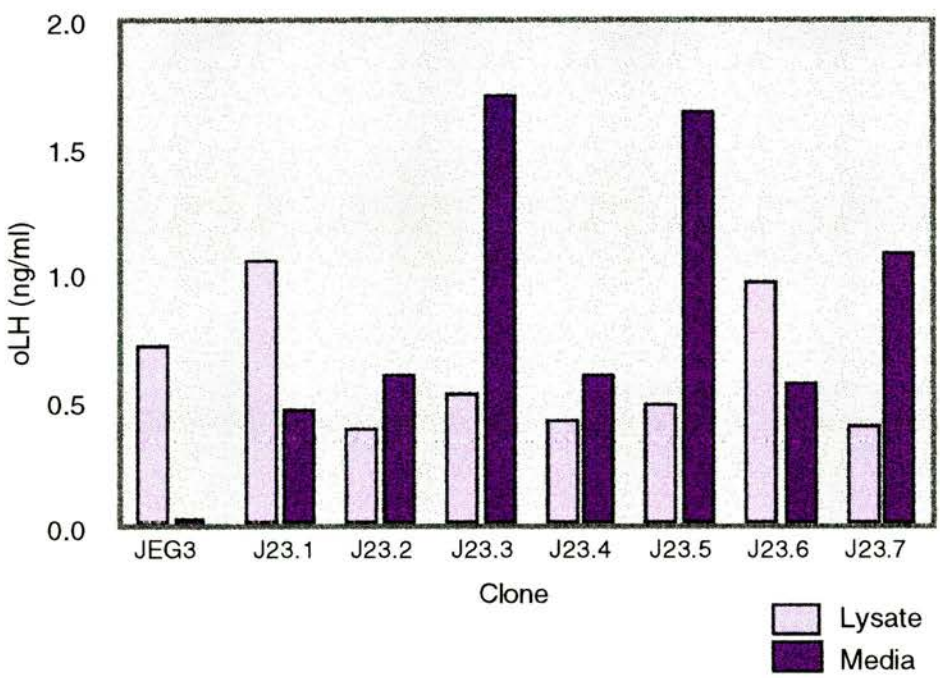

Figure 4.3.4f: Formation of the LH heterodimer from stably integrated oLHβ and endogenous hCGα in JEG3 clones.

oLH was measured in confluent cultures by RIA using the hCG-stripped R29 antisera. In comparison to the oLH detected in lysates from untransfected JEG3 cells, no significant change is apparent in the J23 clones. Media from the control JEG3 cells contained undetectable oLH whereas all J23 clones contained detectable oLH. J23.3 and J23.5 exhibited the highest oLH secretion which exceeded 1.5ng/ml.

RT-PCR analysis of oLH expression by stable transfections J23.1-4 was compared to that of transiently transfected JEG3 cells. Reactions were carried out using primers lh52 and lh33 directed towards the exon 1-2 junction and 3'UT respectively. The reactions containing RNA from J23.1-4 exhibits an amplified DNA fragment of similar size to that produced by RT-PCR of ovine pituitary RNA and transiently transfected JEG3 cells (figure 4.3.3e). Larger products from reactions containing RNA from transiently transfected JEG3 cells were not present in similar reactions containing RNA from J23.1-4. Although the RT-PCR carried out was not performed with any means for quantification it is apparent that the amount of 480bp product in transient and stable transfections is similar. These data indicate that correctly spliced oLHβ mRNA is produced in low abundance by both transient and stable transfections.

Butyric acid treatment was assessed by RIA for its effect upon J22.1-2 and J24.1-2 JEG3 stable transfections. These cells were stably transfected with both ovine α and β gonadotrophin expression constructs and therefore do not require hCGα expression in order to form heterodimers. J22 media and lysates were assayed for oFSH content whereas J24 media was assayed for oLH content. The oFSH RIA results depicted in figure 4.3.4g indicate that all media and lysate fractions contained levels of oFSH equivalent to those expressed by untransfected JEG3 cells. The exception to this is the media fraction collected during butyric acid treatment. All normal JEG3 cells treated with butyric acid show undetectable levels of oFSH with the untreated cells showing 0.09ng/ml. Samples from untreated J22.1 and J22.2 cells contained 0.97 and 1.6ng/ml oFSH respectively with treated cells exhibiting no significant increases irrespective of the butyric acid concentration applied. These levels of oFSH are obtained from the non-linear portion of the RIA standard curve and therefore may not accurately reflect differences in oFSH abundance.

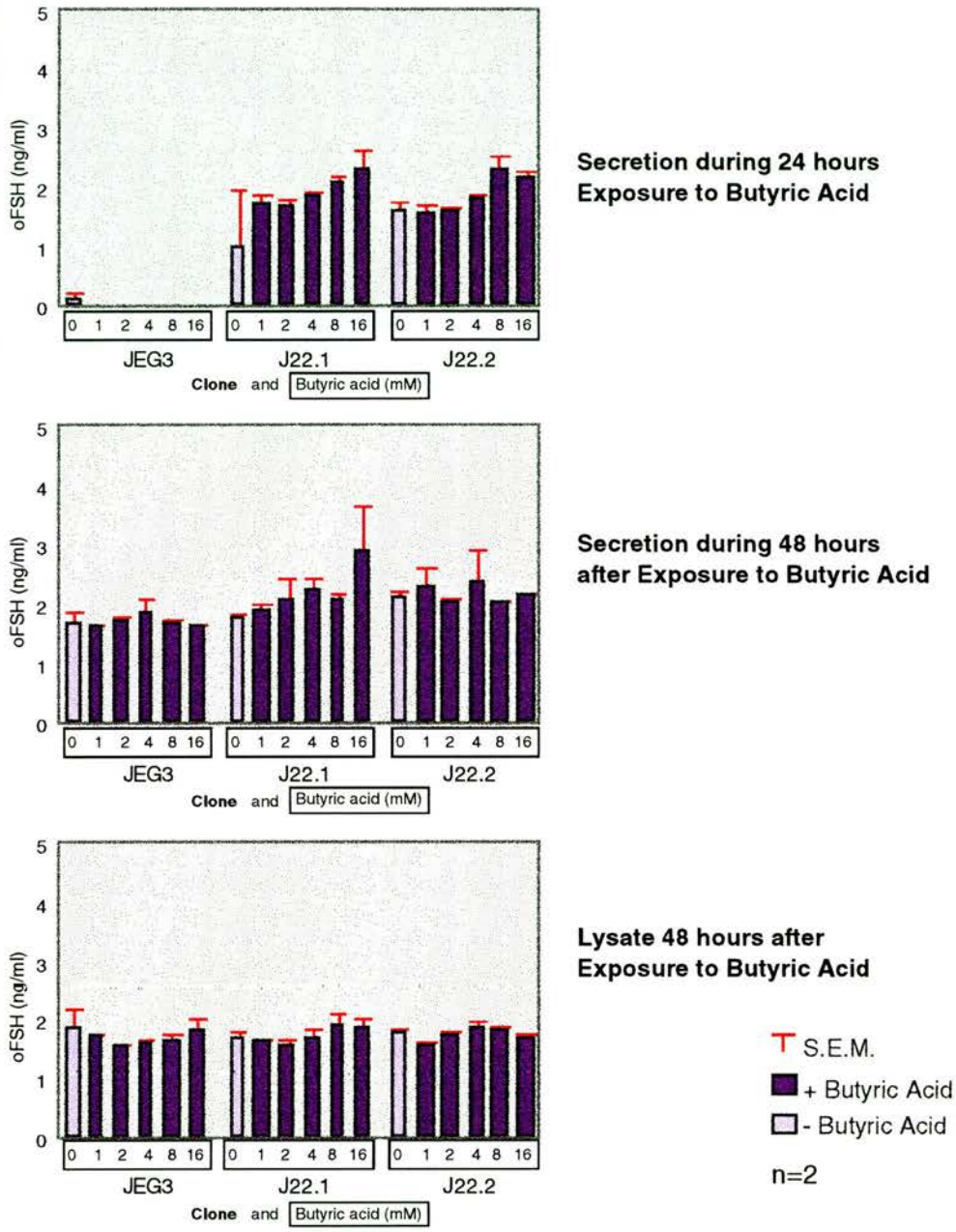

Figure 4.3.4g: Secretion of oFSH from untransfected JEG3 cells and stably transfected clones treated with Butyric acid.

Secreted oFSH was measured by RIA. During butyric acid treatment no oFSH was detected in untransfected cells whereas approximately 2ng/ml was secreted by the J22 clones. However subsequent to butyric acid treatment, secretion and storage of oFSH by the J23 clones did not appear significantly greater than that of untransfected cells. No oFSH was detected in the media during the 48 hours prior to butyric acid treatment (data not shown).

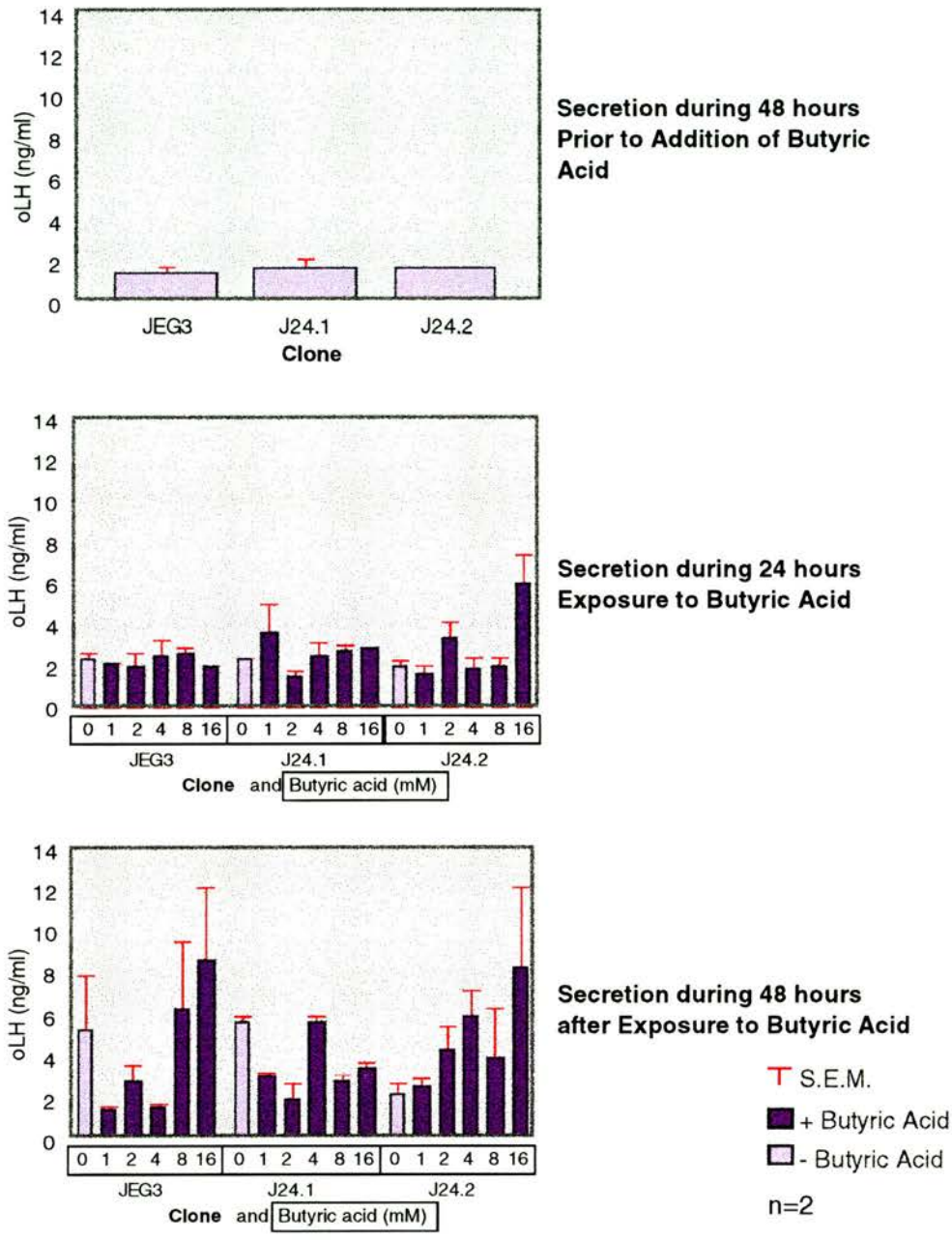

Figure 4.3.4h: Secretion of oLH from untransfected JEG3 cells and stably transfected clones treated with Butyric acid.

Secreted oLH was measured by RIA using the hCG-stripped R29 antisera. In comparison to the oLH detected in lysates from untransfected JEG3 cells, no significant rise was apparent in the J24 clones during or subsequent to butyric acid treatment.

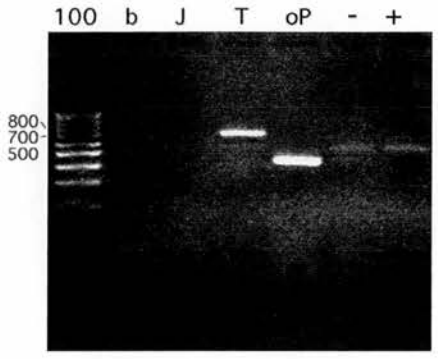

Figure 4.3.4i: oLHβ RT-PCR of RNA from JEG3 cells transfected with poLHβg.

Primers lh53 and lh33 anneal to exon 2 and 3' untranslated sequences respectively. The predicted product size for this reaction is 406bp which is present in the sheep pituitary (oP). This amplified product was not detected in the reactions which contained RNA from JEG3 cells transiently transfected (T) with poLHβg. Stably transfected cells (clone J24.1) either untreated (-) or treated with 16mM butyric acid for 24 hours (+) also did not exhibit this product. Larger products of approximately 700 and 500bp were present in the transiently transfected samples with the former being most abundant. The smaller of these bands was also detected in both the untreated and butyric acid-treated stable J24.1 clones. No products were detected in the reactions containing no RNA (b) or RNA from untransfected JEG3 cells (J). The gel contained 2% agarose and was run in TBE buffer. A 100bp ladder (100) was used for size comparison.

oLH RIA of J24 samples using the hCG-stripped R29 antisera gave results with higher background than that observed for the oFSH assay. However media samples from normal JEG3 cells and stable transfections exhibited oLH over a wide range of concentrations. Despite large differences in oLH measured between treatment groups no clear relationship between butyric acid treatment and oLH secretion was exhibited (figure 4.3.4h).
In light of the high background present in the oLH RIA using the hCG stripped R29 antisera RT-PCR was carried out on RNA from untreated and 16mM butyric acid-treated J24.1 clones. oLHβ mRNA was detected using lh53 and lh33 which anneal to exon 2 and 3'UT sequences respectively (figure 4.3.4i). The predicted amplicon size of 406bp was produced by the reaction containing ovine pituitary RNA. The larger fragment amplified in the transient transfection of JEG3 cells appears approximately 800bp in length which is comparable with that produced by RT-PCR using primers lh52 and lh33. In addition a very faint smaller band is visible at approximately 500bp. RT-PCR of normal and butyric acid-treated J24.1 RNA also produced a fragment of approximately 500bp. The abundance of each band from control and butyric acid-treated J24.1 samples appears similar. The 500bp fragment is present in all reactions containing RNA from poLHβg-transfected JEG3 cells but completely absent from reactions containing normal JEG3 RNA.

4.4 Discussion

Transfection of JEG3 cells using calcium-based techniques provided similar results to those achieved using lipids. However the advantages of using lipids included a reduced incubation time and less labour intensity during the preparation of the transfection mixtures. These two factors were crucial to the studies described in this chapter as they allowed multiple DNA construct combinations to be transfected easily and rapidly. Optimisation of the transfection conditions by adjustment of the lipid:DNA ratio and incubation time did not result in significantly improved transfection efficiencies. This suggests that the guidelines regarding the

ratio of lipid:DNA given by the manufacturer may be applied to transfection of the JEG3 cell line. It also appears that transfection is highly dependent on the lipid used. This was the main feature of the PerFect™ transfection kit which provided a spectrum of different lipids and lipid combinations allowing direct comparison of transfection efficiencies. The advantage of this kit is that it allowed 8 different lipids to be tested using the same methodology and thus did not require repeated adjustments for each lipid.

The exact chemical composition of PerFect™ lipids is not disclosed by the manufacturer, however certain characteristics are described. Pfx4 and Pfx5 both contain 1:1 mixes of cationic lipids whereas Pfx8 and DOTAP each contain only one cationic lipid. The amount of positive charge displayed by the lipids depends largely on the size of the molecules. Interestingly Pfx5 and 8 have the greatest mean molecular weight of the lipids that most effectively transfected JEG3 cells. Although DOTAP and Pfx4 both contain molecules with similar mass, Pfx4 contains a mixture of two types of lipid suggesting that this factor may be more important than the amount of charge alone. The only other lipid mix within the PerFect™ kit with similar molecular weight to Pfx4 is Pfx3. This transfection agent also contains L-dioleoyl phosphatidylethanolamine (DOPE) which suggests that this reduces uptake of DNA by JEG3 cells. Essentially lipid mixtures used in mammalian cell transfections are diverse reflecting the general lack of understanding at this time of the exact mechanisms underlying lipid specificities for different cell lines. The general level of transfection efficiency varies between cell lines and appears to be largely dependent on the rate of proliferation exhibited. Many slow growing neuroendocrine cell lines such as AtT-20 and $L\beta T_2$ prove very difficult to transfect with efficiencies often below 0.5%. Other cell lines such as Chinese hamster ovary (CHO) cells exhibit far higher transfection efficiencies in excess of 30%. The relatively slow growth rate of JEG3 cells and their neuroendocrine origin may predispose them to poor uptake of DNA, although the exact mechanisms which prevent efficient DNA uptake remain unclear.

The model of hCG secretion from JEG3 cells was an attractive one as it was known to be constitutive in nature (Suemizu *et al.*, 1988) and devoid of granins (Howe, 1995). Furthermore at the time this cell line was the only one to secrete dimeric gonadotrophin. Transient transfection of granin expression constructs and subsequent stimulation of hCG expression with 1mM dibutyryl cAMP did not provide any significant differences in hCG storage profiles when compared to untransfected JEG3 cells. Although normal JEG3 cells only secrete hCG and other proteins through a constitutive pathway it was hypothesised that granin-induced aggregation of hCG within the ER and TGN may have led to formation of a regulated pathway detected by a reduction in the proportion of total hCG secreted. The high background of hCG secreted normally from untransfected cells masked any putative effects on secretion induced by expression of granins. This hypothesis is represented schematically below.

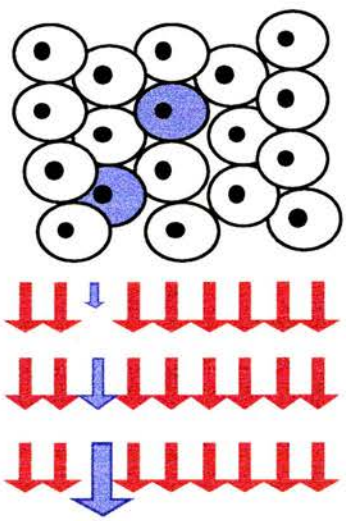

Figure 4.4a: Schematic representation illustrating high background hCG expression masking putative effects of transient granin expression.

hCG expression by transfected (blue) and untransfected cells is stimulated by addition of 1mM dibutyryl cAMP.

Any putative changes in hCG secretion profiles caused by transient gene expression are undetectable by RIA due to the abundance of hCG from untransfected cells (shown in red).

This hypothesis may explain why subtle changes in the proportion of total hCG which is stored were not resolved between untransfected cells and cells expressing granins. This hypothesis did not prevent detection of changes in total hCG expression observed in transfected cells expressing CgA or SgII. Significantly the increase in hCG expression apparently induced by hCgA also occurred in Chinese hamster ovary (CHO) cells

cotransfected with oLH and hCgA expression constructs (see chapter 5). In contrast however bSgII expression had no such effect on oLH expression in transfected CHO cells. An extended 5' untranslated region of hCGβ is not present in LHβ (Bousfield *et al*, 1994) and may allow interaction with SgII facilitating enhancement of translation. Future studies involving removal of this 5' untranslated region or engineering of chimeric hCGβ/LHβ genes may elucidate the role of SgII in β-subunit gene expression. Due to the lack of data reporting uptake of CgA or SgII-derived peptides by placental trophoblasts it is likely that increased hCG expression is occurring in transfected cells within the population. However it remains a possibility that granin-derived peptides exert effects upon hCG expression in untransfected JEG3 cells. This is a major drawback of transient transfection studies measuring hCG secretion in the JEG3 cell line. Although a plethora of granin-derived peptides has been reported to exhibit a wide range of biological effects (see section 1.6.6), enhancement of hCG subunit gene transcription has not been observed. However it is perhaps significant to note that an inhibitory effect of the CgA-derived peptide pancreastatin on PTH and CgA transcription and mRNA stability has been reported (Zhang *et al.*, 1994). Although production of this peptide may lead to an autocrine self-regulation of CgA expression an effect on hCG expression might nevertheless occur. The proteolytic capacity of JEG3 cells has not been reported but novel cleavage of CgA and SgII may lead to production of as yet uncharacterised peptides that enhance expression of hCG genes transcriptionally or at the level of mRNA stability. This may explain the observed stimulatory effect on constitutive secretion of hCG. Cotransfection of all three granin expression constructs abolished the enhancement of hCG expression observed in populations transfected with either phCgA or pbSgII61 alone suggesting an inhibitory role for CgB on the actions of CgA and SgII. Storage of hCG has been reported to occur at a significantly reduced rate in comparison to that of LH *in vitro* due to rapid dimerisation and the presence of the hydrophilic CTP on the hCGβ subunit (Bielinska *et al.*, 1994; Muyan *et al.*, 1996). Therefore it is likely that hCG may never be secreted exclusively via the regulated pathway despite the presence of aggregating factors such as the granins. However it is also likely that the high level of background hCG expressed by untransfected

JEG3 cells may prevent detection of granin-induced hCG storage. This hypothesis was the main reason for attempting stable transfection of the JEG3 cell line.

The study of interactions between multiple gene products using stable transfections requires isolation of separate clones containing each combination of the genes of interest. Although this process would undoubtedly be very time consuming it was undertaken with the goal of clonal expression in mind. Results from initial generation of JEG3 cells containing only the β or α and β expression constructs were disappointing. Southern analysis of JEG3 genomic material for integration of the oFSHβ gene suggested that no copies had stably integrated. Analysis of gene expression by RIA substantiated this initial finding. However Southern hybridisation of other JEG3 transfections clearly indicated the presence of 1-2 copies of oLHβ genes equivalent in size to the control fragments. Clones that appeared to contain integration of half copies are likely to have arisen due to incomplete isolation of clonal populations. For example a population containing cells with 1 copy and others with 2 copies may lead to a signal representing 1.5 integrated copies of the oLHβ gene. The equivalent size of the control and sample bands suggested that the integrated oLHβ sequence had remained intact and therefore was likely to be functional. However the frequency of integration observed was lower than anticipated. Although the selection pressure applied using 200μg/ml G418 was undoubtedly significant, killing 90% of untransfected cells in 7 days, it is possible that a higher concentration is required for multiple copy integration. Alternatively the maintenance dose of 125μg/ml G418 may have been insufficient leading to partial reversal of the integration event. Removal of sufficient selection pressure could over time have led to homologous recombination of concatemerised sequences. This crossover event would return the construct sequences to their original circular form and the transfection would once again become transient. Preferential integration of the neo^R gene is unlikely due to the presence of both the marker and insert on the same molecule. However this may have occurred if secondary structures present within the oLHβ gene prevented recombination with the human genome. Recombination of LHβ

sequences within the human genome is known to have occurred during evolution as sequence comparisons of hLIIβ and hCGβ suggest that the multiple copies of hCGβ arose from hLHβ gene duplications (Talmadge *et al.*, 1984). Despite the difference in species, this event suggests that LHβ sequences are capable of recombining with human genomic sequences.
In light of the expression exhibited by transiently transfected JEG3 cells it may be concluded that the lack of detectable ovine gonadotrophin expression from stably transfected JEG3 cells is in part due to insufficient integrated copies of the requisite genes. In addition it is possible that the site of integration within the human genome is not conducive to high-level gene expression. Of the possible reasons explaining the low frequency of integrated genes, the most likely in my opinion is that insufficient selective pressure was applied during the isolation process.

oLH RIA of J23 cultures using the hCG-stripped R29 antisera failed to demonstrate expression levels significantly in excess of background produced by normal JEG3 cells. The lack of detectable dimeric hormone may have arisen due to a shortage of αGSU in the unstimulated cells or due to poor dimerisation between the ovine and human subunits. RIA of stable transfections containing both α and β subunits for either oFSH or oLH obviated the requirement for cAMP-stimulated αGSU expression. Nevertheless treatment with butyric acid failed to induce expression of either oFSH or oLH. Due to the poor understanding of the mechanisms through which butyric acid exerts its effect it is difficult to provide possible reasons for the lack of efficacy displayed by this agent. It is possible that the reported effect of butyric acid is specific to Vero cells (Wacker *et al.*, 1997) or that the site of gene integration prevents high-level expression in response to this inducing agent.

The appearance of oLHβ-derived amplicons from transfected but not control JEG3 RNA which exceeded the length observed in reactions containing ovine pituitary-derived RNA suggests aberrant splicing of the oLHβ sequence. The use of lh52 which anneals to exon 1 and 2 sequences indicates correct splicing of this intron. However it is apparent that fragments containing this correctly spliced junction exist in low

abundance for both transient and stable transfections. Fragments in excess of the 519 bases encoded by the correctly spliced oLHβ mRNA must contain intronic sequences. RT-PCR using the lh53 primer which anneals to sequences mid-exon 2 appeared to preferentially amplify incorrectly spliced species of oLHβ mRNA. This may have arisen due to secondary structures formed within the correctly spliced oLHβ mRNA reducing the priming ability of lh53. Although the correctly spliced mRNA was detected using lh52 and lh33 in transfected JEG3 cells, using lh53 this mRNA was only detected in the ovine pituitary sample. Application of the same lh53/33 primer pair revealed that transiently transfected JEG3 cells exhibited 2 species of larger transcripts of which the smaller was also expressed by stable transfections. These results suggest that aberrant splicing of oLHβ mRNA occurs in all oLHβ-transfected JEG3 cells. It is likely that in transients a greater abundance of total oLHβ mRNA including correctly spliced oLHβ mRNA accounts for the detectable protein expression. Transient expression of oLH was confirmed in JEG3 cells by indirect immunofluorescence (discussed later). The same method was not applied for detection of protein expression from stable transfections due to their perceived role in providing a means for biochemical assessment of gonadotrophin secretion.

RT-PCR using primers directed towards the 5' and 3' UT regions of oFSH mRNA detected amplicons of only the correct size in samples containing RNA from transiently transfected JEG3 cells. The amplification of the complete coding region with the correct size product suggests that all three exons were correctly spliced. This suggests that expression of an integrated and intact copy of the oFSHβ gene in JEG3 cells would also lead to correct splicing of oFSHβ mRNA. Furthermore the detection of oFSH in the cytoplasm of transiently transfected JEG3 cells indicates that the oFSHβ mRNA is efficiently translated into the correct protein product.

For future biochemical analysis of pituitary gonadotrophin secretion from JEG3 cells stably transfected clones would be required. Two alternatives to this approach include the use of cotransfected reporters allowing purification of the transfected population from the untransfected

background. The pHOOK™ system (Invitrogen, NL) allows isolation of transfected individuals via expression of surface antigens to which immunoreactive magnetic beads may attach. The more conventional fluorescence-activated cell sorting (FACS) may also be used with fluorophores such as enhanced green fluorescent protein (EGFP) to obtain a population containing only transfected cells. The main disadvantages of these approaches is the scale of transfection required to obtain sufficient cell numbers for analysis. Secondly, the variation of transient expression levels between individual cells which is intrinsic to transient transfections may lead to misleading results.

With regard to generation of stably transfected cells this chapter has highlighted two factors that must be improved for future use of JEG3 cells; transfection efficiency and selection pressure. Several DNA transfer methods that were not assessed during these studies include microinjection, electroporation and viral infection. Although effective at transferring DNA into the nucleus, microinjection still relies on chance recombination events for integration. Alternatively electroporation could be used and is often applied in transfection studies as an alternative to chemically-mediated methods. Although effective for certain cell lines electroporation can cause severe loss of viability for others. DNA transfer mediated by viral particles such as attenuated adenovirus is an effective method of gene transfer especially suited for use with cell lines exhibiting a low rate of proliferation.

Although these methods may increase the chance of DNA integration indirectly through increased transfection efficiency, they may not cause the necessary increase in copy number required for high-level gene expression. Assessment of selection pressure during stable transfections requires the processes of selection and isolation to be completed prior to undertaking an appropriate assay. Using G418 selection, selection required 4-6 weeks and a further 3-4 weeks to obtain sufficient numbers for analysis. Assessment of multiple selection conditions in parallel may provide accurate data regarding the relationship between selection pressure and integration of genes. Although this approach may demonstrate an optimum G418 concentration for use with JEG3 cells, it

would require selection and maintenance of several clones for each antibiotic concentration for up to 10 weeks before data from assays would be available. A novel potent antibiotic Blasticidin (Invitrogen, NL) used for selection of pcDNA6-harbouring cells allows isolation of transfected colonies within two weeks. Use of this selection marker may allow assessment of multiple antibiotic concentrations in significantly less time.

Verification of the expression of oFSH and oLH in transiently transfected JEG3 cells by indirect immunofluorescence provided more encouraging results. The appearance of immunoreactive patterns which correlated with those exhibited for hCG in cAMP-stimulated JEG3 cells emphasised the constitutive nature of the pathway by which these cells secrete proteins. The similar intracellular appearance of oFSH and oLH suggests that these hormones are both secreted via the constitutive pathway when expressed at similar levels and in the absence of granins. It may be argued that JEG3 cells are incapable of hormone secretion via a regulated pathway. Recently however the Chinese hamster ovary (CHO) cell line which was previously believed to secrete exclusively via the constitutive pathway has been shown to contain a cryptic regulated pathway capable of secretagogue-stimulated release (Chavez *et al.*, 1996). Transiently transfected CHO cells (see chapter 5) exhibited similar intracellular patterns of oLH and oFSH immunoreactivity to that observed in JEG3 cells. These results suggest that overexpression of pituitary gonadotrophins in cells devoid of granins does not lead to the formation of subcellular aggregates or large secretory vesicles. Transient cotransfection studies using JEG3 cells may allow visualisation of large secretory vesicles induced by granin expression using indirect immunofluorescence or EGFP fusion protein expression. This approach may allow investigation of the effects of granins on gonadotrophin trafficking in individual cells and therefore eliminate background caused by untransfected cells. However the low transfection efficiency of this cell line may slow progress favouring use of an alternative cell line.

The preliminary findings of these studies indicate that oLH and oFSH are secreted via a constitutive pathway in JEG3 cells similar to that through

which hCG is secreted. This suggests that overexpression of the pituitary gonadotrophins like that of hCG is not sufficient to form large secretory granules characteristic of the regulated secretory pathway. The effect of granins and other proteins implicated in exocytosis has yet to be investigated in this model.

These studies have also demonstrated that detection of changes in protein secretion at the individual cell level and at that of the cell population require different approaches. Biochemical observation of the effect of exogenous gene expression on the secretion of endogenously expressed proteins by a population of cells requires that the majority of individuals express the exogenous genes. Clonal populations expressing identical amounts of transfected genes may allow study of secretion using conventional protein assays providing sufficient gene expression is obtained. Analysing secretion of endogenously expressed proteins in transiently transfected populations must be undertaken at the level of the individual cell. Methods such as reverse-haemolytic plaque assay, patch-clamp analysis or indirect immunofluorescence may be used. All future studies using this model would benefit from enhanced transfection efficiency.

If storage of LH and FSH are to be investigated in an *in vitro* system an alternative cell line which is easily manipulated may provide more easily interpretable results. The following chapter details transient transfection studies using the CHO cell line.

Chapter Five

Gonadotrophin Secretion from Chinese Hamster Ovary Cells

5.1 Introduction

The Chinese hamster ovary (CHO) and CHO-K1 cell lines were isolated in 1958 (Puck *et al.*, 1958). CHO cells are fibroblastic in appearance and exhibit relatively rapid proliferation. Secretion of endogenously expressed genes was until recently believed to occur exclusively via a constitutive pathway in these cells. However labelling of glycosaminoglycan chains with $^{[35]}S$ has revealed the presence of post-Golgi vesicles which colocalise with the regulated secretory granule marker Rab3D. Furthermore the release of these vesicles is stimulated by intracellular rises in Ca^{++} or by application of a secretagogue (Chavez *et al.*, 1996). Although details regarding the protein content of these regulated vesicles remain to be revealed, the presence of storage vesicles within CHO cells makes the cell line attractive for use in secretion studies. Unlike the JEG3 cell line, CHO cells do not endogenously express gonadotrophins and no data regarding endogenous expression of granins has been reported. This characteristic provides a 'clean' system in which changes in expression levels of transfected gonadotrophins and granins may be detected with no significant background. CHO cells are widely used for mammalian expression studies and are relatively easy to transfect. Furthermore recombinant human FSH has been expressed on an industrial scale using dihydrofolate reductase (DHFR)-deficient CHO cells as hosts. The quality of hFSH expressed in this system is high and exists predominantly in acidic isoforms which have longer half lives and greater bioactivity (Chappel *et al.*, 1998).

The aims of this study will include formation of a regulated secretory pathway *in vitro*, and demonstration of the factors required for its formation and for differential sorting of LH and FSH. Particular attention will be directed towards the role of the granins in formation of intracellular aggregates facilitating sorting of LH away from other constitutively secreted proteins possibly including FSH.

5.2 Methods

5.2.1 Optimisation of Lipid-based Transfection

Lipids supplied by Invitrogen (PerFect^{TM}) and Promega (Tfx10) were assessed for their ability to mediate transfection of CHO cells. Both lipids were used in accordance with the manufacturers guidelines. PerFect^{TM} lipid transfections were carried out for 3.5 hours whereas Tfx10 transfections were assessed after 4, 6 and 8 hour incubations. In addition the effect of using Opti-MEM (GibcoBRL, UK) during the transfection process in place of DMEM with no FCS added was also assessed.

CHO-K1 transfection was carried out similarly to that of CHO cells using Opti-MEM and PerFect^{TM} lipids.

Transfection efficiency was assessed 48 hours post-transfection by β-galactosidase staining as described in section 2.4.9.

5.2.2 Detection of Gonadotrophin and Granin mRNA by RT-PCR

RNA was extracted from control and transiently transfected CHO cells with Tri-reagent (Sigma-Aldrich, UK) used in accordance with manufacturers guidelines and stored at -70°C.

RT-PCR was carried out to verify expression of inserted genes from transiently transfected constructs. The Titan^{TM} RT-PCR kit (Boehringer Mannheim, UK) was used as described in section 2.3.15. Detection of oFSHβ and oLHβ transcripts was carried out using the primers and conditions described in section 4.2.7. Detection of hCgA, bCgB and bSgII transcripts required the design of novel primers undertaken using GeneJockeyII and GCG software as described in section 2.3.16. Sequence and annealing details of primers assessed for their ability to detect specific transcripts by RT-PCR are contained in table 5.2.2a.

Table 5.2.2a: Primers designed for Amplification of Ovine αGSU RNA and Specific Granin RNA sequences.

Primer name & Target	Binding position	Oligonucleotide Sequence (5'->3') [length]	T_{AN} (°C)	Predicted Product (bp) [pair]
a51 (oαGSU)	-51 to -30 (5' UT)	CAATCAACTCTCCTGACTAC [20]	56	368 [a32]
a52 (oαGSU)	-44 to -42 (5' UT)	CTCTCCTGACTACATTCTG [19]	56	361 [a32]
a32 (oαGSU)	298 to 317	GTTCTCCACTCTGACATTTC [20]	56	368 [a51] 361 [a52]
cga59 (hCgA)	1290 to 1307	GACCAGGAGCTGGAGAGC [18]	67	266 [cga34]
cga34 (hCgA)	1537 to 1556	CAGGCAGGAGTCAGGAGTAG [20]	67	266 [cga59]
cgb51 (bCgB)	1199 to 1218	CTCCACACTAGGCCAAACAG [20]	58	730 [cgb31]
cgb54 (bCgB)	1425 to 1445	CAGTATGCTCCCCATCTCATC [21]	58	504 [cgb31]
cgb31 (bCgB)	1909 to 1928	GGTACCACTGAACTTCTCAG [20]	58	730 [cgb51] 504 [cgb54]
sgii52 (bSgII)	313 to 332	GTGAAGATGAATGGATGAAG [20]	58	416 [sgii33]
sgii53 (bSgII)	340 to 360	CTGAAGCTTTGAGACAGGCTG [21]	58	389 [sgii33]
sgii33 (bSgII)	710 to 728	CACGTCTTCATAGGCAATG [19]	58	416 [sgii52] 389 [sgii53]

Where, T_{AN} is the predicted optimal annealing temperature for the primer pair.

5.2.3 Comparative Expression of oFSHβ Constructs

Total oFSH expression levels in CHO and CHO-K1 cells were measured by RIA 48 or 72 hours after transient cotransfection of the oαGSU expression

construct poαGSU with one of three different oFSHβ expression constructs. Expression levels were compared for poFSHβ containing the full-length cDNA, poFSHβg containing the genomic clone and the EGFP carboxy-terminal fusion to the full-length oFSHβ cDNA (for vector details refer to chapter 3). Addition of 10% pcDNA3.1/His/lacZ plasmid (Invitrogen, NL) to the transfection mixtures allowed variations in transfection efficiency to be estimated by β-galactosidase staining of replicate wells as described in section 2.4.9.

Lysates and media were assayed for oFSH content by RIA as described in section 2.5.5.

5.2.4 Expression of Gonadotrophins and Granins

In order to assess the effect of granins on transient expression of oLH, cotransfections were performed on CHO cells in 12-well plates. All transfection mixtures contained 10% pCAT vector to allow standardisation of results with regard to variations in transfection efficiency by CAT assay (see section 2.5.3). The remaining 90% of DNA in the mixture was divided in two parts so that half would comprise constructs encoding oLH subunits. The remaining 45% of the DNA for transfection would comprise varying quantities of a granin construct. Total DNA in each transfection was maintained at the appropriate level by addition of high purity pBluescript KS+ vector. This DNA ensures that variations in transfection efficiency caused by different ratios of lipid to DNA are reduced. The absence of an efficient eukaryotic promoter within the pBluescript KS+ prevented transcription of bacterial sequences which may cause toxic effects within the transfected mammalian cell.

5.2.5 Visualisation of Intracellular Gonadotrophin Traffic

Combinations of gonadotrophin and granin expression constructs were transiently transfected into CHO and CHO-K1 cells using the respective optimised protocol described previously.

48 to 72 hours after transient transfection cells in chamber slides were fixed and incubated with the appropriate primary antisera overnight at 4°C. Subsequent washing and application of secondary antisera prior to mounting were performed as described in section 2.6.1. Cells transfected

with EGFP constructs were viewed live as described in section 2.6.2. Confocal microscopy was carried out on all samples using a Zeiss Axiovert 100M microscope and LSM510 scanning module (Zeiss, UK) as described in 2.6.3.

5.3 Results

5.3.1 Optimisation of Lipid-based Transfection

CHO cells were effectively transfected with Tfx10 at ratios of lipid to DNA of 3:1 and 5:1 (figure 5.3.1a). Opti-MEM media did not provide consistently increased transfection efficiencies using this lipid. A maximal transfection efficiency of 11.95±2.35% was achieved with the higher ratio of lipid to DNA after a 6 hour incubation. A further increase in transfection efficiency was not observed after an 8 hour incubation with a 5:1 ratio.

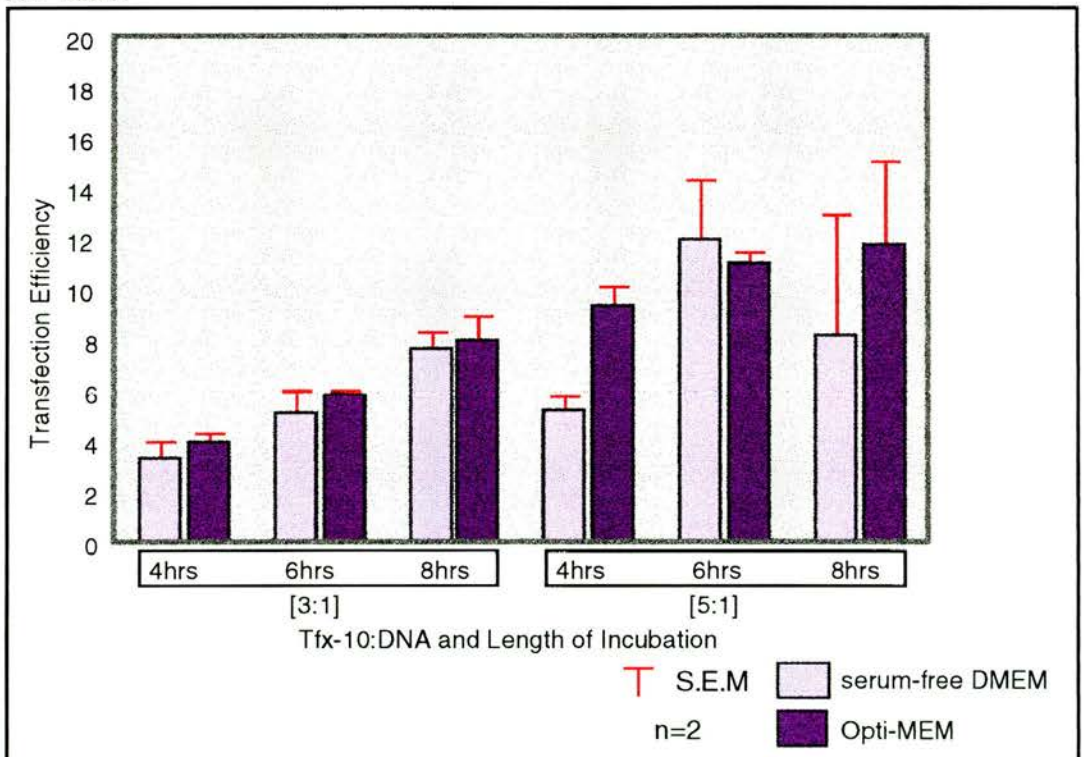

Figure 5.3.1a: Comparison of CHO transfection efficiencies obtained using Tfx10 lipids with either serum-free DMEM or Opti-MEM.

Cells plated in a 12-well dish were transfected with the pcDNA3.1/His/lacZ plasmid and stained for β-galactosidase activity 48 hours posttransfection. 250 cells were counted in four fields of view for each well.

PerFect™ lipids 5 and 8 gave greater transfection efficiencies than the maximum obtained using Tfx10 (figure 5.3.1b). Furthermore Pfx5 exhibited a transfection efficiency of 34.2±0.2% which is almost 3-fold greater than that obtained with Tfx10 and was achieved in only 3.5 hours in comparison to the 6 hour incubation required for Tfx10. A representative photomicrograph of optimally transfected CHO cells after β-galactosidase staining is shown in figure 5.3.1c. Use of Opti-MEM provided increases in transfection efficiency for the majority of PerFect™ lipids tested. The transfection efficiency obtained using Pfx5 was significantly improved from 24.1±0.5% to 34.2±0.2% ($p<0.01$).

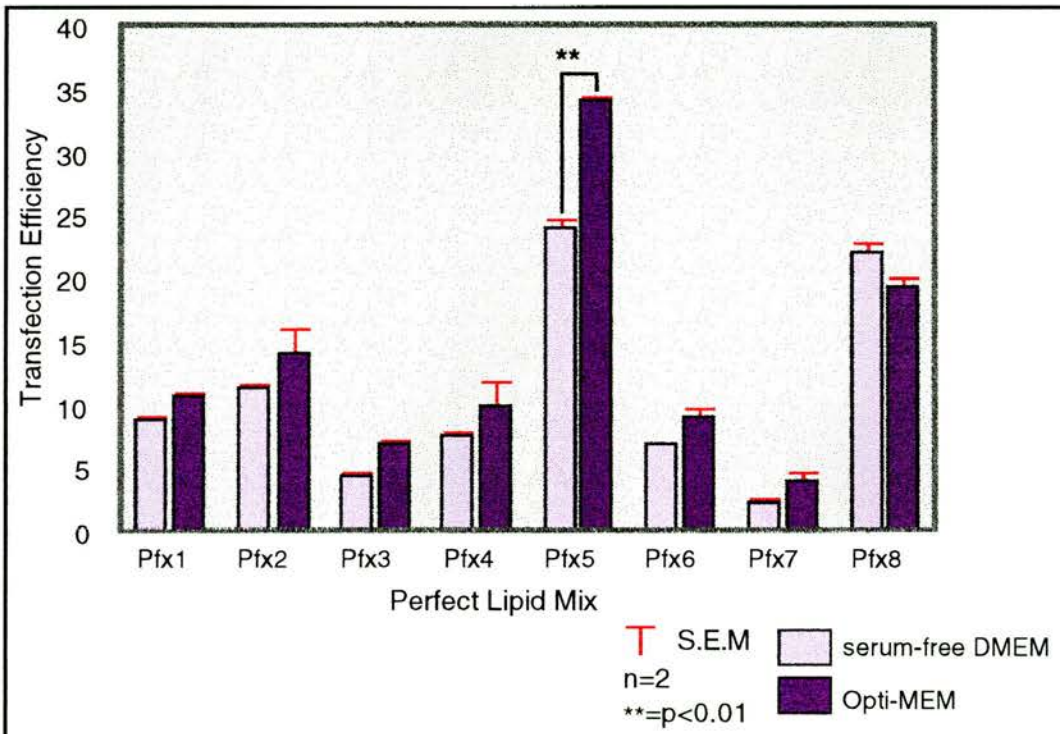

Figure 5.3.1b: Comparison of CHO transfection efficiencies obtained using PerFect lipids with either serum-free DMEM or Opti-MEM.

Cells plated in a 12-well dish were transfected with the pcDNA3.1/His/lacZ plasmid and stained for β-galactosidase activity 48 hours posttransfection. 250 cells were counted in four fields of view for each well.

Transfection of the CHO-K1 cell line was achieved using PerFect™ lipids and Opti-MEM. Surprisingly the most efficient lipid was different to that observed for CHO cells. Pfx1 exhibited a transfection efficiency of

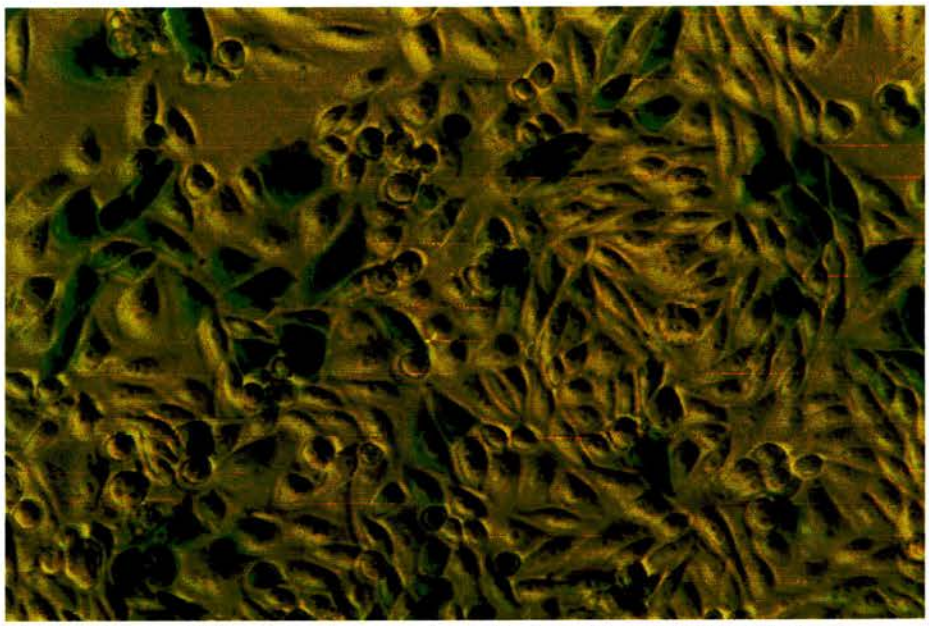

Figure 5.3.1c: CHO cells transiently transfected with pcDNA3.1/His/lacZ.

CHO cells were transiently transfected with pcDNA3.1/His/lacZ using Pfx5. 48 hours posttransfection the cells were fixed and stained for β-galactosidase activity.

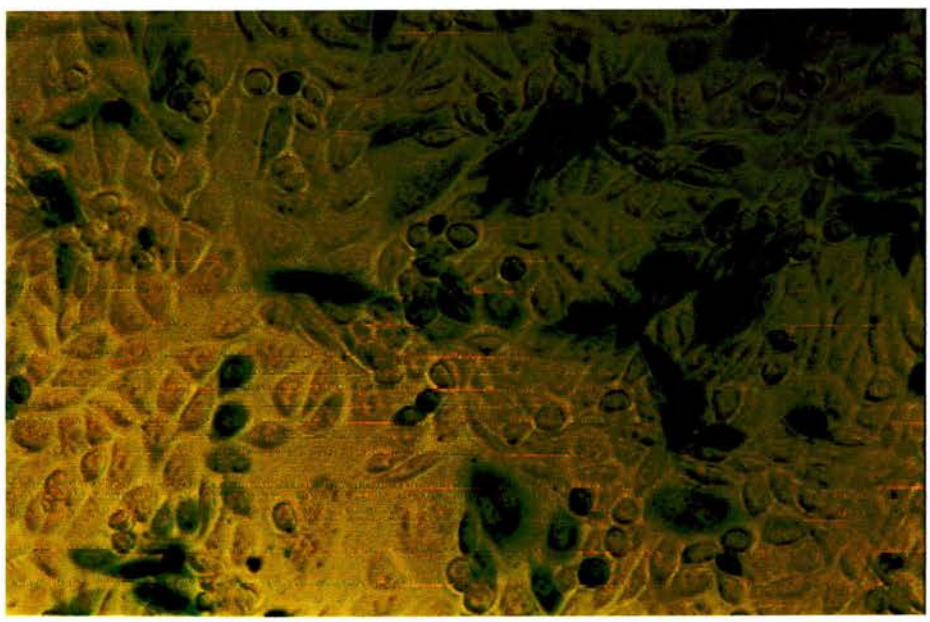

Figure 5.3.1e: CHO-K1 cells transiently transfected with pcDNA3.1/His/lacZ.

CHO-K1 cells were transiently transfected with pcDNA3.1/His/lacZ using Pfx1. 48 hours posttransfection the cells were fixed and stained for β-galactosidase activity.

28.7±0.4% (figure 5.3.1d), similar to that obtained from optimal transfection of CHO cells using Pfx5. A representative photomicrograph of β-galactosidase stained CHO-K1 cells illustrates their appearance after optimal transfection (figure 5.3.1e). Unlike CHO cell transfection in which several lipids demonstrated efficiencies close to or in excess of 10%, only Pfx1 and 7 provided such transfection efficiencies.

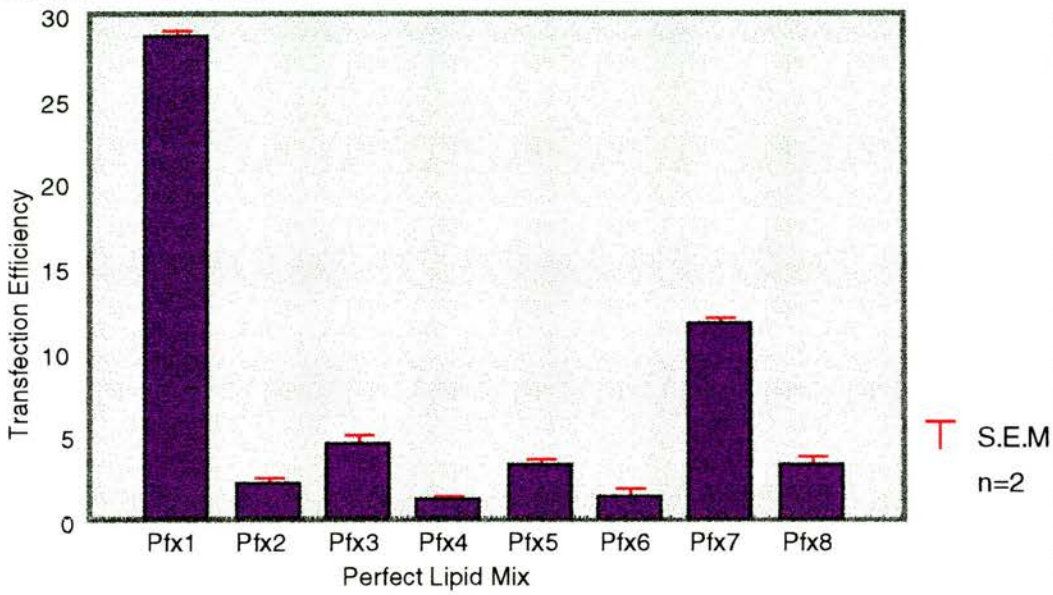

Figure 5.3.1d: CHO-K1 transfection efficiencies obtained using PerFect lipids and Opti-MEM.

Cells plated in a 12-well dish were transfected with the pcDNA3.1/His/lacZ plasmid and stained for β-galactosidase activity 48 hours posttransfection. 250 cells were counted in four fields of view for each well.

5.3.2 Detection of Gonadotrophin and Granin mRNA by RT-PCR

Optimisation of RT-PCR conditions for detection of bCgB, bSgII and oαGSU was undertaken successfully using RNA derived from the ovine pituitary gland (figure 5.3.2a). Optimisation of the hCgA reaction required human pituitary RNA which was unavailable. Expression of specific mRNA in CHO cells was detected for all transiently transfected constructs including phCgA, pbChrB73, pbSgII61, poαGSU, poFSHβg and poLHβg (figures 5.3.2b & c). All products were specific to transfected samples and correlated well with samples containing ovine pituitary-derived RNA with the exception

Figure 5.3.2a: Temperature optimisation of RT-PCRs for ovine αGSU, bovine CgB and bovine SgII.

The ovine αGSU-specific primer combinations were assessed at 54 and 56ºC. Both primer combinations produced the predicted product sizes at each annealing temperature (a51/32-368bp, a52/32-361bp). The bovine CgB-specific primers combinations were assessed at 56, 58 and 60ºC. The predicted products were exhibited for the cgb51/31 (730bp) and cgb54/31 (504bp) reactions. No products were detected for the cgb51/32 or cgb54/32 reactions. The bovine SgII-specific primer combinations were assessed at 58 and 60ºC. Both sgii52/33 and sgii53/33 reactions exhibited the predicted products of 416 and 389bp respectively. No products were detected in any of the control reactions containing no RNA. 100bp ladders were used for size comparison. The gel contained 2% agarose and was run in TBE buffer.

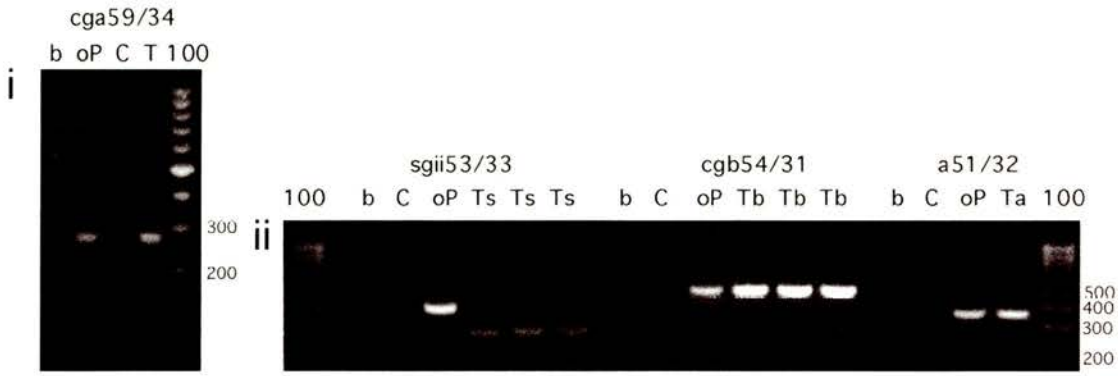

Figure 5.3.2b: Transient expression of granins and ovine αGSU in CHO cells detected by RT-PCR.

i) Primers cga59 and cga34 specific for human CgA exhibited the predicted product size of 266bp in samples containing RNA from sheep pituitary (oP) or CHO cells transiently transfected with the phCgA construct (T). No products were detected in the no RNA control (b) or in samples containing RNA from untransfected CHO cells (C). The reactions were carried out at the annealing temperature of 67°C. ii) Expression of specific mRNA for bSgII, bCgB and ovine αGSU was detected using primers sgii53 and 33, cgb54 and 31 and a51 and 32 respectively. The annealing temperatures used were 58°C for the granin reactions and 56°C for the αGSU reaction. The predicted product sizes were produced for the bCgB reactions (504bp) and oαGSU reactions (368bp) which contained either sheep pituitary RNA (oP) or RNA from CHO cells transiently transfected with either the pbChrB73 (Tb) or poαGSU (Ta) constructs. The bSgII reaction exhibited the predicted product size of 389bp in the sheep pituitary sample but a smaller product (280bp approx.) in samples containing RNA from CHO cells transiently transfected with the pbSgII61 construct (Ts). No products were detected in the no RNA control (b) or in samples containing RNA from untransfected CHO cells (C). RNA was extracted from transiently transfected cells 48 hours posttransfection using Tri-reagent. Both gels contained 2% agarose and were run in TBE buffer. 100bp ladders (100) were used for size comparison.

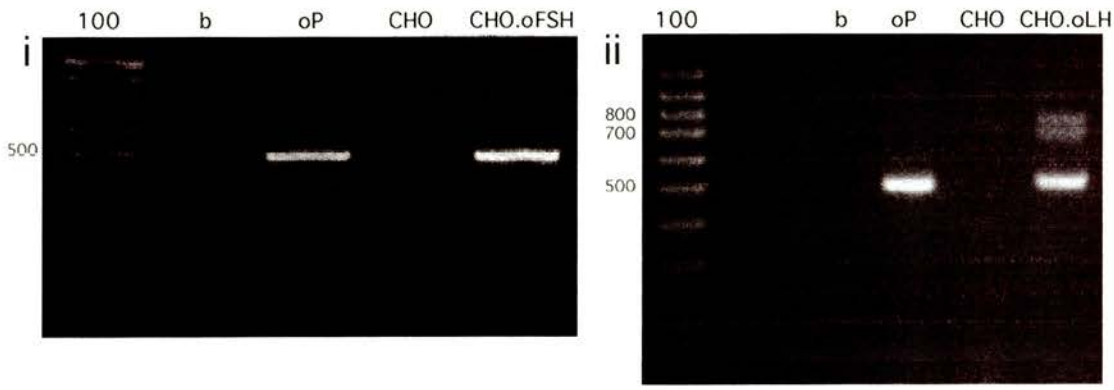

Figure 5.3.2c: Transient expression of ovine gonadotrophin β-subunits detected by RT-PCR.

i) The oFSHβ reactions were carried out using primers fsh51and fsh33 at the annealing temperature of 64°C. The predicted product is 450bp which is approximately the size of that exhibited in reactions containing either sheep pituitary RNA (oP) or RNA from CHO cells transiently transfected with the poαGSU and poFSHβg constructs (CHO.oFSH). No products were present in the no RNA control (b) or untransfected CHO RNA (CHO) samples.
ii) The oLHβ reactions were carried out using primers lh52 and lh33 at the annealing temperature of 70°C. The predicted product is 480bp which is present in samples containing either sheep pituitary RNA (oP) or RNA from CHO cells transiently transfected with with the poαGSU and poLHβg constructs (CHO.oLH). Two additional but less abundant products were detected at approximately 700 and 800bp in the reaction containing RNA from transfected CHO cells. No products were present in the no RNA control (b) or untransfected CHO RNA (CHO) samples.
RNA was extracted from CHO cells 48 hours posttransfection using Tri-reagent. Both gels contained 2% agarose and were run in TBE buffer. 100bp ladders were used for size comparison.

of bSgII which produced a smaller product (280bp) in comparison to that from ovine samples (389bp). The oLHβ RT-PCR also produced 2 less abundant larger products of approximately 700 and 800bp in size. These products were equivalent in size to those produced by RT-PCR of JEG3 cells transiently transfected with the same constructs.

5.3.3 Comparative Expression of oFSHβ Constructs

Prior to RIA of lysates and media fractions β-galactosidase staining of replicate wells was undertaken demonstrating that no significant variations in transfection efficiency occurred (data not shown).

CHO-K1 transiently transfected with the oαGSU construct and either the oFSHβ cDNA, genomic sequence or EGFP fusion produced low expression of oFSH as detected by RIA (figure 5.3.3a).

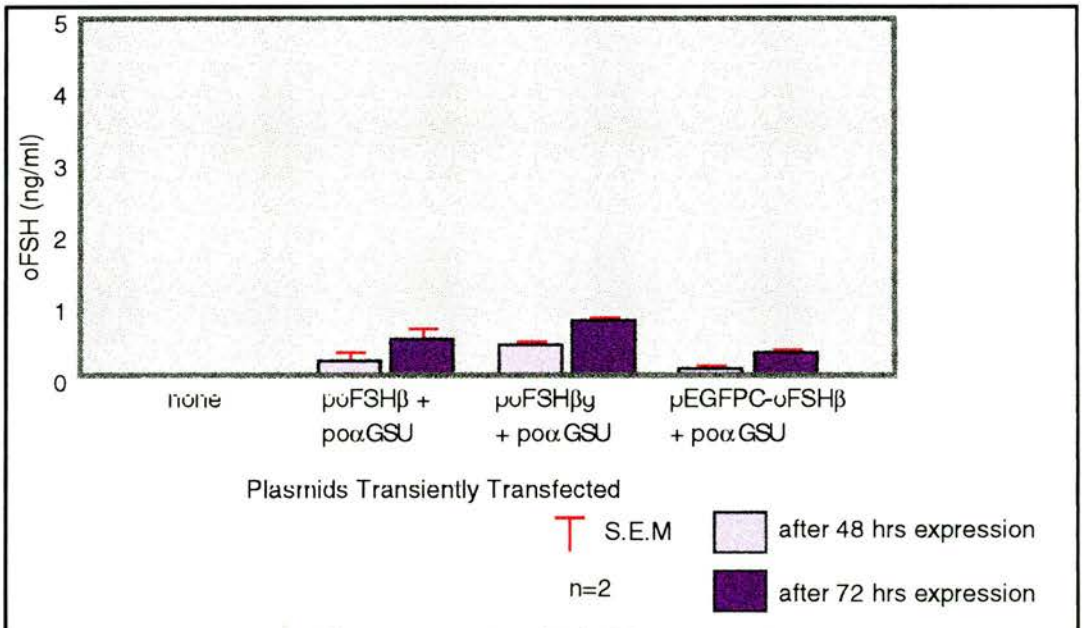

Figure 5.3.3a: Total oFSH expressed by CHO-K1 cells transiently transfected with different oFSHβ expression constructs.

CHO-K1 cells were transfected using Pfx1. Media and lysates were harvested 48 and 72 hours posttransfection. oFSH levels were determined by RIA. poαGSU contains the ovine αGSU cDNA, poFSHβ contains the ovine FSHβ cDNA, poFSHβg contains the ovine FSHβ genomic sequence, pEGFPC-oFSHβ contains the ovine FSHβ cDNA downstream in an ORF with EGFP.

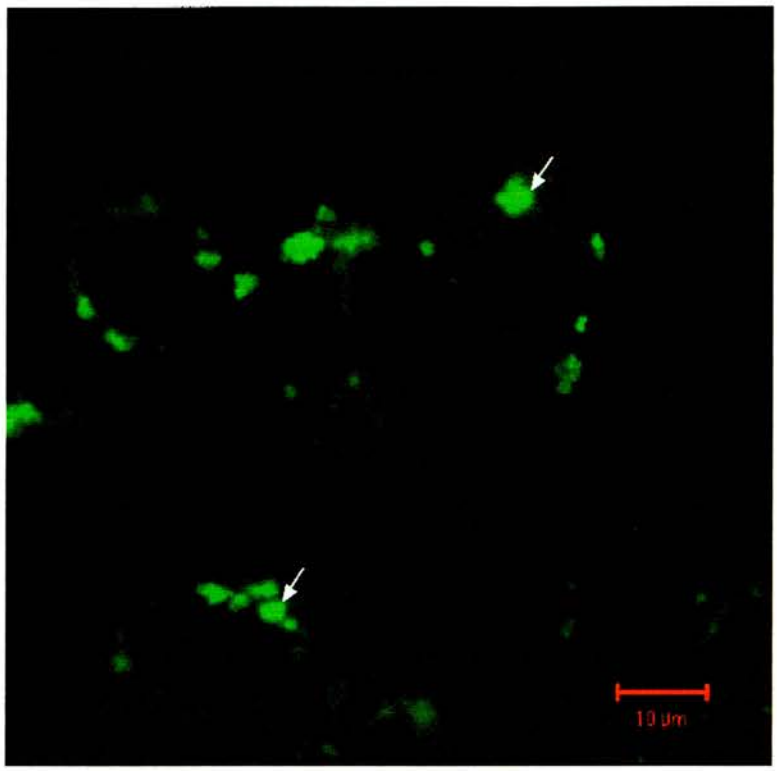

Figure 5.3.3b: Subcellular distribution of oFSHβ in transiently transfected CHO-K1 cells 48 hours posttransfection.

CHO-K1 cells were transiently transfected with poαGSU and poFSHβg. Cells were fixed in Bouins 48 hours posttransfection. Large fluorescence bodies are clearly visible within the perinuclear region of these cells (arrows). The diameter of these intracellular bodies ranges from approximately 1-3µm. FSH antisera (M91) was diluted 1:500 and FITC-conjugated goat anti-rabbit secondary antisera diluted 1:40. Fluorescence was observed using a 488nm argon laser and 505-535nm bandpass filter.

Indirect immunofluorescence of oFSHβ showed bright perinuclear signal coinciding with the subcellular localisation of the endoplasmic reticulum (ER) and *trans*-Golgi network (TGN) (figure 5.3.3b).

Similar transient transfection of CHO cells led to relatively high expression levels from the oFSHβ construct containing the genomic sequence with significantly less expression from the cDNA-containing construct (figure 5.3.3c). The increased expression from the genomic clone was unexpected. Figure 5.3.3c also demonstrates an absence of RIA-detectable oFSH from cells transfected with the EGFPC-oFSHβ fusion construct.

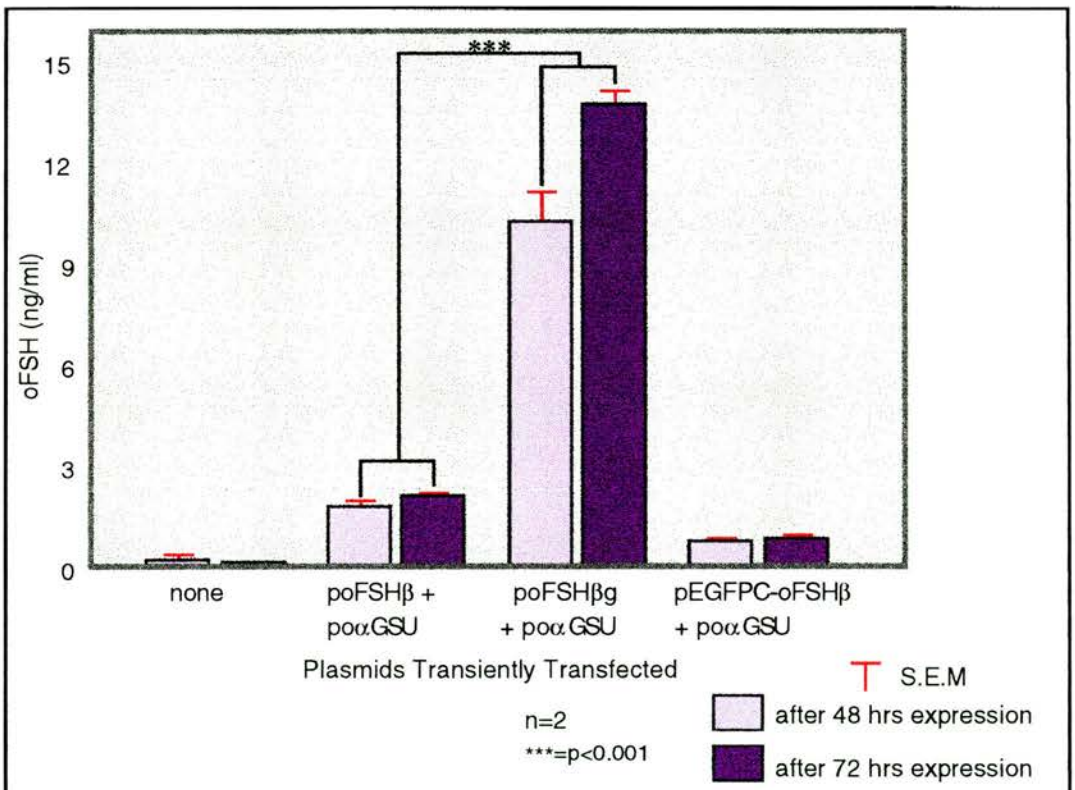

Figure 5.3.3c: Total oFSH expressed by CHO cells transiently transfected with different oFSHβ expression constructs.

CHO cells were transfected using Pfx5. Media and lysates were harvested 48 and 72 hours posttransfection. oFSH levels were determined by RIA. poαGSU contains the ovine αGSU cDNA, poFSHβ contains the ovine FSHβ cDNA, poFSHβg contains the ovine FSHβ genomic sequence, pEGFPC-oFSHβ contains the ovine FSHβ cDNA downstream in an ORF with EGFP.

Comparison of the distribution of oFSH expressed by CHO cells transiently transfected with either the cDNA or genomic clone demonstrated a significant difference (figure 5.3.3d). The cells expressing the genomic clone of oFSHβ exhibited a significantly lower proportion of intracellular oFSH after 48-72 hours expression despite expressing a greater abundance of oFSH intracellularly in comparison to cells transfected with the oFSHβ cDNA expression construct.

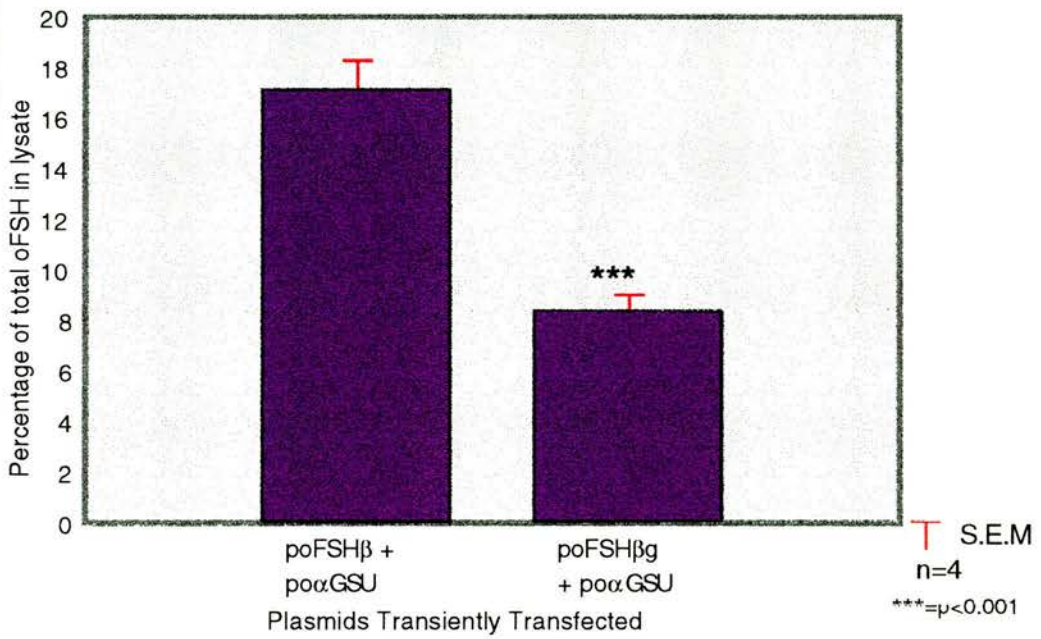

Figure 5.3.3d: Comparison of oFSH storage by CHO cells transiently transfected with different oFSHβ expression constructs.

CHO cells were transfected using Pfx5. Media and lysates were harvested 48 and 72 hours posttransfection. oFSH levels were determined by RIA. The results shown represent the mean of figures determined after 48 and 72 hours of expression. poαGSU contains the ovine αGSU cDNA, poFSHβ contains the ovine FSHβ cDNA, poFSHβg contains the ovine FSHβ genomic sequence.

5.3.4 Expression of oLH and Granins

All oLH measured in lysates and media fractions were standardised against total protein determined by Bradford assays and for variations in transfection efficiency by CAT assay (see sections 2.5.2-3 & figure 4.3.2c).

In comparison to cells expressing only oLH constructs, a significant increase in the total amount of oLH expressed was observed in cells cotransfected with the hCgA expression construct at ratios equal to or in excess of 75% of the oLH expression constructs (figure 5.3.4a).

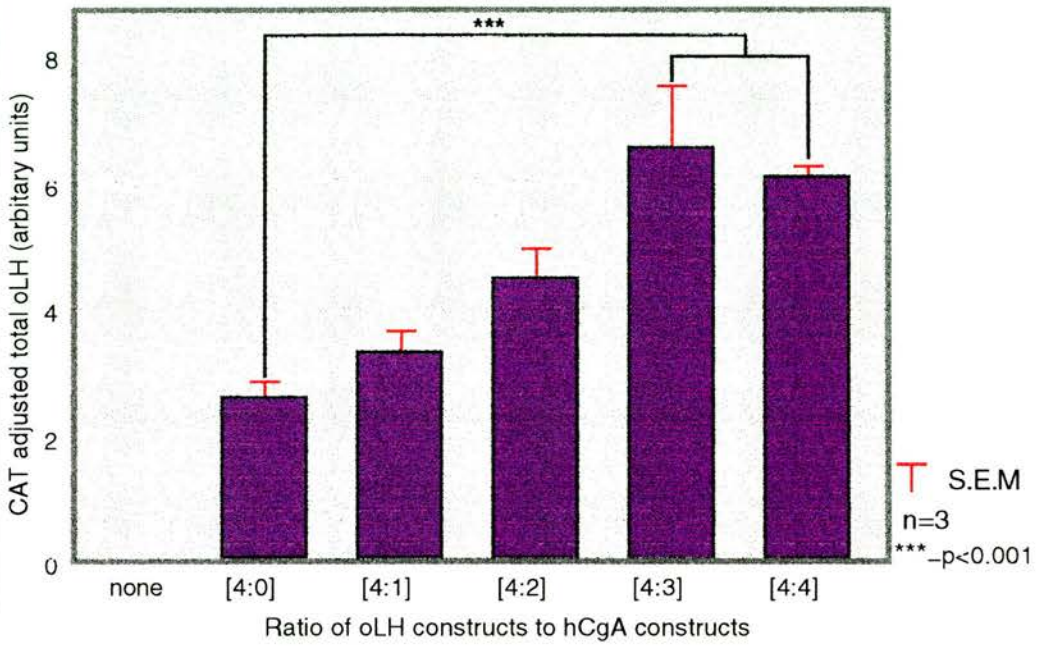

Figure 5.3.4a: Total oLH expression in CHO cells transiently cotransfected with different amounts of the hCgA expression construct.

All transfected cells received an equal amount of poαGSU and poLHβg constituting 45% of the total DNA added to each well. The remaining 45% of the DNA in the transfection mix contained varied amounts of phCgA or pBluescript KS+. Addition of pBluescript KS+ to the transfection mix ensured that the total DNA concentration was maintained in each transfection. The proportion of hCgA expression constructs in the transfection mix was increased from none ([4:0]) to a 1:1 ratio ([4:4]). All transfection mixes contained 10% pCAT as an internal control. oLH in the media and lysate fractions was measured by RIA and standardised against total protein content and CAT activity.

Although total oLH expression was increased by cotransfection of the hCgA expression construct at the ratios shown in figure 5.3.4a, no significant alteration in the proportion of total oLH which remained intracellularly was observed (figure 5.3.4b).

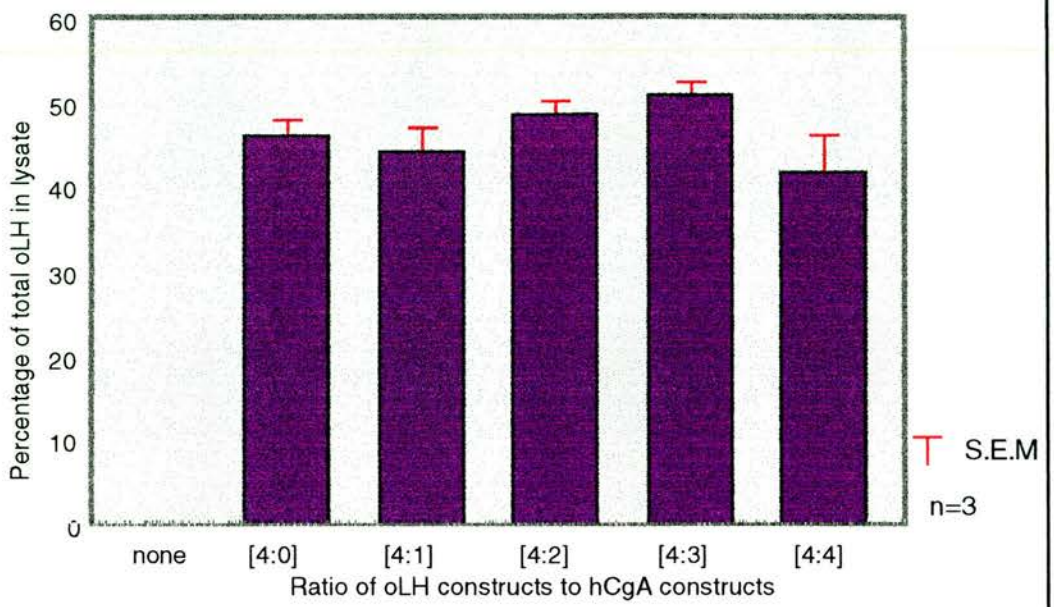

Figure 5.3.4b: Storage of oLH in CHO cells transiently cotransfected with different amounts of the hCgA expression construct.

All transfected cells received an equal amount of poαGSU and poLHβg constituting 45% of the total DNA added to each well. The remaining 45% of the DNA in the transfection mix contained varied amounts of phCgA or pBluescript KS+. Addition of pBluescript KS+ to the transfection mix ensured that the total DNA concentration was maintained in each transfection. The proportion of hCgA expression constructs in the transfection mix was increased from none ([4:0]) to a 1:1 ratio ([4:4]). All transfection mixes contained 10% pCAT as an internal control. oLH in the media and lysate fractions was measured by RIA and standardised against total protein content and CAT activity before determining the proportion of total oLH present in the lysate.

Similar cotransfection of oLH expression constructs with increasing amounts of the bSgII expression construct (pbSgII61) exhibited no significant change in the total amount of oLH transiently expressed by CHO cells in comparison to cells containing only the oLH expression constructs (figure 5.3.4c). However a significant difference was observed between cells transfected with pbSgII61 equalling 50% and 75% of the concentration of oLH expression constructs.

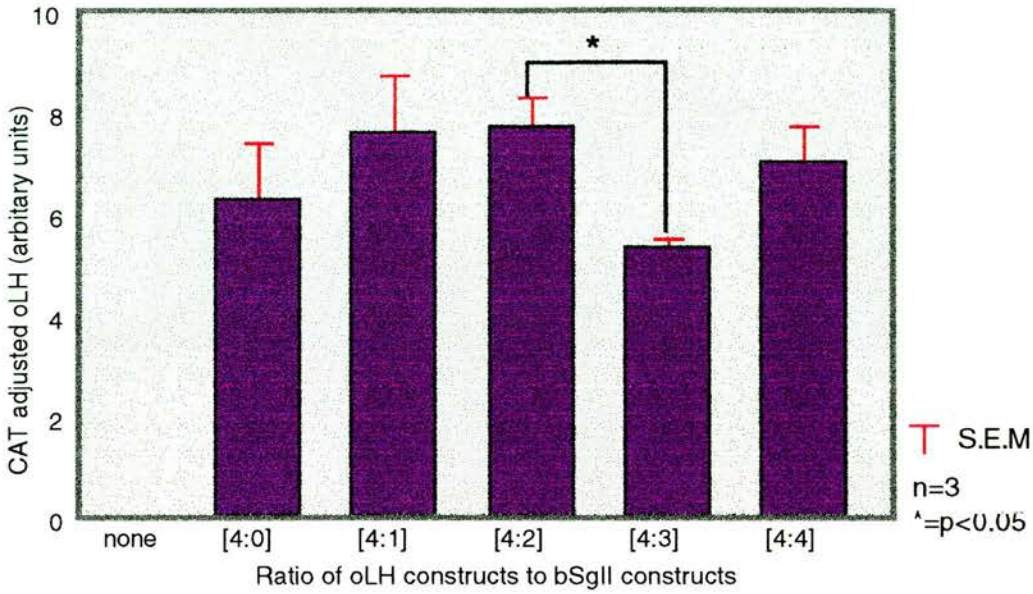

Figure 5.3.4c: Total oLH expression in CHO cells transiently cotransfected with different amounts of the bSgII expression construct.

All transfected cells received an equal amount of poαGSU and poLHβg constituting 45% of the total DNA added to each well. The remaining 45% of the DNA in the transfection mix contained varied amounts of pbSgII61 or pBluescript KS+. Addition of pBluescript KS+ to the transfection mix ensured that the total DNA concentration was maintained in each transfection. The proportion of bSgII expression constructs in the transfection mix was increased from none ([4:0]) to a 1:1 ratio ([4:4]). All transfection mixes contained 10% pCAT as an internal control. oLH in the media and lysate fractions was measured by RIA and standardised against total protein content and CAT activity.

Although no significant difference in total oLH expression was observed during coexpression of the bSgII gene, significant decreases in the proportion of oLH remaining in the lysate fraction were observed particularly for the cells which received the lower concentrations of the pbSgII61 construct (figure 5.4.3d). However no significant differences were observed between cells which received different proportions of the bSgII expression construct.

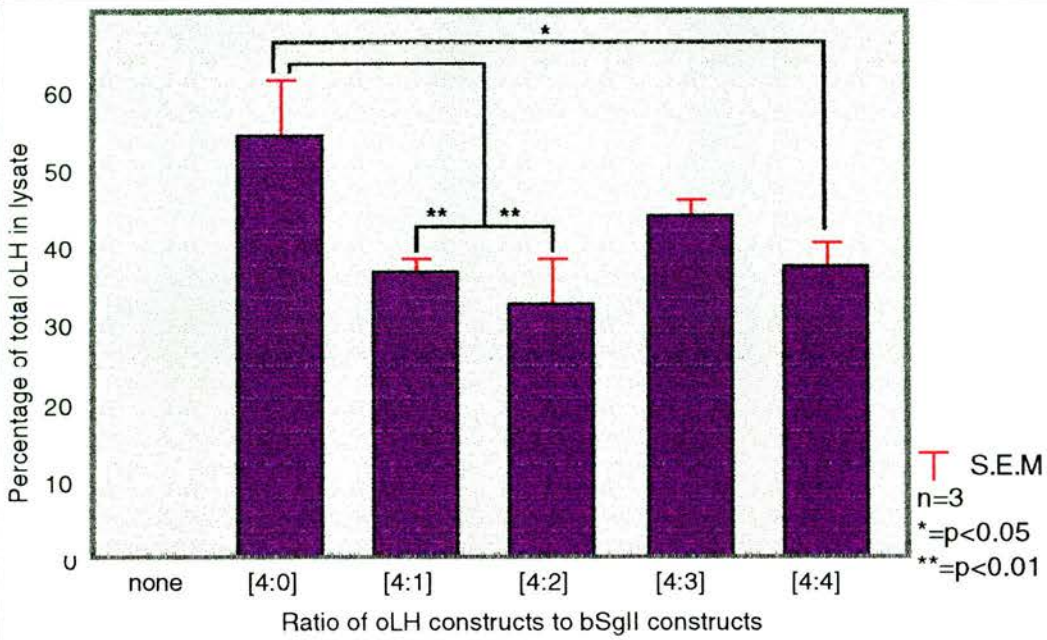

Figure 5.3.4d: Storage of oLH in CHO cells transiently cotransfected with different amounts of the bSgII expression construct.

All transfected cells received an equal amount of poαGSU and poLHβ constituting 45% of the total DNA added to each well. The remaining 45% of the DNA in the transfection mix contained varied amounts of pbSgII61 or pBluescript KS+. Addition of pBluescript KS+ to the transfection mix ensured that the total DNA concentration was maintained in each transfection. The proportion of bSgII expression constructs in the transfection mix was increased from none ([4:0]) to a 1:1 ratio ([4:4]). All transfection mixes contained 10% pCAT as an internal control. oLH in the media and lysate fractions was measured by RIA and standardised against total protein content and CAT activity before determining the proportion of total oLH present in the lysate.

Comparison of the amount of oLH and oFSH stored between separate transfection experiments using the ovine αGSU expression construct in conjunction with either genomic clone for oLHβ or oFSHβ demonstrated a significant difference (figure 5.3.4e).

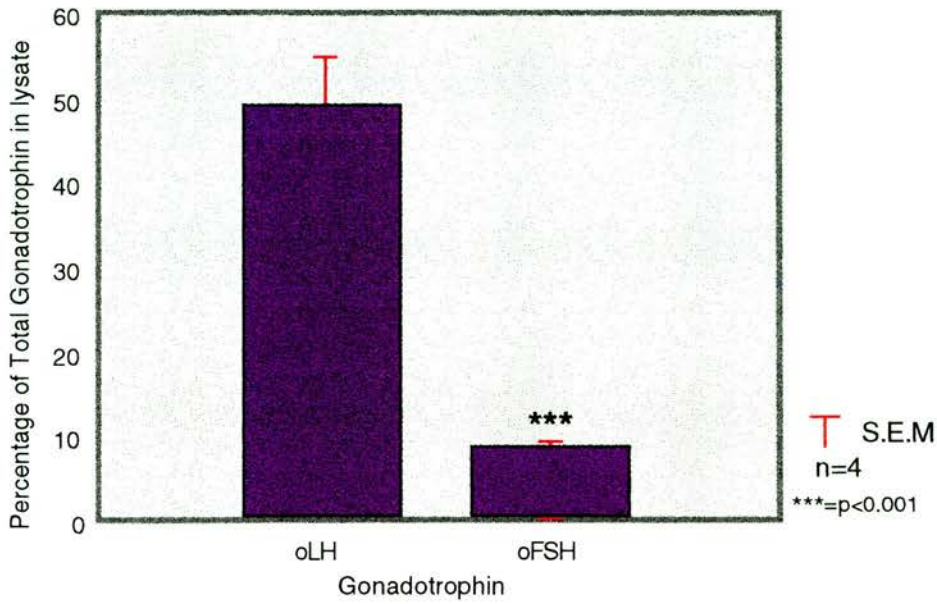

Figure 5.3.4e: Comparison of oLH and oFSH storage by transiently transfected CHO cells.

CHO cells were transfected using Pfx5. Media and lysates were harvested 48 and 72 hours posttransfection. oLH and oFSH levels were determined by RIA. All transfections contained poα GSU at a 1:1 ratio with either genomic clone for oLHβ or oFSHβ.

5.3.5 Visualisation of Intracellular Traffic

No CHO cells exhibited any staining in the absence of the appropriate transfection or primary antisera. Propidium iodide (Sigma-Aldrich, UK) fluorescence appeared restricted to the nucleus and mitochondria.

Indirect immunofluorescence was initially carried out on α-tubulin to verify that the subcellular structures within the fixed cells were intact. Figure 5.3.5a shows tubulin staining in a Bouins fixed untransfected CHO cell and indicates that these relatively fragile cytoskeletal elements are preserved. Staining of the endoplasmic reticulum (ER) and Golgi apparatus using Bodipy 630/650 (Molecular Probes, NL) demonstrated the subcellular localisation of these compartments within CHO cells (figure 5.3.5b). It should be noted that untransfected CHO cells stained with this dye also exhibit several granule-like fluorescent bodies towards the periphery of the cell.

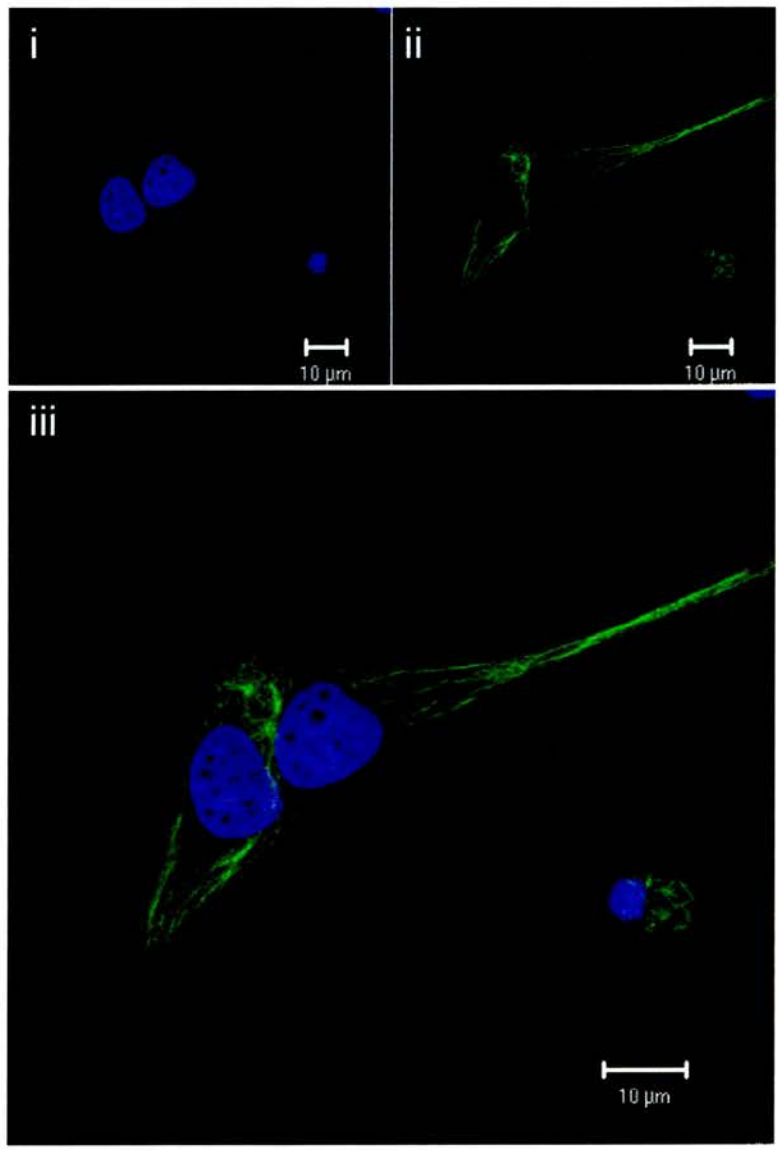

Figure 5.3.5a: Subcellular distribution of α-Tubulin in CHO cells.

CHO cells were fixed in Bouins and stained with the α-Tubulin FITC conjugate. Nucleic acids were detected using 10µg/ml propidium iodide (i). Excitation of the fluorophores was undertaken using the 488nm argon and 543nm HeNe lasers and detected using 505-535nm bandpass (ii) and 580nm longpass (i) filters respectively. The composite image is represented in (iii).

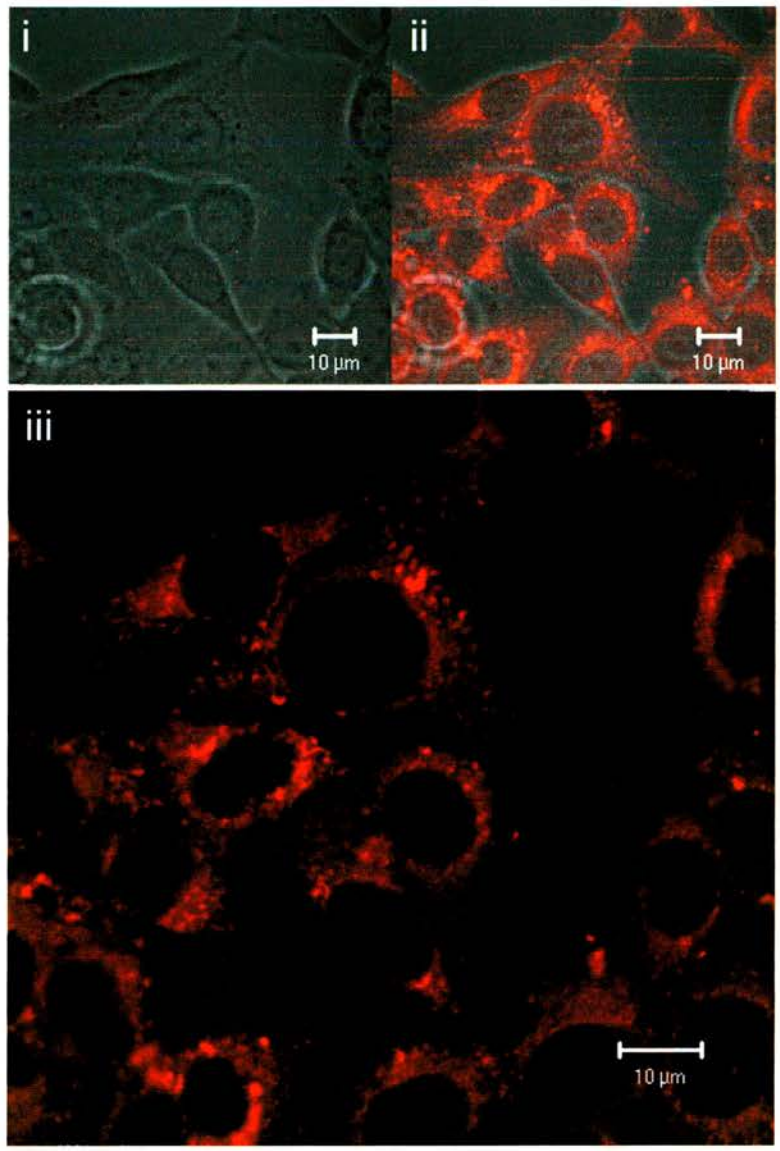

Figure 5.3.5b: CHO cells stained with the endoplasmic reticulum and Golgi apparatus-specific probe Bodipy 630/650.

i) Phase-contrast image. ii) Bodipy 630/650 fluorescence and phase-contrast overlay. iii) Bodipy 630/650 fluorescence. The pattern of fluorescence appears punctate throughout the cytoplasm and particularly concentrated at perinuclear regions. Untransfected CHO cells were fixed in Bouins and mounted in Citifluor containing 10µg/ml Bodipy 630/650. Fluorescence was detected using the HeNe 633nm laser and 640nm longpass filter.

The subcellular localisation of oFSH in transiently transfected CHO cells did not resemble the staining achieved with the ER/Golgi dye Bodipy 630/650. Instead the pattern of staining resembled that of a fine mesh within the cytoplasm (figure 5.3.5c). A small amount of punctate expression was exhibited at 'intersections' within the 'mesh-like' staining. This pattern of staining was almost identical to that of oLH in transiently transfected CHO cells (figure 5.3.5d). No discernible increase in the amount of aggregation was observed in cells transfected with the oFSH expression constructs compared to those transfected with the oLH expression constructs.

CHO cells transfected with expression constructs for individual granins exhibited strikingly different patterns of staining compared to those of the pituitary gonadotrophins alone. However no staining was achieved using antisera against SgII or using the monoclonal CgA antisera. CHO cells transfected with phCgA exhibited staining (using the polyclonal antisera) which resembled the cisternae of the ER and Golgi apparatus throughout the cytoplasm. Furthermore several vesicle-like bodies ranging in diameter between 100-600nm were present towards the periphery of the cell (figure 5.3.5e). Detection of bCgB in transiently transfected CHO cells exhibited relatively large areas of concentrated cytoplasmic staining some of which was located proximal to the plasma membrane (figure 5.3.5f). The transfected cells also exhibited widespread punctate expression with the vesicle-like bodies ranging in diameter between 0.1-2.0μm. The bCgB-immunoreactivity appears similar to the fluorescence produced by the ER and Golgi-specific probe Bodipy 630/650 (figure 5.3.5b).

Colocalisation of oLH with hCgA and bCgB was also exhibited in cotransfected CHO cells. Cells cotransfected with oLH and hCgA expression constructs (figure 5.3.5g) exhibited significant colocalisation throughout the ER and Golgi apparatus. In addition oLH-immunoreactivity appears to predominate at the periphery of the cell. Colocalisation within distinct fluorescent bodies ranging in diameter from 310-640nm appeared transient. Three types of immunoreactivity within these bodies was observed; hCgA only, oLH only and both hCgA and oLH. Vesicles containing hCgA only or both hCgA and oLH appeared throughout the cytoplasm whereas those containing only oLH appeared proximal to the

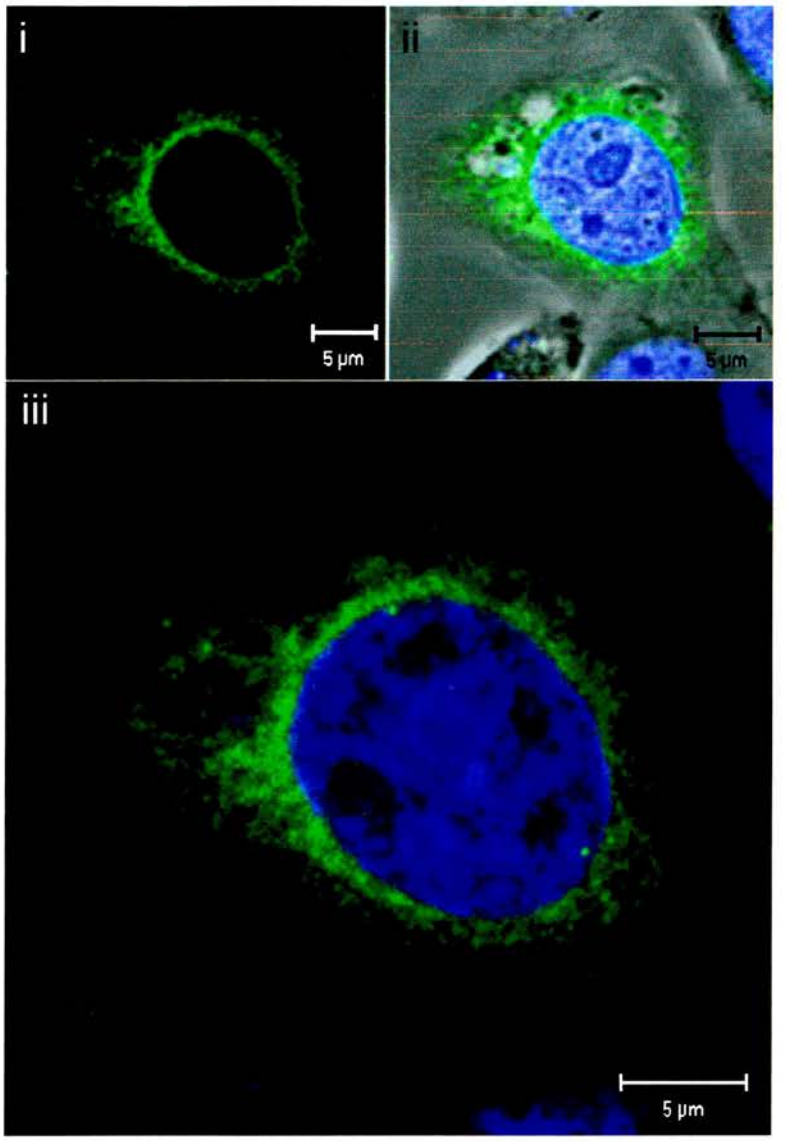

Figure 5.3.5c: Subcellular distribution of oFSH in a transiently transfected CHO cell.

i) FSH-immunoreactivity (green) appears dispersed throughout the cytoplasm in a 'mesh-like' pattern. ii) Overlay of FSH-immunoreactivity, nuclear staining (blue) and phase-contrast. Cells were fixed in Bouins 48 hours posttransfection with poαGSU and poFSHβg. Primary FSH polyclonal antisera (M91) was diluted 1:500. Goat anti-rabbit FITC conjugate was diluted 1:40. Nuclear staining was undertaken using 10µg/ml propidium iodide.

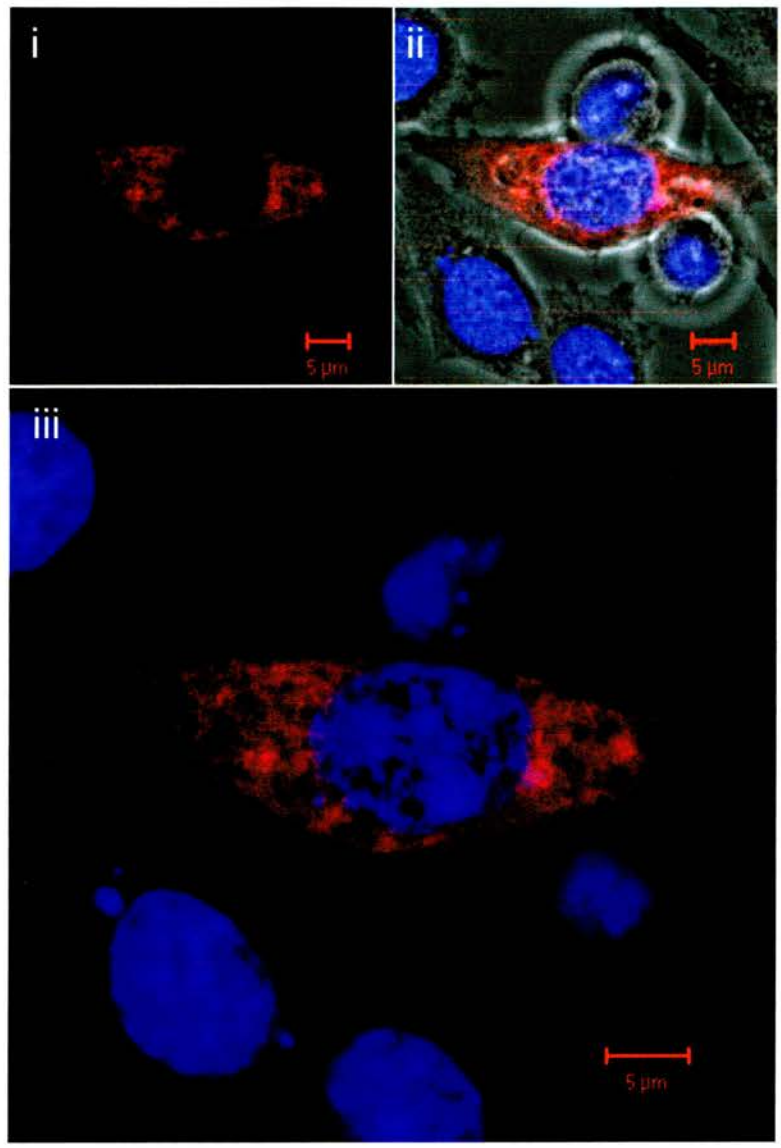

Figure 5.3.5d: Subcellular distribution of oLH in a transiently transfected CHO cell.

i) LH-immunoreactivity appears dispersed throughout the cytoplasm in a dense 'mesh-like' pattern. ii) Overlay of LH-immunoreactivity, nuclear staining (blue) and phase-contrast. Cells were fixed in Bouins 48 hours posttransfection with poαGSU and poLHβg. Primary bLH monoclonal antisera (518B7) was used at 2µg/ml. Goat anti-mouse TRITC conjugate was diluted 1:40. Nuclear staining was undertaken using 10µg/ml propidium iodide.

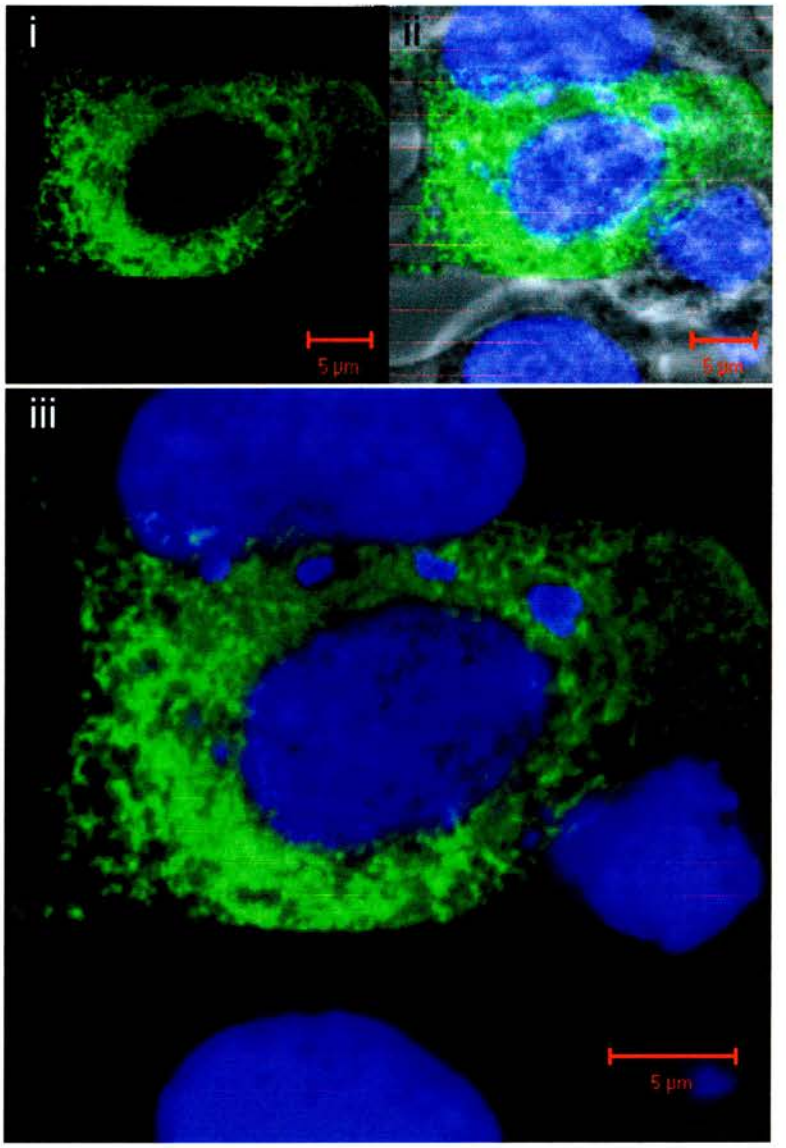

Figure 5.3.5e: Subcellular distribution of hCgA in a transiently transfected CHO cell.

i) hCgA-immunoreactivity appears dispersed throughout the cytoplasm in a network of tubular structures which are presumably the endoplasmic reticulum and Golgi apparatus. In addition several areas of punctate fluorescence are present in regions proximal to the plasma membrane. These fluorescent bodies range from approximately 100-600nm in diameter. ii) Overlay of hCgA-immunoreactivity, nuclear staining (blue) and phase-contrast. Cells were fixed in Bouins 48 hours posttransfection with phCgA. Primary CgA polyclonal antisera was diluted 1:1500. Goat anti-mouse FITC conjugate was diluted 1:40. Nuclear staining was undertaken using 10µg/ml propidium iodide. Cytoplasmic staining of nuclear material may represent mitochondria.

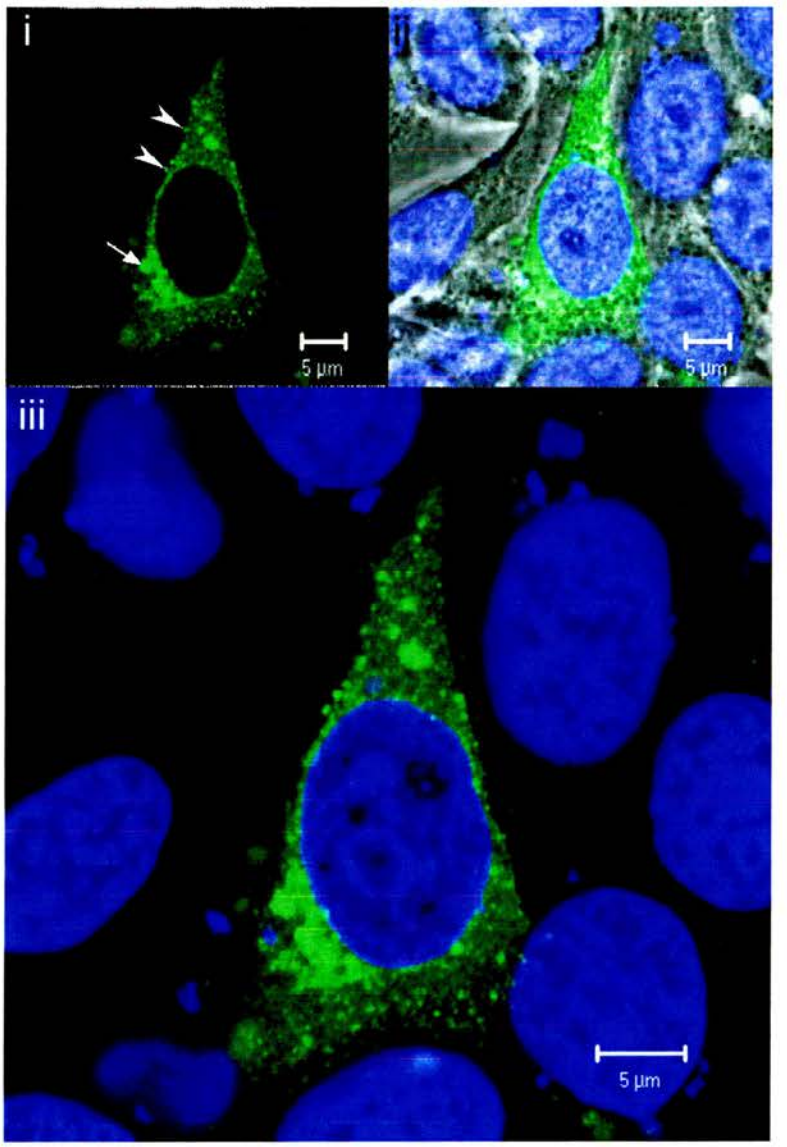

Figure 5.3.5f: Subcellular distribution of bCgB in a transiently transfected CHO cell.

i) Punctate bCgB-immunoreactivity appears dispersed throughout the cytoplasm. These fluorescent bodies range from approximately 100nm to nearly 2µm in diameter. CgB-immunoreactivity is particularly concentrated at the perinuclear region (arrow). Several of the smaller fluorescent bodies appear juxtaposed to the plasma membrane (arrowheads).
ii) Overlay of hCgB-immunoreactivity, nuclear staining (blue) and phase-contrast. Cells were fixed in Bouins 48 hours posttransfection with pbChrB73. Primary CgB polyclonal antisera was diluted 1:1500. Goat anti-mouse FITC conjugate was diluted 1:40. Nuclear staining was undertaken using 10µg/ml propidium iodide. Cytoplasmic staining of nuclear material may represent mitochondria.

plasma membrane. Colocalisation of oLH with bCgB within cotransfected cells (figure 5.3.5h) exhibited different colocalisation to that of oLH and hCgA. bCgB appeared to colocalise with oLH in the ER and Golgi apparatus with no detectable colocalisation within the bCgB-immunoreactive cytoplasmic vesicles. Comparison of figures 5.3.5e & g and 5.3.5f & h indicate that the subcellular distribution of hCgA and bCgB appears different in oLH cotransfected cells to those expressing only the granins. Cells transfected with phCgA and poLHβg appear to contain more hCgA-immunoreactivity within small cytoplasmic vesicles than cells transfected with phCgA alone. In contrast cells transfected with pbChrB73 and poLHβg do not contain the abundant punctate cytoplasmic fluorescence observed in cells expressing bCgB alone. In addition these pbChrB73/poLHβg cotransfected cells did not exhibit the large (1-2μm) bCgB-immunoreactive vesicles present in 'bCgB only' cells.

Comparison of the staining patterns in oLH/granin cotransfected cells with those obtained from cells transfected with only oLH expression constructs (figures 5.3.5d, g & h) revealed striking differences. oLH immunoreactivity appeared relatively dispersed throughout the cytoplasm in CHO cells expressing only oLH expression constructs. Coexpression of hCgA with oLH led to abundance colocalisation within the ER and Golgi apparatus. Notably oLH-immunoreactivity appeared colocalised with hCgA in 310-640nm cytoplasmic vesicles yet alone in peripheral areas of the cell. This punctate expression was absent from cells transfected with oLH expression constructs alone. Colocalisation of oLH and bCgB appeared to be restricted to the ER and Golgi apparatus with no punctate expression of oLH.

Colocalisation of oFSH and granins was not investigated due to a lack of appropriate antisera. Fluorescence from TRITC and FITC conjugates appeared to be inhibited by the ER and Golgi-specific dye Bodipy 630/650 and therefore prevented colocalisation of these signals.

5.3.6 Subcellular Localisation of EGFP-Gonadotrophin β-subunit fusion proteins

CHO cells transiently transfected with equal amounts of poαGSU and pEGFPC-oLHβ were observed directly in DPBS (figure 5.3.6a). Cells

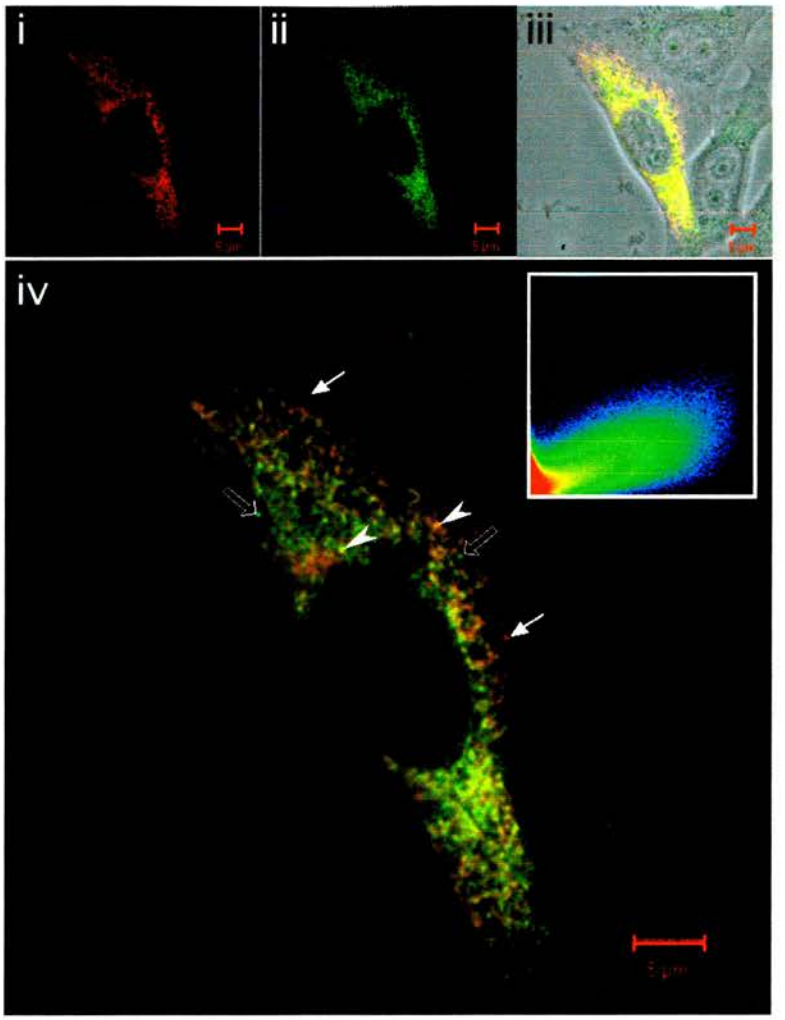

Figure 5.3.5g: Subcellular distribution of oLH and hCgA in a transiently transfected CHO cell.

i) oLH-immunoreactivity appears throughout the cytoplasm and several punctate fluorescent bodies are present in peripheral areas of the cell. ii) hCgA-immunoreactivity appears similarly distributed to oLH with several areas of punctate expression. iii) An overlay of oLH- (red) and hCgA-immunoreactivity (green) with phase-contrast indicates that the punctate areas of oLH fluorescence are located closer to the plasma membrane than that of hCgA. iv) Overlay of oLH- and hCgA-immunoreactivity only. The punctate fluorescent bodies range from 310-640nm and exhibit three types of fluorescence. Some of these putative vesicles contain hCgA only (black arrows) and others contain only oLH (white arrows). Others contain both oLH and hCgA appearing yellow (arrowheads). The inset of panel (iv) demonstrates the degree of colocalisation between oLH and hCgA. Antigens exhibiting no colocalisation show no pixels in the centre of the pixel distribution graph. Identical images exhibit a 45° line from the bottom left corner. oLH and hCgA appear to show significant colocalisation within transiently transfected CHO cells. Cells were transfected with poαGSU, poLHβg and phCgA then fixed in Bouins 48 hours later. LH primary antisera (518B7) was used at 2μg/ml and CgA antisera diluted 1:1000. Goat anti-mouse TRITC and goat anti-rabbit FITC secondary antisera conjugates were diluted 1:40. Fluorescence was detected using HeNe 543nm and argon 488nm lasers with 585nm longpass and 505-535nm bandpass filters for TRITC and FITC respectively.

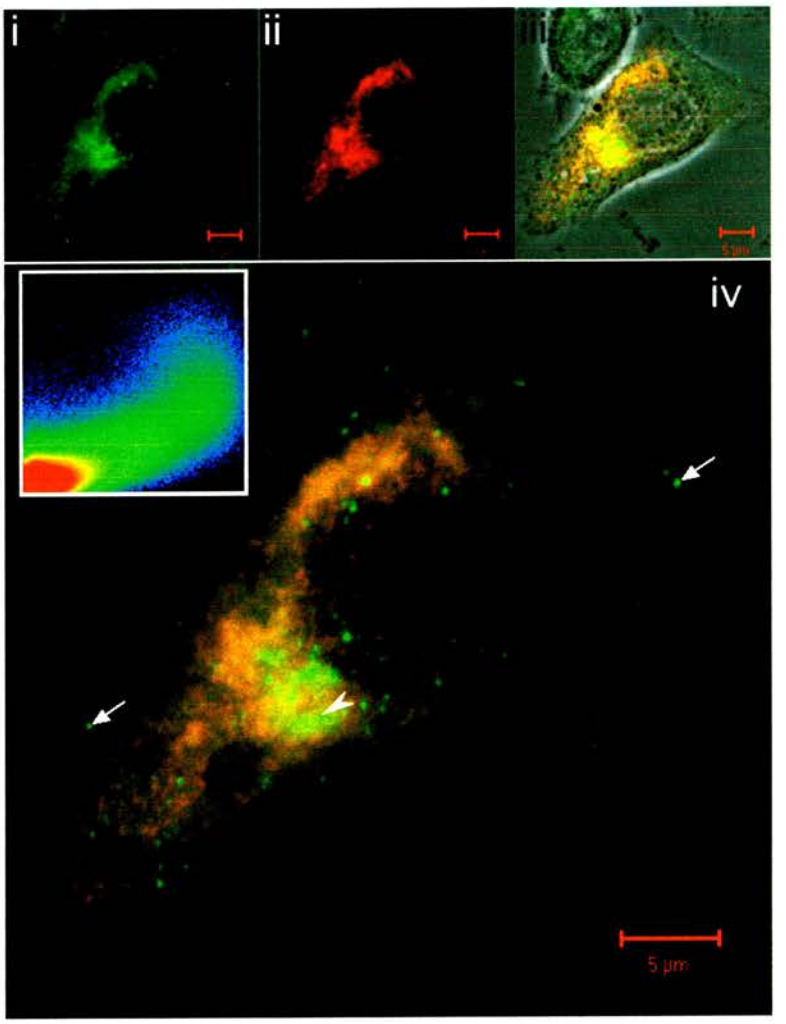

Figure 5.3.5h: Subcellular distribution of oLH and bCgB in a transiently transfected CHO cell.

i) bCgB-immunoreactivity is also concentrated in the ER and TGN. In addition several punctate bodies are present in the periphery of the cell. ii) oLH-immunoreactivity appears throughout the cytoplasm and particularly concentrated in the perinuclear region corresponding to the ER and TGN. iii) An overlay of oLH- (red) and bCgB-immunoreactivity (green) with phase-contrast indicates that the punctate areas of bCgB fluorescence are located in close proximity with the plasma membrane. iv) Overlay of oLH- and bCgB-immunoreactivity only. The punctate fluorescent bodies range from 190-380nm and only contain bCgB (arrows). oLH and bCgB appear colocalised within the ER and TGN (arrowhead). The inset of panel (iv) demonstrates the degree of colocalisation between oLH and bCgB. Antigens exhibiting no colocalisation show no pixels in the centre of the pixel distribution graph. Identical images exhibit a 45º line from the bottom left corner. oLH and bCgB appear to show moderate colocalisation within transiently transfected CHO cells. Cells were transfected with poαGSU, poLHβg and pbChrB73 then fixed in Bouins 48 hours later. LH primary antisera (518B7) was used at 2µg/ml and bCgB antisera diluted 1:1000. Goat anti-mouse TRITC and goat anti-rabbit FITC secondary antisera conjugates were diluted 1:40. Fluorescence was detected using HeNe 543nm and argon 488nm lasers with 585nm longpass and 505-535nm bandpass filters for TRITC and FITC respectively.

transfected with the 'empty' pEGFPC-3 construct alone exhibited fluorescence throughout the cell including the nucleus. Cells transfected with the pEGFPC-3, pEGFPC-oLHβ and poαGSU exhibited punctate expression over a background of EGFP fluorescence throughout the cell. Cells transfected with pEGFPC-oLHβ and poαGSU exhibited similar punctate cytoplasmic bodies in the absence of EGFP background. These fluorescent bodies ranged in size from 1-2μm. Time-lapse scanning of these cells failed to demonstrate their movement.

Cells transfected with poαGSU and pEGFPC-oFSHβ were viewed live 24 (figure 5.3.6b & c) and 48 hours (figure 5.3.6e & f) posttransfection. After 24 hours some cells exhibited fluorescence throughout the cytoplasm and nucleus. Other cells exhibited punctate fluorescence which appeared to move within the cytoplasm in apparently random directions (movie 5.3.6d). These vesicles ranged in diameter between 400-630nm whereas others which did not exhibit movement were much larger (1.69μm). The majority of transfected cells 48 hours posttransfection exhibited punctate cytoplasmic fluorescence. These cytoplasmic bodies ranged in diameter between 110-350nm (figure 5.3.6e). Time-lapse scanning of these cells revealed that many of these vesicles exhibited rapid movement within the cytoplasm (figure 5.3.6f & movie 5.3.6g). An example of an exocytotic event where a single vesicle appeared to fuse with the plasma membrane was also observed. Surprisingly some vesicles localised proximal to the plasma membrane did not exhibit this type of movement and instead appeared to 'wobble' (movie 5.3.6g).

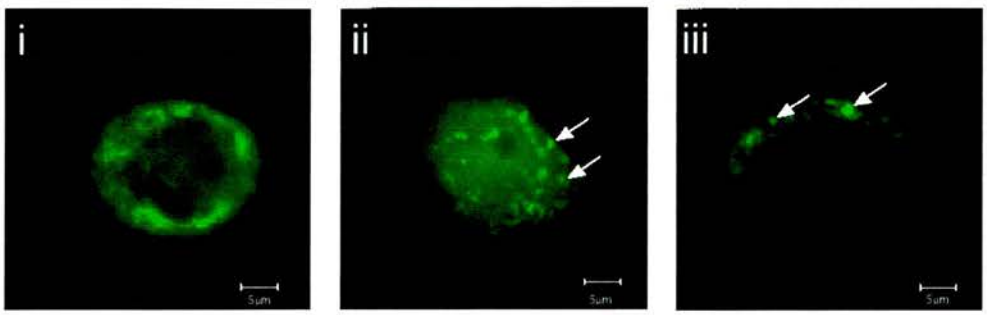

Figure 5.3.6a: EGFP and EGFPC-oLHβ fluorescence in transiently transfected CHO cells.

EGFP and EGFPC-oLHβ fluorescence was observed in living CHO cells 48 hours posttransfection. Panel (i) shows a CHO cell transfected with the 'empty' pEGFP-C3 vector alone and displays fluorescence throughout the cell. The fluorescence is particularly concentrated in the perinuclear region corresponding to the ER and Golgi apparatus. Panel (ii) shows a CHO cell transfected with poαGSU, pEGFP-C3 and pEGFPC-oLHβ. The fluorescence in this cell is also dispersed throughout the cytoplasm and nucleus. In addition several relatively large fluorescent cytoplasmic bodies (arrows) are present with diameters of approximately 1-2µm. Panel (iii) shows a CHO cell transiently transfected with poαGSU and pEGFPC-oLHβ. Fluorescence in this cell is punctate and restricted to the cytoplasm. No diffuse fluorescence is present in this cell. The cytoplasmic bodies (arrows) appear similar to those displayed in panel (ii). EGFP fluorescence was observed using a 488nm argon laser and 505-535nm bandpass filter.

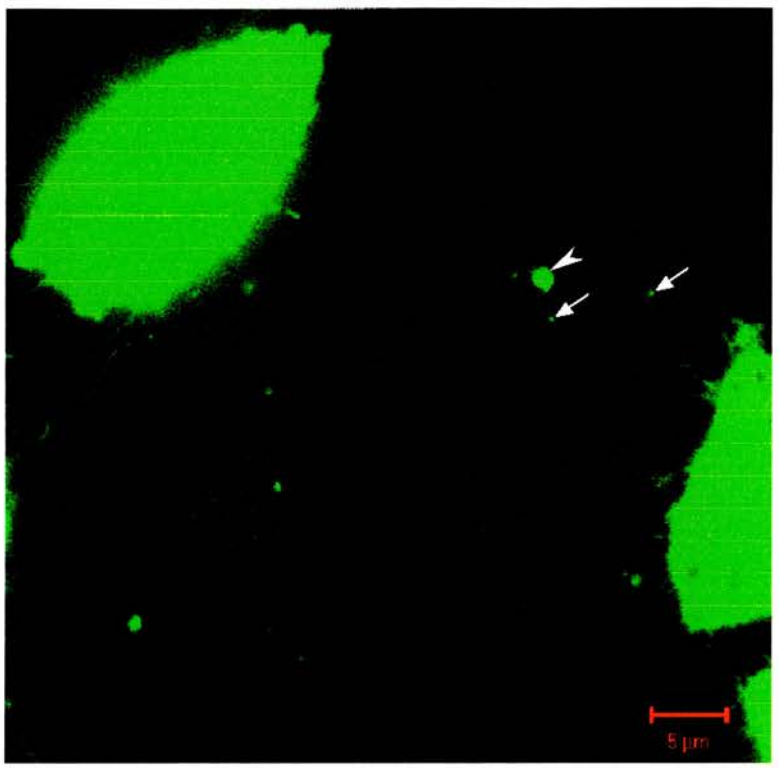

Figure 5.3.6b: EGFPC-oFSHβ fluorescence in transiently transfected CHO cells 24 hours posttransfection.

Several cells are present within the field of view. The cell in the centre of the field of view exhibits punctate fluorescence (arrows). These fluorescent bodies range in diameter between 400-630nm and moved sporadically within the cytoplasm. Other larger fluorescent bodies (1.69µm; arrowhead) remained in a fixed position. Other cells within the field of view exhibit fluorescence throughout their nuclei and cytoplasms. Cells were observed live using a 488nm argon laser and 505-535nm bandpass filter. This image was the first in a series taken at 32.07 second intervals.

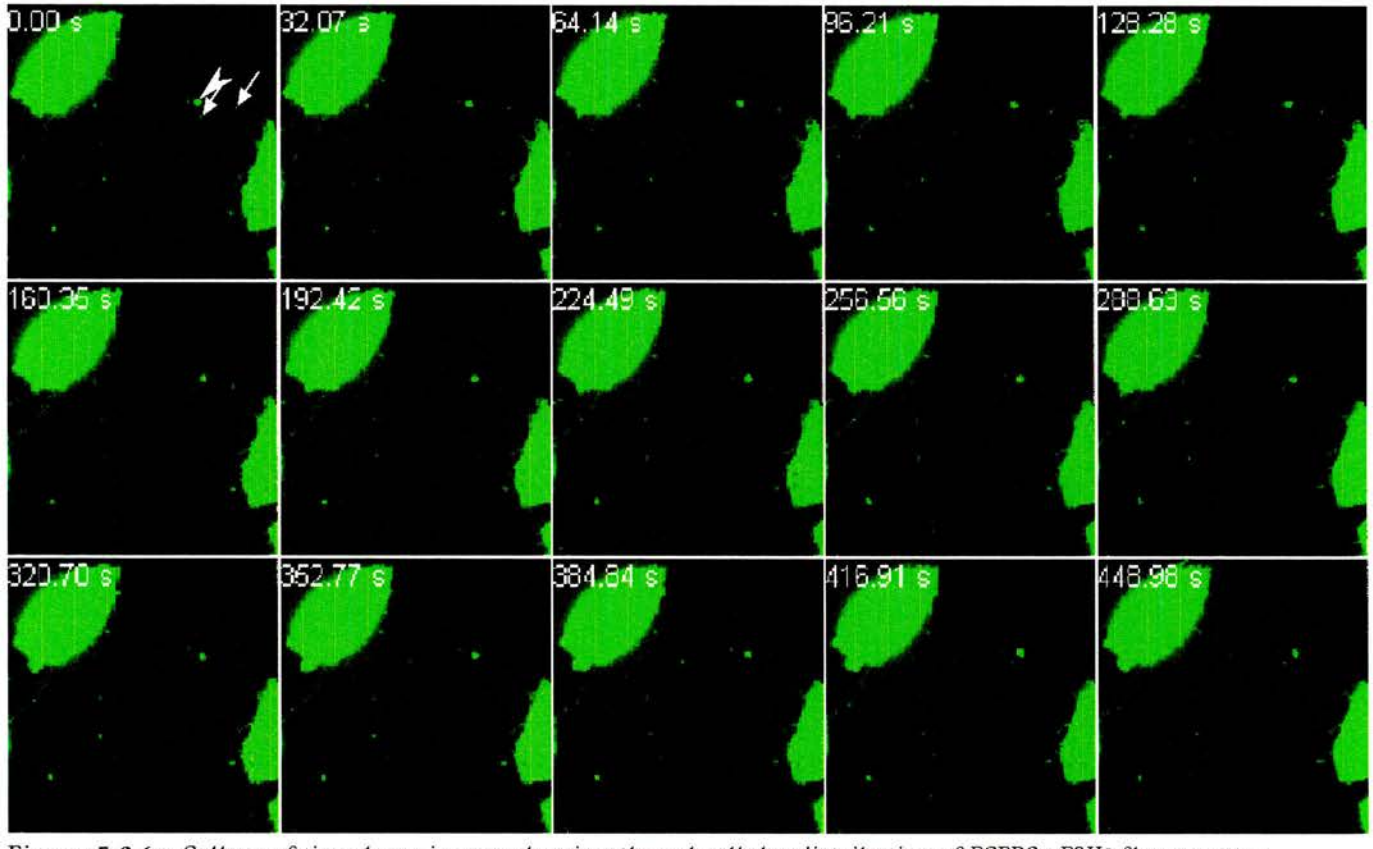

Figure 5 3.6c: Gallery of time-lapse images showing the subcellular distribution of EGFPC-oFSHβ fluorescence in transiently transfected CHO cells 24 hours posttransfection.

Several cells are present within the field of view. The cell in the centre of the field of view exhibits punctate fluorescence (arrows). These fluorescent bodies range in diameter between 400-630nm and moved sporadically within the cytoplasm. Other larger fluorescent bodies (1.69μm; arrowhead) remained in a fixed position. Other cells within the field of view exhibit fluorescence throughout their nuclei and cytoplasms. Cells were observed live using a 488nm argon laser and 505-535nm bandpass filter. Images were taken at 32.07 second intervals.

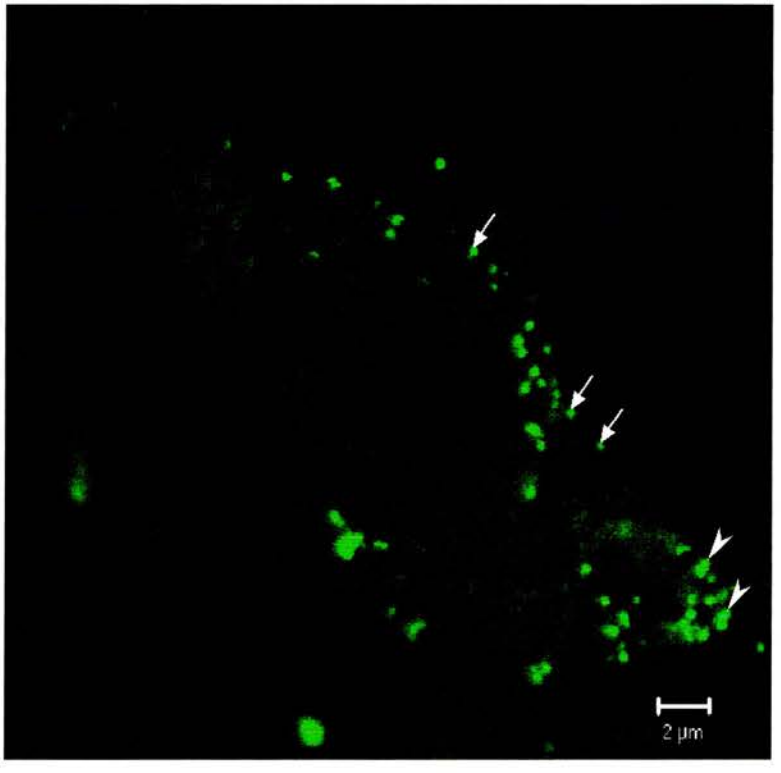

Figure 5.3.6e: EGFPC-oFSHβ fluorescence in a transiently transfected CHO cell 48 hours posttransfection.

CHO cells were transiently transfected with poαGSU and pEGFPC-oFSHβ. Living cells were viewed 48 hours posttransfection. Punctate fluorescence is clearly visible within the cytoplasm of this cell (arrows). The diameter of these intracellular bodies ranges from 110-350nm. Many of these putative vesicles exhibited sporadic movement while others located proximal to the plasma membrane either remained in a fixed position or 'wobbled' (arrowheads). This image is the first in a series taken at 32.07 second intervals. EGFP fluorescence was observed using a 488nm argon laser and 505-535nm bandpass filter.

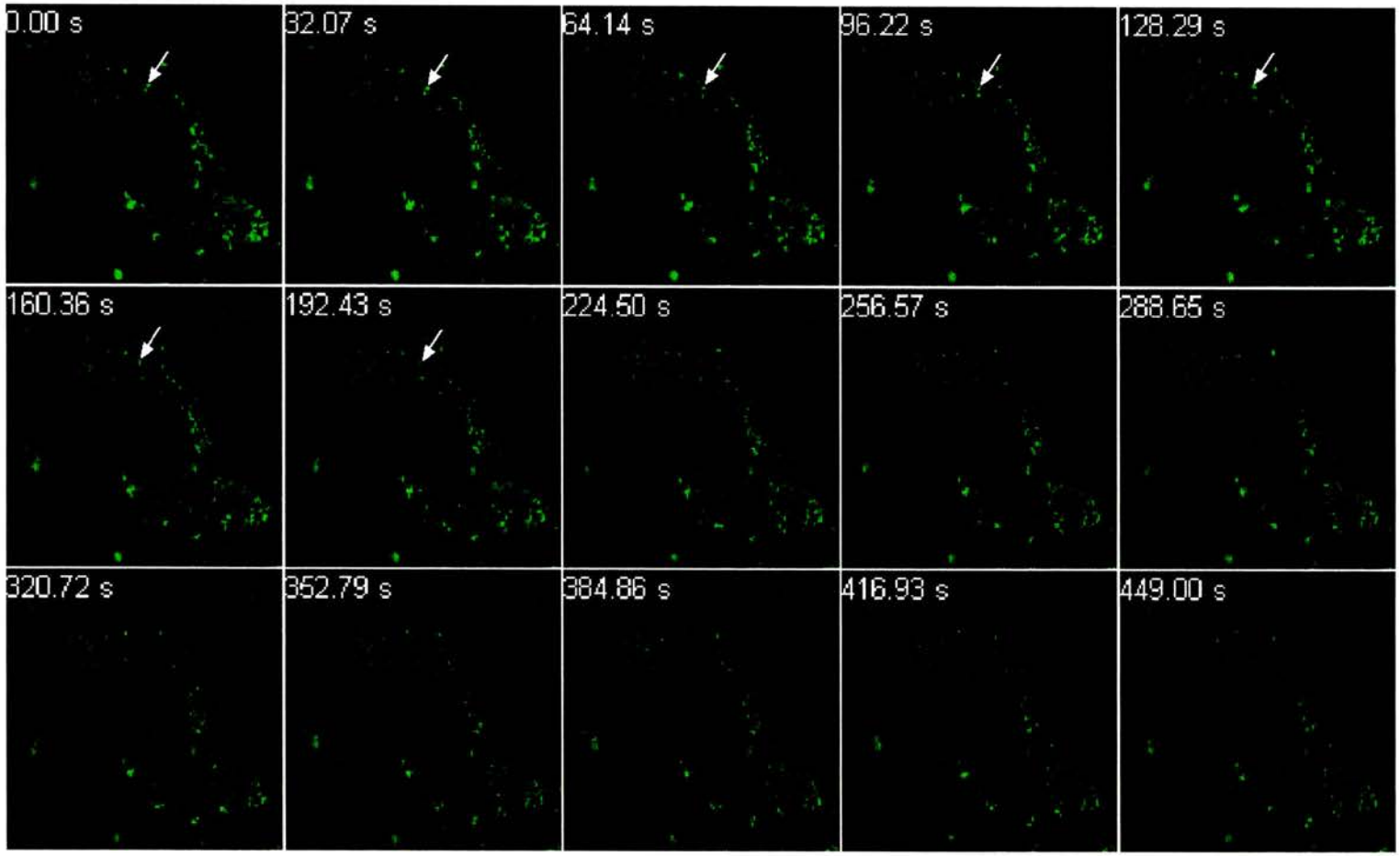

Figure 5.3.6f: Gallery of time-lapse images showing EGFPC-oFSHβ fluorescence in a transiently transfected CHO cell 48 hours posttransfection.

CHO cells were transiently transfected with poαGSU and pEGFPC-oFSHβ. Living cells were viewed 48 hours posttransfection. Punctate fluorescence is clearly visible within the cytoplasm of this cell. The diameter of these intracellular bodies ranges from 110-350nm. Many of these putative vesicles exhibited sporadic movement while others either remained in a fixed position or 'wobbled'. The vesicle marked with an arrow moves and then appears to be exocytosed after fusing with the upper surface of the cell (192.43sec). These images were taken at 32.07 second intervals. EGFP fluorescence was observed using a 488nm argon laser and 505-535nm bandpass filter. The images fade during time due to photobleaching of the EGFP fluorescence.

5.4 Discussion

Transfection of both CHO and CHO-K1 cell lines was achieved after a relatively short optimisation process. Both cell lines were easily transfected using PerFect^{TM} lipids although optimal transfection was not achieved using the same lipid mix for each. This was unexpected due to the assumed similarity of the cell lines. Although the molecular mechanisms involved in the specific nature of each transfection remain to be determined, it is possible that these differences may be derived from differential expression of cell surface proteins.

Transient expression from all constructs used in these studies was confirmed by RT-PCR. Only RT-PCRs carried out on cells transfected with oLHβ expression constructs exhibited larger amplified products in addition to the predicted products. However this larger product was less abundant than the correct size product which is in contrast to the relationship observed in reactions containing RNA from similarly transfected JEG3 samples. Further analysis of the situation leading to the amplification of this product in transfected JEG3 cells suggested that it arose due to aberrant splicing. It is therefore likely that this is also the case in CHO cells although it appears that aberrant splicing of oLHβ mRNA occurs less frequently than in JEG3 cells .

Expression of oFSH in CHO-K1 cells was unexpectedly low. However visualisation of transfected cells by indirect immunofluorescence demonstrated a high concentration of oFSH immunoreactivity in the perinuclear region, presumably proximal to the endoplasmic reticulum (ER) and Golgi apparatus. The lack of further cytoplasmic staining in conjunction with the low yield of oFSH from the lysate and media suggests breakdown of oFSH in lysosomal compartments budding from the Golgi apparatus. The reasons for this are unclear but it is perhaps likely that misfolding or aberrant glycosylation events may have prevented dimerisation of the oFSH molecule. It has been demonstrated *in vivo* that free gonadotrophin β-subunits are digested within post-Golgi lysosomal compartments (Bassetti *et al.*, 1995).

Expression studies in CHO cells revealed that, unexpectedly, higher levels of oFSH were expressed from the combination of constructs containing the oFSHβ genomic clone as opposed to the cDNA. The reasons for this apparent 'preference' for the genomic clone may be due to the presence of cryptic enhancer sequences within the introns. This result contrasts with that observed for $L\beta T_2$ cells (see chapter 6) where higher expression was derived from transient transfection of the cDNA-containing construct and suggests the involvement of regulatory mechanisms specific to the different cell types. Comparison of the proportion of total oFSH present within the lysate fraction in cells transfected with either the cDNA or genomic clone demonstrated a higher level of storage from the cDNA construct. Taken in the context of the lower overall expression level obtained using this construct combination, these results do not suggest concentration dependent retention of oFSH in CHO cells. The significantly greater amount of storage achieved from the oFSHβ cDNA construct compared to the genomic clone despite lower overall expression may be caused by differences in glycosylation although this will require further investigation to substantiate. In contrast, $L\beta T_2$ cells (see chapter 6) exhibited a higher proportion of storage as a result of higher overall expression derived from the oFSHβ cDNA construct. This difference may be facilitated by the lack of granin expression in normal CHO cells in comparison to $L\beta T_2$ cells which is further substantiated by the observation that a higher proportion of oFSH is stored in the gonadotroph cell line compared to CHO cells (compare figures 5.3.3d and 6.3.4d). Future studies may investigate the effect of granin expression on oFSH storage in CHO cells and allow comparison with the level of storage in $L\beta T_2$ cells.

oLH secretion in the presence of individual granins was investigated in transiently transfected CHO cells. However a startling difference in the proportion of oLH stored in comparison to oFSH was apparent in the absence of granin expression. The approximately 5-fold greater level of storage of oLH in comparison to oFSH demonstrates that CHO cells are able to differentially secrete LH and FSH. This difference may represent the sorting of oLH into the cryptic regulated pathway of CHO cells (Chavez *et al.*, 1996) due to the presence of a 7aa hydrophobic region at the carboxy-terminus of LHβ. Removal of this region which is not present on the LH

dimer in the pituitary gland (Talmadge *et al.*, 1984) increases the rate of LH secretion *in vitro* by increasing the efficiency of dimer formation (Matzuk *et al.*, 1989). However to substantiate these preliminary findings in CHO cells further studies must be undertaken to verify the regulated nature of this secretion by application of secretagogues such as forskolin and KCl. It is unlikely that this difference is caused solely by the reported differences in the rates of dimer assembly for LH and FSH (Matzuk *et al.*, 1989; Muyan *et al.*, 1996) due to the 48-72 hour length of expression before assay. However it was surprising that no obvious difference in the subcellular localisation of oLH and oFSH was observed by indirect immunofluorescence. It may therefore be possible that the 5-fold difference in the proportion of oLH and oFSH in the lysate represents variations within the constitutive pathway.

Unexpectedly no significant change in the amount of oLH which remained intracellularly at the time of assay was observed in cells cotransfected with the hCgA expression construct. However the presence of hCgA at 75-100% of the level of oLH did cause more than a 2-fold increase in the relative amount of oLH expressed by CHO cells. This result is very similar to the approximately 2-fold greater increase in cAMP-stimulated hCG expression in JEG3 cells transfected with the hCgA expression construct compared to untransfected cells (see chapter 4). It may be likely that CgA-derived peptides promote oLH expression via mRNA stabilisation. Some evidence exists for interactions between CgA-derived peptides and specific mRNA. For example pancreastatin has been demonstrated to exert an inhibitory effect on parathyroid hormone as well as CgA expression in the parathyroid through mRNA interactions (Zhang *et al.*, 1994). It may be interesting to investigate the longevity of LHβ mRNA in the absence of CgA and its peptides. Previous determination of the rLHβ mRNA half-life (44±0.5 hours) was undertaken in male rat gonadotrophs *in vitro* (Bouamoud *et al.*, 1992). Male gonadotrophs have been demonstrated to contain higher levels of CgA as a consequence of positive regulation by testosterone (Watanabe *et al.*, 1998b) which suggests that the determination of rLHβ mRNA stability may have been subject to the putative regulatory effects of CgA and CgA-derived peptides. Further evidence for a role of CgA in the enhanced expression of LHβ is suggested

by the coincidental decrease in CgA and LHβ levels during repeated passage of the murine gonadotroph $L\beta T_2$ cell line (see chapter 6).

Indirect immunofluorescence carried out on CHO cells expressing oLH and hCgA demonstrated a distinct alteration in the subcellular localisation of oLH in comparison to cells lacking hCgA expression. However in light of the biochemical evidence for increased oLH expression with no significant change in the amount of oLH storage during coexpression of hCgA, it suggests that hCgA increases the efficiency of oLH secretion during higher levels of expression. Observation of fixed cells did not permit analysis of the speed of vesicle traffic. The colocalisation of oLH and hCgA immunoreactivity within the ER and TGN together with the appearance of dual staining cytoplasmic vesicles suggests that hCgA aggregates with oLH in the ER and TGN and enhances the rate of gonadotrophin release via formation of larger cytoplasmic vesicles. The apparent divergence of hCgA and oLH within what appears to be the late regulated secretory pathway at regions proximal to the plasma membrane is similar to that observed *in vivo* (see chapter 7) (Watanabe *et al.*, 1991; Thomas *et al.*, 1998). The appearance of these subplasmalemmal 'LH only' vesicles in CHO cells cotransfected with phCgA suggests that CgA may initiate entry of LH into the cryptic regulated secretory pathway in CHO cells (Chavez *et al.*, 1996). It is important to note that the apparent maturation of the LH-containing granule occurs in the absence of SgII recently demonstrated to co-migrate with LH in <200nm granules during E_2 treatment. This suggests the presence of conserved molecular mechanisms in cells of non-neuroendocrine origin which permit granule maturation. Future studies of SNARE proteins in this model may elucidate their role in this process. It is possible that the low abundance of these 'LH only' vesicles within the cotransfected cell represents their rapid and sporadic movement from the TGN to the plasma membrane. Evidence for this type of movement has been provided by analysis of living cells by time-lapse confocal microscopy discussed later. Definitive biochemical evidence for an increase in oLH turnover during coexpression of hCgA may be obtained by pulse-chase analysis of stably transfected cells.

Similar investigations of LH secretion in the GH_3 cell line which possess a visually recognisable regulated pathway have indicated that a threshold of

expression must be reached prior to LH storage (Bielinska *et al.*, 1994). It is therefore possible that in CHO cells the high level of oLH expression which is further enhanced by the presence of hCgA exceeds this threshold. However the oLH dimers are not stored effectively in characteristic granules due to the absence of the necessary molecular machinery expressed by gonadotrophs *in vivo*. The key molecules required remain to be defined but it is likely that these involve other granins and novel proteins such as Rab3B (Tasaka *et al.*, 1998). No evidence for the expression of Rab3B in CHO cells has been reported and future studies may investigate its presence. A recent antisense study in cultured female rat gonadotrophs has indicated that Rab3B is crucial for both constitutive and regulated release of gonadotrophins (Tasaka *et al.*, 1998). However in light of the observed secretion of LH and FSH it is likely that CHO cells do posses Rab3B or a protein with similar functional characteristics which facilitate vesicle release. If this is the case then it may be possible to 'knock-out' this protein using antisense technology 'forcing' the CHO cell to either store or breakdown the excess gonadotrophins. Alternatively the role of F-actin may be the critical factor in vesicle retention. Further analysis of this cytoskeletal protein by indirect immunofluorescence may reveal an absence of the necessary barrier required to partition granules away from sites of exocytosis.

The effect of bSgII on the total level of oLH expressed did not differ significantly from expression of oLH alone in CHO cells. This was the expected outcome of bSgII expression on that of oLH. However this effect of bSgII differed from that observed for hCG in JEG3 cells perhaps reflecting differences in cell type or regulation of the respective β-subunits (see chapter 4). Differences in cell type may lead to alternate processing of SgII with production of different peptides. Alternatively the observed difference between hCG and oLH may have arisen due to the extended 5' UT of hCGβ (Bousfield *et al*, 1994) through which SgII or SgII-derived peptides may interact and exert their effect. However in contrast to the studies carried out in JEG3 cells, bSgII expression significantly reduced the proportion of oLH which remained in the lysate. *In vivo* observations of the subcellular localisation of SgII have demonstrated its

colocalisation with LH in small (<200nm) regulated secretory granules (Watanabe *et al.*, 1991) which co-migrate during E_2 treatment (Thomas *et al*, 1998) and are preferentially released during the LH surge (Currie & McNeilly, 1995). These results suggest a role for SgII in the final stages of LH secretion and perhaps in the promotion of exocytosis *in vitro*. The exact mechanisms involved in this putative role of SgII are as yet uncharacterised. SgII-derived peptides such as secretoneurin and secretogranin LT have been demonstrated as secretagogues for dopamine and related molecules (You *et al.*, 1996). Future *in vivo* studies may investigate the interaction of SgII-derived peptides with the gonadotroph as an autocrine or paracrine (lactotrophs also express SgII) mechanism for gonadotrophin granule release. It is possible that a mechanism such as this may allow amplification of LH release during surge-type events. Future *in vitro* studies may include cotransfection of oLH expression constructs with both phCgA and pbSgII61 to investigate the combined effect of these granins on LH expression and secretion. Unfortunately a lack of suitable antisera prevented visualisation of bSgII within transfected cells and its putative colocalisation with oLH. This experiment may pinpoint subcellular colocalisation of oLH and bSgII to sites of exocytosis within transfected CHO cells.

Expression of EGFP carboxy-terminal β-subunit fusions in CHO cells allowed for the first time visualisation of gonadotrophin secretion in living cells. Certain differences were observed between the oLHβ and oFSHβ fusions. The oLHβ fusion appeared to remain within the TGN as suggested by the absence of cytoplasmic vesicles. It is likely that the relatively inefficient dimerisation of LH (Matzuk *et al.*, 1989) was abolished by the presence of the EGFP structure on the β-subunit. The EGFP molecule at approximately 27kDa is considerably larger than the LHβ subunit at approximately 15kDa and may severely impede the dimerisation of LH. It is possible that future studies may benefit from oLHβ fusions to the amino terminus of EGFP. However this fusion may require prior removal of the sequences encoding the 7aa hydrophobic carboxy-terminus of the β-subunit as the putative cleavage of this region may disintegrate the fusion protein.

Similar studies using the EGFPC-oFSHβ fusion protein yielded novel data regarding the intracellular trafficking of oFSH in living cells. The size of these fluorescent vesicles is in accordance with reported diameters of regulated secretory granules in gonadotrophs (Watanabe *et al.*, 1998b) and their type of movement correlates with that reported for similar CgB fusions expressed in Vero cells (Wacker *et al.*, 1997). It is likely that these represent trafficking of the dimerised FSH hormone as free β-subunits are retained in the ER and eventually digested (Bassetti *et al.*, 1995) which appears to occur with EGFPC-oLHβ as previously discussed. The rapid yet sporadic movement of regulated secretory granules might be unexpected due to their relatively large size. However evidence presented in the following chapter demonstrates the rapid movement of similar granules in transfected $L\beta T_2$ cells suggesting that this observation is not limited to cells of non-neuroendocrine origin. Evidence for the secretory nature of these vesicles is provided by the observation of a vesicle which appears to fuse with the plasma membrane and release its contents. Although this does not occur at the periphery of the cell one must bear in mind the three-dimensional structure of cells which may permit vesicles to fuse with the uppermost surface of the cell. Regular fusion events were not observed which may reflect the relatively short periods of observation undertaken. Future studies will undoubtedly benefit from the use of a heated perfusion chamber allowing prolonged observation of living cells at controlled temperatures. A further advantage of such a system includes the ability to infuse secretagogues into the media and observe the effects on vesicle traffic in real time. An unexpected observation was the apparent polarisation of EGFPC-oFSHβ vesicles to the periphery of some transfected CHO cells. Gonadotrophs *in vivo* display this characteristic exclusively for LH immunoreactive granules during E_2 treatment (Thomas & Clarke, 1997). Although this phenomenon occurred in only a very limited number of transfected cells it nevertheless suggests that basic mechanisms within diverse cell types exist that permit this type of vesicle trafficking. However large (>100nm) cytoplasmic granules such as those observed in cells expressing the EGFP-oFSHβ fusion protein were not apparent in cells transfected with the normal oFSH expression constructs suggesting EGFP-induced aggregation of the oFSH dimer. This may hinder

'live cell' investigations into the granin-induced aggregation of gonadotrophins although it is possible that further aggregation may be observed during granin cotransfection studies. Conventional biochemical means for detecting the expression of the EGFP fusion protein appeared to be prevented possibly due to epitope-masking by the relatively large EGFP structure. Should future studies require immunological assessment of EGFP fusion protein secretion it may be necessary to undertake western analysis using EGFP antisera. However this technique does not easily allow measurement of specific protein content in high numbers of samples unlike RIA.

The use of the CHO cell line as a 'proof of concept' model has provided some interesting preliminary data regarding gonadotrophin secretion and the role of granins. Notably the increased proportion of total oLH which remains intracellularly in comparison to that of oFSH suggests the involvement of basic molecular mechanisms expressed in cells derived from neuroendocrine as well as non-neuroendocrine tissues. The positive regulatory effect of hCgA on oLH expression has been demonstrated without an increase in the proportion of oLH stored suggesting a role for CgA in increasing the efficiency of oLH secretion. In contrast the effect of bSgII expression demonstrated no effect on the level of oLH expression but did show a clear reduction in the proportion of oLH which remained intracellularly. In the context of previously reported subcellular localisation and secretion studies this may suggest a role for SgII in promoting exocytosis of LH-containing vesicles. Indirect immunofluorescence demonstrated colocalisation of both hCgA and bCgB with oLH in the ER and TGN of cotransfected cells suggesting specific co-aggregation. Furthermore the appearance of secretory granules containing oLH and hCgA but not bCgB correlates with *in vivo* data (Watanabe *et al.*, 1991). This suggests that coexpression of these regulated secretory proteins within a cell of non-neuroendocrine origin may permit molecular interactions similar to those which occur *in vivo*. The use of novel EGFP fusion constructs has provided preliminary data correlating with previous reports of the lower efficiency of LH dimerisation compared to that of FSH. The intracellular trafficking of EGFP-tagged oFSH within a

cell of non-neuroendocrine origin has demonstrated that relatively large secretory granules, possibly within the regulated pathway, exhibit rapid movement, membrane fusion and targeting towards the plasma membrane. Future studies will include further investigation of the effect of granins and combinations of granins on not only LH expression and secretion but also that of FSH. In order to achieve this, generation of stably transfected CHO cells may be advised. With a clonal population of cells expressing combinations of gonadotrophin subunits and granins pulse-chase analysis may be carried out. This may allow more accurate determination of the effects of granins and combinations of granins on basal rates of secretion as well as to investigate secretagogue-stimulated exocytosis of putatively stored gonadotrophins.

Chapter Six

Gonadotrophin Secretion from the LβT2 Gonadotroph Cell line

6.1 Introduction

In vitro studies on gene regulation and secretion of pituitary gonadotrophins have been hindered in the past by the absence of a suitable cell line. Up until 1996 the JEG3 human choriocarcinoma (Kohler & Bridson, 1971) (see chapter 4) and the αT3-1 mouse gonadotroph (Windle *et al.*, 1990) were the only cell lines to endogenously express the αGSU. Although the αT3-1 had the advantage over JEG3 cells of being pituitary-derived and expressing functional GnRH-R, it did not express either of the gonadotrophin β-subunit genes whereas JEG3 cells expressed hCGβ. Furthermore neither the JEG3 nor αT3-1 cells appeared to secrete endogenously expressed proteins via a regulated pathway. Although non-gonadotroph derived cell lines such as the rat somatomammotroph GH_3 (Tashjian *et al.*, 1968) and mouse adrenocorticotroph AtT-20 (Gumbiner & Kelly, 1982) cell lines did exhibit regulated secretory pathways, they did not provide direct relevance to secretion by the gonadotroph. In 1996 a novel mouse gonadotroph-derived cell line was described by the same group that had previously isolated the αT3-1 cell line. The $L\beta T_2$ cell line was obtained using similar methodology to that used previously for the αT3-1 cell line. Oncogenesis directed specifically to the gonadotroph was previously carried out using the SV40 T-antigen under control of the αGSU promoter whereas in the case of the $L\beta T_2$ cell line LHβ promoter sequences were used (Thomas *et al.*, 1996). The characteristics of $L\beta T_2$ cells include LH secretion under control of the GnRH-R. Indeed the secretory characteristics of the $L\beta T_2$ cell line appear almost identical to those of *in vivo* gonadotrophs with the exception that this cell line does not express the FSHβ gene (Thomas *et al.*, 1996). As yet no investigations into the role of granins or the effect of FSHβ expression within this cell line have been reported. Due to the presence of a regulated pathway specifically suited to secrete LH in a pulsatile manner, the $L\beta T_2$ cell line provided the best model for investigation of the molecular mechanisms involved with particular reference to the role of granins and their assumed co-ordinate expression.

Furthermore by transfection of FSHβ expression constructs it may be possible to investigate the mode of high level FSH secretion.
Two main objectives were set for these studies using $L\beta T_2$ cells. Firstly to assess the hormonal regulation of granin gene expression during a controlled GnRH regime previously demonstrated to prime LH secretion (Turgeon *et al.*, 1996). Secondly to investigate the mode of secretion employed by $L\beta T_2$ cells during expression of high levels of ovine FSHβ from 3' truncated (stabilised) mRNA.

6.2 Methods

6.2.1 Radioimmunoasay of rat LH

The rLH radioimmunoassay (RIA) was carried out as using the general methodology described in section 2.5.5 . Primary antisera against rLH (rLH-S-11) was used at a dilution of 1:150000. rLH-RP-3 tracer material (NIDDK, USA) for the rLH RIA was iodinated as described in section 2.5.4. Normal rabbit serum (NRS; SAPU, UK) and Donkey anti-rabbit serum (DARS; SAPU, UK) were used at dilutions of 1:400 and 1:16 respectively.

6.2.2 Basal LH Expression

Unstimulated LH secretion was determined by rLH RIA of media from confluent cultures of $L\beta T_2$ cells at different passage numbers ranging from 6 to 103 passages. In addition lysates from confluent cultures of $L\beta T_2$ cells at passage 38 and 103 were obtained by incubation at room temperature for 1 hour with occasional vortexing in extraction solution containing 62.5mM Tris.HCl pH6.8, 2% sodium dodecyl sulphate (SDS), 10% glycerol and Complete™ protease inhibitor (Boehringer Mannheim, UK). The protein concentration of the lysates was determined by Bradford assay (Bio-Rad, UK).
SDS-PAGE was undertaken as described in chapter 2. 5% and 10% acrylamide were used for the stacking and resolving gels respectively. Samples containing 45μg of total protein were prepared in either reducing or non-reducing buffers prior to loading. After electrophoresis the proteins were transferred to nitrocellulose membranes after which LH

and CgA were detected using the ECF kit (Amersham, UK). The monoclonal primary antisera bLH518B7 was diluted to 1μg/ml whereas bCgA antisera was used at a dilution of 1:2500.

6.2.3 Basal GnRH-R Expression

Radioligand receptor binding assays were carried out by Elena Faccenda in order to verify expression of the GnRH-R.

6.2.4 Inositol 1,4,5-trisphosphate Production by the GnRH-R

Elena Faccenda assessed GnRH-R activity by measuring production of the intracellular second messenger molecule inositol 1,4,5-trisphosphate (IP_3). Basal and 10^{-6}M GnRH-stimulated activity were compared.

6.2.5 GnRH Regimes

In order to assess the effect of GnRH on gene expression and protein secretion $L\beta T_2$ cells were periodically exposed to the hypothalamic decapeptide over a 3-4 day period. Cells were plated in 6 or 12 well dishes at $1x10^6$ or $5x10^5$ cells per well 24-48 hours prior to commencing the GnRH regime. Cells were plated onto the normal culture surface or onto Thermanox coverslips (GibcoBRL, UK) coated with a 1:4 dilution of Matrigel (Becton-Dickinson, UK). All culture media contained 100 units/ml penicillin and 0.1 mg/ml streptomycin. Either cDMEM or phenol red-free DMEM supplemented with 10% charcoal-stripped FCS (efDMEM) was used. Cells were cultured in efDMEM or efDMEM containing 0.2nM E_2 and 20nM dexamethasone (Sigma-Aldrich, UK). Exposure to GnRH lasted 15 minutes with a 75 minute interpulse period. Either 3 pulses for three days or 4 pulses for four days was carried out. GnRH (Sigma-Aldrich, UK) was added to the cultures at a final concentration of either 10nM or 1μM.

6.2.6 RNase Protection Assays

Pamela Brown and Joanne McVerry undertook the RNase protection assays (RPAs) for the LHβ and αGSU respectively. RPAs were carried out in order to quantify changes in mRNA for LHβ and αGSU. Antisense RNA directed at GAPDH was used to quantify protected fragments in each RPA. The control

reactions were carried out separately and loaded in separate wells to avoid loss of LHβ or αGSU signal caused by background from the GAPDH reaction.

6.2.7 Detection of Mouse Granin and GnRH-R mRNA by RT-PCR

RT-PCR primers were designed following the guidelines detailed in section 2.3.16 to detect expression of the murine CgA, CgB, SgII and GnRH-R genes. Details regarding the primers used are contained in the table below.

Table 6.2.7a: Mouse RT-PCR primers.

Primer name	Binding position	Oligonucleotide Sequence (5'->3') [length]	T_{AN} (°C)	Predicted Product (bp) [pair]
mcga51	974 to 996	TCCAGAAAGATGATGGTCAGTCG [23]	58	295
mcga31	1249 to 1268	CTCTGCTGTCAGCTCTTTGGC [21]	58	295
mcgb51	316 to 338	GCTCCAGTAGAAGACTCTCAAGG [23]	58	230
mcgb31	525 to 546	TTCACCAGCATCTTCCCTGTGC [22]	58	230
msgii51	593 to 613	CTACCCTGGAGTCTGTGTTCC [21]	58	350
msgii31	921 to 943	AGGTGATAACTTTGGAGGCATCC [23]	58	350
gnrhR51	103 to 123	GGAAAGATCCGAGTGACCGTG [21]	63	369
gnrhR31	451 to 473	GACTGTTCAAGCTTGCTGTTGC [22]	63	369

Where, T_{AN} is the predicted optimal annealing temperature for the primer pair.

Detection of the specific mRNA species was undertaken using the Titan™ kit (Boehringer Mannheim, UK) on $L\beta T_2$ lysates harvested using Tri-reagent (Sigma-Aldrich, UK). RNA concentration was determined by spectrophotometrical analysis and 500ng of total RNA was added to each reaction. Amplified products were visualised by 2% agarose gel electrophoresis in TBE buffer (see Appendix I).

6.2.8 Optimisation of Lipid-based Transfection

Optimisation of transfections using the PerFect^{TM} lipid system (Invitrogen, NL) was carried out using 24-well dishes seeded with approximately $2x10^5$ cells per well. Transfections were undertaken on cultures exhibiting 60-80% confluency for 6-7 hours with a ratio of lipid to DNA of 6:1. Transfection efficiency was assessed by β-galactosidase staining as described in section 2.4.9 .

6.2.9 Transient FSH Expression

Cells were transfected using Pfx3 for 6 hours with the αGSU expression construct poαGSU and either poFSHβ, poFSHβg or pEGFPC-FSHβ. Media and lysates were harvested after 48 or 72 hours as described in section 2.5.1. Additionally similar transfections carried out on cells plated in glass chamber slides were fixed in Bouins fixative (Appendix I) and subjected to either indirect immunofluorescence or direct visualisation of EGFP as described in sections 2.6.2-3 . Analysis of EGFP fluorescence in transiently transfected $L\beta T_2$ cells was also carried out as described in section 2.6.3.

6.3 Results

6.3.1 Basal Gene Expression

rLH RIAs undertaken with media from unstimulated confluent cultures of $L\beta T_2$ cells revealed that even after 103 passages basal LH secretion was exhibited (figure 6.3.1a). This data demonstrates the variability of expression during progressive passaging of $L\beta T_2$ cells. The lack of adequate samples for each passage prevents statistical comparisons but does demonstrate that detectable LH is secreted from cultures even after prolonged passaging.

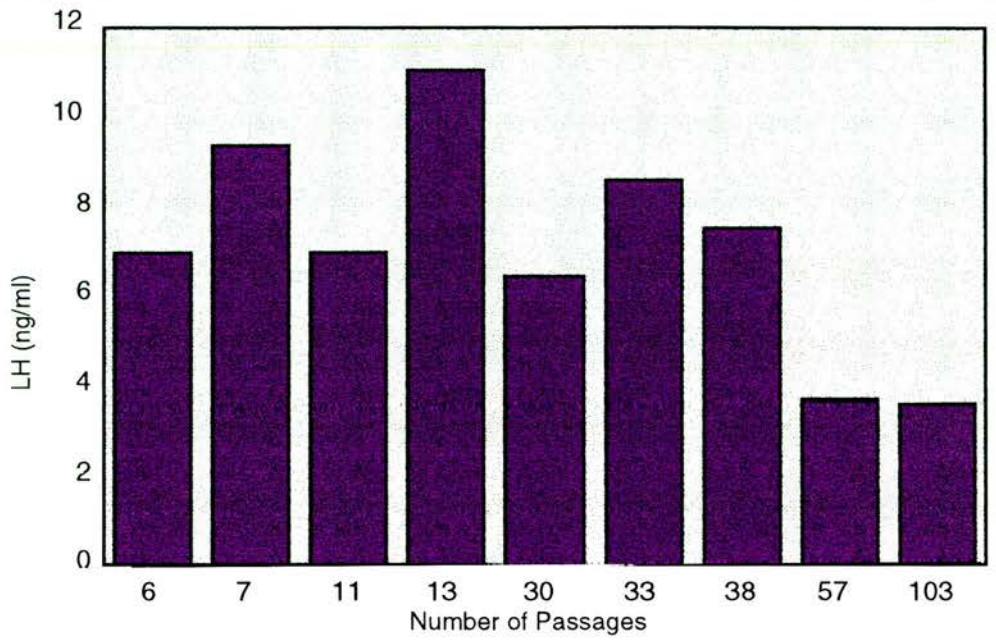

Figure 6.3.1a: Secretion of rLH from $L\beta T_2$ cells after increasing numbers of passage in culture.

Media from confluent $L\beta T_2$ cultures incubated for 24 hours was measured for LH content by rLH RIA.

SDS-PAGE using lysates from two representative passage numbers (p38 and p103) revealed that both expressed detectable levels of rLHβ and CgA. However the amount of rLHβ signal detected at the predicted size of approximately 15kDa in the p38 sample far exceeded that of the p103 sample (figure 6.3.1b). This result correlates with the suggested decline in secreted LH detected by rLH RIA (figure 6.3.1a). It should be noted however, that the observed difference in intracellular LHβ abundance between these two samples appears far greater than that observed for secreted LH. Interestingly neither sample produced an immunoreactive band at the predicted size when treated with the reducing loading buffer containing β-mercaptoethanol. The samples probed for CgA content presented a strong band between the 64 and 98kDa markers in the p38 samples treated with non-reducing or reducing loading buffers which is in agreement with the reported migration of CgA during SDS-PAGE (figure 6.3.1c) (Winkler & Fischer-Colbrie, 1992). Lanes containing p103 did not

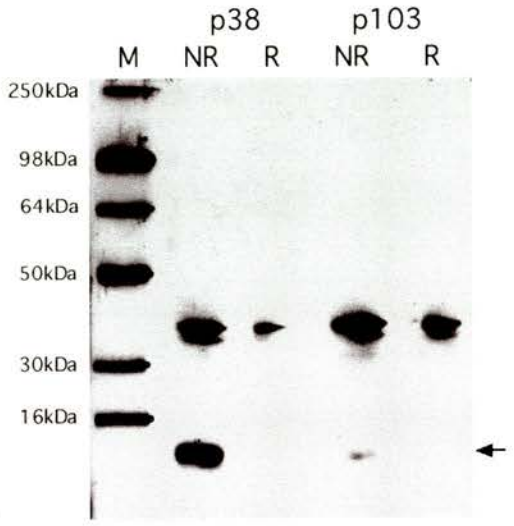

Figure 6.3.1b: Comparison of LHβ abundance in $L\beta T_2$ cell lysates after different lengths of passage.

Lysates from cells after 38 and 103 passages were prepared in non-reducing (NR) and reducing (R) loading buffers. A band corresponding to the reported size of the LHβ subunit (15kDa approx.) was detected (arrow) in samples prepared in non-reducing buffer but not in reducing buffer. The abundance of LHβ in p103 was much less than that observed for lysates after 38 passages. 45μg of total protein was loaded per lane. LH primary antisera (517B8) was used at 1μg/ml. Protein detection was undertaken using the ECL kit.

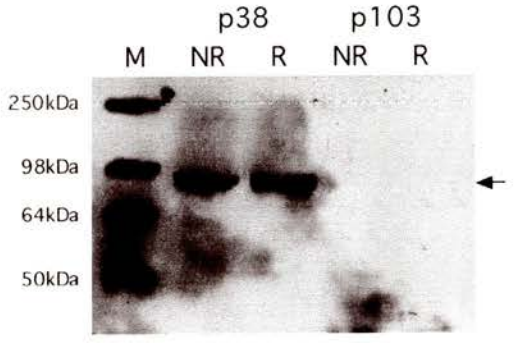

Figure 6.3.1c: Comparison of CgA abundance in $L\beta T_2$ cell lysates after different lengths of passage.

Lysates from cells after 38 and 103 passages were prepared in non-reducing (NR) and reducing (R) loading buffers. A band corresponding to the reported size of monomeric CgA (70-85kDa) was detected (arrow) in p38 samples prepared in non-reducing buffer and reducing buffer. This band was not visible in lysates taken after 103 passages. 45μg of total protein was loaded per lane. CgA primary antisera was diluted 1:2500. Protein detection was undertaken using the ECL kit.

show immunoreactivity at this position even after extended incubation (data not shown).

Assessment of basal GnRH-R expression by radioligand binding demonstrated significant displacement of ^{125}I-labelled GnRH by 10^{-6}M of the D-Trp^{6} GnRH ethylamide peptide as shown in figure 6.3.1d. The figure also indicates that the amount of non-specific binding of the radiolabelled ligand is very low representing less than 8% of the total binding to $L\beta T_2$ membranes.

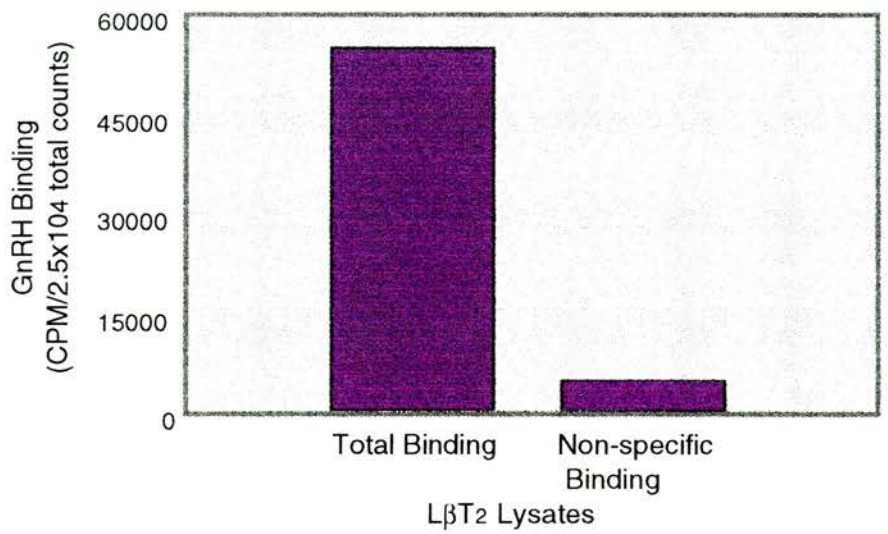

Figure 6.3.1d: Displacement of ^{125}I-GnRH binding from LβT2 membranes using 10-6M D-Trp6 GnRH ethylamide.

Membranes isolated from a single culture of LβT2 cells after 62 passages were assessed for their ability to specifically bind GnRH. The difference between total binding and non-specific binding is equivalent to the specific GnRH binding ability of LβT2 cells.

6.3.2 Effects of GnRH Treatment

Application of 10^{-6}M GnRH to $L\beta T_2$ after 62 passages produced an approximate 40-fold increase in IP_3 production in comparison to untreated cells (figure 6.3.2a).

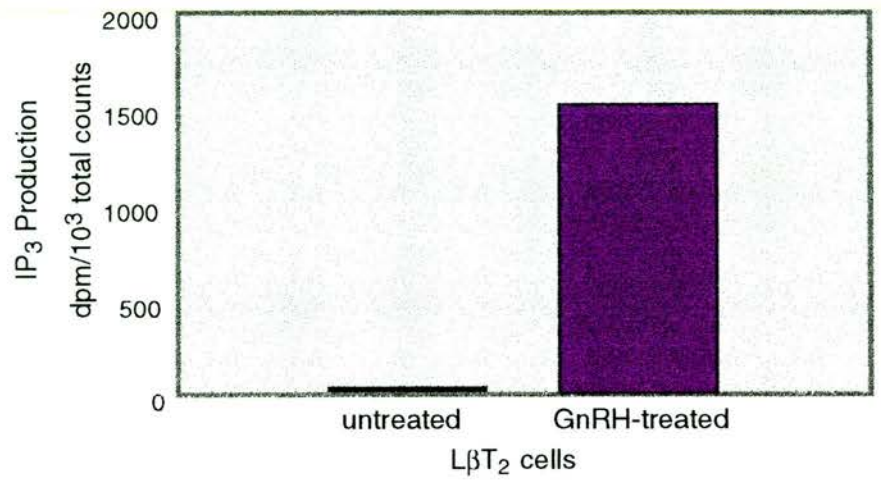

Figure 6.3.2a: Effect of 10^{-6}M GnRH treatment on IP_3 production from $L\beta T_2$ cells.

$L\beta T_2$ cells after 62 passages were labelled with tritiated inositol for 24 hours. Subsequently each culture was either mock-treated or given a single dose of 10^{-6}M GnRH. Lysates were then harvested and assayed for radioactive IP_3 content.

Despite efficient detection of 0.5pg of the 128-base sense strand of mouse LHβ (mLHβ), no mLHβ was detected in the $L\beta T_2$ lysates after pulsatile treatment with 10^{-8}M GnRH. The predicted 197bp protected fragment was not detected in lysates from untreated $L\beta T_2$ cells or those which received either 2 or 3 days of GnRH pulses (figure 6.3.2b).

The RPA carried out to detect the murine αGSU mRNA in 10^{-8}M GnRH-treated cells did detect the protected fragment at the predicted size of 230bp (figure 6.3.2c). However larger fragments presumably a result of inefficient RNase digestion of the 300-base probe were also present. The αGSU mRNA signal was quantified with regard to the parallel detection of GAPDH mRNA which produced the predicted fragment at 316bp and is also shown in figure 6.3.2c. The GAPDH-corrected αGSU mRNA levels are represented in figure 6.3.2d.

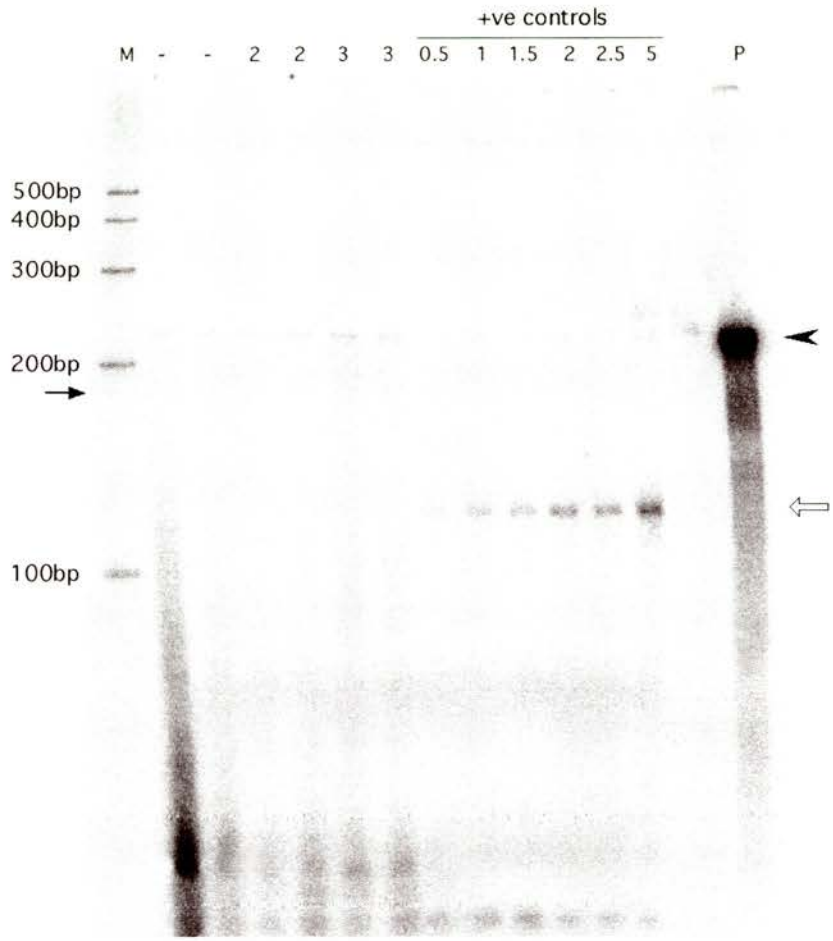

Figure 6.3.2b: mLHβ RNase protection assay of $L\beta T_2$ cells after treatment with 10nM GnRH.

Cells were grown on Matrigel-coated coverslips in the presence of 0.2mM oestradiol and 20nM dexamethasone. GnRH-treated cells received three 10nM pulses per day (15 minute pulse and 75 minute interval). All samples including untreated (-), 2 days of GnRH (2) and 3 days of GnRH (3) did not exhibit the protected fragment of 197bp (filled arrow). Undigested probe is visible in the samples which corresponds to the 248bp band in lane containing only the mLHβ probe (EMBL no.Y10418) shown in lane 'P' and the arrowhead. Positive controls demonstrated efficient protection of the 128bp fragment down to 0.5pg of the sense strand (empty arrow). 'M' denotes the lane containing a 100bp marker.

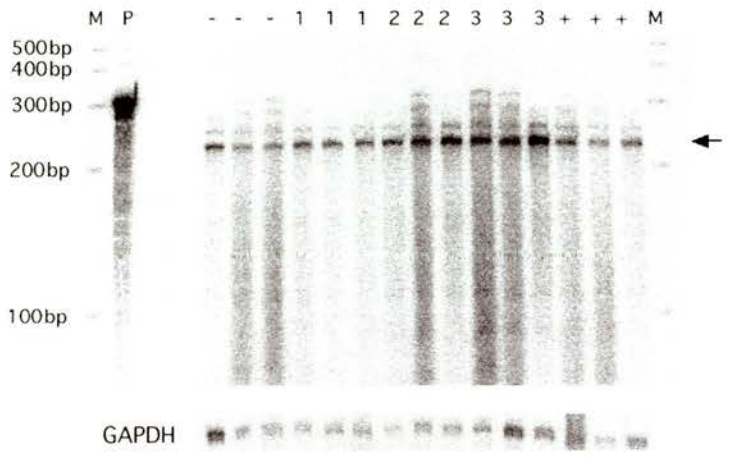

Figure 6.3.2c: mαGSU RNase protection assay of LβT$_2$ cells after treatment with 10nM GnRH.

All cells were grown in the presence of 0.2mM oestradiol and 20nM dexamethasone except for lanes marked (-). GnRH-treated cells received three 10nM pulses per day (15 minute pulse and 75 minute interval). All samples including untreated without oestradiol and dexamethasone (-), untreated with oestradiol and dexamethasone (+), 1 day of GnRH (1), 2 days of GnRH (2) and 3 days of GnRH (3) exhibited the protected fragment of approximately 230bp (arrow). Undigested probe is visible in the samples and in the lane containing only the mαGSU probe (P). Internal controls measuring GAPDH mRNA abundance were carried out separately and are shown in the panel below the main gel. Increased abundance of the mαGSU mRNA was apparent in samples which had received 2 days of GnRH treatment (i.e. 6 pulses) in comparison to controls and cells treated for 1 and 3 days. 'M' denotes the lane containing a 100bp marker. All cells were grown on Matrigel-coated coverslips.

show immunoreactivity at this position even after extended incubation (data not shown).

Assessment of basal GnRH-R expression by radioligand binding demonstrated significant displacement of ^{125}I-labelled GnRH by 10^{-6}M of the dTrp6 GnRH peptide as shown in figure 6.3.1d. The figure also indicates that the amount of non-specific binding of the radiolabelled ligand is very low representing less than 8% of the total binding to $L\beta T_2$ membranes.

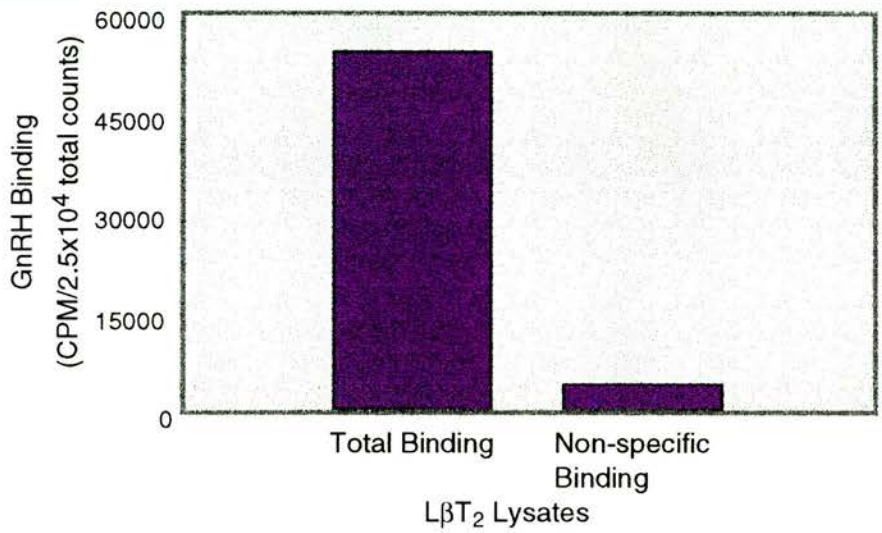

Figure 6.3.1d: Displacement of ^{125}I-GnRH binding from $L\beta T_2$ membranes using 10^{-6}M dTrp6 GnRH.

Membranes isolated from a single culture of $L\beta T_2$ cells after 62 passages were assessed for their ability to specifically bind GnRH. The difference between total binding and non-specific binding is equivalent to the specific GnRH binding ability of $L\beta T_2$ cells.

6.3.2 Effects of GnRH Treatment

Application of 10^{-6}M GnRH to $L\beta T_2$ after 62 passages produced an approximate 40-fold increase in IP_3 production in comparison to untreated cells (figure 6.3.2a).

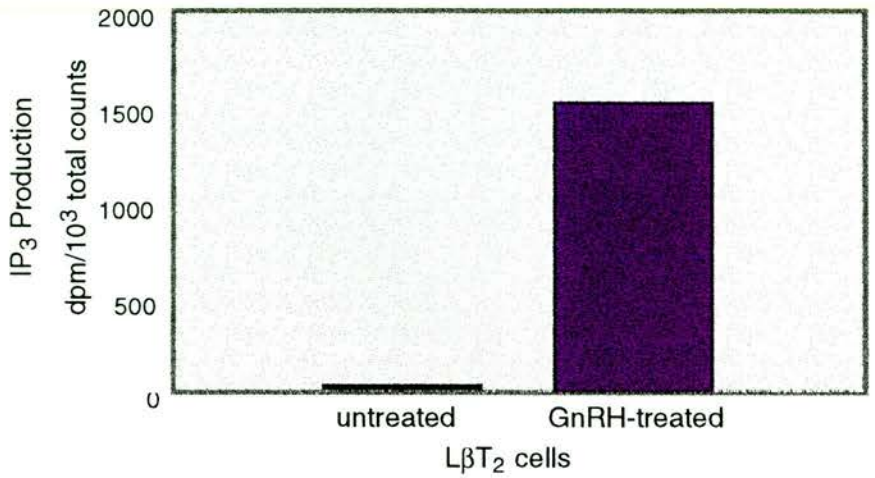

Figure 6.3.2a: Effect of 10^{-6}M GnRH treatment on IP_3 production from $L\beta T_2$ cells.

$L\beta T_2$ cells after 62 passages were labelled with tritiated inositol for 24 hours. Subsequently each culture was either mock-treated or given a single dose of 10^{-6}M GnRH. Lysates were then harvested and assayed for radioactive IP_3 content.

Despite efficient detection of 0.5pg of the 128-base sense strand of mLHβ, no mLHβ was detected in the $L\beta T_2$ lysates after pulsatile treatment with 10^{-8}M GnRH. The predicted 197bp protected fragment was not detected in lysates from untreated $L\beta T_2$ cells or those which received either 2 or 3 days of GnRH pulses (figure 6.3.2b).

The RPA carried out to detect the murine αGSU mRNA in 10^{-8}M GnRH-treated cells did detect the protected fragment at the predicted size of 230bp (figure 6.3.2c). However larger fragments presumably a result of inefficient RNase digestion of the 300-base probe were also present. The αGSU mRNA signal was quantified with regard to the parallel detection of GAPDH mRNA which produced the predicted fragment at 316bp and is also shown in figure 6.3.2c. The GAPDH-corrected αGSU mRNA levels are represented in figure 6.3.2d.

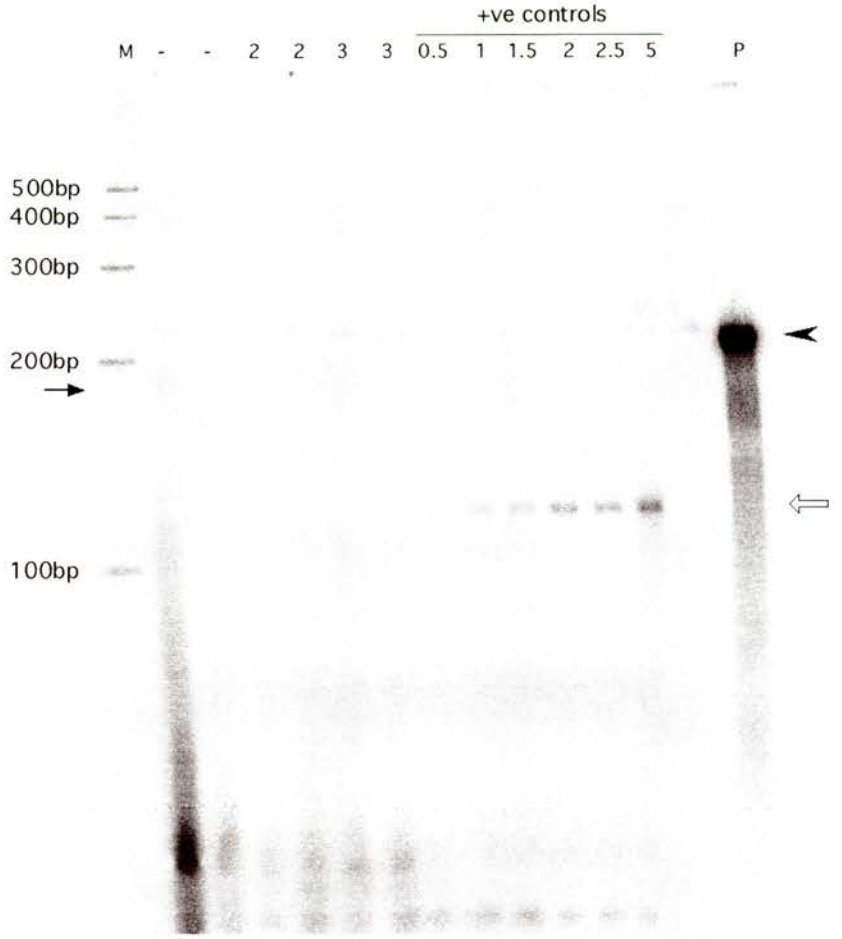

Figure 6.3.2b: mLHβ RNase protection assay of $L\beta T_2$ cells after treatment with 10nM GnRH.

Cells were grown on Matrigel-coated coverslips in the presence of 0.2mM oestradiol and 20nM dexamethasone. GnRH-treated cells received 3 10nM pulses per day (15 minute pulse and 75 minute interval). All samples including untreated (-), 2 days of GnRH (2) and 3 days of GnRH (3) did not exhibit the protected fragment of 197bp (filled arrow). Undigested probe is visible in the samples which corresponds to the 248bp band in lane containing only the mLHβ probe (EMBL no.Y10418) shown in lane 'P' and the arrowhead. Positive controls demonstrated efficient protection of the 128bp fragment down to 0.5pg of the sense strand (empty arrow). 'M' denotes the lane containing a 100bp marker.

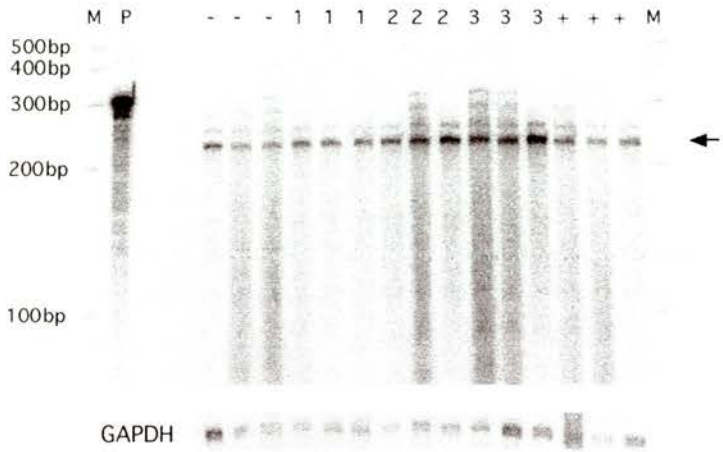

Figure 6.3.2c: mαGSU RNase protection assay of $L\beta T_2$ cells after treatment with 10nM GnRH.

Cells were grown on Matrigel-coated coverslips in the presence of 0.2mM oestradiol and 20nM dexamethasone except for lanes marked (-). GnRH-treated cells received three 10nM pulses per day (15 minute pulse and 75 minute interval). All samples including untreated without oestradiol and dexamethasone (-), untreated with oestradiol and dexamethasone (+), 1 day of GnRH (1), 2 days of GnRH (2) and 3 days of GnRH (3) exhibited the protected fragment of approximately 230bp (arrow). Undigested probe is visible in the samples and in the lane containing only the mαGSU probe (P). Internal controls measuring GAPDH mRNA abundance were carried out separately and are shown in the panel below the main gel. Increased abundance of the mαGSU mRNA was apparent in samples which had received 2 days of GnRH treatment (i.e. 6 pulses) in comparison to controls and cells treated for 1 and 3 days. 'M' denotes the lane containing a 100bp marker.

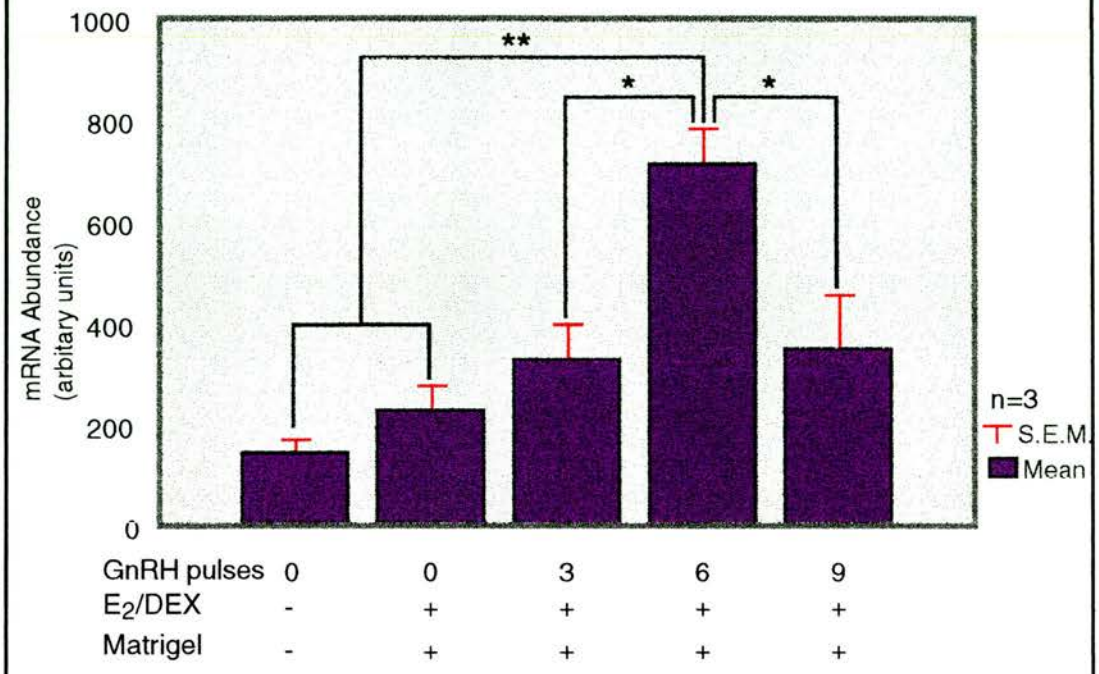

Figure 6.3.2d: Quantification by RPA of murine αGSU in $L\beta T_2$ cells treated with pulsatile 10^{-8}M GnRH.

RNase protection assays (RPAs) were carried out on lysates of control and GnRH-treated $L\beta T_2$ cells. 3 GnRH pulses were given daily to cells cultured in the presence of Matrigel, 0.2nM oestradiol and 20nM dexamethasone. The untreated control samples were taken at the begining of the experiment whereas the E_2/DEX and Matrigel treated control samples were harvested at the end of day three. Where *=$p<0.05$ and **=$p<0.001$.

The control sample which did not receive GnRH, E_2 or DEX and was plated on standard culture surface exhibited the lowest abundance for αGSU mRNA. No significant rise in αGSU mRNA abundance was apparent in lysates harvested from cultures after three days in media containing 0.2nM E_2 and 20nM DEX whilst plated on Matrigel. Maximal stimulation of αGSU mRNA abundance was evident after 2 days and a total of 6 pulses. Lysates harvested after 3 or 9 GnRH pulses (days 1 and 3) exhibited significantly lower levels of αGSU mRNA abundance.

In correlation with the lack of mLHβ mRNA detection by RPA, rLH detected in the media of GnRH-treated and untreated $L\beta T_2$ cells was equivalent to background levels (data not shown). This level of LH expression is lower than that observed for basal LH secretion (figure 6.3.1a) and showed no significant response to GnRH treatment despite the presence of Matrigel, E_2 and DEX. This experiment was undertaken with $L\beta T_2$ cells after approximately 75 passages.

A GnRH regime consisting of four 1μM pulses per day for four days did not reduce the basal LH secretion in $L\beta T_2$ cells after 44 passages. LH levels secreted by GnRH-treated and untreated cells on the final day of the regime are shown in figure 6.3.2e.

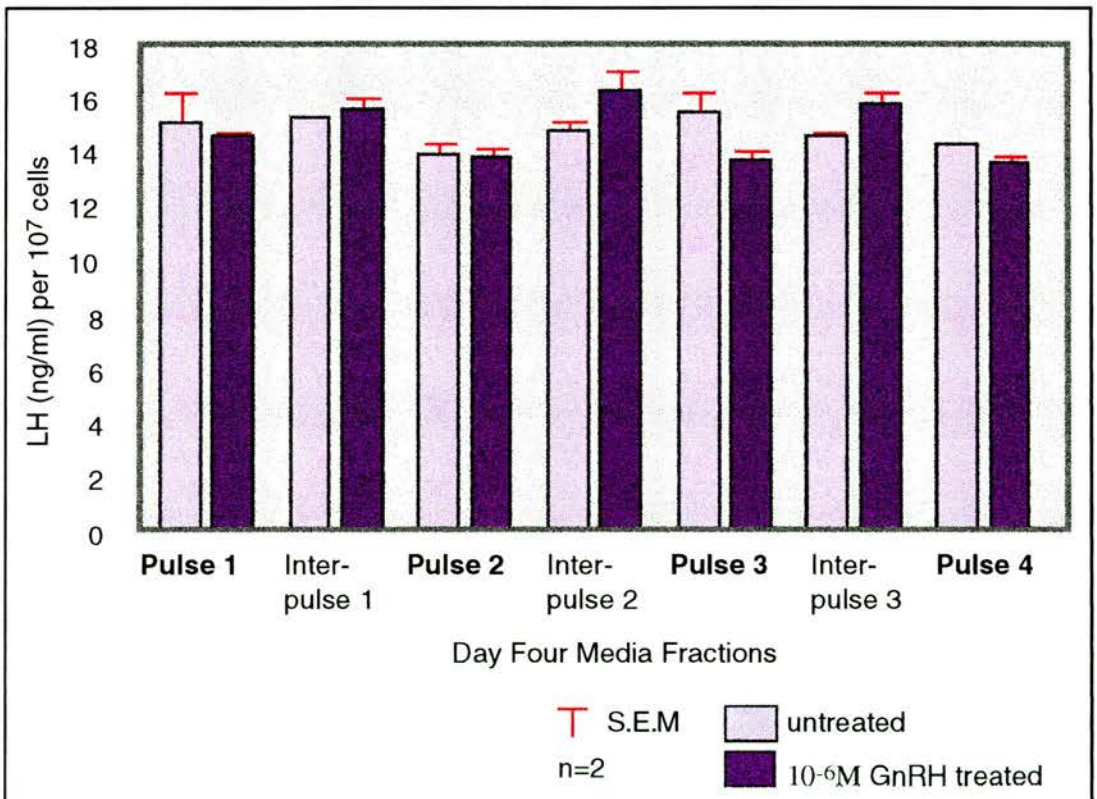

Figure 6.3.2e: Secretion of LH by control and 10^{-6}M GnRH-treated $L\beta T_2$ cells on day four of a 4 pulses per day regime.

LH was assayed by rLH RIA. Media fractions represent LH secretion during the 15 minute GnRH pulse period or the 75 minute inter-pulse period.

Although no difference in the amount of LH secreted from control and GnRH-treated cells was observed, a marked difference in the amount of LH present intracellularly between control and GnRH-treated cells was evident (figure 6.3.2f).

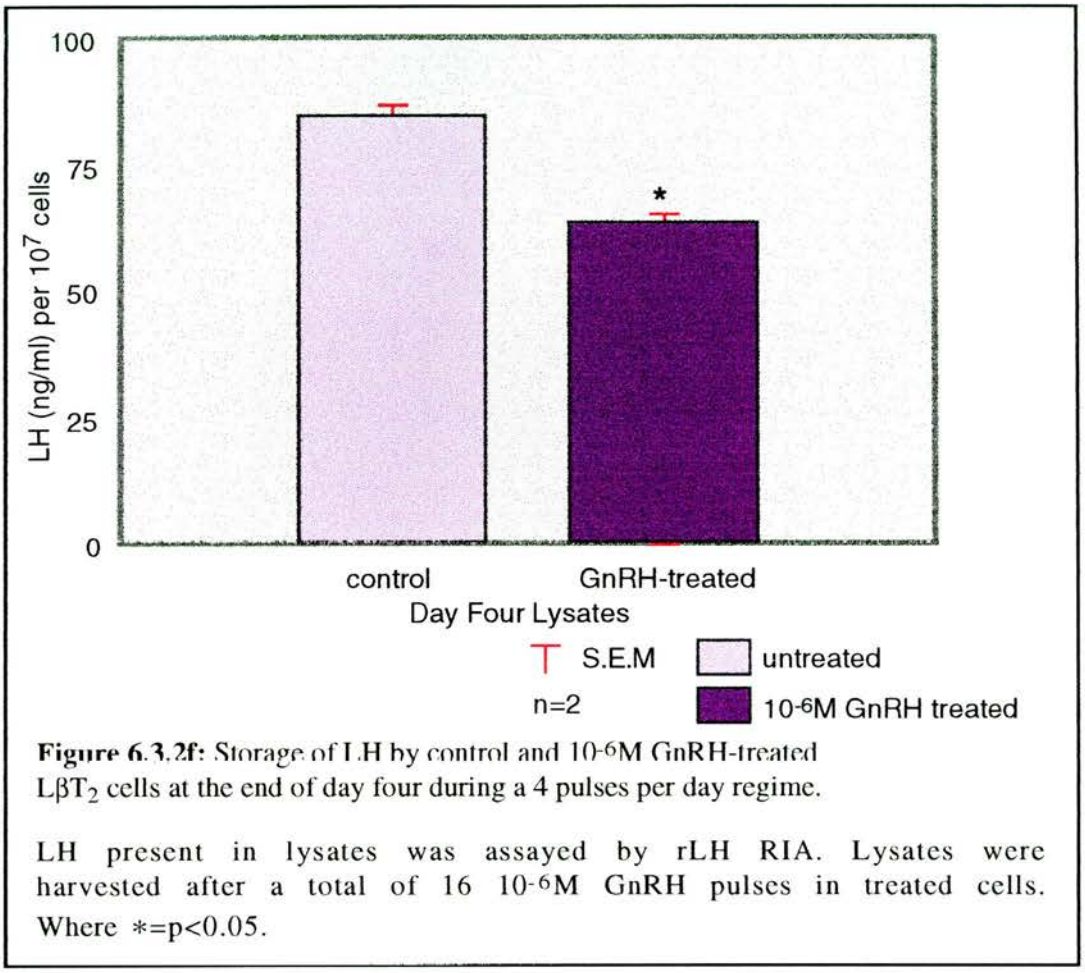

Figure 6.3.2f: Storage of LH by control and 10^{-6}M GnRH-treated $L\beta T_2$ cells at the end of day four during a 4 pulses per day regime.

LH present in lysates was assayed by rLH RIA. Lysates were harvested after a total of 16 10^{-6}M GnRH pulses in treated cells. Where *=p<0.05.

Furthermore increased LH release was apparent during the overnight incubations. Whereas untreated cells secreted 19±1.5ng LH per 10^7 cells in 17 hours over the 3 nights, cells treated with 1μM GnRH secreted on average 27.5±0.7ng during the same 17 hour periods which is significantly greater (p=<0.001) as shown below in figure 6.3.2g.

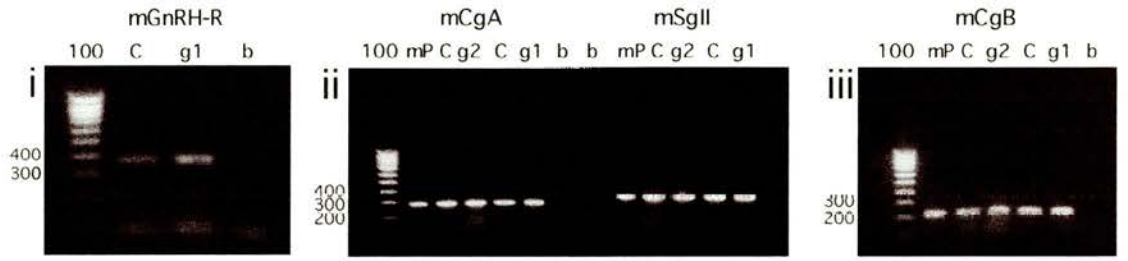

Figure 6.3.2h: Effect of GnRH on expression of GnRH-R and granins in LβT_2 cells detected by RT-PCR.

i) GnRH-R expression was detected by the appearance of the amplified product corresponding to the predicted size of 370bp. The band is present in both untreated (C) and LβT_2 cells which received 10nM GnRH pulses 4 times daily over four days (g1). No products were detected in the control reaction which contained no RNA (b). (ii) & (iii) CgA, SgII and CgB expression was detected by the appearance of amplified products corresponding to the predicted sizes of 295, 350 and 230bp. Similar size products were detected in reactions containing RNA from LβT_2 cells after no treatment (C), after 4 days of four 10nM GnRH pulses (g1) and after 4 days of four 1μM GnRH pulses (g2). These products were also present in reactions which contained mouse pituitary RNA (mP). No products were detected in the control reactions which contained no RNA (b).

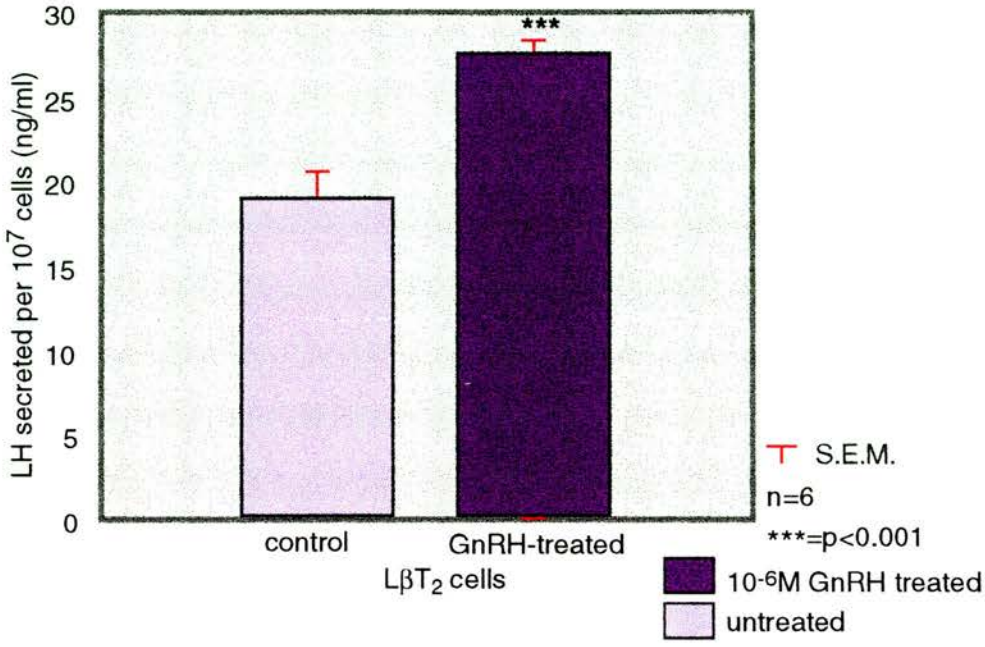

Figure 6.3.2g: Effect of 10^{-6}M GnRH treatment on LH secretion by $L\beta T_2$ cells during 17 hour overnight incubations.

Media from untreated $L\beta T_2$ cells and $L\beta T_2$ cells treated with 10^{-6}M GnRH four times per day were isolated 17 hours after the last pulse each day. The data represents the mean LH determined after days 1, 2 and 3 of the four day regime by rLH RIA.

RT-PCR detected CgA, CgB, SgII and GnRH-R mRNA before and after treatment with either 10^{-6} or 10^{-8}M GnRH (see figure 6.3.3h). Although these reactions were not carried out using primers amplifying an internal control such as GAPDH, these results indicate that specific target RNA was present in all samples.

6.3.3 Optimisation of Lipid-based Transfection

Initial attempts to transfect the $L\beta T_2$ cell line did not provide significant transfection efficiencies as illustrated by the photomicrograph of β-galactosidase stained cells in figure 6.3.3ai. However repeated passaging of the cell line using the diluted trypsin-EDTA solution resulted in morphological changes which appeared to aid adherence to the culture surface. Transfection of cultures after approximately 50 passages were

i

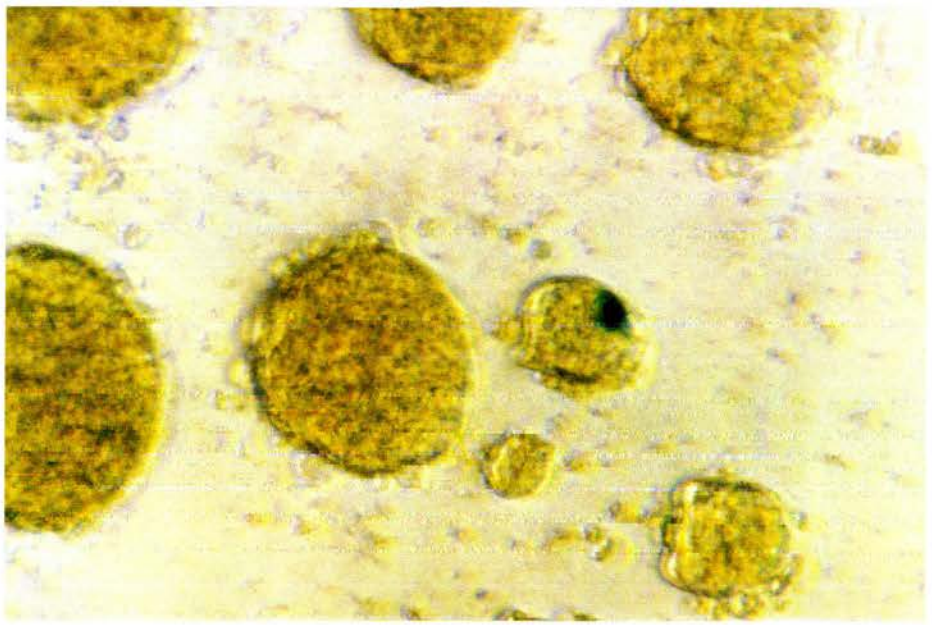

ii

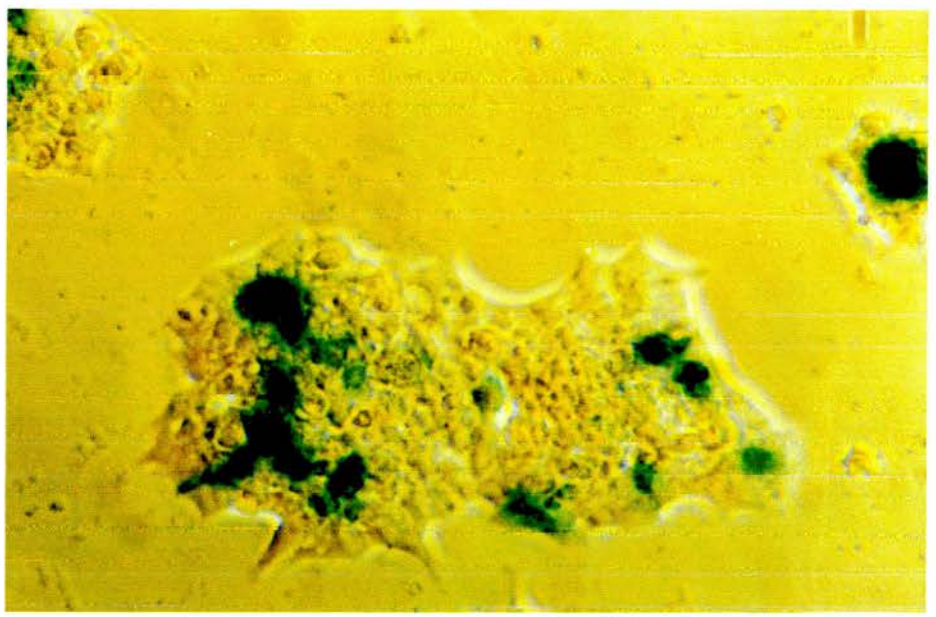

Figure 6.3.3a: $L\beta T_2$ cells transiently transfected with pcDNA3.1/His/lacZ and stained for β-galactosidase activity 48 hours later.

i) Low passage $L\beta T_2$ cells grow in clumps and transfect relatively poorly.
ii) $L\beta T_2$ cells after approximately 55 passages exhibit greater adherence to the culture surface and a higher transfection efficiency. Magnification = x200.

significantly more successful as shown by the photomicrograph in figure 6.3.3aii. This figure represents the optimal transfection efficiency obtained after screening with the eight lipids in the PerFect^{TM} transfection kit (Invitrogen, NL) which provided the transfection efficiencies shown below.

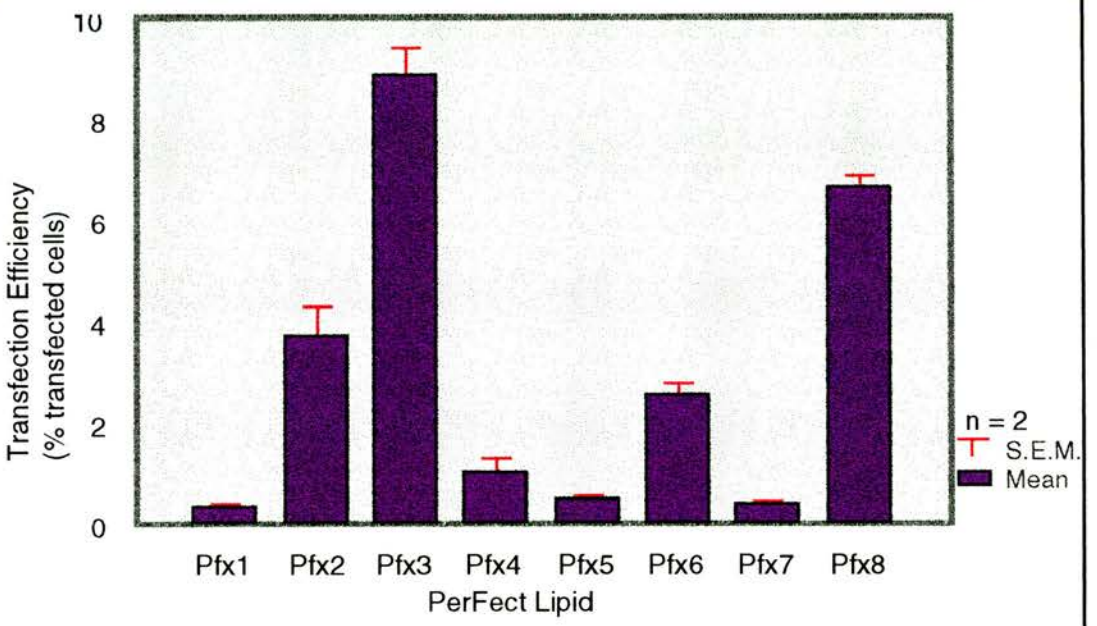

Figure 6.3.3b: Transfection of $L\beta T_2$ cells using PerFect lipids.

Cells were transfected in 12 well dishes for 3.5 hours using each lipid mix at a 6:1 ratio to DNA. The proportion of cells expressing the transfected *lacZ* gene (pcDNA3.1/His/lacZ) was determined 48 hours posttransfection by β-galactosidase staining. 1000 cells were counted per well and the proportion stained blue represented the transfection efficiency.

Transfection using Pfx3 provided the most efficient transfection of approximately 9%. Lipids Pfx2, 6 and 8 also provided relatively high transfection efficiencies in comparison to the remaining lipids and the almost undetectable transfection of lower passage $L\beta T_2$ cells (figure 6.3.3ai).

6.3.4 Transient FSH Expression

As expected control $L\beta T_2$ cells transfected with only the poαGSU construct did not express FSH. Cells transfected with the poFSHβg construct alone which therefore relied on endogenous αGSU expression to form the heterodimeric FSHαβ hormone, produced significant amounts of FSH as did cells transfected with both poαGSU and poFSHβg constructs (figure 6.3.4a).

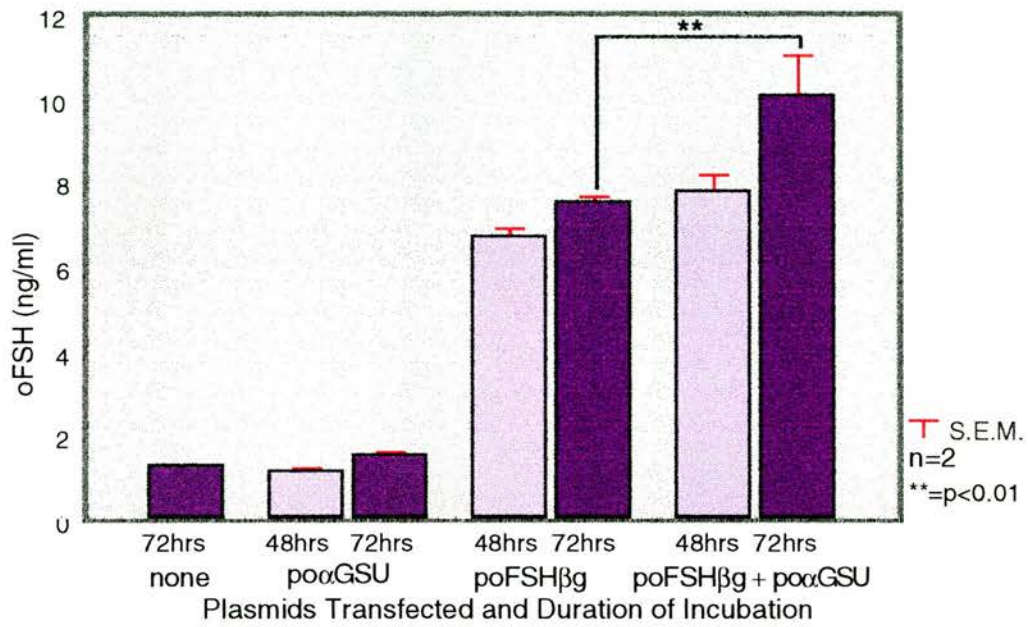

Figure 6.3.4a: Total oFSH expressed by LβT2 cells transiently transfected with either the oFSHβ subunit expression construct alone or in conjunction with the ovine αGSU expression construct.

Cells were mock-transfected or transfected with the poαGSU alone. FSH heterodimer formation was assessed in cells transfected with only the oFSHβ subunit expression construct which therefore relied upon endogenous murine αGSU. This was compared with cells transfected with both the ovine αGSU and FSHβ expression constructs after 48 and 72 hours of expression.

Comparisons of the percentage of total oFSH which remained intracellularly after 48-72 hours in cells transfected with either poFSHβg alone or both poFSHβg and poαGSU revealed a significant difference (figure 6.3.4b). Cells transfected with both ovine expression constructs (intra-species heterodimer) exhibited storage of only 26.7±2.9% compared to 37.0±0.6% in cells expressing the inter-species FSH heterodimer.

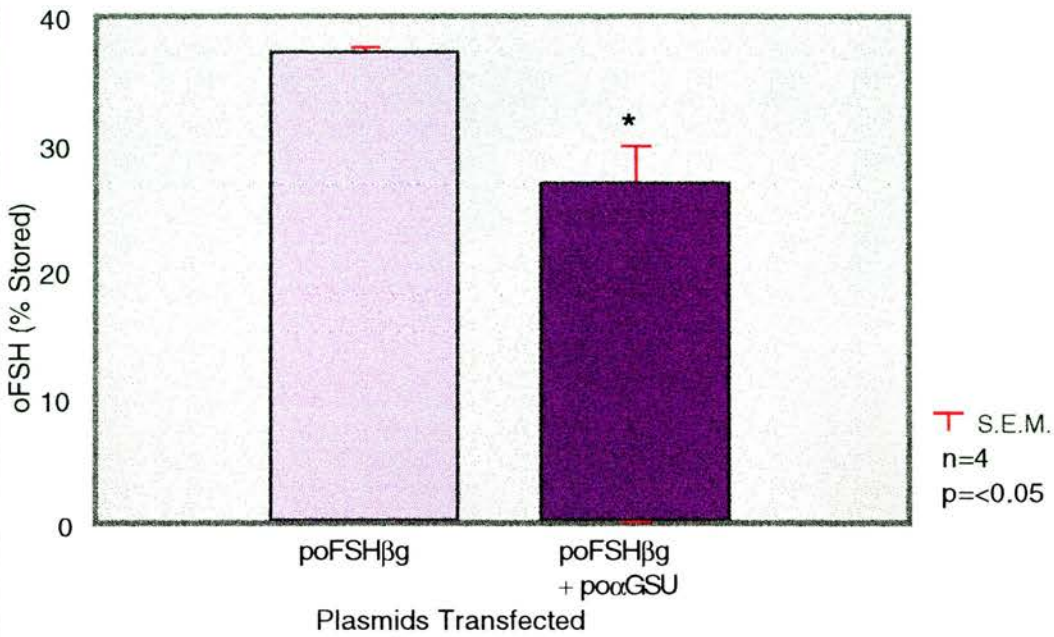

Figure 6.3.4b: Comparison of the proportion of FSH stored in $L\beta T_2$ cells transfected with the oFSHβ subunit alone or in conjunction with the αGSU expression construct.

oFSH was assayed by RIA in the lysates and media of transiently transfected cells after 48 or 72 hours. Cells transfected with the oFSHβ subunit expression construct alone required endogenous murine αGSU to form the FSH heterodimer detectable by RIA. The data represented in the bar chart represents the mean figures for the proportion of the total oFSH which remained intracellularly after 48 and 72 hours in cells transfected with the β-subunit construct alone or both the αGSU and β-subunit constructs.

The total amounts of oFSH expressed by $L\beta T_2$ cells were compared between transfections containing poαGSU in conjunction with poFSHβ or poFSHβg or pEGFPC3-oFSHβ. The differences in oFSH detected are shown in figure 6.3.4c. Mock-transfected cells expressed little detectable oFSH as expected. However cells transfected with the EGFP-oFSHβ construct expressed similar background levels of oFSH as detected by RIA. $L\beta T_2$ cells transfected with the ovine αGSU and oFSHβ cDNA constructs exhibited significantly higher expression than cells transfected with the ovine αGSU and genomic oFSHβ

constructs. This difference was apparent between samples taken after 48 and 72 hours.

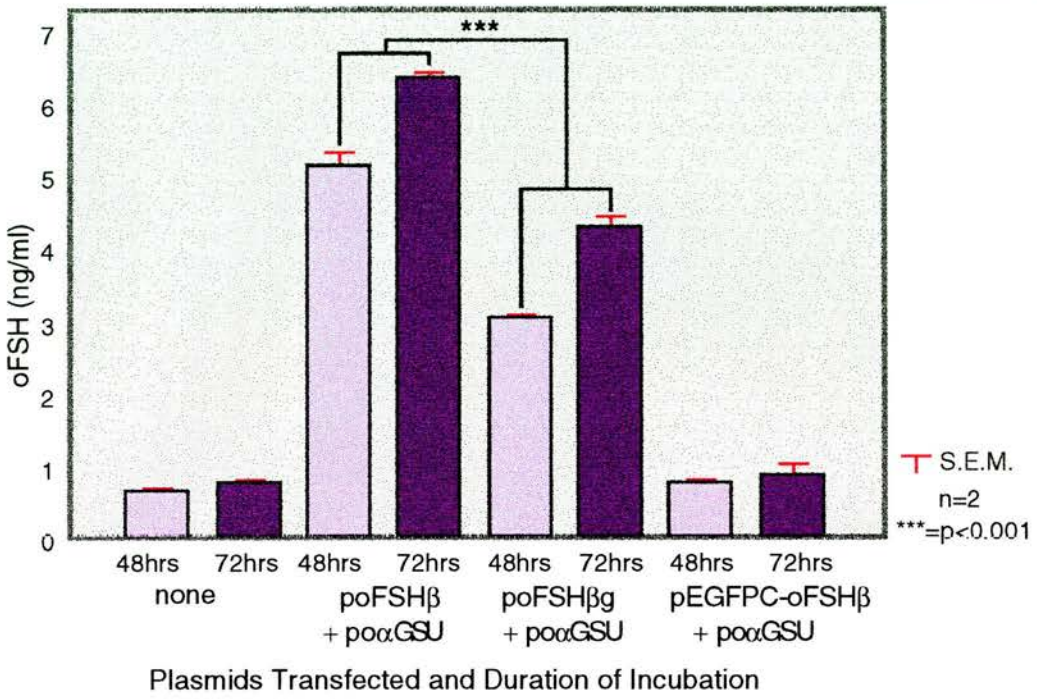

Figure 6.3.4c: Total oFSH expressed by LβT2 cells transiently transfected with the αGSU expression construct and different oFSHβ constructs.

oFSH was determined 48 or 72 hours posttransfection by RIA of lysates and media. FSH detected in mock-transfected LβT2 cells indicates the level of background. The ovine FSHβ cDNA construct exhibited significantly higher expression than that of the genomic oFSHβ clone after 48 and 72 hours. No significant oFSH was detected in cells transfected with the EGFPC-FSHβ fusion construct.

Comparison between the percentage of total oFSH stored in cell transfected with the poαGSU and either poFSHβ or poFSHβg also revealed significant differences. $L\beta T_2$ cells transfected with the genomic clone for oFSHβ exhibited reduced storage in comparison to cells transfected with the cDNA construct (figure 6.3.4d).

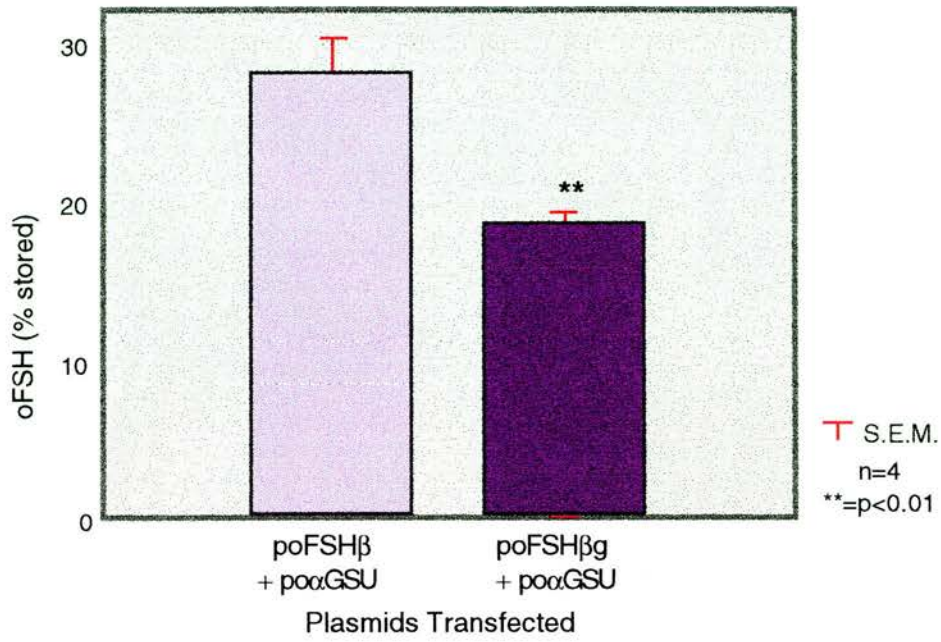

Figure 6.3.4d: Storage of oFSH in transiently transfected $L\beta T_2$ cells.

$L\beta T_2$ cells were transiently transfected with either the cDNA or genomic clone for oFSHβ in conjunction with the oαGSU expression construct. oFSH in media and lysates was measured by RIA after 48 or 72 hours. The percentage of total oFSH which was present intracellularly was compared between cells transfected with either oFSHβ construct.

However the proportion of oFSH storage observed in cells transfected with the αGSU and genomic oFSHβ constructs also appears to have declined between the experiments shown in figure 6.3.4b and d. This reduction from 26.7±2.9 to 18.5±0.8 is statistically significant (n=4, $p<0.05$). It is important to note that these investigations were carried out using the same batch of $L\beta T_2$ cells but after different numbers of passages. The previous experiment investigating the secretion of hybrid FSH molecules used cells after 44 passages whereas in the latter experiment the cells had undergone 65 passages.

6.3.5 Intracellular Trafficking of FSH fusion proteins

$L\beta T_2$ cells transiently transfected with the poαGSU and pEGFPC-oFSHβ constructs were viewed after fixing in Bouins. Although the cells appear

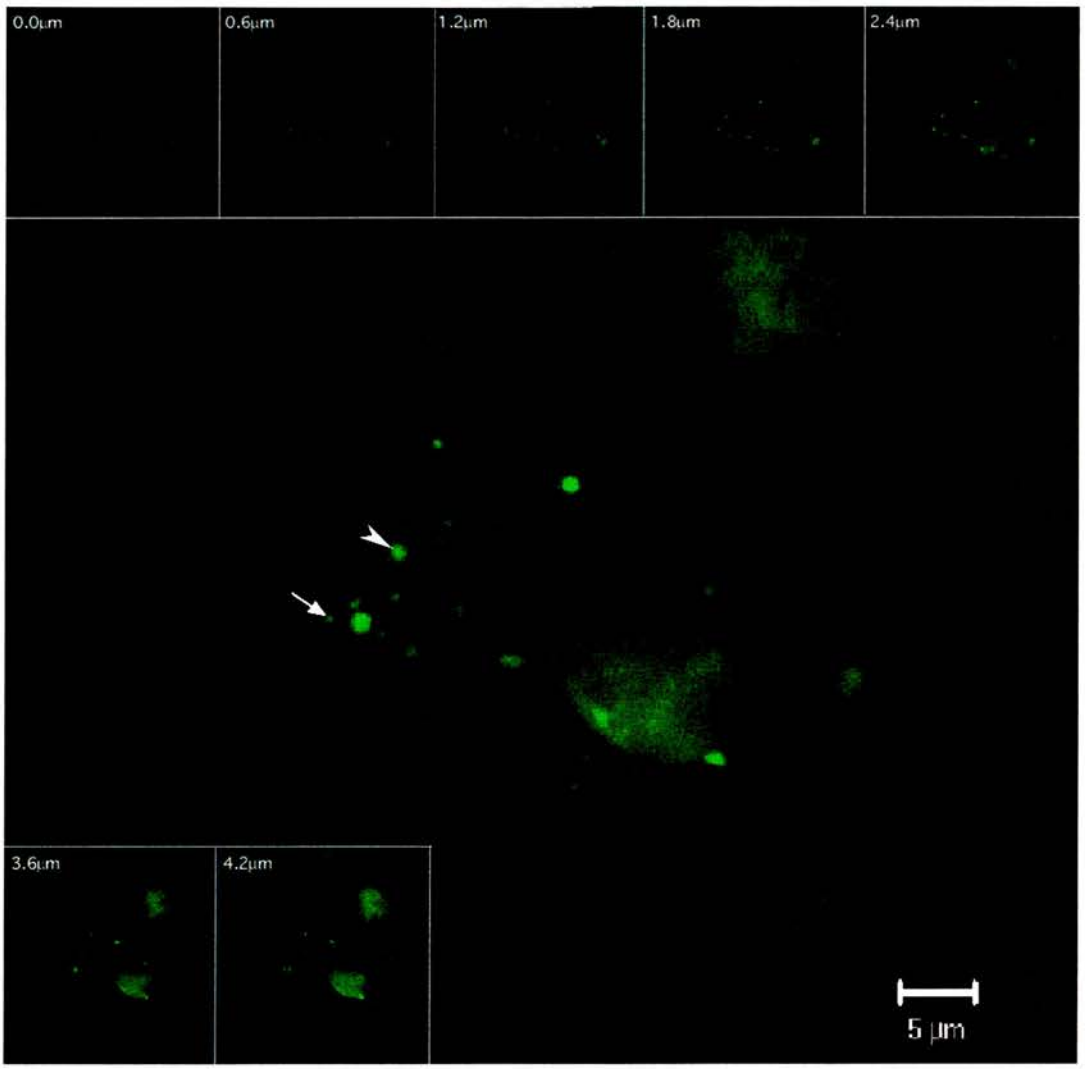

Figure 6.3.5a: Series of Z-scan images from $L\beta T_2$ cells transiently transfected with poαGSU and pEGFPC-oFSHβ.

Optical sections were taken through the Z-plane at 0.6μm intervals. The main picture shows a clump of several $L\beta T_2$ cells in which some are expressing the transfected constructs. Fluorescent bodies are present within the cytoplasm towards the periphery of the cell. These putative vesicles range from 500nm (arrow) to 1.1μm (arrowhead) in diameter. EGFP fluorescence was observed in fixed cells 48 hours posttransfection using a 488nm argon laser and 505-535nm bandpass filter.

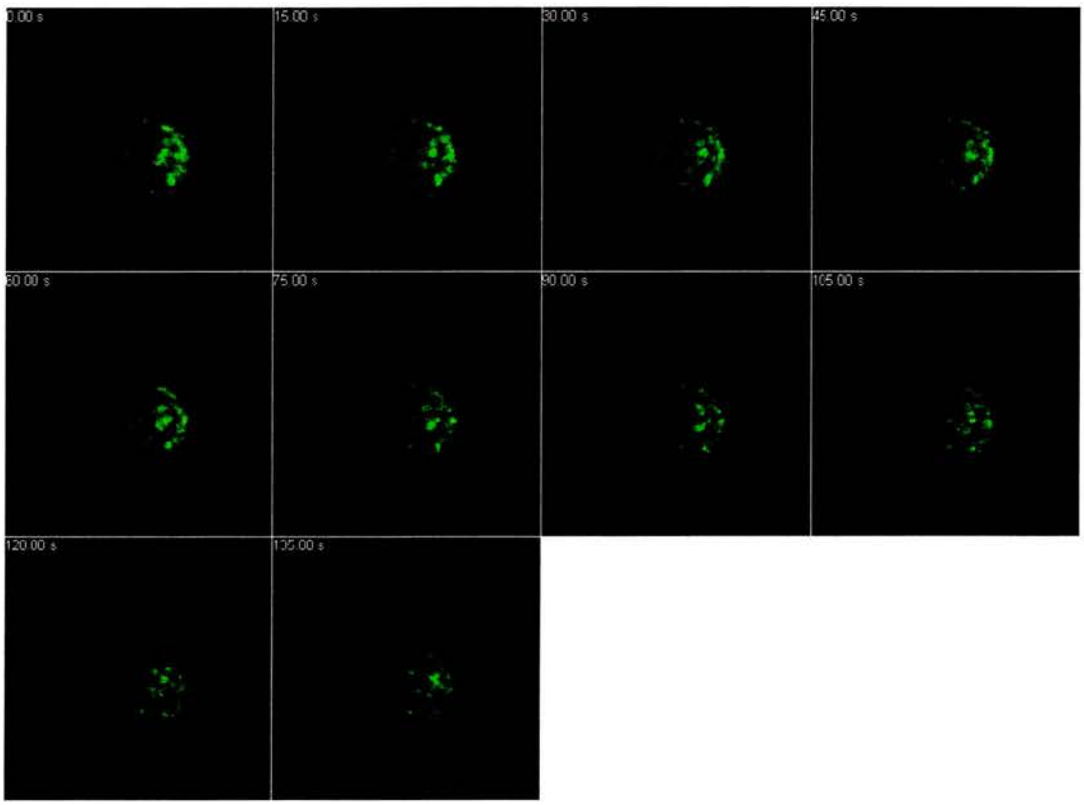

Figure 6.3.5b: Gallery of time-lapse images of EGFPC-oFSHβ fluorescence from a transiently transfected $L\beta T_2$ cell.

This rounded $L\beta T_2$ cell exhibits punctate fluorescence ranging from 280-990nm in diameter. These fluorescent bodies exhibit apparently random movement within the $L\beta T_2$ cell. Images were taken 48 hours posttransfection with poαGSU and pEGFPC-oFSHβ. Scans were performed at 15 second intervals. EGFP fluorescence was observed in fixed cells 48 hours posttransfection using a 488nm argon laser and 505-535nm bandpass filter. The fluorescence begins to fade over time due to photobleaching.

poorly attached to the glass surface of the chamber slide, a serial Z-scan revealed the presence of several areas of punctate fluorescence located towards the cell periphery (figure 6.3.5a). These structures ranged from approximately 500 to 1100nm in diameter.

Similar analysis of a living $L\beta T_2$ cells transfected with the same combination of constructs demonstrated the rapid movement of these fluorescent bodies (figure 6.3.5b and movie 6.3.5c). The individual images within the series were taken at 15 second intervals demonstrating the relatively rapid movement of the fluorescent bodies. It can be seen that the direction of their movement appears to be largely random and to occur sporadically.

6.4 Discussion

Studies on the control of endogenous LH expression from $L\beta T_2$ cells were hampered by the apparent transient nature of the LHβ subunit gene expression. $L\beta T_2$ cells were derived from the mouse pituitary by targeted expression of the SV40 T-antigen to LHβ-expressing gonadotrophs (Thomas *et al.*, 1996). This popular method for deriving cell lines inhibits tumour suppressing proteins responsible for maintenance of DNA integrity. The SV40 T-antigen interacts with several of these proteins leading to mutations which in time may cause uncontrolled proliferation. For example binding of the T antigen to the hypophosphorylated form of p105-RB which normally prevents cell proliferation by inhibiting expression of the proto-oncogene c-*myc*, leads to unregulated cell proliferation (Marshall, 1991). In isolated cell lines the SV40 T-antigen continues to be expressed interfering with maintenance of the genomic structure. During repeated passaging in culture the effects of the mutations arising due to T-antigen expression may become apparent. In these studies several effects were observed including most notably a drastic decrease in LHβ mRNA expression. Although this effect was without doubt the most detrimental to these studies other effects were also apparent. CgA expression appeared unchanged when analysed by RT-PCR but western analysis clearly showed

reduced expression of the unprocessed protein suggesting increased susceptibility to the processing enzyme prohormone convertase PC1. CgA has been demonstrated as a substrate for PC1 in the mouse adrenocorticotroph AtT-20 cell line (Eskeland *et al.*, 1996). It is also possible that due to an accumulation of mutations in the CgA gene, the mature protein exhibits structural anomalies which predispose it to a lysosomal destination thus accounting for unchanged mRNA expression and reduced immunoreactivity for CgA.

Significantly reduced storage of transiently expressed oFSH was also apparent between passages 44 and 65. Although endogenous LH expression appeared drastically reduced in passage 103 compared to that of passage 38, the proportion of intracellular LH in the lower passage cells appeared much higher which also suggests reduced storage with increasing passage. Despite the putative effects of lower LH abundance within high passage cells,

it is likely that reduced storage of LH and FSH was a direct effect of the reduction in CgA abundance intracellularly. Certainly the role of CgA as a mediator of LH sorting to the regulated pathway suggested by its aggregative nature (Yoo & Albanesi, 1990a), interaction with membrane proteins (Yoo, 1994) and colocalisation with LH in immature or condensing vesicles (Watanabe *et al.*, 1991) strongly implicates CgA as a key protein in the regulated pathway. Exclusive *in vitro* aggregation of LH induced by lysates containing CgA further implicates the granin in the gonadotroph regulated pathway (Colomer *et al.*, 1995). Evidence for a role of CgA in LH and FSH aggregation in gonadotrophs is also suggested by their colocalisation in large granules (Watanabe *et al.*, 1991) demonstrating that CgA may interact with both pituitary gonadotrophins. The reduced storage of LH and FSH coinciding with an apparent reduction in expression of intact CgA in $L\beta T_2$ cells implicates this granin in intracellular accumulation of the pituitary gonadotrophins. To further substantiate these preliminary findings future studies may involve targeted disruption of CgA expression using antisense oligonucleotides in lower passage $L\beta T_2$ cells. Alternatively treatment of $L\beta T_2$ cells with dexamethasone which upregulates CgA expression (Fischer-Colbrie *et al.*, 1989) may reveal this granin's effect on LH storage *in vitro*. Comparisons of granule

morphology in rat gonadotrophs has demonstrated decreased diameter of CgA-immunoreactive granules in castrated males compared to controls (Watanabe *et al.*, 1998b). Whether this directly effects LH storage may be revealed by future studies using the $L\beta T_2$ cell line.

Morphological differences were also observed during these studies with an overall change from round 'clumpy' cells to those with increased adherence and neuron-like processes. Coupled with these morphological changes was an increase in the rate of proliferation by approximately two-fold which may have accounted for the significant rise in transfection efficiency. Clearly this increase in transfection efficiency aided studies of oFSHβ expression but the relevance of any findings made under these circumstances could be disputed in light of changes in LHβ and CgA expression. The initial attraction of the $L\beta T_2$ cell line was due to its apparent regulated expression of LH secretion (Turgeon *et al.*, 1996). Nevertheless comparison of gene expression in low and high passage $L\beta T_2$ cells may allow assignment of key proteins involved in formation of the regulated secretory pathway. Use of differential display in which multiple semi-specific RT-PCRs are carried out on cell lysates allows comparison of gene expression by changes in mRNA profiles. Application of this technique may not only reveal proteins involved in regulated secretion but also gonadotroph-specific transcription factors.

Despite the aberrant expression of LHβ and CgA in the $L\beta T_2$ cell line after repeated passage some significant findings regarding gonadotrophin expression during GnRH stimulation were observed. The cells used during the 10nM GnRH treatment were not in excess of 103 passages yet did not exhibit LHβ expression. However $L\beta T_2$ cells analysed by western analysis were derived from fully confluent cultures and hence were not undergoing rapid growth which may explain their detectable LH expression. During GnRH regimes cells were not plated at the same high density as $L\beta T_2$ cells tended to clump and detach from the culture surface easily and this may have been exaggerated by the repetitive liquid manipulations during this type of experiment. It is therefore likely that the reduced LHβ expression occurring as a result of high passage was

compounded by a cell density effect such that cells undergoing growth exhibited further reduction in LHβ expression. It may also be noted that expression of the LHβ subunit may be derived from only a few mRNA molecules due to the relatively long half-life of LHβ mRNA demonstrated to be approximately 44 hours (Bouamoud *et al.*, 1992). αGSU mRNA was detected in these cells and expression was clearly affected by application of 10nM GnRH displaying a biphasic response. Over the three day experiment a total of nine GnRH pulse were administered with maximal stimulation of αGSU mRNA levels occurring after the second day or six GnRH pulses. This result is in accord with observations made on αGSU mRNA abundance in αT3-1 cells treated with 100nM GnRH continuously for 1 to 120 hours. This study also demonstrated maximal stimulation after 24 and 48 hour exposure after which αGSU mRNA levels were reduced (Windle *et al.*, 1990). Reduction of the αGSU mRNA abundance to levels equivalent to those after day one suggests delayed negative regulation perhaps mediated by a specific regulatory protein. Assignment of this protein may be undertaken using differential display. It is important to recognise that the changes in αGSU mRNA levels were not investigated with regard to changes in free αGSU abundance. The aims of these studies were to investigate the secretion of LH so that changes in αGSU expression should be taken in this context. In the absence of detectable LH levels further investigation of αGSU expression was deemed inappropriate to the aims of the study. Future studies in which secreted LH may be detected will allow any effects of changes in αGSU expression to investigated.

The use of $L\beta T_2$ cells after reduced passage allowed the effect of application of a higher dose of GnRH to be investigated. The relatively high dose of 1μM GnRH on LH secretion provided evidence for delayed stimulation of the constitutive pathway. During administration of the 1μM GnRH pulses LH secretion appeared unchanged in comparison with untreated cells suggesting that this level of basal secretion was obtained by a constitutive pathway. The presence of a regulated pathway in these cells would have been observed by an increased release of LH in GnRH-stimulated cells in comparison to untreated cells (Turgeon *et al.*, 1996). The high level of GnRH repeatedly applied to the cells prevented accumulation of LH

intracellularly as evidenced by the lack of increased secretagogue-stimulated LH secretion. Furthermore intracellular LH was also reduced in cells treated with 1μM GnRH suggesting that untreated $L\beta T_2$ cells contain some LH within a releasable pool. This persistent basal level of LH secretion and reduction in intracellular abundance correlates with an *in vivo* study investigating the effects of continuous high-level application of GnRH to ewes and suggests a level of basal LH secretion independent of control by GnRH presumably occurring through a constitutive pathway (McNeilly *et al.*, 1991b). However a delayed effect of GnRH on this constitutive LH secretion was observed during the relatively long overnight incubations between the daily GnRH pulses. GnRH-treated cells displayed a significantly greater amount of LH release during the 17 hour periods in comparison to untreated cells. This low level LH secretion immediately following a series of high-level GnRH stimulation may represent an attempt to replenish the intracellular stores for future regulated secretory episodes. However due to the repeatedly high dose of GnRH applied, significant intracellular accumulation of LH may not occur. A transcriptional mechanism for regulation of constitutive LH secretion may exist. GnRH-R activation stimulates delayed PKC activity promoting the MAP-kinase pathway leading to formation of the AP-1 complex for which a binding site exists in the rLHβ promoter (Shupnik, 1996b; Naor *et al.*, 1998). The apparent 'leakage' of LH from GnRH-stimulated cells overnight must represent constitutive secretion in the absence of GnRH-induced Ca^{++} fluxes. However the delayed nature of PKC activation may account for the transcriptional effect of GnRH-R activation after a prolonged interval. The reasons why this LH is not immediately diverted from the constitutive to the regulated pathway so that stores may be replenished are uncertain. It is likely that a threshold level of constitutive LH secretion must be achieved in order to obtain sufficient LH to form storage granules. Indeed constitutive secretion has been shown to precede storage of LH in GH_3 cells (Bielinska *et al.*, 1994). As the initial characterisation of the $L\beta T_2$ cell line demonstrated efficient augmentation of LH stores during pulsatile administration of 10nM GnRH-R agonist (Turgeon *et al.*, 1996), it is likely that the 100-fold higher dose of GnRH stimulates a predominantly secretory response with a reduced but not

intracellularly evident by the lack of increased secretagogue-stimulated LH secretion. Furthermore intracellular LH was also reduced in cells treated with 1μM GnRH suggesting that untreated $L\beta T_2$ cells contain some LH within a releasable pool. This persistent basal level of LH secretion and reduction in intracellular abundance correlates with an *in vivo* study investigating the effects of continuous high-level application of GnRH to ewes and suggests a level of basal LH secretion independent of control by GnRH presumably occurring through a constitutive pathway (McNeilly *et al.*, 1991b). However a delayed effect of GnRH on this constitutive LH secretion was observed during the relatively long overnight incubations between the daily GnRH pulses. GnRH-treated cells displayed a significantly greater amount of LH release during the 17 hour periods in comparison to untreated cells. This low level LH secretion immediately following a series of high-level GnRH stimulation may represent an attempt to replenish the intracellular stores for future regulated secretory episodes. However due to the repeatedly high dose of GnRH applied, significant intracellular accumulation of LH may not occur.

A transcriptional mechanism for regulation of constitutive LH secretion may exist. GnRH-R activation stimulates delayed PKC activity promoting the MAP-kinase pathway leading to formation of the AP-1 complex for which a binding site exists in the rLHβ promoter (Shupnik, 1996b; Naor *et al.*, 1998). The apparent 'leakage' of LH from GnRH-stimulated cells overnight must represent constitutive secretion in the absence of GnRH-induced Ca^{++} fluxes. However the delayed nature of PKC activation may account for the transcriptional effect of GnRH-R activation after a prolonged interval. The reasons why this LH is not immediately diverted from the constitutive to the regulated pathway so that stores may be replenished are uncertain. It is likely that a threshold level of constitutive LH secretion must be achieved in order to obtain sufficient LH to form storage granules. Indeed constitutive secretion has been shown to precede storage of LH in GH_3 cells (Bielinska *et al.*, 1994). As the initial characterisation of the $L\beta T_2$ cell line demonstrated efficient augmentation of LH stores during pulsatile administration of 10nM GnRH-R agonist (Turgeon *et al.*, 1996), it is likely that the 100-fold higher dose of GnRH stimulates a predominantly secretory response with a reduced but not

abolished effect upon LHβ transcription thus preventing sufficient intracellular accumulation of LH to form a regulated pathway. Recent use of antisense molecules directed at Rab3B have demonstrated its importance in both regulated and constitutive secretion form gonadotrophs (Tasaka *et al.*, 1998). Similar application of this technique to $L\beta T_2$ cells chronically treated with GnRH may prevent release of low levels of LH leading to intracellular accumulation. Ultrastructural examination of these cells may determine the threshold of LH required to form the dense-core secretory granules representative of the regulated pathway.

Transfection of $L\beta T_2$ cells was only achieved using passage numbers in excess of 55 reflecting an increase in adhesion and rate of proliferation. Without this beneficial side of passage-induced change no data on oFSH expression would have been obtained. FSHβ dimerisation with endogenous αGSU or that derived from expression of poαGSU resulted in secretion of FSH. However significant differences in storage profiles between cells expressing the ovine and inter-species molecule suggests preferential retention of the inter-species FSH heterodimer. This data is particularly interesting in light of studies carried out on oLHβ/oFSHβ transgenic mice that overexpress the oFSHβ gene (P.Brown - in press) and therefore also form an inter-species FSH heterodimer (see chapter 7). Overexpression of the oFSHβ gene increased intracellular levels of FSH to four times the level of mFSH. This inter-species FSH heterodimer did not appear significantly different in size when compared to the endogenous mFSH molecule suggesting that differential glycosylation did not play a role in this phenomenon. Analysis of the colocalisation of LH and FSH in this transgenic model suggests that overexpression of oFSHβ leads to increased colocalisation of the gonadotrophins within peripheral areas of the gonadotroph normally exclusive to LH (see chapter 7). These data suggest that storage of the inter-species FSH molecule occurs both *in vitro* and *in vivo* and that this may occur more efficiently than storage of oFSHαβ *in vitro*. The mechanisms by which this occurs remain to be determined but they may involve slower intracellular transit time of the inter-species heterodimer due to less efficient dimerisation which predisposes FSH to sorting into the regulated pathway. A reduced rate of dimerisation

between subunits of LH in comparison to those of CG has been demonstrated and may represent a possible mechanism for the more efficient storage of LH in transfected GH_3 cells (Muyan *et al.*, 1996). Dimerisation of FSH has been reported to occur at a rapid rate similar to that of CG *in vitro* (Matzuk *et al.*, 1989). However the studies detailed in this thesis have been carried out using the oFSHβ gene without its native 3' UT region which allows higher FSH expression (Mountford *et al.*, 1992). It is likely that cells with basal levels of αGSU expression form the FSHαβ less efficiently than cells which have been cotransfected with the poαGSU expression construct and therefore express αGSU levels equivalent to those of oFSHβ. Furthermore although cells transfected with only the poFSHβg construct may express significantly lower amounts of FSH dimer, individual cells may express much higher amounts of the oFSHβ subunit due to its exclusivity within the transfection mixture. In these cells the oFSHβ subunit may have been more likely to exceed the abundance of endogenous dimerisation rate-limiting αGSU thus decreasing the amount of FSH dimer formed. However this 'loitering' of the oFSHβ subunit within the ER and *trans*-Golgi network (TGN) may potentiate sorting of the FSHαβ dimer to the regulated pathway.

Further analysis of transient oFSH expression in $L\beta T_2$ cells revealed that the construct containing the oFSHβ cDNA resulted in significantly greater expression levels than those obtained with the genomic clone. This difference may have arisen due to the presence of intronic regulatory sequences although these have yet to be characterised. In light of the differences in level of expression the greater proportion of oFSH stored in cells transfected with the cDNA construct in comparison to the genomic construct suggests that aggregation may be caused by high level expression and lead to increased storage. These results are not definitive as further investigation must be carried out to assess whether an intracellular pool does exist and whether it is releasable under secretagogue stimulation. These results contrast with similar experiments carried out on Chinese Hamster ovary (CHO) cells (see chapter 5) which demonstrated reduced oFSH storage in cells transfected with the αGSU and oFSHβ genomic clone despite higher expression than that obtained with

the cDNA construct. CHO cells unlike $L\beta T_2$ cells do not endogenously express granins and therefore may not benefit from their aggregative properties which may promote sorting of abundant gonadotrophins to a regulated pathway.

Expression of the EGFPC-oFSHβ fusion protein was not detectable by oFSH RIA in the lysates or media of transfected cells presumably due to masking of the epitope. This was also the case for transiently transfected CHO cells (see chapter 5) suggesting that this effect was not cell-specific. Confocal analysis of transiently transfected $L\beta T_2$ cells demonstrated that the fusion protein had been packaged into discrete intracellular bodies of comparable size to regulated secretory granules. It is not clear from these analyses whether the intracellular bodies indeed represent FSH within the regulated pathway *in vitro*. Observation of EGFPC-oFSHβ fluorescence in living cells demonstrated rapid movement of the putative vesicles. Furthermore these vesicles exhibited the apparently random movement previously associated with microtubule-dependent transport of fluorescently-tagged CgA in Vero cells (Wacker *et al.*, 1997). This suggests that the EGFPC-oFSHβ subunit had dimerised with αGSU as no reports of free β-subunit packaging exist. In the gonadotrophs of castrated rats where β-subunits abundance is greater than that of the αGSU, the former are retained in the endoplasmic reticulum (ER) and eventually degraded (Bassetti *et al.*, 1995). It is therefore likely that free EGFPC-oFSHβ would also be retained in the ER if dimerisation did not occur and that this would eventually be followed by lysosomal breakdown.

Real-time observation of secretagogue-stimulated release of these vesicles will require a perfusion chamber accessory for the confocal microscope. This may allow verification that these fluorescent bodies do indeed represent granules of the regulated pathway. Observation of two fluorescent protein fusions in the same cell may be possible using the enhanced yellow fluorescent protein (EYFP) which has different excitation and emission spectra to EGFP. Expression of both gonadotrophin β-subunits each labelled with a different fluorophore may allow real-time observation of the differential sorting of LH and FSH.

Similar experiments undertaken using CHO cells (see chapter 5) have also demonstrated vesicle formation with similar characteristics. This is surprising due to the assumed lack of molecular machinery required for regulated pathway formation. There are at least two scenarios that may explain these findings. The first is that the fluorescent vesicles present in both transiently transfected CHO and $L\beta T_2$ cells represent the constitutive secretory pathway. This may be verified by stimulation of transfected cells with a suitable secretagogue during real-time observation. The second is that the presence of EGFP stabilises the gonadotrophin dimer which allows preferential self-aggregation independently of more conventional granin mediated means. Future experiments may benefit from novel destabilised EGFP variants (Clontech, USA) which may contribute less structural stability to the β-subunit structure and therefore reduce the opportunity for self-aggregation.

These studies have demonstrated the complexity of the $L\beta T_2$ cell line. Although initially shown to express LH in a regulated manner (Turgeon *et al.*, 1996), these studies have been hampered by the apparent transient nature of LHβ expression. This basal level of LHβ expression appeared to decrease after repeated passage in culture. Furthermore the coincidental decrease in intact CgA abundance intracellularly appeared to reduce the storage ability of the cells.

Two important responses to pulsatile GnRH administration have been demonstrated. Firstly, that in accordance with observed effects in the αT3-1 cell line (Windle *et al.*, 1990), αGSU mRNA abundance peaks after 48 hours of stimulation with 10nM GnRH and falls thereafter. Perhaps more relevant to this thesis is the observation of a persistent level of basal LH secretion similar to that observed in ewes (McNeilly *et al.*, 1991b) which may be transcriptionally upregulated in a delayed fashion after pulsatile administration of a higher 1μM GnRH dose. This effect appeared after one day (4 pulses) of GnRH treatment and was maintained over a three day period. This increased expression of LH was not sufficient to enter the regulated pathway suggesting that a threshold for regulated secretion may occur. This is particularly important as it suggests a mechanism whereby low level expression of gonadotrophins such as FSH may result in

constitutive secretion despite similar protein structure to LH which is secreted primarily but not exclusively via the regulated pathway.

Transient transfection studies also revealed data regarding expression of oFSH in the $L\beta T_2$ cell line. High expression of the oFSH subunits leads to a significantly greater proportion of oFSH remaining intracellularly after 48-72 hours suggesting that in granin-expressing $L\beta T_2$ cells a concentration-dependent sorting mechanism may exist. Furthermore the observed decrease in intact CgA abundance intracellularly may account for the reduction in oFSH storage observed during experiments carried out on cells after different lengths of passage.

Overall the findings of these studies have strengthened the hypothesis that differential sorting of gonadotrophins occurs due to differences in their intracellular abundance thus influencing their aggregation which is mediated by granins, particularly CgA.

Chapter Seven

Gonadotrophins and Granins in Murine Gonadotrophs

7.1 Introduction

Studies covered previously within this thesis have been undertaken completely *in vitro*. As a means of comparison, investigation of gonadotrophin expression in mouse pituitaries will be carried out. Although predominantly ovine and bovine genes were used during *in vitro* investigations, murine tissue will be used for two reasons. Firstly, murine tissue is readily available and easily obtained. Secondly and more importantly, a transgenic mouse model relevant to these studies has been engineered (P.Brown *et al* - paper submitted).

The transgenic mouse developed by Brown *et al* contains the oFSHβ gene under control of the oLHβ promoter. Furthermore to counteract the negative posttranscriptional regulation of the oFSHβ mRNA the 3' UT of the molecule was replaced with the HSV-IE polyadenylation signal. The objective of this oLHβ/oFSHβ construct was to drive high level expression of oFSHβ comparable to that of oLHβ exclusively in gonadotrophs. This construct is similar to the oFSHβ expression construct poFSHβg used in the previous chapters (see section 3.2.3) except that the plasmid construct directs oFSHβ via the CMV promoter instead of the oLHβ sequence. Comparison of expression by these essentially similar constructs *in vitro* and *in vivo* may yield important data regarding the intracellular trafficking of FSH in these systems.

Use of *in vivo* models to study complex interaction of intracellular molecules has the advantage of presenting a functional system complete with all the necessary molecular machinery. Previously described use of cell lines (chapters 4, 5, and 6) has required additional gene expression in order to create a model equivalent to the *in vivo* gonadotroph. Although such an approach may be useful in assigning roles to individual proteins, it may not allow the study of interactions between many proteins in the presence of as yet uncharacterised factors. For this reason analysis of *in vivo* murine gonadotrophs will be undertaken.

The use of confocal microscopy has already been demonstrated in this thesis as a powerful tool for dissection of intracellular interactions. Stereological aspects of pituitary gland anatomy with respect to spatial

orientation of gonadotrophs and their close relationship with lactotrophs requires extensive serial sectioning of pituitary tissue. Confocal microscopy obviates the need for preparation of 5μm sections due to the ability to 'filter out' fluorescence from tissue above and below the optical plane (figure 2.6.3a). This characteristic allows observation of relatively thick sections and compilation of a series of images by optical sectioning. The studies described in this chapter will include confocal analyses of gonadotrophin and granin expression in the murine pituitary gland. Analysis of the oLHβ/oFSHβ transgenic model will also be carried out with regard to the level of FSH expression intracellularly and its subcellular localisation.

7.2 Methods

7.2.1 Extraction of Pituitary Glands

All animal manipulations were undertaken by Judith McNeilly and Pamela Brown. Pituitaries were removed from adult male non-transgenic and oLHβ/oFSHβ transgenic mice immediately *post-mortem* after being killed by a Home Office Schedule 1 procedure using CO_2. The pituitary glands were then either placed in Bouins fixative (see Appendix I) for confocal analyses or stored in liquid nitrogen.

7.2.2 Observation of Pituitaries by Indirect Immunofluorescence

Essentially indirect immunofluorescence using intact pituitaries from adult mice was performed as described for cell lines with some modifications. Samples were maintained in an intact form and not mounted until after all antisera and washes had been carried out. Antisera applications and PBS washes were undertaken in microcentrifuge tubes. Due to the intact structure of the pituitary gland all incubations of antisera and PBS washes were extended so as to obtain maximal penetration of the tissue. The method used was a modification of that described by Thomas & Clarke (Thomas & Clarke, 1997). Incubation in Bouins fixative

was extended to 5 hours after which tissue was stored at room temperature in 70% ethanol. Rehydration of tissue was carried out by sequential washing in 50% and 25% ethanol followed by PBS (Sigma-Aldrich, UK) with each stage lasting approximately 1 hour. Permeabilisation and blocking were carried out simultaneously in PBS containing 1% BSA (Sigma-Aldrich, UK) and 10% normal Goat serum (SAPU, UK) with 0.3% Triton X-100 (Sigma-Aldrich, UK) for 24 hours at 4°C with gentle agitation. Addition of primary antisera was followed by incubation in the same conditions for a further 72 hours. LH was detected using the monoclonal bLH 518B7 antisera (J.Rosen, USA) diluted to 5µg/ml. FSH was detected using the polyclonal M91 antisera (A.S.McNeilly, MRC CRB) at a 1:200 dilution whereas CgA antisera (R.Fischer-Colbrie, Austria) was diluted to 1:1000. After extended PBS washes secondary antisera diluted 1:20 in blocking/ permeabilising buffer were added and incubated for 24 hours at 4°C with gentle agitation. After washing the samples were sectioned by hand using a razor blade and dissecting microscope. Thick sections of between 0.5 and 1.5 mm were mounted in Citifluor (UKC, UK) using Easiseal adhesive chambers (Hybaid, UK) and glass coverslips. Slides were then viewed immediately by confocal microscopy or stored in the dark at 4°C until later visualisation.

Comparison of levels of FSH expression in negative and positive transgenic pituitaries was undertaken using LH as a reference. Signal detected for FSH in negative mice was adjusted using the amplification settings within the LSM510 module software (Zeiss, UK) to match that of LH. Positive pituitaries were then analysed while maintaining these settings so that any changes in FSH abundance could be related to that of LH.

7.2.3 Western Analysis of Pituitary Extracts

Pituitaries stored in liquid nitrogen were removed and thawed at room temperature. The tissue was then homogenised in 100mM sodium carbonate containing Complete™ protease inhibitor (Boehringer Mannheim, UK) using a mini-pestle (Kontes, USA) and microcentrifuge tube.

Electrophoresis under non-denaturing conditions (as described in section 2.5.7) was undertaken using either 10 or 20µg total protein (determined by Bradford assay - see section 2.5.2) per lane in a 5% stacking and either a 7.5% or 10% resolving gel. Non-denatured marker proteins (Sigma-Aldrich, UK) also run on the gel were separately stained using 0.1% Amido black in 20% ethanol and 7% acetic acid. Detection of the transferred proteins from pituitary samples was undertaken using the ECF kit (Amersham, UK) in accordance with the manufacturers guidelines. Primary antisera was used at the following dilutions. bLH518B7 (J.Rosen, USA) was diluted to 1µg/ml, M91 (A.S.McNeilly, MRC CRB) was used at a 1:1000 dilution and hSgII antisera (C-19; Santa Cruz Biotechnologies, USA) was diluted to 0.5µg/ml. Detection of the fluorescent signal produced by the conjugated secondary antisera was carried out using a STORM$^{T\ M}$ PhosphorImager (Molecular Dynamics, UK) on blue fluorescence mode in accordance with the manufacturers guidelines.

7.3 Results

7.3.1 Gonadotrophins and Granins in Normal Gonadotrophs

Preparation of whole pituitary glands from male mice for indirect immunofluorescence showed excellent penetration of the tissue by the antisera providing detectable signal throughout the tissue. Furthermore the appearance of pituitary cells appeared undamaged in comparison to semi-thick sections (data not shown). Complete preservation of blood vessels and cells throughout the gland allowed their close relationship with gonadotrophs to be observed.

Gonadotrophs identified by immunoreactivity for LH appeared either alone or in clusters of 2-3 cells. All gonadotrophs appeared to be bihormonal as FSH immunoreactivity showed a high degree of colocalisation with that of LH. No monohormonal cells were observed although the ratio of LH to FSH did not appear identical in all gonadotrophs (figures 7.3.1a, b & c and movie 7.3.1d). Many gonadotrophs were demonstrated to exist juxtaposed to blood vessels (figures 7.3.1e and 7.3.1h). The divergent subcellular localisation of LH and FSH is suggested by the

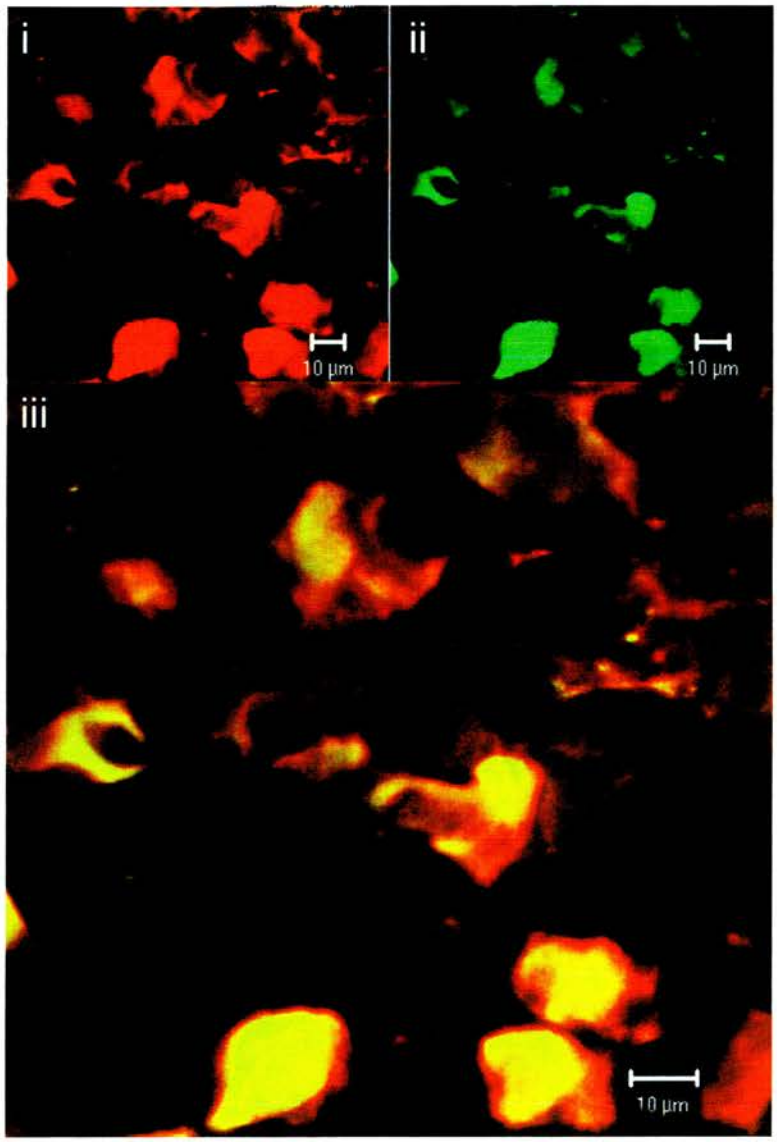

Figure 7.3.1a: Projection of LH and FSH immunoreactivity in a 12.8µm series of optical sections through a murine pituitary gland.

LH immunoreactivity (i) is shown in red and FSH immunoreactivity (ii) in green. The overlaid images (iii) demonstrate that peripheral areas of gonadotrophs contain LH immunoreactivity exclusively. Colocalisation of LH and FSH (yellow) occurs in the central cytoplasmic areas of the gonadotrophs. This image was compiled from 21 optical sections of a pituitary tissue slice approximately 1-2mm thick. LH antisera (518B7) was used at 5µg/ml and FSH antisera (M91) diluted 1:200. Secondary TRITC and FITC conjugates were diluted 1:20. TRITC and FITC fluorescence were observed using 543nm HeNe and 488nm argon lasers with 585nm longpass and 505-535nm bandpass filters respectively.

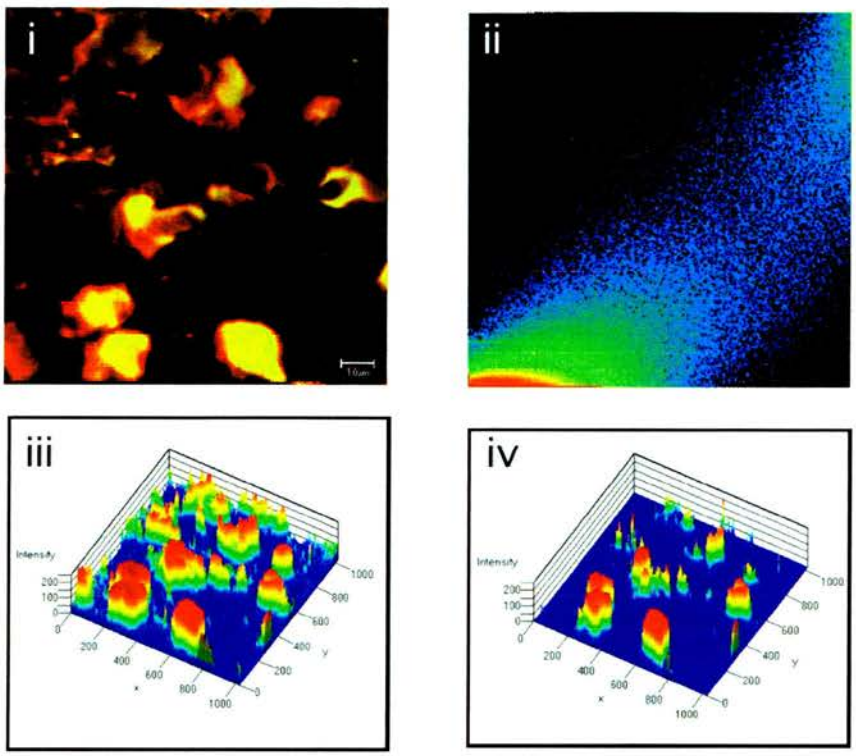

Figure 7.3.1b: Colocalisation of LH and FSH immunoreactivity in a 12 8μm optical section through a murine pituitary gland.

i) Overlay of LH immunoreactivity (red) and FSH immunoreactivity (green) demonstrate that peripheral areas of gonadotrophs contain LH immunoreactivity exclusively. Colocalisation of LH and FSH (yellow) occurs in the central cytoplasmic areas of the gonadotrophs. This image was compiled from 21 optical sections of a pituitary tissue slice approximately 1-2mm thick. LH antisera (518B7) was used at 5μg/ml and FSH antisera (M91) diluted 1:200. Secondary TRITC and FITC conjugates were diluted 1:20. TRITC and FITC fluorescence were observed using 543nm HeNe and 488nm argon lasers with 585nm longpass and 505-535nm bandpass filters respectively.
ii) Colocalisation of pixels from LH-and FSH-immunoreactivity. Overlay of identical images would produce a red 45º line from the bottom left hand corner of the graph. The thickness of the 45º line containing predominantly blue pixels indicates that LH and FSH show moderate colocalisation.
iii) Intense (red) LH-immunoreactivity appears distributed over a larger area of the gonadotrophs than FSH-immunoreactivity (iv) depsite similar levels of maximal fluorescence (artificially adjusted). This demonstrates that the absence of FSH-immunoreactivity at the periphery of the gonadotroph is not due to a lower level of maximal fluorescent intensity.

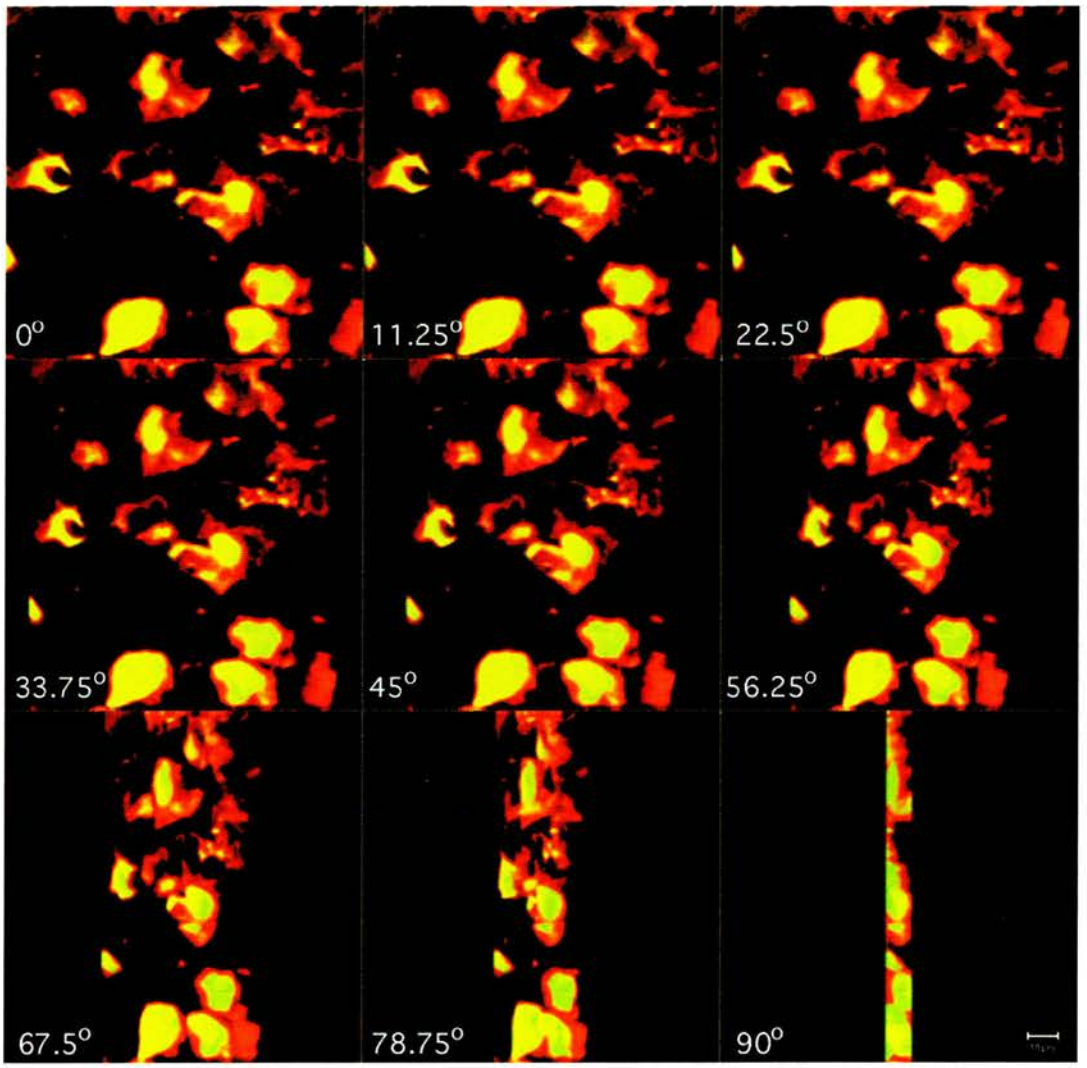

Figure 7.3.1c: Rotation of a Z-scan projection of LH and FSH immunoreactivity in murine gonadotrophs.

Colocalisation of LH (red) and FSH (green) immunoreactivity is depicted by yellow. All gonadotrophs contain peripheral LH immunoreactivity with FSH colocalised within more central regions of the cells. The 12.8μm thick projected image was derived from 21 serial optical sections. This image was obtained from a pituitary tissue slice approximately 1-2mm thick. LH antisera (518B7) was used at 5μg/ml and FSH antisera (M91) diluted 1:200. Secondary TRITC and FITC conjugates were diluted 1:20. TRITC and FITC fluorescence were observed using 543nm HeNe and 488nm argon lasers with 585nm longpass and 505-535nm bandpass filters respectively. Bar = 10μm.

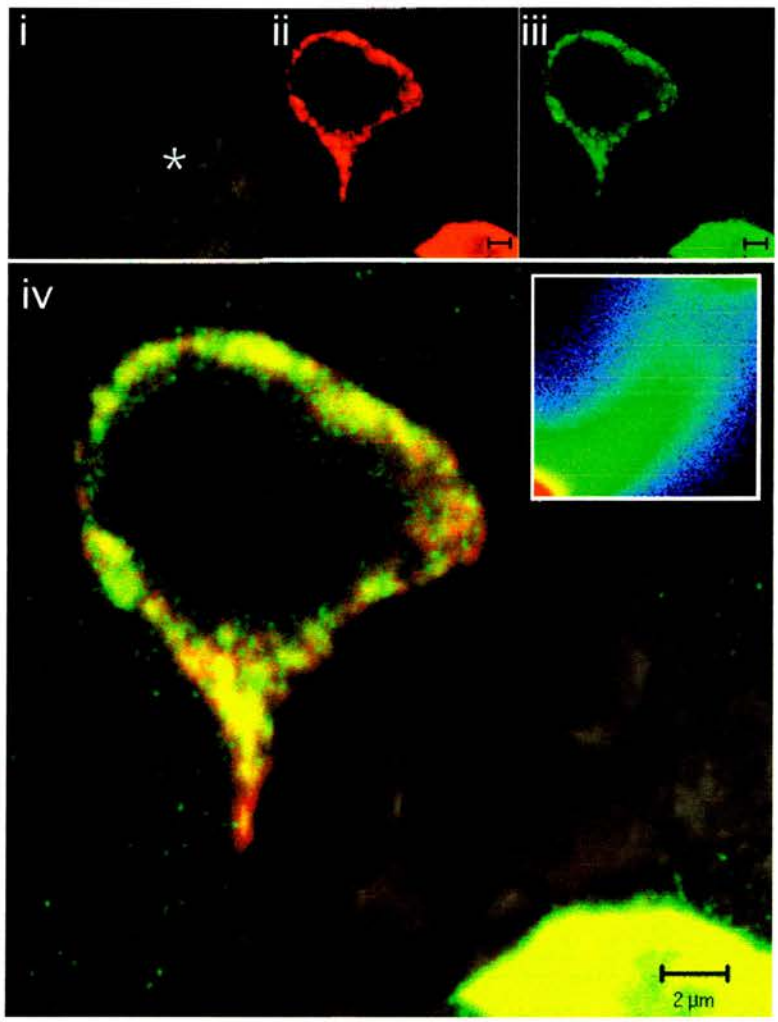

Figure 7.3.1e: LH and FSH immunoreactivity in a gonadotroph juxtaposed to a capillary.

Panels (i)-(iii) contain the phase contrast, TRITC (LH) and FITC (FSH) images respectively. When overlaid these images produce the composite image depicted in panel (iv). The close association of the gonadotroph with the blood vessel (marked '*' in panel (i)) is clearly depicted. The inset of panel (iv) shows the degree of colocalisation exhibited by LH and FSH. The thickness of the 45º line containing predominantly blue pixels indicates that LH and FSH show moderate colocalisation. Overlay of identical images would produce a red 45º line from the bottom left hand corner of the graph. This image was obtained from a pituitary tissue slice approximately 1-2mm thick. LH antisera (518B7) was used at 5µg/ml and FSH antisera (M91) diluted 1:200. Secondary TRITC and FITC conjugates were diluted 1:20. TRITC and FITC fluorescence were observed using 543nm HeNe and 488nm argon lasers with 585nm longpass and 505-535nm bandpass filters respectively.

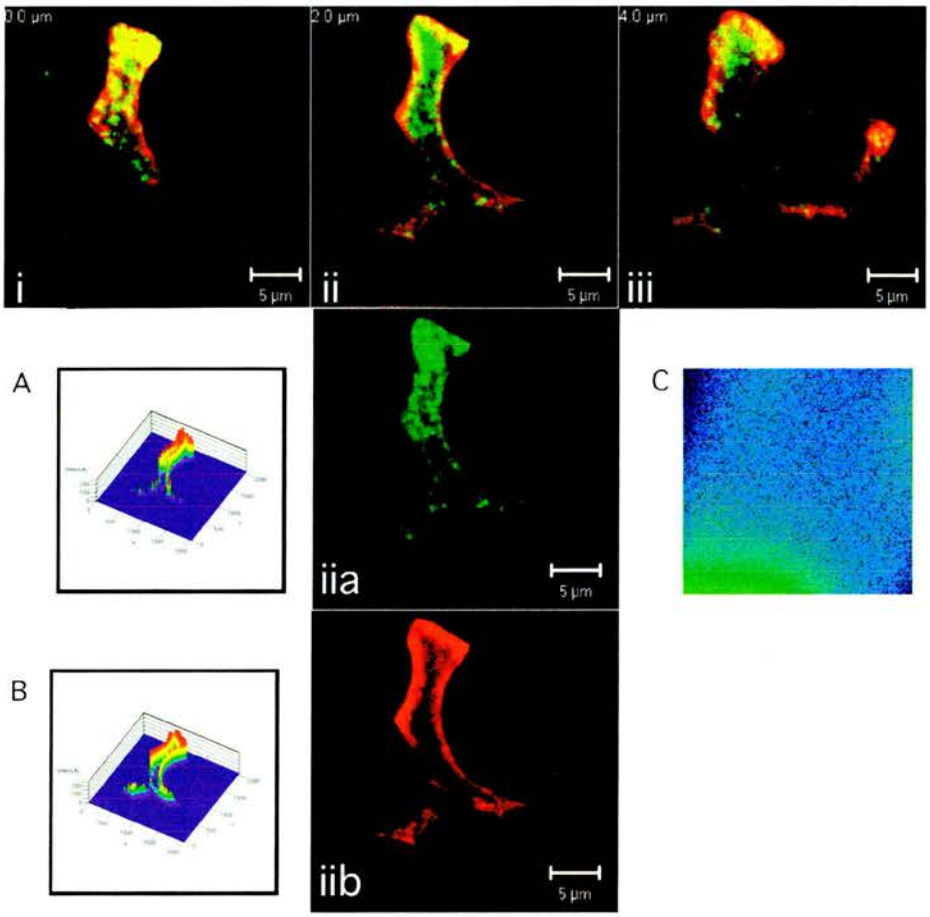

Figure 7.3.1f: Z-scan of a murine gonadotroph showing a semi-divergent subcellular distribution of LH and FSH.

Images (i)-(iii) show dual indirect immunofluorescence of LH (red) and FSH (green) in optical sections of an intact gonadotroph taken at 2µm intervals. Image (ii) is split to show the individual levels of FSH (iia) and LH (iib). These images are also represented graphically in panels 'A' and 'B'. LH immunoreactivity is clearly at the periphery of the gonadotroph whereas FSH immunoreactivity appears predominantly in the central cytoplasmic areas. Some LH immunoreactivity is also present in the peri-nuclear area. The semi-divergent nature of LH and FSH immunoreactivity is depicted in the pixel distribution graph (C) which shows no clear 45º line from the bottom left corner which would indicate colocalisation. However the two antigens are not completely segregated as this would be represented by an absence of pixels in the centre of the graph. This image was obtained from a pituitary tissue slice approximately 1-2mm thick. LH antisera (518B7) was used at 5µg/ml and FSH antisera (M91) diluted 1:200. Secondary TRITC and FITC conjugates were diluted 1:20. TRITC and FITC fluorescence were observed using 543nm HeNe and 488nm argon lasers with 585nm longpass and 505-535nm bandpass filters respectively.

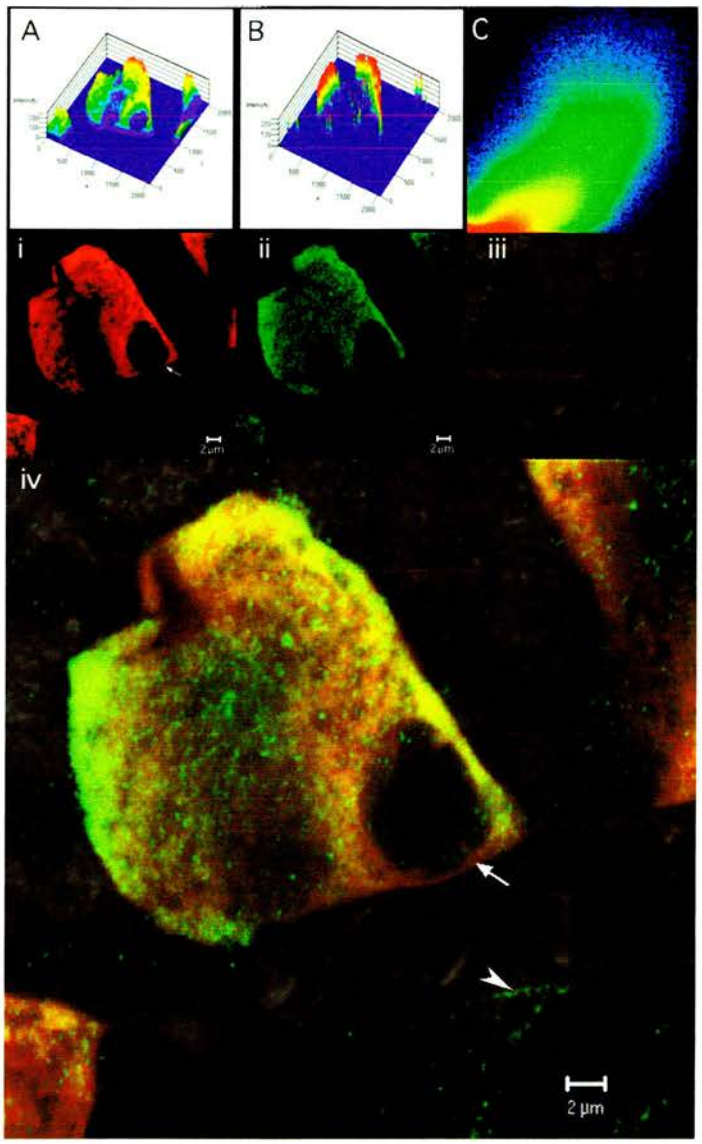

Figure 7.3.1g: LH and CgA immunoreactivity in a gonadotroph juxtaposed to a capillary.

Panels (i)-(iii) contain the TRITC (LH) and FITC (CgA) and phase contrast images respectively. When overlaid these images produce the composite image depicted in panel (iv). Panels 'A' and 'B' show the intensity of TRITC and FITC fluorescence. Panel 'C' shows the colocalisation of pixels for LH and CgA. LH immunoreactivity appears throughout the cytoplasm of the gonadotroph but particularly concentrated towards the plasma membrane. CgA shows distribution within the gonadotroph similar to that of LH but with less intense fluorescence in the central cytoplasmic regions. CgA-immunoreactivity is absent from the plasma membrane region proximal to the blood vessel whereas LH-immunoreactivity remains (arrow). LH and CgA exhibit colocalisation as depicted by the intensity of pixel distribution within panel 'C'. In addition an outer area of lower colocalisation is apparent by the blue pixels in the graph (overlay of identical images would produce a red 45º line from the bottom left hand corner of the graph). Weak CgA-immunoreactivity is also present within the cell opposite the gonadotrophs (arrowhead). This image was obtained from a pituitary tissue slice approximately 1-2mm thick. LH antisera (518B7) was used at 5µg/ml and CgA antisera was diluted 1:1000. Secondary TRITC and FITC conjugates were diluted 1:20. TRITC and FITC fluorescence were observed using 543nm HeNe and 488nm argon lasers with 585nm longpass and 505-535nm bandpass filters respectively.

red halo appearance of LH immunoreactivity when superimposed with FSH immunoreactivity and by the difference in distribution of immunoreactivity despite similar fluorescent intensity (figure 7.3.1b). The pixel distribution diagram shown in the inset of figure 7.3.1b indicates that FSH and LH show moderate colocalisation. In a series of higher magnification optical sections taken at 2μm intervals LH immunoreactivity can clearly be seen to exist at the periphery whereas FSH is confined to more central areas of the gonadotroph cytoplasm (figure 7.3.1f). Colocalisation of LH and FSH is demonstrated by the pixel distribution diagram which indicates a semi-divergent relationship within this gonadotroph.

CgA immunoreactivity also appeared to occur in gonadotrophs although some faint staining was also observed in neighbouring cells, presumably lactotrophs (figure 7.3.1h). Examination of the subcellular localisation of LH and CgA revealed that although CgA immunoreactivity appeared throughout the cytoplasm, it was particularly concentrated at the periphery of the gonadotroph with LH. This relationship appeared conserved around the gonadotroph plasma membrane except at the interface between the cell and blood vessel (figure 7.3.1h). In this region of the gonadotroph LH immunoreactivity predominates with a complete absence of CgA. The pixel distribution diagram in figure 7.3.1h indicates that the majority of LH and CgA immunoreactivity is colocalised (yellow and green pixels). However the halo of blue pixels indicates a lesser degree of divergence between these two proteins.

7.3.2 Gonadotrophins and Granins in Gonadotrophs of Transgenic Mice

Pituitaries from positive male oLHβ/oFSHβ transgenic mice were analysed by indirect immunofluorescence with regard to their expression of oFSHβ (figure 7.3.2a). Initial observation of FSH immunoreactivity demonstrated that it was localised exclusively to gonadotrophs as in negative mice. FSH levels in gonadotrophs from negative mice were compared to those of positive mice using the same pinhole, laser power and amplification settings. Whereas LH and FSH levels were adjusted to appear equivalent in

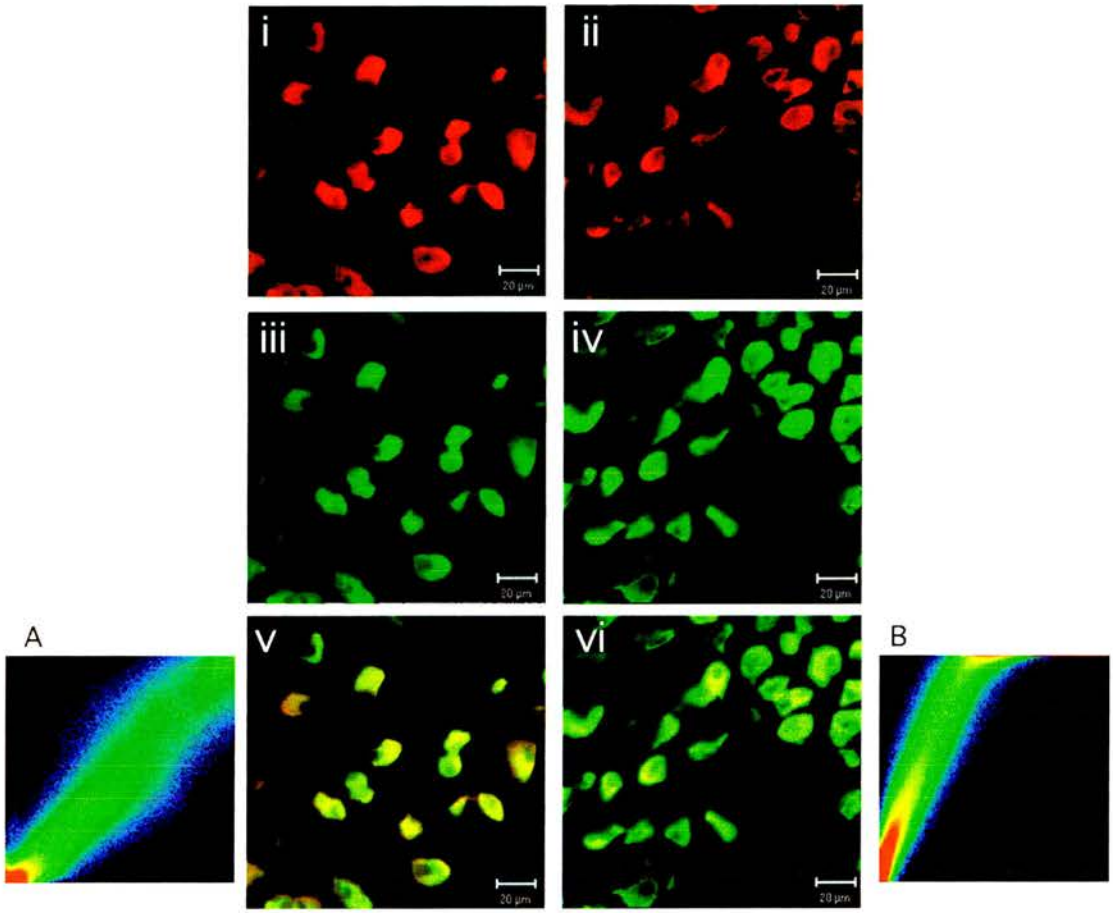

Figure 7.3.2a: Dual indirect immunofluorescence for LH and FSH in non-transgenic and oLHβ/oFSHβ transgenic mouse pituitary glands.

Panels (i) and (ii) depict LH immunoreactivity in non-transgenic and oLHβ/oFSHβ transgenic gonadotrophs respectively. The levels of LH appear similar in both samples. FSH immunoreactivity is depicted for non-transgenic and transgenic pituitary glands in panels (iii) and (iv) respectively. FSH abundance appears greater in the oLHβ/oFSHβ transgenic model compared to the gonadotrophs of non-trangenic mice. The overlaid LH and FSH images for the non-trangenic and oLHβ/oFSHβ transgenic mice are shown in panels (v) and (vi) respectively. The red halo of LH immunoreactivity predominant in non-transgenic gonadotrophs is absent from all oLHβ/oFSHβ transgenic gonadotrophs. The effect of increased FSH expression in the transgenic model is also depicted by the pixel distribution graphs for non-transgenic (A) and oLHβ/oFSHβ transgenic (B) gonadotrophs. LH and FSH exhibit moderate colocalisation in non-transgenic gonadotrophs indicated by the relatively thick 45º line in 'A'. The level of colocalisation in the transgenic model appears increased as evident by the comparatively narrow and more intense pixel distribution. The angle of this line is also increased in the transgenic model reflecting the greater abundance of FSH immunoreactivity in comparison to that of LH.
This image was obtained from a pituitary tissue slice approximately 1-2mm thick. LH antisera (518B7) was used at 5μg/ml and FSH antisera (M91) diluted 1:200. Secondary TRITC and FITC conjugates were diluted 1:20. TRITC and FITC fluorescence were observed using 543nm HeNe and 488nm argon lasers with 585nm longpass and 505-535nm bandpass filters respectively.

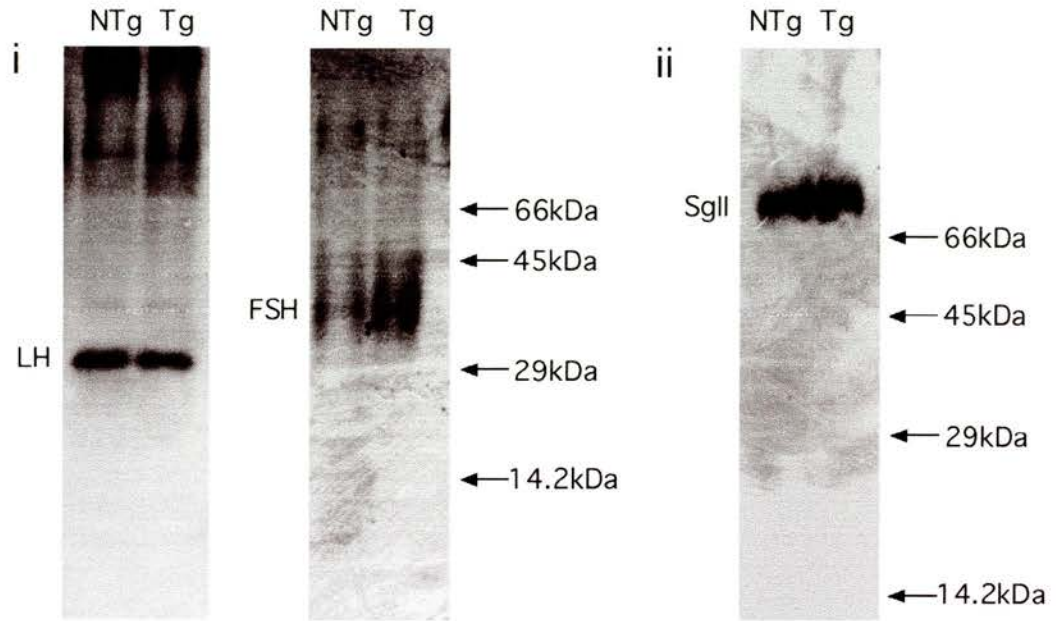

Figure 7.3.2b: Comparison of LH, FSH and SgII expression in the pituitary glands of non-transgenic and oLHβ/oFSHβ transgenic mice by PAGE under non-denaturing conditions.

i) LH was detected using monoclonal primary antisera (518B7) at 1μg/ml. The LH dimer is present at approximately 29kDa in accordance with its predicted molecular mass. No significant difference in size or abundance of LH was apparent between the non-transgenic (NTg) and transgenic (Tg) samples. FSH was detected using the polyclonal M91 primary antisera diluted 1:1000. The FSH dimer is present at approximately 35kDa in both NTg and Tg pituitary samples.
FSH appears 4-fold more abundant in the Tg sample. Both 10% acrylamide gels were loaded with 20μg total protein per lane. ii) SgII was detected using monoclonal hSgII antisera (C-19) at 0.5μg/ml. A single band was present in both NTg and Tg samples which corresponded to approximately 75kDa. The Tg sample contained approximately 2-fold greater SgII than the NTg sample. 10μg total protein was loaded per lane. The resolving gel contained 7.5% acrylamide. Fluorescent conjugates of secondary antisera (components of the ECF kit) were detected and quantified using a STORM PhosphorImager.

negative mice, FSH exhibited greater abundance over LH in transgenic gonadotrophs and therefore over levels of FSH in normal gonadotrophs. This is indicated by the differences between the pixel distribution diagrams from non-transgenic and oLHβ/oFSHβ transgenic mice. In tissue from non-transgenic mice where the fluorescent intensities from LH and FSH immunoreactivity were adjusted to similar levels, the pixel distribution forms a 45° line. In transgenic tissue the pixel distribution forms a much steeper line reflecting an approximate 2-fold excess of signal from the FSH (FITC) channel over the LH (TRITC) channel. In addition the colocalisation of LH and FSH in the oLHβ/oFSHβ gonadotrophs also appears altered. This is indicated by the comparatively narrow distribution of pixels in the image from the transgenic pituitary compared to that of the non-transgenic pituitary (figure 7.3.2a).

Pituitary content of LH, FSH and SgII were also compared in normal and transgenic mice by Western analysis after PAGE under non-denaturing conditions (figure 7.3.2b). Quantification of the fluorescent signal from each LH band (figure 7.3.2c) shows that LH levels appear essentially unchanged between normal and transgenic male pituitaries.

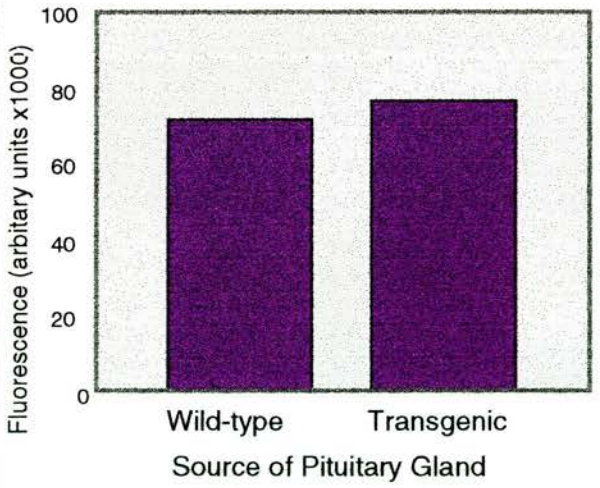

Figure 7.3.2c: Abundance of LH in normal and transgenic mouse pituitary glands.
Protein was extracted from pituitaries of adult male mice and 20μg separated by PAGE under non-denaturing conditions. LH abundance was determined using the ECF kit (Amersham, UK) and a STORM™ PhosphorImager.

However the abundance of total FSH in pituitary tissue derived from oLHβ/oFSHβ transgenic mice appears approximately 3.8-fold greater than

in negative mice (figure 7.3.2d). This level of increase is twice as large as that observed by confocal microscopy. It is also important to note that formation of the inter-species FSH molecule containing oFSHβ and mαGSU results in a heterodimer of equivalent size to that of the endogenous mFSH (figure 7.3.2d).

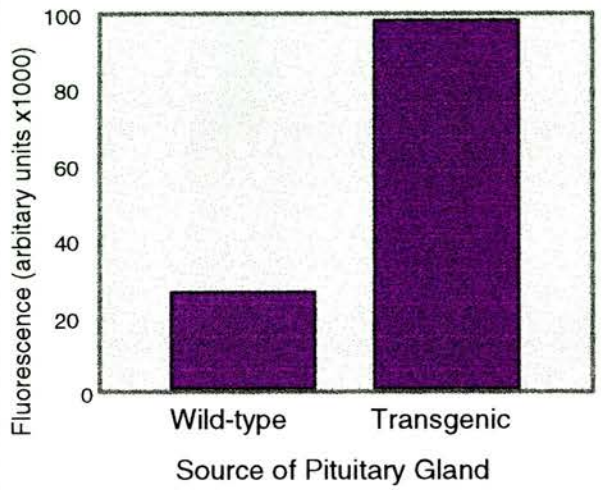

Figure 7.3.2d: Abundance of FSH in normal and transgenic mouse pituitary glands.

Protein was extracted from pituitaries of adult male mice and 20μg separated by PAGE under non-denaturing conditions. FSH abundance was determined using the ECF kit (Amersham, UK) and a STORM™ PhosphorImager.

The lack of significant change in LH levels was expected as was the increased levels of FSH. However unexpectedly quantification of the abundance of SgII revealed an approximate 1.7-fold increase in abundance of this granin in transgenic pituitaries compared to normal pituitaries (figure 7.3.2e).

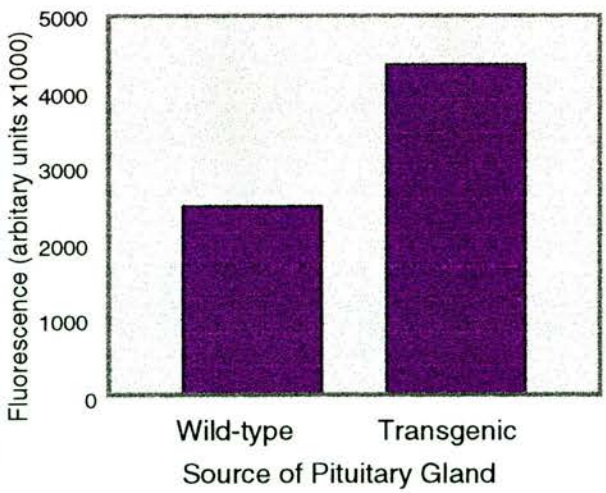

Figure 7.3.2e: Abundance of Secretogranin II in normal and transgenic mouse pituitary glands.

Protein was extracted from pituitaries of adult male mice and 10μg separated by PAGE under non-denaturing conditions. SgII abundance was determined using the ECF kit (Amersham, UK) and a STORM™ PhosphorImager.

7.4 Discussion

The presence of entirely bihormonal gonadotrophs in both wild-type male mice and oLHβ/oFSHβ transgenic male mice suggests that overexpression of oFSHβ under control of the oLHβ promoter exhibited complete gonadotroph specificity. The tissue specificity of the oLHβ promoter has previously been demonstrated using a CAT reporter in transgenic mice (Brown *et al.*, 1993). The close association of gonadotrophs with capillaries was demonstrated for the majority of gonadotrophs despite limitation of phase contrast image collection to the cut surface. This association has obvious biological consequences including exposure to systemic regulatory factors such as GnRH and E_2 and a direct path for release of gonadotrophins into the bloodstream. The deliberate nature of the interaction is suggested by the observation of the gonadotroph in figure 7.3.1b which appears at least partly, to wrap itself around the capillary thus increasing the surface area via which systemic interactions may occur. It is also interesting to note that in many of the gonadotrophs the nucleus was located towards the blood vessel which may aid reception of systemic factors which act via transcriptional responses.

The subcellular colocalisation of LH and CgA correlates with previous data regarding their presence in large FSH-containing granules (Watanabe *et al.*, 1991). However the novel observation of their colocalisation at the periphery of the gonadotroph suggests a role for CgA during shunting of LH granules to the site of release. Most significantly CgA immunoreactivity was absent at this site next to the capillary suggesting a change in granule morphology perhaps to that of the smaller LH and SgII only subclass demonstrated to be preferentially released during the LH surge (Watanabe *et al.*, 1991; Currie & McNeilly, 1995; Thomas *et al.*, 1998). It is not clear what happens to CgA at this stage but it is likely that the granin may be proteolytically cleaved by enzymes such as prohormone convertase 2 (PC2) which has been demonstrated to interact with CgA (Seidah *et al.*, 1987). Subsequent conformational changes in the structure of CgA may prevent immunodetection and facilitate the final stages of granulogenesis prior to exocytosis. Future studies will undoubtedly benefit

from antisera to granin-derived peptides with which this final stage of LH secretion may be investigated.

The divergent subcellular localisation of LH and FSH is similar to that reported in ewes treated with E_2 (Thomas & Clarke, 1997). It is possible that in males this effect is derived from metabolism of testosterone which may be studied using castrate mice. However this may have negative effects on CgA expression as reported in rats which leads to abnormal granule morphology (Watanabe *et al.*, 1998). Furthermore the biological significance of what appears to be gonadotroph priming in male mice remains uncertain promoting the direction of future studies towards that of divergent subcellular gonadotrophin localisation in female mice during the oestrus cycle. The intracellular behaviour of high levels of oFSHβ during the oestrus cycle of transgenic mice may reveal the secretory mechanisms which result in the biological effects of increased litter size compared to non-transgenic mice (P.Brown - personal communication). As demonstrated by these studies using males, the divergent subcellular localisation of LH and FSH in transgenic gonadotrophs where FSH is overexpressed is abolished. This suggests that the colocalisation of LH and FSH which does exist in normal gonadotrophs is promoted in this transgenic line due to high level expression. This increased colocalisation within gonadotrophs suggests that FSH is packaged into what are exclusively LH-containing granules in normal gonadotrophs. To verify this hypothesis secretagogue stimulated release of FSH at levels comparable to LH may be undertaken. Further physiological investigations of this transgenic line are currently underway (P.Brown - personal communication). Fine detail from electron microscopy (EM) regarding the granule morphology and colocalisation of LH and FSH as well as granins in these transgenic gonadotrophs may yield compelling evidence for significant entry of FSH into the regulated secretory pathway.

Although these results suggest that FSH may enter the regulated pathway as a result of increased expression, it is not clear what effect this has on expression of granins in gonadotrophs. The localisation of CgA with LH at

discrete subcellular locations suggests a specific role for CgA in LH granule biogenesis. More specifically the absence of CgA colocalisation with LH at the putative site for exocytosis next to the capillary suggests that CgA does not participate directly in the final stages of LH secretion. Previous reports have demonstrated LH colocalisation with CgA and SgII in larger granules but exclusively with SgII in smaller granules (Watanabe *et al.*, 1991; Thomas *et al.*, 1998). It may be likely that maturation of granules occurs and that CgA is present during mobilisation of LH granules but is either excluded immediately prior to the exocytosis or is subject to proteolytic processing preventing immunodetection at the release site. Although limitations regarding availability of primary antisera prevented colocalisation studies of FSH and CgA it may be assumed by the localisation of CgA to central cytoplasmic areas that some degree of colocalisation with FSH occurs. It is likely that this perinuclear area represents the location of the Golgi network and suggests that CgA has a role in the early differential sorting of LH and FSH. The limited availability of transgenic pituitaries prevented investigation of CgA colocalisation with LH in this system. However the other key granin implicated in LH secretion, SgII, may have undergone changes in expression as a result of increased intracellular FSH abundance. Although the small sample size prevented statistical analysis of the comparative abundancies, it is clear that SgII abundance is increased in the transgenic pituitary. However the SgII antiserum was ineffective for indirect immunofluorescence on whole pituitaries and thus prevented clarification regarding the cell type in which SgII appears to be upregulated. SgII has previously been reported to colocalise exclusively with LH in small (200nm) granules and with LH, CgA and FSH in larger (500nm) granules. It may be likely that as a result of increased FSHβ expression promoting colocalisation of FSH with LH, more small electron-dense granules are formed. Although the mechanism of regulation has not been determined it may be likely that SgII expression is upregulated to meet the increased requirement for small vesicles. A mechanism of positive feedback within gonadotrophs may occur via changes in cytoskeletal elements caused by the assumed increase in the abundance of granules.

In conclusion these studies have demonstrated that confocal microscopy on preparations of whole pituitaries allows visualisation of indirect immunofluorescence in conjunction with collection of phase-contrast images. It is this combination of semi-intact tissue preparation and the multi-channel capabilities of confocal microscopy which have permitted visualisation of the close relationship between gonadotrophs and blood vessels. Dual labelling with antisera directed towards LH and FSH as well as LH and CgA has demonstrated their subcellular localisations with regard to each other. As previously demonstrated in ewes treated with oestradiol (Thomas & Clarke, 1997), LH and FSH in the gonadotrophs of male mice exhibit differential subcellular localisation with LH predominantly located at the cell's periphery. Due to the preserved structure of the pituitary gland blood vessels this relationship between LH and FSH was put in context of the cellular end point of gonadotroph function that being secretion into the juxtaposed capillary. LH appeared to concentrate in the subplasmalemmal areas of the gonadotroph furthest from the blood vessel suggesting a process of preparation prior to shunting around the cell periphery to the site of release. Further detail regarding the role of CgA in this process was suggested by its colocalisation with LH during the stages leading to exocytosis. Notably however CgA appeared absent at the putative site of release suggesting perhaps a regulatory role facilitated by its proteolytic cleavage or perhaps recycling to aid sorting of newly synthesised LH molecules. In the novel transgenic mouse model where a stabilised form of the oFSHβ mRNA is expressed under control of the LHβ promoter, levels of hybrid FSH 2 to 4-fold greater than in normal mice were detected. This FSH appeared to migrate at a similar rate to that of mFSH suggesting similar glycosylation of the respective subunits. Most importantly this hybrid FSH appears to colocalise with mLH in the subplasmalemmal area of gonadotrophs suggesting that high-level expression of FSH is sufficient for its entry into the regulated pathway. Future analysis of similar female transgenics may allow this altered intracellular trafficking to be put in context of the oestrus cycle with particular relevance to the impact on reproductive physiology.

Chapter 8

General Discussion

The approaches used during this thesis have involved both *in vitro* and *in vivo* systems. This combination has proved successful as it has allowed comparison of observations for each protein investigated in a variety of systems. The initial choice of cell line was difficult, mainly due to the lack of a suitable cell line. However, limited success was achieved using the constitutively secreting JEG3 choriocarcinoma cell line. Other cell lines with regulated secretory pathways such as the murine adrenocorticotroph AtT-20, murine gonadotroph αT3-1 and rat somatomammotroph GH_3 cell lines proved inappropriate for lipid-based transfection studies due to slow growth rates and poor transfection efficiencies (data not reported). The easily transfected CHO cell line enabled investigation of gonadotrophin secretion in the presence of individual granins. Although these transfections were transient, some interesting preliminary data regarding an apparent upregulation of oLH expression by CgA and a reduction in oLH storage by SgII were obtained. In addition the use of confocal microscopy enabled visualisation of LH colocalised with CgA and CgB at different stages of secretion. Encouragingly the semi-divergent colocalisation of LH and CgA in CHO cells also appeared to occur in murine gonadotrophs *in vivo*. Finally a suitable gonadotroph cell line, $L\beta T_2$ (Thomas *et al*, 1996) was engineered during the course of these studies. Although use of this novel cell line was hampered by transient LHβ expression and poor adherence to culture surfaces, three key observations were made. Firstly, upregulation of αGSU expression by pulsatile GnRH administration peaked on the second day of treatment before falling again in accordance with previous data from the αT3-1 cell line (Windle *et al.*, 1990). Secondly, a relatively high dose GnRH regime caused increased constitutive secretion of LH, presumably via a transcriptional mechanism. This data correlates with previous findings in ewes chronically treated with GnRH (McNeilly *et al.*, 1991). Thirdly, high passage $L\beta T_2$ cells demonstrated an absence of CgA in conjunction with a reduction in the proportion of LH remaining intracellularly. This is further evidence which supports a role of this granin during regulated secretion.

The novel use of EGFP fusion proteins to study gonadotrophin secretion *in vitro* provided exciting visualisation of FSH vesicle traffic in CHO and $L\beta T_2$ cells. Although the carboxy-terminal EGFP structure appeared to enhance aggregation of the FSH heterodimers in the absence of granins, this technique enabled observation of movement and fusion of FSH granules within a living cell for the first time. This important development in the study of gonadotrophin secretion may in the future, allow real-time observation of LH and FSH secretion in a single cell. This will require engineering of an EGFP/oLHβ construct which is capable of heterodimer formation and may involve use of an amino-terminus fusion vector. In addition some specialised equipment for confocal microscopy including bandpass filters for distinction of EGFP and EYFP signals will be required as their emission spectra differ by only 10-15nm.

Indirect immunofluorescence carried out on semi-intact murine pituitary glands has for the first time enabled visualisation of LH and FSH or CgA in gonadotrophs which were clearly juxtaposed to blood vessels. This technique has confirmed the semi-divergent colocalisation of LH with FSH (Thomas & Clarke, 1997) and LH with CgA (Watanabe *et al.*, 1991) and related them to the position of the nearby sinusoid. Although carried out on untreated males this technique will be essential for observation of colocalisation events during the oestrus cycle. Perhaps most significantly of all this technique has allowed the visualisation of enhanced colocalisation of LH and FSH in the oLHβ/oFSHβ transgenic model. This suggests that 4-fold overexpression of FSH levels in gonadotrophs can lead to FSH entering the small (>200nm) LH/SgII/CSP-only granules (Thomas *et al.*, 1998) which occur at the periphery of the gonadotroph. Further EM-based investigation carried out on females may reveal whether FSH is colocalised with LH or is alone in similar FSH-only granules responding to GnRH-induced $[Ca^{++}]_i$ fluxes and E_2 treatment in a similar manner to LH.

These results in conjunction with previously reported data have enabled construction of the model for gonadotrophin secretion shown in figure 8a. This model raises specific questions regarding differential gonadotrophin secretion and the role of granins. In the remainder of this chapter these questions and the strategies that might be used to address them will be discussed.

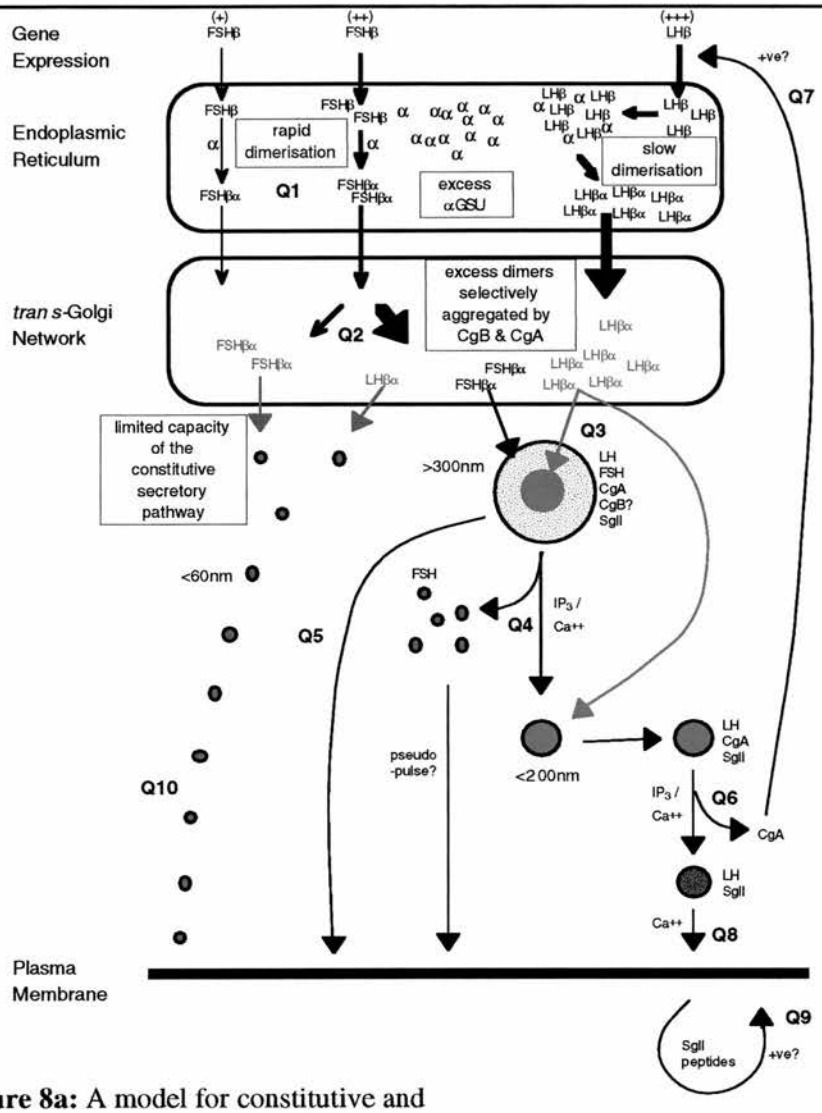

Figure 8a: A model for constitutive and regulated gonadotrophin secretion.

Q1: Does the high rate of dimerisation prevent FSH sorting to the regulated pathway?

Q2: If FSHβ is expressed at high levels (i.e. equivalent to LHβ), can it be sorted to the regulated pathway?

Q3: Can LH be packaged directly into >300nm and <200nm secretory vesicles?

Q4: Do large granules mature into smaller LH-only granules and if so what happens to the FSH?

Q5: Do large bihormonal granules contain IP3-Rs, SNAREs etc. and are they capable of fusion with the plasma membrane?

Q6: What happens to CgA prior to LH release?

Q7: Do CgA/CgA-derived peptides enhance translation of LHβ ?

Q8: Does SgII have a role during the fusion event?

Q9: Are SgII-derived peptides produced by gonadotrophs and do they have an autocrine effect on LH release?

Q10: What is the maximum capacity for constitutive release of LH/FSH and are they the same and are they altered by granins?

Several key points of gonadotrophin secretion are contained within boxes in the model. Notably the rates of dimerisation for LH and FSH are different and it has been proposed that this may represent a mechanism whereby LH and FSH are differentially sorted (Muyan *et al.*, 1994). The rate at which inter-species FSH forms a heterodimer has not been investigated in transiently transfected $L\beta T_2$ cells or the oLHβ/oFSHβ transgenic model despite increased storage in comparison to the intra-species FSH heterodimers. This difference in the rate of dimerisation may still represent the reason FSH is normally secreted via the constitutive pathway. To resolve this question it may be necessary to engineer a transgenic model in which high levels of an intra-species FSH heterodimer are expressed. This model may also confirm the preliminary findings from the oLHβ/oFSHβ transgenic model which suggest that FSH enters the regulated secretory pathway when overexpressed. However it still remains to be determined whether the increased colocalisation of LH and FSH in this transgenic model truly represents FSH sorting to the final stages of the regulated pathway. To answer this question ongoing studies of the oLHβ/oFSHβ transgenic model may involve EM analysis during E_2 treatment to observe whether FSH exhibits priming as reported for LH granules in sheep (Thomas *et al* 1998). In addition it may be necessary to sample hypophyseal blood during administration of pulsatile GnRH to establish whether FSH exhibits the reported time-lag observed between GnRH and LH release (Padmanabhan *et al.*, 1997). This may indicate that FSH is present within either similar or the same secretory vesicles as LH.

LH is present in at least two types of granule; the larger FSH-containing and the smaller LH-only varieties (Watanabe *et al.*, 1991). Do these morphologically distinct granules represent two separate regulated secretory pathways? If they do then this would imply that the larger bihormonal granules are capable of fusion with the plasma membrane. However if these granules represent the same secretory pathway this would suggest that the larger granules condense and form the smaller LH-only granules. In this scenario what happens to the FSH at the periphery of the granule? In order to answer these questions two approaches may be taken. Firstly an *in vitro* study of $L\beta T_2$ cells stably transfected with EGFP and EYFP fusions of FSH and LH respectively. This system would enable

real-time visualisation of FSH and LH transit through the regulated pathway. Colocalisation in post-Golgi vesicles may be followed by divergence closer to the plasma membrane. Real-time analysis of transgenic animals expressing fluorophore fusion hormones has yet to be reported. The presence of the fluorescent proteins on LH and FSH may prevent their biological function and this could be verified by bioassay of proteins secreted by cell lines. Targeting gene expression to gonadotrophs in adults using adenoviral vectors or GnRH-polylysine transporters may avoid disruption to reproductive development caused by the fluorescent proteins. Primary culture of these genetically modified gonadotrophs may enable real-time visualisation of LH and FSH secretion in a more physiological context. The recent report by Tasaka *et al* demonstrated the efficacy of inhibiting both constitutive and regulated secretion by gonadotrophs *in vitro* through application of Rab3B antisense oligonucleotides (Tasaka *et al.*, 1998). Using this approach together with a pulsatile GnRH regime it may be possible to observe an increase in the proportion of smaller (more mature) LH granules. This observation would suggest that in response to GnRH, gonadotrophin granules migrate towards the plasma membrane and mature as they do so. If granules do indeed mature in response to GnRH-R activation this would raise the question of how this message is conveyed to the granule and the signal converted into a cellular response? Since CgA has been observed on the periphery of bihormonal granules (Currie & McNeilly - personal communication) and has been demonstrated to bind the IP_3-R (Yoo, 1994), this granin is a leading candidate for effecting changes in granule morphology. A possible mechanism for this may involve conformational changes in CgA structure or the degree of aggregation in response to a reduction in calcium concentration within the granule lumen. This change may be facilitated through activation of the IP_3-R calcium channel by its agonist produced during GnRH-R activation. CgA unlike CgB requires high calcium concentrations for aggregation and may therefore be well-suited to a role where relatively small reductions in calcium concentration are a signal.

Indirect immunofluorescence carried out on transfected CHO cells and murine gonadotrophs demonstrated colocalisation of CgA with LH except at

putative exocytosis sites. In CHO cells CgA-only granules were apparent although not at peripheral areas of the cell. In murine gonadotrophs CgA-immunoreactivity appeared absent from the subplasmalemmal areas juxtaposed to the blood vessel. What happens to CgA prior to LH exocytosis *in vivo*? At least two possibilities could account for the lack of CgA-immunoreactivity immediately prior to LH exocytosis. Firstly, CgA may be proteolytically digested within the granule thus altering its conformation and requiring use of antisera directed at specific peptides. Secondly, recycling of CgA and CgA-derived peptides may also occur. To establish whether either of these hypotheses are correct antisera directed at CgA-derived peptides may be used in immunohistochemical applications and RIAs to determine the location of processed CgA *in vivo*.

The observed enhancement of oLH expression from CHO cells cotransfected with the CgA expression construct and similar enhancement of hCG expression suggests a possible interaction of CgA or CgA-derived peptides during translation of these β-subunit genes. By creating a transgenic knockout of the CgA gene in mice it may be possible to observe the effects of CgA removal on levels of LH expression as well as the formation of the regulated secretory pathway. Recent work by Watanabe *et al* has demonstrated a reduction in the diameters of CgA-positive granules following castration (Watanabe *et al.*, 1998). It is possible that a complete absence of CgA in the gonadotroph may completely abolish granule formation and therefore the regulated secretory pathway. Alternatively stable transfection of the $L\beta T_2$ cell line with antisense directed towards CgA may be carried out as this may yield similar results more rapidly.

The colocalisation of SgII and CSP with LH in granules which are preferentially released during the LH surge (Thomas *et al.*, 1998; Currie & McNeilly, 1995) has led to speculation that SgII has a role during fusion of the granule with the plasma membrane. This hypothesis is strengthened by a report which has observed that rat gonadotrophs lack the calcium sensor synaptotagmin which is involved in fusion pore formation (Jacobsson & Meister, 1996). To test this hypothesis a similar approach may be taken to that described for the previous question. The generation of a SgII knockout and application of antisense technology to $L\beta T_2$ cells may determine a role for this granin in LH secretion.

In addition the hypothesis that SgII-derived peptides act on the gonadotroph as a means of autocrine regulation which is perhaps heightened during the LH surge may be tested by application of these peptides to gonadotrophs either *in vivo* or *in vitro*. As a prerequisite for this experiment it would be necessary to verify by RIA that SgII-derived peptides are released during the preovulatory LH surge. Investigation of serum levels of SgII in the oLHβ/oFSHβ transgenic model may strengthen the hypothesis that SgII levels are raised in the gonadotroph during increased regulated secretion.

The final question raised by this model relates to the constitutive secretory pathway. As observed in $L\beta T_2$ cells and ewes (McNeilly *et al.*, 1991) chronically treated with GnRH, LH like FSH can be released via the constitutive pathway. Expression of LH and FSH at high levels enables their entry into the regulated pathway in the presence of granins. Is there a threshold of gonadotrophin expression that must be exceeded before entry into the regulated pathway and it is the same for LH and FSH? Also, is this threshold lowered by the presence of one or more granins? Stable transfection of $L\beta T_2$ cells with an inducible FSH expression system may allow determination of this threshold. Determination of this putative level for LH may require similar transfection of primary cultures of gonadotrophs from the NGF1-A knockout mouse which does not express endogenous LH (Lee *et al.*, 1996).

In conclusion this thesis has demonstrated further evidence for the role of granins during regulated secretion of gonadotrophins *in vitro* and *in vivo*. Transient transfection studies carried out on CHO cells have suggested that CgB colocalises with LH in the Golgi apparatus only whereas CgA also colocalises with LH in granules located in non-peripheral areas of the cytoplasm. Additionally, CgA appears to exert significant enhancement of oLH expression in cotransfected CHO cells suggesting an interaction at the post-transcriptional level. Surprisingly cotransfection studies involving oLH and SgII suggested that this granin reduced the amount of oLH storage in CHO cells. Use of the novel $L\beta T_2$ cell line has demonstrated an increase in constitutive secretion of LH during chronic GnRH treatment and reduction in the proportion of LH stored in the

absence of intracellular CgA. Indirect immunofluorescence carried out on male murine gonadotrophs *in vivo* has demonstrated a semi-divergent relationship between CgA and LH where the granin appears to exit the granule prior to exocytosis. Similar confocal analysis of the oLHβ/oFSHβ transgenic model which expresses FSH at four times the wild-type level has suggested that FSH entry into the regulated secretory pathway of gonadotrophs may be enhanced by its overexpression.

Appendix I

This appendix lists the recipes for solutions referred to in the materials and miscellaneous methods sections throughout this thesis.

Bouins Fixative

21ml 40% formaldehyde
400ml Acetic acid
8 litres Picric acid-saturated water

10x Blue Loading Buffer:

50% glycerol
1mM EDTA (pH8.0)
0.1mg/ml bromophenol blue

Church & Gilbert Hybridisation buffer (Church & Gilbert 1984)

0.5M $NaPO_4$ pH7.2
7% SDS
1mM EDTA pH8
1% BSA
15% formamide

HEPES-buffered saline (HBS)

137mM NaCl
125mM HEPES
5mM Na_2HPO_4
adjusted to pH7.0 with NaOH

10x MOPS buffer

0.2M MOPS (pH7.0)
80mM NaAc
10mM EDTA (pH8.0)

Native PAGE: **Running buffer**

(stored at room temperature)
25mM Tris
192mM glycine
distilled H_2O
pH 8.8

5x Loading Buffer

312.5mM TrisHCl (pH6.8)
50% glycerol
0.05% bromophenol blue

6x OJ Loading Buffer:

18% Ficoll
0.06% SDS
24mM EDTA pH8
0.15% Orange S

SDS-PAGE: Running buffer
(stored at room temperature)
25mM Tris
192mM glycine
0.1% SDS
distilled H_2O
pH8.3

5x Reducing/Non-reducing Loading buffer
(stored at room temperature)
60mM TrisHCl (pH6.8)
25% glycerol
2% SDS
14.4mM β-mercaptoethanol*
0.1% bromophenol blue
distilled H_2O

*only in Reducing loading buffer

Siliconised Pasteur Pipettes (Sambrook *et al* 1989)
In a fume hood:
Place glass wool in bottom of glass measuring cylinder
Add glass Pasteur pipettes
Pour in Repelcote
Swirl gently for 30 seconds
Remove Repelcote
Leave to dry in fume hood
Wrap in foil and seal with autoclave tape
Autoclave

20x SSC buffer
300mM Sodium Chloride
300mM Sodium Citrate

10x TAE Buffer
400mM Tris-acetate
10mM EDTA (pH8.0)

10x TBE Buffer
450mM Tris-borate
10mM EDTA (pH8.0)

TE buffer pH8
10mM TrisHCl
1mM EDTA

Wet-blot buffer for Transfer of SDS-coated Proteins
25mM Tris
192mM glycine
20% Methanol
distilled H_2O

Appendix II

This appendix contains contact addresses for academic and commercial suppliers of materials described throughout this thesis.

Academic Sources

T.E.Adams
University of Melbourne
Parkville
Victoria 3052
Australia

P.Brown
MRC Reproductive Biology Unit
Centre for Reproductive Biology
37 Chalmers Street
Edinburgh EH3 9EW
UK
Tel: 0131 229 2575 ext. 2216
Fax: 0131 228 5571
e-mail: p.brown@ed-rbu.mrc.ac.uk

R.Fischer-Colbrie
Department of Pharmacology
University of Innsbruck
Peter-Mayr-Straβe 1
A-6020 Innsbruck
Austria
Tel: (00 43 5222) 724-2410

A.S.McNeilly
MRC Reproductive Biology Unit
Centre for Reproductive Biology
37 Chalmers Street
Edinburgh EH3 9EW
UK
Tel: 0131 229 2575 ext. 2206
Fax: 0131 228 5571
e-mail: a.mcneilly@ed-rbu.mrc.ac.uk

P.Mellon
The Salk Institute
PO Box 85800
San Diego
CA 92138-9216
USA
Tel: (619) 453 4100

B.Miller
Department of Biochemistry
North Carolina State University
Raleigh
North Carolina 27695-7622
USA

J.Rosen
Department of Animal Science
University of California, Davis
CA 95616-8521
USA

P.Taylor
MRC Reproductive Biology Unit
Centre for Reproductive Biology
37 Chalmers Street
Edinburgh EH3 9EW
UK
Tel: 0131 229 2575 ext. 2006
Fax: 0131 228 5571
e-mail: p.taylor@ed-rbu.mrc.ac.uk

Commercial Suppliers

Amersham Pharmacia Biotech Ltd
Amersham Place
Little Chalfont
Bucks HP7 9NA,
ENGLAND
Tel: 0870 606 1921
Fax: 44 1494 544350
Technical enquiries: 0800 616928

American Type Culture Collection (ATCC)
10801 University Boulevard,
Manassas,
VA 20110-2209
Tel: 703-365-2700

Anachem Ltd
Anachem House
Charles Street
Luton
Bedfordshire
LU2 0EB

Boehringer Mannheim UK
(Diagnostics & Biochemicals) Limited
Bell Lane, Lewes
East Sussex BN7 1LG
UNITED KINGDOM
Tel: 0800 521578
Fax: 0800 181087
Email: biochem_uk@bmg.boehringer-mannheim.com

CamBio
34 Newnham Road
Cambridge CB3 9EY
UK

Tel: 01223 366500
Fax: 01223 350069

Cambridge Bioscience Ltd.
25, Signet Court
Swann's Road
Cambridge
Cambridgeshire CB5 8LA
UK
Tel:+44 1223 316855
Fax:+44 1223 360732

CLONTECH Laboratories UK Ltd.
Unit 2, Intec 2,
Wade Road,
Basingstoke,
Hampshire RG24 8NE
UK
TEL: 01256 476500
FAX: 01256 476499
E-MAIL: products@clontech.com

CoStar UK Ltd.
High Wycombe,
UK
Tel: 44-1494-471207
Fax: 44-1494-464891

DuPont NEN
BRU/BRU/40349
P.O. Box 66
TW5 9RT
UK
Tel: 0800 896046
Fax: 0800 891715

Dynamic Microsystems, Inc.
13003 Bucaneer Road
Silver Spring MD 20904
U.S.A.
Tel: 301 384 2754
Fax: 301 384 0826

European Collection of Cell Cultures (ECACC)
Centre for Applied Microbiology and Research
Salisbury SP4 OJG,
UK.
Tel: (44 1980) 612512. Fax: (44 1980) 611315.
E-mail: ecacc@ecacc.demon.co.uk.

Elkay Products, Inc.
PO Box 4247
Shrewsbury, MA 01545
Tel: 508-845-2116 or Fax: 508-842-1338

Genosys Biotechnologies (Europe) Ltd.
London Road
Pampisford
Cambridge
CB2 4EF, UK
Phone: (+44) (0)1223 839000
Fax: (+44) (0)1223 839200

Gibco Life Technologies, Inc.
9800 Medical Center Drive
Post Office Box 6482
Rockville, MD 20849 - 6482,
U.S.A.
Tel: 1-800-338-5772

Greiner Labortechnik
C.A.Greiner & Sohne GmbH
A-4550 Kremsmunster
Bad Hallerstr 32
Austria

Hayman Ltd.
Eastways Park
Witham
Essex CM8 3YE
UK

Hybaid Limited
Action Court,
Ashford Road,
Ashford,
Middlesex TW15 1XB
Tel: +44(0)1784 425000 or Fax: +44(0)1784 248085

Invitrogen BV
PO Box 2312
9704 CH Groningen
The Netherlands
Tel: 00800 5345 5345
Fax: 00800 7890 7890

Jencons (Scientific) Ltd
Cherrycourt Way
Stanbridge Road
Leigton Buzzard
Bedfordshire
LU7 8UA
England
Telephone : (+44) 1525 372010
Fax: (+44) 1525 379547

KONTES Scientific Instruments
Vineland
New Jersey 08360
USA

MacWarehouse Ltd
Horizon One
Studio Way
Borehamwood
WD6 5WH
Tel: 0990 168740

Merck Ltd (BDH)
Merck House
POOLE
Dorset
BH15 1TD
Tel: +44 (0) 1202 669700
Fax: +44 (0) 1202 665599

Millipore (UK) Ltd
The Boulevard
Blackmoor Lane
Watford
Hertfordshire
WD1 8YW
Tel. (01923) 816375
Fax. (01923) 818297

Molecular Dynamics
World Headquarters
928 East Arques Avenue
Sunnyvale, CA 94086-4520 USA
Telephone: 1-408-773-1222
Fax: 1-408-773-1493
e-mail: info@mdyn.com

Molecular Probes Europe BV
PoortGebouw
Rijnsburgerweg 10
2333 AA Leiden
The Netherlands
Tel. +31-71-5233378 or Fax: +31-71-5233419

Nalge Nunc International
Nalge (Europe) Limited
Foxwood Court
Rotherwas Industrial Estate
Hereford HR2 6JQ
UK
TEL: 01432 263933
FAX: 01432 351923

NIDDK
National Hormone and Pituitary Program
685 Lofstrand Lane,
Rockville
MD 20850
USA
ogden@access.digex.net

OLYMPUS Optical Co. (UK.) Ltd.
2-8 Honduras Street
London EC1Y OTX
UK
Tel: 0171 25 32 772
Fax: 0171 25 16 330

Perkin-Elmer Analytical Instruments
Seer Green Customer Centre
Chalfont Road
Seer Green
Bucks HP9 2FX
Phone (01494) 676161
Fax (01494) 679331/3

Promega UK Ltd,
Delta House,
Chilworth Research Centre,
Southampton SO16 7NS
Tel 01703-760225
Fax 01703-767014

Santa Cruz Biotechnology, Inc.
Ludolf-Krehl-Straβe 33
69120 Heidelberg
Germany
Tel: +800 4573 8000
Fax: 49(0) 6221 4503 45

Scottish Antibody Production Unit (SAPU)
Law Hospital
Carluke
Lanarkshire
Scotland ML8 5ES

Serono Diagnostics France SNC
18, rue des Pyrenees
Silic 321
94598 Rungis Cedex
FRANCE
Tel: 01 45 12 89 00
Fax: 0222 8940357

Serotec Ltd,
22 Bankside,
Station Approach,
Kidlington,
Oxford, OX5 1JE
Tel +44 (0) 1865 852722
Fax +44 (0) 1865 373899

Sigma-Aldrich
Fancy Road
Poole
Dorset BH12 4QH
England

Sorvall (UK) Ltd
International Centre
Boulton Road
Stevanage
Herts SG1 4QX

Stratagene Ltd.
Cambridge Innovation Centre,
Cambridge Science Park,
Milton Road,
Cambridge CB4 4GF
UK
Tel: 0800 585370
Fax: 01223 420234

UKC
Chem Lab
Canterbury CT2 7NH

Wallac UK (EG&G Ltd)
Milton Keynes
20 Vincent Avenue
Crownhill Business Centre
Crownhill
Milton Keynes, MK8 0AB
Tel. 44-1908-265 744
Fax. 44-1908-265 956
e-mail: wallac-uk@wallac.com

Carl Zeiss Ltd.
17-20 Woodfield Road
P.O.Box 78
Welwyn Garden City
Hertfordshire AL7 1L
Tel.: 0044-1-707-871200
Fax: 00441-707/871287

Bibliography

Aardal, S. & Helle, K. B. (1992). The vasoinhibitory activity of bovine chromogranin A fragment (vasostatin) and its independence of extracellular calcium in isolated segments of human blood-vessels. *Regulatory Peptides* **41,** 9-18.

Aiyer, M. S., Chiappa, S. A. & Fink, G. (1974a). A priming effect of luteinizing hormone releasing factor on the anterior pituitary gland in the female rat. *Journal of Endocrinology* **62,** 573-588.

Aiyer, M. S., Fink, G. & Greig, F. (1974b). Changes in the sensitivity of the pituitary gland to luteinizing hormone releasing factor during the oestrous cycle of the rat. *Journal of Endocrinology* **60,** 47-64.

Akbar, A. M., Nett, T. M. & Niswender, G. D. (1974). Metabolic clearance and secretion rates of gonadotrophins at different stages of the estrous cycle in ewes. *Endocrinology* **94,** 1318-1324.

Allaerts, W., Mignon, A. & Denef, C. (1991). Selectivity of juxtaposition between cup-shaped lactotrophs and gonadotrophs from rat anterior pituitary in culture. *Cell Tissue Res* **263,** 217-225.

Anderson, B., Kennedy, G. & Nilson, J. (1990). A *cis*-acting element located between the cAMP response elements and the CCAAT box augments cell-specific expression of the glycoprotein hormone alpha subunit gene. *Journal of Biological Chemistry* **265,** 21874-21880.

Anderson, L. (1996). Intracellular mechanisms triggering gonadotrophin secretion. *Reviews of Reproduction* **1,** 193-202.

Andrews, W. V., Hansen, J. R., Janovick, J. A. & Conn, P. M. (1990). Gonadotropin-releasing hormone modulation of protein kinase-C activity in perifused anterior pituitary cells. *Endocrinology* **127,** 2393-2399.

Anouar, Y. & Duval, J. (1992). Direct estradiol down-regulation of secretogranin II and chromogranin A mRNA levels in rat pituitary cells. *Molecular and Cellular Endocinology* **88,** 97-104.

Arora, K. K., Sakai, A. & Catt, K. J. (1995). Effects of second intracellular loop mutations on signal transduction and internalization of the gonadotropin-releasing hormone receptor. *Journal of Biological Chemistry* **270,** 22820-22826.

Attardi, B. & Winters, S. J. (1993). Decay of Follicle-stimulating hormone-β messenger RNA in the presence of transcriptional inhibitors and/or inhibin, activin, or follistatin. *Molecular Endocrinology* **7,** 668-680.

Augustine, G. & Neher, E. (1992). Calcium requirements for secretion in bovine chromaffin cells. *Journal of Physiology* **450,** 247-271.

Baird, D. T., Campbell, B. K., Mann, G. E. & McNeilly, A. S. (1991). Inhibin and oestradiol in the control of FSH secretion in the sheep. *Journal of Reproduction and Fertility Suppl* **43,** 125-138.

Baird, D. T. & McNeilly, A. S. (1981). Gonadotrophic control of follicular development and function during the oestrous cycle of the ewe. *Journal of Reproduction and Fertility Suppl* **30,** 119-133.

Baker, P. F. & Knight, D. E. (1978). Calcium-dependent exocytosis in bovine adrenal medullary cells with leaky plasma membranes. *Nature* **276,** 620-622.

Barbosa, J. A., Gill, B. M., Takiyyuddin, M. A. & O'Connor, D. T. (1991). Chromogranin-A - Posttranslational Modifications in Secretory Granules. *Endocrinology* **128,** 174-190.

Bassetti, M., Huttner, W. B., Zanini, A. & Rosa, P. (1990). Co-localisation of secretogranins/chromogranins with thyrotropin and luteinizing hormone in secretory granules of cow anterior pituitary. *Journal of Histochemistry and Cytochemistry.* **38,** 1353-1363.

Bassetti, M., Pasini, D. L. & Rosa, P. (1995). Degradation of Gonadotropin Beta-subunits Retained in the Endoplasmic Reticulum of the Gonadotropes of Castrated Rats. *Endocrinology* **136,** 1168-1176.

Bauer, J. W. & Fischer-Colbrie, R. (1991). Primary Structure of Bovine Chromogranin-B Deduced from cDNA Sequence. *Biochimica Et Biophysica Acta* **1089,** 124-126.

Begeot, M., Hemming, F. J., Dubois, P. M., Combarnous, Y., Dubois, M. P. & Aubert, M. L. (1984). Induction of pituitary lactotrope differentiation by luteinizing hormone α subunit. *Science* **226,** 566-567.

Belchetz, P., Plant, T. M., Nakai, Y., Keogh, E. J. & Knobil, E. (1978). Hypophysial responses to continuous and intermittent delivery of hypothalamic gonadotrophin releasing hormone. *Science* **202,** 631-633.

Bello, P. A., Mountford, P. S., Brandon, M. R. & Adams, T. E. (1989). Cloning and DNA sequence analysis of the cDNA for the common alpha-subunit of the ovine pituitary glycoprotein hormones. *Nucleic Acids Research* **17,** 10494-.

Bidart, J. M., Baudin, E., Troalen, F., Bellet, D. & Schlumberger, M. (1997). Eutopic and ectopic production of glycoprotein hormone alpha and beta subunits. *Annales De Endocrinologie* **58,** 125-128.

Bielinska, M., Rzymkiewicz, D. & Boime, I. (1994). Human Luteinizing-Hormone and Chorionic-Gonadotropin Are Targeted to a Regulated Secretory Pathway in GH_3 Cells. *Molecular Endocrinology* **8,** 919-928.

Blake, C. A. & Kelch, R. P. (1981). Administration of antiluteinizing hormone-releasing hormone serum to rats: effects on periovulatory secretion of luteinizing hormone and follicle stimulating hormone. *Endocrinology* **109,** 2175-2179.

Blithe, D. L., Richards, R. G. & Skaulis, M. C. (1991). Free alpha molecules from pregnancy stimulate secretion of prolactin from human decidual cells. *Endocrinology* **129,** 2257-2259.

Block, M. R., Glick, B. S., WWilcox, C. A., Wieland, F. T. & Rothman, J. E. (1988). Purification of an N-ethylmaleimide-sensitive protein catalyzing vesicular transport. *Proceedings of the National Academy of Sciences USA* **85,** 7852-7856.

Bo, M. & Boime, I. (1992). Identification Of the Transcriptionally Active Genes Of the Chorionic Gonadotropin-Beta Gene-Cluster in vivo. *Journal of Biological Chemistry* **267,** 3179-3184.

Bokar, J. A., Keri, R. A. & Farmerie, T. A. (1989). Expression of the glycoprotein hormone alpha-subunit requires a functional cyclic AMP response element, whereas a different *cis*-acting element mediates pituitary-specific expression. *Molecular and Cellular Biology* **9,** 5113-5122.

Bouamoud, N., Lerrant, Y., Ribot, G. & Counis, R. (1992). Differential stability of mRNAs coding for α and gonadotropin β subunits in cultured rat pituitary cells. *Molecular and Cellular Endocrinology* **88,** 143-151.

Bousfield, G. R., Perry, W.M., Ward, D.N. (1994). Gonadotrophins. The Physiology of Reproduction (Ed. E. Knobil, Neill, J.D.) New York, Raven Press Ltd. Second Edition, 1749-1792.

Bradford, M. (1976). A rapid and sensitive method for the quantitation of microgram quantities of protein utilizing the principle of protein-dye binding. *Analytical Biochemistry* **72,** 248-254.

Braks, J. A. M. & Martens, G. J. M. (1994). 7B2 is a Neurooendocrine Chaperone that Transiently interacts with Prohormone Convertase PC2 in the Secretory Pathway. *Cell* **78,** 263-273.

Brooks, A. N., Lamming, G. E., Lees, P. D. & Haynes, N. B. (1986). Opioid modulation of LH secretion in the ewe. *Journal of Reproduction and Fertility.* **76,** 693-708.

Brooks, J. & McNeilly, A. S. (1994). Regulation of gonadotrophin-releasing hormone receptor mRNA expression in the sheep. *Journal of Endocrinology* **143,** 175-182.

Brooks, J., Taylor, P. L., Saunders, P. T. K., Eidne, K. A., Struthers, W. J. & McNeilly, A. S. (1993). Cloning and sequencing of the sheep pituitary gonadotropin-releasing hormone receptor and changes in expression of its mRNA during the estrous cycle. *Molecular and Cellular Endocrinology* **94,** R23-R27.

Brown, P. & McNeilly, A. S. (1997). Steroidogenic Factor-1 (SF-1) and the regulation of expression of luteinising hormone and follicle-stimulating hormone beta-subunits in the sheep anterior pituitary *in vivo*. *International Journal of Biochemical and Cellular Biology* **29,** 1513-1524.

Brown, P., McNeilly, J. R., Wallace, R. M., McNeilly, A. S. & Clark, A. J. (1993). Characterization Of the Ovine LH-Beta-Subunit Gene - the Promoter Directs Gonadotrope-Specific Expression In Transgenic Mice. *Molecular and Cellular Endocrinology* **93,** 157-165.

Burgoyne, R. D. & Handel, S. E. (1994). Activation Of Exocytosis By GTP Analogs In Adrenal Chromaffin Cells Revealed By Patch-Clamp Capacitance Measurement. *FEBS Letters* **344,** 139-142.

Burgoyne, R. D. & Morgan, A. (1993). Regulated Exocytosis. *Biochemical Journal* **293,** 305-316.

Burzawa-Gerard, E., Fontaine Y-A. (1976). Formation d'une molecule hybride douee d'une activite gonadotrope sur la grenouille, a partir de la sous-unite a de l'hormone luteinisante bovine et d'une sous-unite de l'hormone gonadotrope d'un poisson teleosteen. *CR Acad Sci Paris* **282,** 97-100.

Caldani, M., Batailler, M., Thiery, J.-C. & Dubois, M. P. (1988). LHRH-immunoreactive structures in the sheep brain. *Histochemistry* **89,** 129-139.

Campbell, B. K., McNeilly, A. S., Picton, H. M. & Baird, D. T. (1990). The effect of a potent gonadotrophin-releasing hormone antagonist on ovarian secretion of oestradiol, inhibin, and androstenedione and the concentration of LH and FSH during the follicular phase of the sheep oestrous cycle. *Journal of Endocrinology* **126,** 377-384.

Campbell, B. K., Scaramuzzi, R. J. & Webb, R. (1995). The control of antral follicle development and selection in sheep and cattle. *Journal of Reproduction and Fertility.Suppl* **49,** 335-350.

Canaff, L., Bevan, S., Wheeler, D. G., Mouland, A. J., Rehfuss, R. P., White, J. H. & Hendy, G. N. (1998). Analysis of molecular mechanisms controlling neuroendocrine cell specific transcription of the chromogranin A gene. *Endocrinology* **139,** 1184-1196.

Carbajal, M. E. & Vitale, M. L. (1997). The Cortical Actin Cytoskeleton of Lactotropes as an Intracellular Target for the Control of Prolactin Secretion. *Endocrinology* **138,** 5374-5384.

Carroll, R. S., Corrigan, A. Z., Gharib, S. D., Vale, W. & Chin, W. W. (1989). Inhibin, activin, and follistatin: regulation of follicle-stimulating hormone messenger ribonucleic acid levels. *Molecular Endocrinology.* **3,** 1969-1976.

Carroll, R. S., Corrigan, A. Z., Vale, W. & Chin, W. W. (1991). Activin stabilizes follicle-stimulating hormone-beta messenger ribonucleic acid levels. *Endocrinology* **129,** 1721-1726.

Cesnjaj, M., Catt, K. J. & Stojikovic, S. S. (1994). Coordinate actions of calcium and protein kinase C in the expression of primary response genes in pituitary gonadotrophs. *Endocrinology* **135,** 692-701.

Chanat, E., Weiss, U. & Huttner, W. B. (1994). The Disulfide Bond In Chromogranin-B, Which Is Essential For Its Sorting to Secretory Granules,

Is Not Required For Its Aggregation In the Trans-Golgi Network. *FEBS Letters* **351,** 225-230.

Chappel, S., Kelton, C. & Nugent, N. (1998). Basic knowledge about recombinant gonadotropic hormone production. Treatment of Infertility (Ed. Howells, C.R. & Jacobs, H.) Serono Symposium 95-102.

Chavez, R. A., Miller, S. G. & Moore, H. P. H. (1996). A Biosynthetic Regulated Secretory Pathway In Constitutive Secretory-Cells. *Journal of Cell Biology* **133,** 1177-1191.

Chen, C. & Okayama, H. (1987). High-Efficiency Transformation of Mammalian Cells by Plasmid DNA. *Molecular and Cellelar Biology* **7,** 2745-2752.

Chi, L., Zhou, W., Prikhozhan, A., Flanagan, C., Davidson, J. S., Golembo, M., Illing, N., Millar, R. P. & Sealfon, S. C. (1993). Cloning and characterization of the human GnRH receptor. *Molecular and Cellular Endocrinology* **91,** R1-R6.

Chung, S. H., Takai, Y. & Holz, R. W. (1995). Evidence That the Rab3A-Binding Protein, Rabphilin3A, Enhances Regulated Secretion - Studies In Adrenal Chromaffin Cells. *Journal of Biological Chemistry* **270,** 16714-16718.

Church, G. M. & Gilbert, W. (1984). Genomic Sequencing. *Proceedings of the National Academy of Sciences USA* **81,** 1991-1995.

Clark, J. R., Dierschke, D. J., Meller, P. A. & Wolf, R. C. (1979). Hormonal regulation of ovarian folliculogenesis in rhesus monkeys. II Serum concentrations of estradiol 17β and follicle stimulating hormone associated with growth and identification of the preovulatory follicle. *Biology of Reproduction* **21,** 497-503.

Clarke, I. J. & Cummins, J. T. (1982). The temporal relationship between gonadotropin releasing hormone (GnRH) and luteinizing hormone (LH) secretion in ovariectomized ewes. *Endocrinology* **11,** 1737-1739.

Clarke, I. J., Cummins, J. T., Crowder, M. E. & Nett, T., M. (1987). Pituitary receptors for gonadotropin-releasing hormone in relation to changes in pituitary and plasma luteinizing hormone in ovariectomized-hypothalamo pituitary disconnected ewes. I. Effect of changing frequency of gonadotropin-releasing hormone pulses. *Biology of Reproduction* **37,** 749-754.

Clarke, I. J., Cummins, J. T., Crowder, M. E. & Nett, T. M. (1988). Pituitary receptors for gonadotropin-releasing hormone in relation to changes in pituitary and plasma gonadotropins in ovariectomized hypothalamo/pituitary disconnected ewes. II. A marked rise in receptor number during the acute feedback effects of estradiol. *Biology of Reproduction* **39,** 349-354.

Clarke, I. J., Cummins, J. T., Findlay, J. K., Burman, K. J. & Doughton, B. W. (1984). Effects on plasma luteinizing hormone and follicle-stimulating hormone of varying the frequency and amplitude of

gonadotropin-releasing hormone pulses in ovariectomized ewes with hypothalamo-pituitary disconnection. *Neuroendocrinology* **39,** 214-221.

Clarke, I. J., Fraser, H. M. & McNeilly, A. S. (1978). Active immunization of ewes against luteinizing hormone releasing hormone, and its effects on ovulation and gonadotrophin, prolactin and ovarian steroid secretion. *Journal of Endocrinology* **78,** 39-47.

Clarke, I. J., Rao, A., Fallest, P. C. & Shupnik, M. A. (1993). Transcription rate of the FSH-beta gene is reduced by inhibin in sheep but this does not fully explain the decrease in mRNA. *Molecular and Cellular Endocrinology* **91,** 211-216.

Clary, D. O., Griff, I. C. & Rothman, J. E. (1990). SNAPs, a family of NSF attachment proteins involved in intracellular membrane fusion in animals and yeast. *Cell* **61,** 709-721.

Colomer, V., Kicska, G. A. & Rindler, M. J. (1995). Secretory granule content proteins and the Luminal Domains of granule membrane proteins aggregate in vitro at mildly acidic pH. *Journal of Biological Chemistry* **271,** 48-55.

Conn, P. M., Rogers, D. C. & Sandhu, F. S. (1979). Alteration of intracellular calcium level stimulates gonadotropin release from cultured rat pituitary cells. *Endocrinology* **105,** 1122-1127.

Conn, P. M., Marian, J., McMillian, M. & Rogers, D. (1980a). Evidence for calcium mediation of gonadotropin releasing hormone action in the pituitary. *Cell Calcium* **1,** 7-20.

Conn, P. M., Kilpatrick, D. & Kirshner, N. (1980b). Ionophoretic Ca^{2+} mobilization in rat gonadotropes and bovine adrenomedullary cells. *Cell Calcium* **1,** 129-133.

Conn, P. M. (1984). Molecular Mechanism of Gonadotropin-Releasing Hormone Action. *Biochemical Actions of Hormones* **11,** 67-92.

Conn, P. M., Janovick, J. A., Braden, T. D., Maurer, R. A. & Jennes, L. (1992). SIIp - a Unique Secretogranin/Chromogranin of the Pituitary Released in Response to Gonadotropin-Releasing-Hormone. *Endocrinology* **130,** 3033-3040.

Conn, P. M., McArdle, C. A., Andrews, W. V. & Huckle, W. R. (1987). The Molecular-Basis of Gonadotropin-Releasing Hormone (GnRH) Action in the Pituitary Gonadotrope. *Biology of Reproduction* **36,** 17-35.

Conn, P. M., Rogers, D. C. & Seay, S. G. (1983). Structure-function relationships of calcium ion channel antagonists at the pituitary gonadotrope. *Endocrinology* **113,** 1592-1595.

Conn, P. M., Rogers, D. C. (1980c). Gonadotropin release from pituitary cultures following activation of endogenous ion channels. *Endocrinology* **107,** 2133-2134.

Cool, D. R., Normant, E., Shen, F. S., Chen, H. C., Pannell, L., Zhang, Y. & Loh, Y. P. (1997). Carboxypeptidase E is a regulated

secretory pathway sorting receptor: Genetic obliteration leads to endocrine disorders in $Cpe^{(fat)}$ mice. *Cell* **88,** 73-83.

Couzinet, B. & Schaison, G. (1993). The Control Of Gonadotropin-Secretion By Ovarian-Steroids. *Human Reproduction* **8,** 97-101.

Crowley, W. R., McArthur., J. W. (1980). Stimulation of the normal menstrual cycle in Kallmann's syndrome by pulatile administration of luteinizing hormone-releasing hormone (LH-RH). *Journal of Clinical Endocrinology and Metabolism* **51,** 173-175.

Cumming, I. A., Brown, J. M., Blockley, M. A. D., Wilfield, C. G., Baxter, R. & Godling, J. R. (1971). Constancy of the interval between the LH release and ovulation in the ewe. *Journal of Reproduction and Fertility* **24,** 134-135.

Currie, R. J. W. & McNeilly, A. S. (1995). Mobilization Of LH Secretory Granules In Gonadotrophs In Relation to Gene-Expression, Synthesis and Secretion of LH During the Preovulatory Phase of the Sheep Estrous-Cycle. *Journal of Endocrinology* **147,** 259-270.

de Kretser, D. M. & Robertson, D. M. (1989). The isolation and physiology of inhibin and related proteins. *Biology of Reproduction.* **40,** 33-47.

Deftos, L. J. & Abrahamsson, P. A. (1998). Granins and prostate cancer. *Urology* **51,** 141-145.

Deftos, L. J., Fitzgerald, P. A., Wilson, C. B. & O'Connor, D. T. (1987). Chromogranin-A (CgA) is produced by pituitary-tumors. *Clinical Research* **35,** A 646.

del-Pozo, E. & Martin-Perez, J. (1985). Effect of dopamine receptor stimulation on the inhibition of LH pulsatility by a met-enkephalin (FK33-824). *Acta Neurochir. Wien.* **75,** 88-90.

Delegeane, A. M., Ferland, L. H. & Mellon, P. L. (1987). Tissue-Specific Enhancer of the Human Glycoprotein Hormone Alpha-Subunit Gene - Dependence on cyclic AMP-Inducible Elements. *Molecular and Cellular Biology* **7,** 3994-4002.

Delegeane, A. M. & Mellon, P. L. (1987). A Composite Enhancer Regulates the Glycoprotein Hormone Alpha-Subunit Gene Promoter. *Journal of Cellular Biochemistry* 72-72.

Dierschkle, D. L., Bhattachatya, A. N., Atkinson, L. E. & Knobil, E. (1970). Circhorial oscillations of plasma LH levels in the ovariectomized rhesus monkey. *Endocrinology* **87,** 850-853.

Dorrington, J. H., Roller, N. F. & Fritz, I. B. (1975). Effects of follicle-stimulating hormone on cultures of Sertoli cell preparations. *Molecular and Cellular Endocrinology* **3,** 57-70.

Drees, B. M. & Hamilton, J. W. (1994). Processing Of Chromogranin-A By Bovine Parathyroid Secretory Granules - Production and Secretion Of N-Terminal Fragments. *Endocrinology* **134,** 2057-2063.

Eiden, L. E., Huttner, W. B., Mallet, J., O'Connor, D. T., Winkler, H. & Zanini, A. (1987). A Nomenclature Proposal For the Chromogranin/Secretogranin Proteins. *Neuroscience* **21,** 1019-1021.

Eidne, K. A., Sellar, R. E., Couper, G., Anderson, L. & Taylor, P. L. (1992). Molecular cloning and characterisation of the rat pituitary gonadotropin-releasing hormone (GnRH) receptor. *Molecular and Cellular Endocrinology* **90,** R5-R9.

Ellis, G. I., Desjardins, C. & Fraser, H. M. (1983). Control of pulsatile LH release in male rats. *Neuroendocrinology* **37,** 177-183.

Esbenshade, K. L. & Britt, J. H. (1985). Active immunization of gilts against gonadotropin-releasing hormone: effects on secretion of gonadotropins, reproductive function and responses to agonists of gonadotropin-releasing hormone. *Biology of Reproduction* **33,** 569-577.

Eskeland, N. L., Zhou, A., Dinh, T. Q., Wu, H. J., Parmer, R. J., Mains, R. E. & O'Connor, D. T. (1996). Chromogranin-A Processing and Secretion - Specific Role of Endogenous and Exogenous Prohormone Convertases in the Regulated Secretory Pathway. *Journal of Clinical Investigation* **98,** 148-156.

Evans, N. P., Dahl, G. E., Padmanabhan, V., Thrun, L. A. & Karsch, F. J. (1997). Estradiol requirements for induction and maintenance of the gonadotropin-releasing hormone surge: Implications for neuroendocrine processing of the estradiol signal. *Endocrinology* **138,** 5408-5414.

Fasciotto, B. H., Gorr, S.-U., DeFranco, D. J., Levine, M. A. & Cohn, D. V. (1989). Pancreastatin, a presumed product of chromogranin-A (secretory protein-I) processing, inhibits secretion from porcine parathyroid cells in culture. *Endocrinology* **125,** 1617-1622.

Fedorcsak, I. & Ehrenberg, L. (1966). Effects of diethyl pyrocarbonate and methyl methanosulfonate on nucleic acids and nucleases. *Acta Chem. Scand.* **20,** 107.

Feinberg, A. P. & Vogelstein, B. (1983). A technique for radiolabelling DNA restriction endonuclease fragments to high specific activity. *Analytical Biochemistry* **132,** 6-13.

Fiddes, J. C., Talmadge, K. (1984). Structure, expression and evolution of the genes for the human glycoprotein hormones. *Recent Progress in Hormone Research* **40,** 43-74.

Fiete, D., Srivastava, V., Hindsgaul, O. & Baenziger, J. U. (1991). A hepatic reticuloendothelial cell receptor specific for SO4-GalNAcβ1,4GlcNAcβ1,2Manα that mediates rapid clearance of lutropin. *Cell* **67,** 1103-1110.

Fischer-Colbrie, R. (1996). Processing of Chromogranins to Functional Peptides. *Journal of Neurochemistry* **66,** S 14-S 14.

Fischer-Colbrie, R., Gutierrez, J., Hsu, C. M., Iacangelo, A. & Eiden, L. E. (1990). Sequence-Analysis, Tissue Distribution and

Regulation By Cell Depolarization, and 2nd Messengers of Bovine Secretogranin-II (Chromogranin-C) Messenger-RNA. *Journal of Biological Chemistry* **265,** 9208-9213.

Fischer-Colbrie, R., Hagn, C. & Schober, M. (1987). Chromogranin-A, Chromogranin-B, and Chromogranin-C - Widespread Constituents of Secretory Vesicles. *Annals of the New York Academy of Sciences* **493,** 120-134.

Fischer-Colbrie, R. & Schober, M. (1987). Isolation and Characterization of Chromogranin-A, Chromogranin-B, and Chromogranin-C From Bovine Chromaffin Granules and a Rat Pheochromocytoma. *Journal of Neurochemistry* **48,** 262-270.

Fischer-Colbrie, R., Wohlfarter, T., Schmid, K. W., Grino, M. & Winkler, H. (1989). Dexamethasone Induces an Increased Biosynthesis of Chromogranin-A in Rat Pituitary-Gland. *Journal of Endocrinology* **121,** 487.

Fraser, H. M. & McNeilly, A. S. (1982). Effects of immunoneutralization of luteinizing hormone releasing hormone on the estrogen-induced luteinizing hormone and follicle stimulating hormone surges in the ewe. *Biology of Reproduction* **27,** 548-555.

Fraser, H. M. & McNeilly, A. S. (1983). Differential effects of LH-RH immunoneutralization on LH and FSH secretion in the ewe. *Journal of Reproduction and Fertility* **69,** 569-577.

Fritzler, M. J. (1995). Molecular characterization of Golgin-245, a novel Golgi Complex Protein containing a Granin Signature. *Journal of Biological Chemistry* **270,** 31262-31268.

Funakoshi, A., Mikasaka, K., Nakamura, R., Kitani, K., Funakoshi, S., Tamamura, H., Fujii, N. & Yajima, H. (1988). Bioactivity of synthetic human pancreastatin on exocrine pancreas. *Biochemical and Biophysical Research Communications* **156,** 1237-1242.

Furuhashi, M., Ando, H., Bielinska, M., Pixley, M. R., Shikone, T., Hsueh, A. J. W. & Boime, I. (1994). Mutagenesis Of Cysteine Residues In the Human Gonadotropin Alpha-Subunit - Roles Of Individual Disulfide Bonds In Secretion, Assembly, and Biologic Activity. *Journal of Biological Chemistry* **269,** 25543-25548.

Furuichi, T., Yoshikawa, S., Miyawaki, A., Wada, K., Maeda, N. & Mikoshiba, K. (1989). Primary structure and functional expression of the inositol 1,4,5-trisphosphate-binding protein P400. *Nature* **342,** 32-38.

Galindo, E., Rill, A., Bader, M. F. & Aunis, D. (1991). Chromostatin, a 20-amino acid peptide derived from Chromogranin A, inhibits chromaffin cell secretion. *Proceedings of the National Academy of Sciences USA* **88,** 1426-1430.

Gasparri, A., Sidoli, A., Sanchez, L. P., Longhi, R., Siccardi, A. G., Marchisio, P. C. & Corti, A. (1997). Chromogranin A fragments modulate cell adhesion - Identification and characterization of a pro-adhesive domain. *Journal of Biological Chemistry* **272,** 20835-20843.

Gerdes, H.-H., Rosa, P., Phillips, E., Baeuerle, P. A., Frank, R., Argos, P. & Huttner, W. B. (1989). The Primary Structure of Human Secretogranin II, a Widespread Tyrosine-sulfated Secretory Granule Protein That exhibits Low pH- and Calcium-induced Aggregation. *Journal of Biological Chemistry* **20,** 12009-12015.

Gharib, D. S., Roy, A., Wierman, M. E. & Chin, W. W. (1989). Isolation and characterisation of the gene encoding the beta-subunit of rat follicle-stimulating hormone. *DNA* **8,** 339-349.

Gharib, S. D., Wierman, M. E., Shupnik, M. A. & Chin, W. W. (1990). Molecular biology of the pituitary gonadotropins. *Endocrine Reviews* **11,** 177-199.

Gill, B. M., Barbosa, J. A., Dinh, T. Q., Garrod, S. & O'Connor, D. T. (1991). Chromogranin-B - Isolation From Pheochromocytoma, N-Terminal Sequence, Tissue Distribution and Secretory Vesicle Processing. *Regulatory Peptides* **33,** 223-235.

Gomez, G., Udupi, V. & Greeley, G. H. (1997). Interaction of nicotine and a H-2-receptor antagonist, famotidine, on gastrin and chromogranin A expression. *Regulatory Peptides* **69,** 77-82.

Goodman, R. L. & Karsch, F. J. (1980). Control of seasonal breeding in the ewe: importance of changes in response to sex-steroid feedback. *Progress in Reproductive Biology* **5,** 134-154.

Goodman, R. L. & Karsch, F. J. (1981). Control of seasonal breeding in the ewe: importance of changes in response to sex-steroid feedback. Biological Clocks in Seasonal Reproductive Cycles (Eds. B. K. Follett and D. E. Follett) Bristol, John Wright and Sons Ltd. 223-236.

Gorman, C. (1986). High Efficiency Gene Transfer into Mammalian cells. DNA cloning: A Practical Approach . 143-165.

Gorman, C. M., Moffat, L. F. & Howard, B. H. (1982). Recombinant genomes which express chloramphenicol acetyltransferase in mammalian cells. *Molecular and Cellular Biology* **2,** 1044-1051.

Gorospe, W. C. & Conn, P. M. (1987). Agents That Decrease Gonadotropin-Releasing Hormone (GnRH) Receptor Internalization Do Not Inhibit GnRH-Mediated Gonadotrope Desensitization. *Endocrinology* **120,** 222-229.

Gough, J. A. & Murray, N. E. (1983). Sequence diversity among related genes for recognition of specific targets in DNA molecules. *Journal of Molecular Biology* **166,** 1-19.

Graham, F. & Van der Eb, A. (1973). A new technique for the assay of infectivity of human adenovirus 5 DNA. *Virology* **52,** 456.

Greenwald, G. S. & Roy, S. K. (1994). Follicular Development and its Control. Physiology of Reproduction (Eds. E. Knobil and J. D. Neill) New York, Raven Press. 2nd ed. 629-724.

Gumbiner, B. & Kelly, R. B. (1982). Two distinct intracellular pathways transport secretory and membrane glycoproteins to the surface of pituitary tumor cells. *Cell* **28,** 51-59.

Guzman, K., Miller, C. D., Phillips, C. L. & Miller, W. L. (1991). The gene encoding ovine follicle-stimulating hormone β: isolation, characterization, and comparison to a related ovine genomic sequence. *DNA and Cell Biology* **10(8),** 593-601.

Halvorson, L. M., Kaiser, U. B. & Chin, W. W. (1996). Stimulation of Luteinizing Hormone Beta gene Promoter Activity by the Orphan Nuclear Receptor, Steroidogenic Factor-1. *Journal of Biological Chemistry* **271,** 6645-6650.

Hanahan, D. (1983). Studies on transformation of *Escherichia coli* with plasmids. *Journal of Molecular Biology* **166,** 557-580.

Hashimoto, S., Fumagalli, G., Zanini, A. & Meldolesi, J. (1987). Sorting of 3 secretory proteins to distinct secretory granules in acidophilic cells of cow anterior-pituitary. *Journal of Cell Biology* **105,** 1579-1586.

Hauger, R. L., Karsch, F. J. & Foster, D. L. (1977). A new concept for control of the estrous cycle of the ewe based on the temporal relationships between luteinizing hormone, estradiol and progesterone in peripheral serum and evidence that progesterone inhibits tonic LH secretion. *Endocrinology* **101,** 807-817.

Hawes, B. E., Marzen, J. E., Waters, S. B. & Conn, P. M. (1992a). Sodium-Fluoride Provokes Gonadotrope Desensitization to Gonadotropin-Releasing-Hormone (GnRH) and Gonadotrope Sensitization to A23187 - Evidence For Multiple G-Proteins in GnRH Action. *Endocrinology* **130,** 2465-2475.

Hawes, B. E., Waters, S. B., Janovick, J. A., Bleasdale, J. E. & Conn, P. M. (1992b). Gonadotropin-Releasing Hormone-Stimulated Intracellular Ca^{2+} Fluctuations and Luteinizing-Hormone Release can be Uncoupled From Inositol Phosphate Production. *Endocrinology* **130,** 3475-3483.

Helman, L. J., Ahn, T. G., Levine, M. A., Allison, A., Cohen, P. S., Cooper, M. J., Cohn, D. V. & Israel, M. A. (1988). Molecular cloning and primary structure of human chromogranin A (secretory protein I) cDNA. *Journal of Biological Chemistry* **263,** 11559-11563.

Hendy, G. N., Bevan, S., Mattei, M. G. & Mouland, A. J. (1995). Chromogranin-A. *Clinical and Investigative Medicine* **18,** 47-65.

Hillarp, N.-A. (1958). Enzymatic systems involving adenosinephosphates in the adrenaline andnoradrenaline containing granules of the adrenal medulla. *Acta Physiol Scand* **42,** 144-165.

Hixon, J. E., Pimentel, C. A., Weston, P. G., Chafetz, E. P., Shanks, R. D. & Hansel, W. (1983). A luteolytic interaction between oestradiol benzoate and prostaglandin F2α in cattle. *Journal of Animal Science* **56,** 1190-1197.

Holthius, J. C. M., Jansen, E. J. R. & Martens, G. J. M. (1996). Secretogranin III is a Sulfated Protein undergoing Proteolytic Processing in the Regulated Secretory Pathway. *Journal of Biological Chemistry* **271,** 17755-17760.

Holz, R. W., Bittner, M. A., Peppers, S. C., Senter, R. A. & Eberhard, D. A. (1989). MgATP-independent and MgATP-dependent exocytosis. Evidence that MgATP primes adrenal chromaffin cells to undergo exocytosis. *Journal of Biological Chemistry* **264,** 5412-5419.

Horn, F., Windle, J. J., Barnhart, K. M. & Mellon, P. L. (1992). Tissue-Specific Gene-Expression In the Pituitary - the Glycoprotein Hormone Alpha-Subunit Gene Is Regulated By a Gonadotrope-Specific Protein. *Molecular and Cellular Biology* **12,** 2143-2153.

Horton, R. J. E., Francis, H. & Clarke, I. J. (1989). Seasonal and steroid-dependent effects on the modulation of LH secretion in the ewe by intercerebroventricularly administered β–endorphin or naloxone. *Journal of Endocrinology* **122,** 509-517.

Howe, A. (1995). Granins and the Packaging of Luteinising Hormone. Obstetrics and Gynaecology. Edinburgh, MSc Thesis, University of Edinburgh. 1-47.

Hsiao, R. J., Neumann, H. P. H., Parmer, R. J., Barbosa, J. A. & O'Connor, D. T. (1990). Chromogranin-A in Familial Pheochromocytoma - Diagnostic Screening Value, Prediction of Tumor Mass, and Postresection Kinetics Indicating 2-Compartment Distribution. *American Journal of Medicine* **88,** 607-613.

Huckle, W. R. & Conn, P. M. (1987). The Relationship Between Gonadotropin-Releasing Hormone-Stimulated Luteinizing-Hormone Release and Inositol Phosphate Production - Studies With Calcium-Antagonists and Protein Kinase-C Activators. *Endocrinology* **120,** 160-169.

Huckle, W. R. Conn, P. M. (1988). Molecular mechanism of gonadotropin releasing hormone action. II. The effector system. *Endocrine Reviews* **9,** 387-395.

Huttner, W. B. & Natori, S. (1995). Regulated Secretion - Helper Proteins For Neuroendocrine Secretion. *Current Biology* **5,** 242-245.

Iacangelo, A., Affolter, H. U., Eiden, L. E., Herbert, E. & Grimes, M. (1986). Bovine chromogranin A sequence and distribution of its messenger RNA in endocrine tissues. *Nature* **323,** 82-86.

Iacangelo, A. L. & Eiden, L. E. (1995). Chromogranin-A - Current Status as a Precursor For Bioactive Peptides and a Granulogenic/Sorting Factor In the Regulated Secretory Pathway. *Regulatory Peptides* **58,** 65-88.

Iacangelo, A. L., Fischer-Colbrie, R., Koller, K. J., Brownstein, M. J. & Eiden, L. E. (1988). The Sequence of Porcine Chromogranin-A Messenger-RNA Demonstrates Chromogranin-A Can Serve as the Precursor For the Biologically-Active Hormone, Pancreastatin. *Endocrinology* **122,** 2339-2341.

Iacangelo, A. L., Grimes, M. & Eiden, L. E. (1991). The bovine chromogranin A gene: structural basis for hormone regulation and generation of biologically active peptides. *Molecular Endocrinology* **5,** 1651-1660.

Illing, N., Jacobs, G. F. M., Becker, I. I., Flanagan, C. A., Davidson, J. S., Eales, A., Zhou, W., Sealfon, S. C. & Millar, R. P. (1993). Comparative sequence analysis and functional characterization of the cloned sheep gonadotropin-releasing hormone receptor reveal differences in primary structure and ligand specificity among mammalian receptors. *Biochemical and Biophysical Research Communications* **196,** 745-751.

Ischia, R., Lovisetti-Scamihorn, P., Hogue-Angeletti, R., Wolkersdorfer, M., Winkler, H. & Fischer-Colbrie, R. (1997). Molecular cloning and characterisation of NESP55, a Novel Chromogranin-like precursor of a Peptide with 5-HT1B Receptor Antagonist Activity. *Journal of Biological Chemistry* **272,** 11657-11662.

Ishizuka, J., Tatemoto, K., Cohn, D. V., Thompson, J. C. & Greeley Jr, G. H. (1991). Effects of pancreastatin and chromogranin A on insulin release stimulated by various insulinotrophic agents. *Regulatory Peptides* **34,** 25-32.

Izumi, S., Stojilkovic, S. S., Iida, T., Krsmanovic, T., Omelijanivk, R. J. & Catt, K. J. (1990). Role of voltage-sensitive calcium channels in $[Ca^{2+}]i$ and secretory responses to activators of protein kinase C in pituitary gonadotrophs. *Biochemical and Biophysical Research Communications* **170,** 359-367.

Jackson, G. L., Thurmon, J. & Nelson, D. (1975). Estrogen-induced release of LH in the ovariectomized ewe: independence of time of day. *Biology of Reproduction* **13,** 358-362.

Jacobsson, G. & Meister, B. (1996). Molecular-Components Of the Exocytotic Machinery In the Rat Pituitary-Gland. *Endocrinology* **137,** 5344-5356.

Jameson, J. L., Becker, C. B., Lindell, C. M. & Habener, J. F. (1988a). Human follicle-stimulating hormone beta-subunit gene encodes multiple messenger ribonucleic acids. *Molecular Endocrinology* **2,** 806-815.

Jameson, L. J., Deutsch, P. J., Gallagher, G. D., Jaffe, R. C. & Habener, J. F. (1987). *trans*-Acting Factors Interact with a Cyclic AMP Response Element to Modulate Expression of the Human Gonadotropin alpha gene. *Molecular and Cellular Endocrinology* **7,** 3032-3040.

Jameson, J. L., Jaffe, R. C., Deutsch, P. J., Albanese, C. & Habener, J. (1988b). The gonadotrophin alpha-gene contains multiple protein binding domains that interact to modulate basal and cAMP-responsive transcription. *Journal of Biological Chemistry* **263,** 9879-9886.

Jameson, J. L. & Lindell, C. M. (1988). Isolation and characterization of the human chorionic gonadotrophin beta subunit (CG beta) gene cluster:

Regulation of transcriptionally active CG beta gene by cyclic AMP. *Molecular and Cellular Biology* **8,** 5100-5107.

Janovick, J. A., Jennes, L. & Conn, P. M. (1995). GH_3 Cells Transfected With Gonadotropin-Releasing-Hormone (GnRH) Receptor Complementary Deoxyribonucleic-Acid Release Secretogranin-II Through a Constitutive Pathway After GnRH Analog-Regulated Synthesis - Evidence That Secretory Proteins Do Not Contain a Sequence That Obligates Processing Through a Secretory Granule or By Regulated Secretion. *Endocrinology* **136,** 202-208.

Jenkins, N. A., Mattei, M. G., Gilbert, D. J., Linard, C. G., Mbikay, M., Chretien, M. & Copeland, N. G. (1991). Assignment of secretogranin I locus to mouse chromosome 2 by *in situ* hybridisation and interspecific backcross analysis. *Genomics* **11,** 479-480.

Jennes, L., Eyigor, O., Janovick, J. A. & Conn, P. M. (1997). Brain gonadotropin releasing hormone receptors: Localization and regulation. *Recent Progress in Hormone Research* **52,** 475-491.

Jin, L., Scheithauer, B. W., Young, W. F., Davis, D. H., Klee, G. G. & Lloyd, R. V. (1996). Pancreastatin Secretion By Pituitary-Adenomas and Regulation Of Chromogranin-B Messenger-RNA Expression. *American Journal Of Pathology* **148,** 2057-2066.

Jirgensons, B. & Ward, D. N. (1970). Circular dichroism of ovine luteinizing hormone and its subunits. *Tex Rep Biol Med* **28,** 553-559.

Johnson, M. S., MacEwan, D. J., Simpson, J. & Mitchell, R. (1993). Characterisation of protein kinase C isoforms and enzymatic activity from the alpha-T3-1 gonadotroph-derived cell line. *FEBS Letters* **333,** 67-72.

Jones, L. C., Day, R. N., Pittler, S. J., Valentine, D. L. & Scammell, J. G. (1996). Cell-Specific Expression Of the Rat Secretogranin-II Promoter. *Endocrinology* **137,** 3815-3822.

Jones, L. C. & Scammel, J. G. (1998). The cAMP-response element mediates induction of secretogranin II by cycloheximide and forskolin in GH4C1 cells. *American Journal of Physiology* **274,** E656-664.

Kakar, S. S., Musgrove, L. C., Devor, D. C., Sellers, J. C. & Neill, J. D. (1992). Cloning, sequencing and expression of human gonadotropin releasing hormone (GnRH) receptor. *Biochemical and Biophysical Research Communications* **189,** 289-295.

Kang, Y. K. & Yoo, S. H. (1997). Identification of the secretory vesicle membrane binding region of chromogranin A. *FEBS Letters* **404,** 87-90.

Karsch, F. J., Foster, D. L., Bittman, E. L. & Goodman, R. L. (1983). A role for estradiol in enhancing luteinizing hormone pulse frequency during the follicular phase of the estrous cycle of sheep. *Endocrinology* **113,** 1333.

Karsch, F. J., Noveroske, J. W., Roche, J. F., Norton, H. W. & Nalbandov, A. V. (1970). Maintenance of ovine corpora lutea in the absence of ovarian follicles. *Endocrinology* **87,** 1228-1236.

Katayama, T. & Conn, P. M. (1994). Activin Modulates the Intracellular Signaling System Activated By Gonadotropin-Releasing-Hormone - Dual Effect On Calcium Messenger System and Protein-Kinase-C Pathway. *Endocrinology* **134,** 119-125.

Keene, J. L., Matzuk, M. M., Otani, T., Fauser, B., Galway, A. B., Hsueh, A. J. W. & Boime, I. (1989). Expression of Biologically-Active Human Follitropin in Chinese Hamster Ovary Cells. *Journal of Biological Chemistry* **264,** 4769-4775.

Keisel, L. (1993). Molecular mechanisms of gonadotrophin releasing hormone-stimulated gonadotrophin secretion. *Human Reproduction* **8,** 23-28.

Kendall, S. K., Samuelson, L. C., Saunders, T. L., Wood, R. I. & Camper, S. A. (1995). Targeted Disruption Of the Pituitary Glycoprotein Hormone Alpha-Subunit Produces Hypogonadal and Hypothyroid Mice. *Genes & Development* **9,** 2007-2019.

Kennedy, G., Anderson, B., Nilson, J. (1990). The human alpha subunit glycoprotein hormone gene utilizes a unique CCAAT binding factor. *Journal of Biological Chemistry* **265,** 6279-6285.

Keri, R. A., Andersen, B., Kennedy, G. C., Hamernik, D. L., Clay, C. M., Brace, A. D., Nett, T. M., Notides, A. C. & Nilson, J. H. (1991). Estradiol inhibits transcription of the human glycoprotein hormone alpha-subunit gene despite the absence of a high affinity binding site for estrogen receptor. *Molecular Endocrinology* **5,** 725-733.

Keri, R. A. & Nilson, J. H. (1996). A Steroidogenic Factor-1 binding site is required for activity of Luteinizing Hormone Beta Subunit Promoter in Gonadotropes of Transgenic Mice. *Journal of Biological Chemistry* **271,** 10782-10785.

Kim, K. E., Day, K. H., Howard, P., Salton, S. R. J., Roberts, J. L. & Maurer, R. A. (1990). DNA sequences required for expression of the LHβ promotor in primary cultures of rat pituitary cells. *Molecular and Cellular Endocrinology* **74,** 101-107.

Kim, K. E., Gordon, D. F. & Maurer, R. A. (1988). Nucleotide sequence of the bovine gene for follicle-stimulating hormone beta-subunit. *DNA* **7,** 227-233.

Kishimoto, A., Takai, Y., Mori, T., Kikkawa, U. & Nishizuka, Y. (1980). Activation of calcium and phospholipid-dependant protein kinase by diacylglycerol, its possible relation to phosphatidylinositol turnover. *Journal of Biological Chemistry* **255,** 2272-2276.

Knobil, E. (1981). Patterns of hypophysiotropic signals and gonadotrophin secretion in the rhesus monkey. *Biology of Reproduction.* **24,** 44-49.

Knobil, E., Plant, T. M., Wildt, L., Belchetz, P. E. & Marshall, G. (1980). Control of the rhesus monkey menstrual cycle: permissive role of hypothalamic gonadotropin-releasing hormone. *Science* **207,** 1371-1373.

Koch, Y., Chobsieng, P., Zor, U., Fridkin, M. & Lindner, H. R. (1973). Suppression of gonadotrophin secretion and prevention of ovulation in the rat by antiserum to synthetic gonadotrophin releasing hormone. *Biochemical and Biophysical Research Communications* **55,** 623-629.

Kohler, P. O. & Bridson, W. E. (1971). Isolation of Hormone-producing Clonal Cell Lines of Human Choriocarcinoma. *Journal of Clinical Endocrinology* **32,** 683-687.

Kourides, I. A., Landon, M. B., Hoffman, B. J. & Weintraub, B. D. (1980). Excess free alpha relative to beta subunits of the glycoprotein hormones in normal and abnormal human pituitary glands. *Clinical Endocrinology* **12,** 407.

Krisch, K., Horvat, G., Krisch, I., Wengler, G., Alibeik, H., Neuhold, N., Ulrich, W., Braun, O. & Hochmeister, M. (1988). Immunochemical characterization of a novel secretory protein (defined by monoclonal antibody HISL-19) of peptide hormone producing cells which is distinct from chromogranin A, B, and C. *Laboratory Investigation* **58,** 411-420.

Kromer, A., Glombik, M. M., Huttner, W. B. & Gerdes, H. H. (1998). Essential role of the disulfide-bonded loop of chromogranin B for sorting to secretory granules is revealed by expression of a deletion mutant in the absence of endogenous granin synthesis. *Journal of Cell Biology* **140,** 1331-1346.

Kumar, T. R., Wang, Y., Lu, N. F. & Matzuk, M. M. (1997). Follicle stimulating hormone is required for ovarian follicle maturation but not male fertility. *Nature Genetics* **15,** 201-204.

Laemmli, U. K. (1970). Cleavage of structural proteins during the assembly of the head of bacteriophage T4. *Nature* **227,** 680.

Lahlou-Kassi, A., Schams, D. & Glatzel, P. (1984). Plasma gonadotrophin concentrations during the oestrous cycle and after ovariectomy in two breeds of sheep with high and low fecundity. *Journal of Reproduction and Fertility* **70,** 165-173.

Lapthorn, A. J., Harris, D. C., Littlejohn, A., Lustbader, J. W., Canfield, R. E., Machin, K. J., Morgan, F. J. & Isaacs, N. W. (1994). Crystal structure of human chorionic gonadotrophin. *Nature* **369,** 455-461.

Laverriere, J. N., Richard, J. L., Morin, A., Buisson, N., Tixier-Vidal, A., Huttner, W. B. & Gourdji, D. (1991). Secretogranin I (chromogranin B) mRNA accumulation is hormonally regulated in GH3B6 rat pituitary tumor cells. *Mollecular and Cellular Biology* **80,** 41-51.

Lee, S. L., Sadovsky, Y., Swirnhoff, A. H., Polish, J. A., Goda, P., Gavrilina, G. & Milbrandt, J. (1996). Luteinizing Hormone Deficiency and Female Infertility in Mice Lacking the Transcription Factor NGFI-A (Egr-1). *Science* **273,** 1219-1221.

Legerski, R. J. & Robberson, D. L. (1985). Analysis and optimization of recombinant DNA joining reactions. *Journal of Molecular Biology* **181,** 297-312.

Lehman, M. N., Robinson, J. E., Karsch, F. J. & Silverman, A. J. (1986). Immnuocytochemical localization of luteinizing hormone-releasing hormone (LHRH) pathways in the sheep brain during anestrous and the mid luteal phase of the estrous cycle. *J.ournal of Comparative Neurology* **244,** 19-35.

Levine, J. E., Pau, K.-Y., Ramirez, V. D. & Jackson, G. I. (1982). Simultaneous measurement of luteinizing hormone-releasing hormone and luteinizing hormone release in unanaesthetized, ovariectomized sheep. *Endocrinology* **111,** 1449-1455.

Lewis, C. E., Richards, P. S. M. & Morris, J. F. (1989). Heterogeneity of responses to LH-releasing hormone and phorbol ester among rat gonadotrophs: a study using a reverse haemolytic plaque assay for LH. *Journal of Molecular Endocrinology* **2,** 55-63.

Lewis, J. J., Zdon, M. J., Adrian, T. E. & Modlin, I. M. (1988). Pancreastatin, a novel peptide inhibitor of parietal cell secretion. *Surgery* **104,** 1031-1036.

Leyendecker, G., Wildt, L. & Hansmann, M. (1980). Pregnancies following chronic intermittent (pulsatile) administration of GnRH by means of a portable pump (Zyklomat): a new approach in the treatment of fertility in hypothalamic amenorrhea. *Journal of Clinical Endocrinology and Metabolism* **51,** 1214-1216.

Li, C. H., Starman, B., (1964). Molecular weight of sheep pituitary interstitial cell-stimulating hormone. *Nature* **202,** 291-292.

Liao, T.-H., Pierce, J.G. (1970). The presence of a common type of subunit in bovine thyroid-stimulating and luteinizing hormones. *Journal of Biological Chemistry* **245,** 3275-3281.

Lincoln, G. A. & Fraser, H. M. (1979). Blockade of episodic secretion of luteinizing hormone in the ram by administration of antibodies to luteinizing hormone releasing hormone. *Biology of Reproduction* **21,** 1239-1245.

Mahata, S. K., Kozak, C. A., Szpirer, J., Szpirer, C., Modi, W. S., Gerdes, H. H., Huttner, W. B. & O'Connor, D. T. (1996). Dispersion of Chromogranin/Secretogranin Secretory Protein Family Loci in Mammalian Genomes. *Genomics* **33,** 135-139.

Marshall, C. J. (1991). Tumor Suppressor Genes. *Cell* **64,** 313-326.

Martens, G. J. M. (1988). Cloning and sequence analysis of human pituitary cDNA encoding the novel polypeptide 7B2. *FEBS Letters* **234,** 160-164.

Matzuk, M. M. & Boime, I. (1989). Mutagenesis and gene transfer define site-specific roles of the gonadotropin oligosaccharides. *Biology of Reproduction* **40,** 48-53.

Matzuk, M. M., Keene, J. L. & Boime, I. (1989). Site Specificity of the Chorionic-Gonadotropin N-Linked Oligosaccharides in Signal Transduction. *Journal of Biological Chemistry* **264,** 2409-2414.

Matzuk, M. M., Spangler, M. M., Camel, M., Suganuma, N. & Boime, I. (1989). Mutagenesis and Chimeric Genes Define Determinants in the Beta- Subunits of Human Chorionic-Gonadotropin and Lutropin For Secretion and Assembly. *Journal of Cell Biology* **109,** 1429-1438.

McArdle, C. A., Forrestowen, W., Davidson, J. S., Fowkes, R., Bunting, R., Mason, W. T., Poch, A. & Kratzmeier, M. (1996). Ca^{2+} Entry In Gonadotrophs and αT3-1 Cells - Does Store- Dependent Ca^{2+} Influx Mediate Gonadotropin-Releasing-Hormone Action. *Journal Of Endocrinology* **149,** 155-169.

McNatty, K. P., Gibb, M., Dobson, C., Thurley, D. C. & Findlay, J. K. (1981). Changes in the concentration of gonadotrophic and steroidal hormones in the antral fluid of ovarian follicles throughout the oestrous cycle of the sheep. *Australian Journal of Biological Science* **34,**

McNeilly, A. S. (1984). Changes in FSH and the pulsatile secretion of LH during the delay in oestrus induced by treatment of ewes with bovine follicular fluid. *Journal of Reproduction and Fertility* **72,** 165-172.

McNeilly, A. S., Picton, H. M., Campbell, B. K. & Baird, D. T. (1991a). Gonadotrophic control of follicle growth in the ewe. *Journal of Reproduction and Fertility Suppl* **43,** 177-186.

McNeilly, J. R., Brown, P., Clark, A. J. & McNeilly, A. S. (1991b). Gonadotropin-Releasing-Hormone Modulation Of Gonadotropins In the Ewe - Evidence For Differential-Effects On Gene-Expression and Hormone-Secretion. *Journal of Molecular Endocrinology* **7,** 35-43.

Midgley, A. R., McFadden, K., Ghazzi, M., Karsch, F. J., Brown, M. B., Mauger, D. T. & Padmanabhan, V. (1997). Nonclassical secretory dynamics of LH revealed by hypothalamo-hypophyseal portal sampling of sheep. *Endocrine* **6,** 133-143.

Milenkovic, L., D'Angelo, G., Kelly, P. A. & Weiner, R. I. (1994). Inhibition of gonadotropin hormone-releasing hormone release by prolactin from GT1 Neuronal cell lines through prolactin receptors. *Proceedings of the National Academy of Sciences USA* **91,** 1244-1247.

Milsted, A., Cox, R. P. & Nilson, J. H. (1987). Cyclic AMP regulates transcriptional control of the genes encoding human chorionic gonadotrophin with different kinetics. *DNA* **6,** 213-219.

Mise, T. & Bahl, O. P. (1980). Assignment of disulphide bonds in the alpha subunit of human chorionic gonadotrophin. *Journal of Biological Chemistry* **255,** 8516-8522.

Misro, M. M. & Conn, P. M. (1988). Isolation and characterization of gonadotropin-rich secretory granules from rat: depletion by GnRH and by a high affinity agonist. *Molecular and Cellular Endocrinology* **55,** 131-140.

Mocharla, H., Mocharla, R. & Hodes, M. E. (1990). Coupled reverse transcription-polymerase chain reaction (RT-PCR) as a sensitive and rapid method for isoenzyme genotyping. *Gene* **93,** 271-275.

Moenter, S. M., Caraty, A., Locatelli, A. & Karsch, F. J. (1991). Pattern of gonadotropin-releasing hormone (GnRH) secretion leading up to ovulation in the ewe: Existence of a preovulatory GnRH surge. *Endocrinology* **129,** 1175-1182.

Moore, R. M. (1974). The ovarian follicle of the sheep: inhibition of oestrogen secretion by luteinizing hormone. *Journal of Endocrinology* **61,** 455-463.

Mooseker, M. S. & Cheney, R. E. (1995). Unconventional Myosins. *Annual Review of Cell and Developmental Biology* **11,** 633-676.

Morgan, F. J., Canfield, R.E. (1971). Nature of the subunits of human chorionic gonadotrophin. *Endocrinology* **88,** 1045-1053.

Mouland, A. J., Bevan, S., White, J. H. & Hendy, G. N. (1994). Human Chromogranin A gene: molecular cloning, structural analysis, and neuroendocrine cell-specific expression. *Journal of Biological Chemistry* **269,** 6918-6926.

Mountford, P. S., Brandon, M. R. & Adams, T. E. (1992). Removal of the 3' untranslated sequences dramatically enhances transient expression of ovine follicle-stimulating hormone beta gene messenger RNA. *Journal of Neuroendocrinology* **4,** 655-658.

Muller, L., Barret, A., Picart, R. & Tougard, C. (1997). Proteolytic processing of sulfated secretogranin II in the *trans*-Golgi network of GH3B6 prolactin cells. *Journal of Biological Chemistry* **272,** 3669-3673.

Muller, L. & Tougard, C. (1995). Production and Secretion Of N-Terminal Secretogranin-II Derived Peptides In GH3B6 Prolactin Cells. *Molecular and Cellular Endocrinology* **112,** 101-112.

Mullis, K., Faloona, F., Scharf, S., Saiki, R., Horn, G. & Erlich, H. (1986). Specific enzymatic amplification of DNA in vitro: the polymerase chain reaction. *Cold Spring Harbour Symposium of Quantitative Biology* **51,** 263-273.

Murray, S. S., Deaven, L. L., Burton, D. W., O'Connor, D. T., Mellon, P. L. & Deftos, L. J. (1987). The Gene For Human Chromogranin-A (CgA) Is Located On Chromosome-14. *Biochemical and Biophysical Research Communications* **142,** 141-146.

Muyan, M., Furuhashi, M., Sugahara, T. & Boime, I. (1996). The Carboxy-Terminal Region of the Beta-Subunits of Luteinizing Hormone and Chorionic Gonadotropin Differentially Influence Secretion and Assembly of the Heterodimers. *Molecular Endocrinology* **10,** 1678-1687.

Muyan, M., Ryzmkiewicz, D. M. & Boime, I. (1994). Secretion of Lutropin and Follitropin From Transfected GH_3 Cells - Evidence For Separate Secretory Pathways. *Molecular Endocrinology* **8,** 1789-1797.

Naar, A., Boutin, J.-M., Lipki, S., Yu, V., Holloway, J., Glass, C. & Rosenfeld, M. (1991). The orientation and spacing of core DNA-binding motifs dictate selective transcriptional responses to three nuclear receptors. *Cell* **65,** 1267-1279.

Nagayama, Y., Russo, D., Chazenbalk, G. D., Wadsworth, H. L. & Rapport, B. (1990). Extracellular domain chimeras of the TSH and LH/CG receptors reveal the mid-region (amino acids 171-260) to play a vital role in high affinity TSH binding. *Biochemical and Biophysical Research Communications* **173,** 1150-1156.

Naor, Z., Harris, D. & Shacam, S. (1998). Mechanism of GnRH Receptor Signalling: Combinatorial Cross-talk of calcium and Protein Kinase C. *Frontiers in Neuroendocrinology* **19,** 1-19.

Natori, S., King, A., Hellwig, A., Weiss, U., Iguchi, H., Tsuchiya, B., Kameya, T., Takayanagi, R., Nawata, H. & Huttner, W. B. (1998). Chromogranin B (secretogranin I), a neuroendocrine-regulated secretory protein, is sorted to exocrine secretory granules in transgenic mice. *EMBO Journal* **17,** 3277-3289.

Naylor, S. L., Chin, W. W., Goodman, H. M., P.A., L., Grzeschik, K. H. & Sakaguchi, A. Y. (1983). Chromosome assignment of genes encoding the alpha and beta subunits of glycoprotein hormone in man and mouse. *Somatic Cell Genetics* **9,** 757-770.

Neuhold, N. & Ullrich, R. (1993). Secretogranin IV immunoreactivity in medullary thyroid carcinoma: an immunohistochemical study of 62 cases. *Virchows Arch A Pathol Anat Histopatol* **423,** 85-89.

Nickolics, K., Mason, A. J., Szonyi, E., Ramachandran, R. & Seeburg, P. H. (1985). A prolactin inhibiting factor within the precursor for human gonadotrophin releasing hormone. *Nature* **316,** 511-517.

Nolan, E. M., Cheung, T. C., Burton, D. W. & Deftos, L. J. (1996). Transcriptional regulation of the human chromogranin A gene by its 5' distal regulatory element: Novel effects of orientation, structure, flanking sequences, and position on expression. *Molecular and Cellular Endocrinology* **124,** 51-62.

Nolan, E. M., Helman, L. J., Burton, D. W. & Deftos, L. J. (1994). Cloning Of the Human Chromogranin-A Promoter and Identification of a Sequence That Possesses Enhancer-Like Activity. *Endocrine* **2,** 891-897.

Normant, E. & Loh, Y. P. (1998). Depletion of carboxypeptidase E, a regulated secretory pathway sorting receptor, causes misrouting and constitutive secretion of proinsulin and proenkephalin, but not chromogranin A. *Endocrinology* **139,** 2137-2145.

O'Connor, D. T. (1983). Chromogranin - Widespread Immunoreactivity in Polypeptide Hormone Producing Tissues and in Serum. *Regulatory Peptides* **6,** 263-280.

O'Connor, D. T. (1984). Human-Plasma Chromogranin-A (CgA) - Detection By Radioimmunoassay (RIA), and Elevation in Pheochromocytoma and in Essential-Hypertension. *Clinical Research* **32,** A336.

O'Connor, D. T. (1985). Plasma Chromogranin-A - Initial Studies in Human Hypertension. *Hypertension* **7,** I-79.

Orci, L., Ravazzola, M., Amherdt, M., Perrelet, A., Powell, S. K., Quinn, D. L. & Moore, H.-P. H. (1987). The *trans*-most cisternae of the Golgi complex; a compartment for sorting of secretory and plasma membrane proteins. *Cell* **51,** 1039-1051.

Ornberg, R. L., Furuya, S., Goping, G. & Kuijpers, G. A. J. (1995). Granule swelling in stimulated bovine adrenal chromaffin cells: regulation by internal granule pH. *Cell and Tissue Research* **279,** 85-92.

Ortmann, O., Stojilkovic, S. S., Cesnjaj, M., Emons, G. & Catt, K. J. (1992). Modulation of cytoplasmic calcium signaling in rat pituitary gonadotrophs by estradiol and progesterone. *Endocrinology* **131(3),** 1565-1567.

Ottiger, H.-P., Battenberg, E. F., Tsou, A. P., Bloom, F. E. & Sutcliffe, J. G. (1990). 1B1075: a brain- and pituitary-specific mRNA that encodes a novel chromogranin/secretogranin-like component of intracellular vesicles. *Journal of Neuroscience.* **10,** 3135-3147.

Padmanabhan, V., McFadden, K., Mauger, D. T., Karsch, F. J. & Midgley, R. (1997). Neuroendocrine control of follicle-stimulating hormone (FSH) secretion .1. Direct evidence for separate episodic and basal components of FSH secretion. *Endocrinology* **138,** 424-432.

Pant, H. C., Hopkinson, C. R. N. & Fitzpatrick, R. J. (1977). Concentrations of oestradiol, progesterone, luteinizing hormone and follicle stimulating hormone in the jugular venous plasma of ewes during the oestrous cycle. *Journal of Endocrinology* **73,** 247-255.

Parsons, T. F., Bloomfield, G. A. & Pierce, J. G. (1983). Purification of an alternate form of the alpha subunit of the glycoprotein hormones from bovine pituitaries and identification of its O-linked oligosaccharide. *Journal of Biological Chemistry* **258,** 240-244.

Paul, S. J., Ortolano, G. A., Haisenleder, D. J., Stewart, J. M., Shupnik, M. A. & Marshall, J. C. (1990). Gonadotropin subunit messenger RNA concentrations after blockade of gonadotropin-releasing hormone action: testosterone selectively increases follicle-stimulating hormone beta-subunit messenger RNA by posttranscriptional mechanisms. *Molecular Endocrinology* **4,** 1943-1955.

Perheentupa, A., Bergendahl, M., Dejong, F. H. & Huhtaniemi, I. (1993). Differential Regulation Of FSH and Inhibin Gene-Expression and Synthesis By Testosterone In Immature and Mature Male-Rats. *Journal of Endocrinology* **137,** 69-79.

Picton, H. M., Tsonis, C. G. & McNeilly, A. S. (1990). FSH causes a time-dependent stimulation of preovulatory follicle growth in the absence

of pulsatile LH secretion in ewes chronically treated with gonadotrophin-releasing hormone agonist. *Journal of Endocrinology* **126,** 297-307.

Pohl, T. M., Philips, E., Song, K. & Gerdes, H.-H. (1990). The organization of the mouse chromogranin B (secretogranin I) gene. *FEBS Letters* **262,** 219-224.

Puck, T. T., Cieciura, S. J. & Robinson, A. (1958). Genetics of Somatic Mammalian Cells. III Long-term cultivation of euploid cells from human and animal subjects. *Journal of Experimental Medicine* **108,** 945-955.

Rao, K., Paik, W. Y., Zheng, L. X., Jobin, R. M., Tomic, M., Jiang, H., Nakanishi, S. & Stojilkovic, S. S. (1997). Wortmannin-sensitive and -insensitive steps in calcium-controlled exocytosis in pituitary gonadotrophs: Evidence that myosin light chain kinase mediates calcium-dependent and wortmannin-sensitive gonadotropin secretion. *Endocrinology* **138,** 1440-1449.

Reader, S. C. J., Robertson, W. R. & Diczfalusy, E. (1983). Microheterogeneity of luteinizing hormone in pituitary glands from women of pre- and postmenopausal age. *Clinical Endocrinology* **19,** 355-363.

Reinhart, J., Mertz, L. M. & Catt, K. J. (1992). Molecular cloning and expression of cDNA encoding the murine gonadotropin-releasing hormone receptor. *Journal of Biological Chemistry* **267,** 21281-21284.

Robinson, LJ. & Martin, T.F.J. (1998) Docking and fusion in neurosecretion. *Current Opinion in Cell Biology*, **10**, (4), p483-492.

Roche, J. F. (1996). Control and Regulation of folliculogenesis - a symposium in perspective. *Reviews in Reproduction* **1,** 19-27.

Rosa, P., Bassetti, M., Weiss, U. & Huttner, W.B. (1992). Widespread Occurence of Chromogranins/Secretogranins in the Matrix of Secretory Granules of Endocrinologically Silent Pituitary Adenomas *Journal of Histochemistry and Cytochemistry* **40,** 523-533.

Rosen, C. B. & Weber, G. (1969). Dimer formation from 1-anilino-8-naphthalenesulfonate catalyzed by Bovine serum albumin. A new fluorescent molecule with exceptional binding properties. *Biochemistry* **8,** 3915-3920.

Sairam, M. R., Seidah, N. G. & Chretien, M. (1981). Primary structure of the ovine pituitary follitropin beta subunit. *Biochemical Journal* **197,** 541-552.

Salmonsen, L. A., O, W.-S., Doughton, B. & Findlay, J. K. (1985). The effects of estrogen and progesterone in vivo on protein synthesis and secretion by cultured epithelial cells from sheep endometrium. *Endocrinology* **117,** 2148-2159.

Sambrook, J., Fritsch, E. F. & Maniatis, T. (1989). Molecular Cloning - A laboratory manual. New York, Cold Spring Harbour.

Santoro, N., Filicori, M. & Crowley W. F. (1986). Hypogonadotropic disorders in men and women: diagnosis and therapy with pulsatile gonadotropin-releasing hormone. *Endocrine Reviews* **7,** 11-23.

Sarafian, T., Aunis, D. & Bader, M.-F. (1987). Loss of proteins from digitonin-permeabilized adrenal chromaffin cells essential for exocytosis. *Journal of Biological Chemistry* **262,** 16671-16676.

Saria, A., Troger, J., Kirchmair, R., Fischer-Colbrie, R., Hogueangeletti, R. & Winkler, H. (1993). Secretoneurin Releases Dopamine From Rat Striatal Slices - a Biological Effect of a Peptide Derived From Secretogranin-II (Chromogranin-C). *Neuroscience* **54,** 1-4.

Sato, A., Perlas, E., BenMenahem, D., Kudo, M., Pixley, M. R., Furuhashi, M., Hsueh, A. J. W. & Boime, I. (1997). Cystine knot of the gonadotropin alpha subunit is critical for intracellular behavior but not for in vitro biological activity. *Journal of Biological Chemistry* **272,** 18098-18103.

Sato, S. (1980). Postnatal development, sexual difference and sexual cyclic variation of prolactin cells in rats: special reference to the topographic affinity to gonadotroph. *Endocrinology Japan* **27,** 573-583.

Scaramuzzi, R. J., Adams, N. R., Baird, D. T., Campbell, B. K., Downing, J. A., Findlay, J. K., Henderson, K. M., Martin, G. B., McNatty, K. P., McNeilly, A. S. & Tsonis, C. G. (1993). A model for follicle selection and the determination of ovulation rate in the ewe. *Reproduction , Fertility and Development.* **5,** 459-478.

Schally, A. V., Arimura, A., Kastin, A. J., Matsuo, H., Baba, Y., Redding, T. W., Nair, R. M. G. & Debeljuk, L. (1971). The gonadotrophin-releasing hormone: one peptide regulates the secretion of luteinizing hormone and follicle stimulating hormones. *Science* **173,** 1036-1038.

Schimmel, A., Braunling, O., Ruther, U., Huttner, W. B. & Gerdes, H. H. (1992). The organisation of the mouse secretogranin II gene. *FEBS Letters* **314,** 375-380.

Schmid, K. W., Kroll, M., Hittmair, A., Maier, H., Totsch, M., Gasser, R., Finkenstett, G., Hogueangeletti, R. & Fischer-Colbrie, R. (1991). Chromogranin-A and Chromogranin-B in Adenomas of the Pituitary - an Immunohistochemical Study of 42 Cases. *American Journal of Surgical Pathology* **15,** 1072-1077.

Schmid, K. W., Schroder, S., Dockhorndworniczak, B., Kirchmair, R., Totsch, M., Bocker, W. & Fischer-Colbrie, R. (1994). Immunohistochemical Demonstration of Chromogranin-A, Chromogranin-B, and Secretogranin-II in Extraadrenal Paragangliomas. *Modern Pathology* **7,** 347-353.

Schneider, F. H., Smith, A. D. & Winkler, H. (1967). Secretion from the adrenal medulla: biochemical evidence for exocytosis. *BR. Journal of Pharmacology and Chemotherapy* **31,** 94-104.

Schvartz, I. & Hazum, E. (1987). Internalization and recycling of receptor-bound gonadotropin-releasing hormone agonist in pituitary gonadotropes. *Journal of Biological Chemistry* **262,** 17046-17050.

Sealfon, S. C., Laws, S. C., Wu, J. C., Gillo, B. & Miller, W. L. (1990). Hormonal regulation of gonadotropin-releasing hormone receptors and messenger RNA activity in ovine pituitary culture. *Molecular Endocrinology* **4,** 1980-1987.

Secco, G. B., Campora, E., Fardelli, R., Lapertosa, G., Delucchi, F., Gianquinto, D. & Bonfante, P. (1996). Chromogranin-A Expression In Neoplastic Neuroendocrine Cells and Prognosis In Colorectal-Cancer. *Tumori* **82,** 390-393.

Seidah, N. G., Hendy, G. N., Hamelin, J., Paquin, J., Lazure, C., Metters, K. M., Rossier, J. & Chretien, M. (1987). Chromogranin A can act as a reversible processing enzyme inhibitor. Evidence from the inhibition of the IRCM-serine protease 1 cleavage of pro-enkephalin and ACTH at pairs of basic amino acids. *FEBS Letters* **211,** 144-150.

Seeburg, P. H. & Adelman, J. P. (1984). Characterization of cDNA for precursor of human luteinizing hormone releasing hormone. *Nature* **311,** 666-668.

Seeburg, P. H., Mason, A. J., Stewart, T. A. & Nikolics, K. (1987). The mammalian GnRH gene and its pivotal role in reproduction. *Recent Progress in Hormone Research* **42,** 69-98.

Sekiya, K., Ghatei, M. A., Salahuddin, M. J., Bishop, A. E., Hamid, Q. A., Ibayashi, H., Polak, J. M. & Bloom, S. R. (1989). Production of GAWK (chromogranin B 420-493)-like immunoreactivity by endocrine tumours and possible diagnostic value. *Journal of Clinical Investigation* **83,** 1834-1842.

Shangold, G. A., Murphy, S. N. & Miller, R. J. (1988). Gonadotropin-releasing hormone-induced Ca^{2+} transients in single identified gonadotropes require both intracellular Ca^{2+} mobilization and Ca^{2+} influx. *Proceedings of the National Academy of Sciences USA* **85,** 6566-6570.

Shapiro, D. J. (1981). Quantitative ethanol precipitation of nanogram quantities of DNA and RNA. *Analytical.Biochemistry* **110,** 229.

Sharpe, R. M. (1994). Regulation of Spermatogenesis. The Physiology of Reproduction Ed. E. Knobil, Neill, J.D. New York, Raven Press Ltd. 2nd ed. 1363-1434.

Sherline, P., Lee, Y. C. & Jacobs, L. S. (1977). Binding of microtubules to pituitary secretory granules and secretory granule membranes. *Journal of Cell Biology* **72,** 380-389.

Sherwood, N. M., Chiappa, S. A. & Fink, G. (1976). Immunoreactive luteinizing hormone releasing factor in pituitary stalk blood from female rats: sex steroid modulation of response to electrical stimulation of preoptic area or median eminence. *Journal of Endocrinology* **70,** 501-511.

Shoemaker, J., Simons, A. M. H., Osnabrugge, G. J. C. V., Lutenburg, C. & Kessel, H. V. (1981). Pregnancy after prolonged pulsatile administration of luteinizing hormone-releasing hormone in a patient with clomiphene-resistant secondary amenorrhea. *Journal of Clinical Endocrinology and Metabolism* **52,** 882-885.

Short, R. V. (1985). Species differences in reproductive systems. Reproduction in Mammals. (Eds. C. R. Austin and R. V. Short.) Cambridge, Cambridge University Press. 24-61.

Shupnik, M. A. (1996a). Gonadal Hormone Feedback On Pituitary Gonadotropin Genes. *Trends In Endocrinology and Metabolism* **7,** 272-276.

Shupnik, M. A. (1996b). Gonadotropin Gene Modulation By Steroids and Gonadotropin-Releasing- Hormone. *Biology of Reproduction* **54,** 279-286.

Shupnik, M. A. & Rosenzweig, B. A. (1991). Identification of an estrogen-reponsive element in the rat LHβ gene. *Journal of Biological Chemistry* **266,** 17084-17091.

Silverman, A. J., Livne, I. & Witkin, J. W. (1987). The gonadotrophin-releasing hormone (GnRH) Neuronal systems: Immunocytochemistry and *in situ* hybridisation. The Physiology of Reproduction (Eds. E. Knobil, Neill, J.D.) New York, Raven Press Ltd. 2nd ed. 1683-1710.

Simon-Chazottes, D., Wu, H., Parmer, R. J., Rozansky, D. J., Szpirer, J., Levan, G., Kurtz, T. W., Szpirer, C., Guenet, J. L. & O'Connor, D. T. (1993). Assignment of the chromogranin A (CgA) locus to homologous regions on mouse chromosome 12 and rat chromosome 6. *Genomics* **17,** 252-255.

Simmons, D. M., Voss, J. W., Ingraham, H. A., Holloway, J. M., Broide, R. S., Rosenfeld, M. G. & Swanson, L. W. (1990). Pituitary cell phenotypes involve cell-specific Pit-1 mRNA translation and synergistic interactions with other classes of transcription factors. *Genes and Development* **4,** 695-711.

Skinner, D. C., Caraty, A. & Evans, N. P. (1998). Does gonadotropin-releasing hormone in the cerebrospinal fluid modulate luteinizing hormone release? *Neuroendocrinology* **67,** 37-44.

Smeaton, T. C. & Robertson, H. A. (1971). Studies on the growth and atresia of Graafian follicles in the ovary of the sheep. *Journal of Reprod.uction and Fertility* **25,** 243-252.

Smith, P. F., Frawley, L. S. & Neill, J. D. (1984). Detection of LH release from individual pituitary cells by the reverse haemolytic plaque assay: estrogen increases the fraction of gonadotropes responding to GnRH. *Endocrinology* **115,** 2484-2486.

Smith, P. L. & Baenziger, J. U. (1988). A pituitary *N*-acetylgalactosamine transferase that specifically recognizes glycoprotein hormones. *Science* **242,** 930.

Smith, P. L. & Baenziger, J. U. (1992). Molecular basis of recognition by the glycoprotein hormone-specific *N*-acetylgalactosamine-transferase. *Proceedings of the National Academy of Sciences USA* **89,** 329-333.

Snabels, M. C. & Kelch, R. P. (1979). Acute inhibitory effects of antiserum to gonadotropin-releasing hormone in ovariectomised rats. *Neuroendocrinology* **29,** 34-41.

Soliman, E., Canaff, L., Fox, J. & Hendy, G. N. (1997). In vivo regulation of chromogranin A messenger ribonucleic acid in the parathyroid by 1,25-dihydroxyvitamin D: Studies in normal rats and in chronic renal insufficiency. *Endocrinology* **138,** 2596-2600.

Sollner, T., Whitehart, S. W., Brunner, M., Erdjument-Bromage, H., Geromanos, S., Tempst, P. & Rothman, J. E. (1993). SNAP receptors implicated in vesicle targeting and fusion. *Nature* **362,** 318-324.

Southern, E. M. (1975). Detection of specific sequences among DNA fragments separated by gel electrophoresis. *Journal of Molecular Biology* **98,** 503-17.

Soszynski, D., Metz-Boutigue, M.-H., Aunis, D. & Bader, M.-F. (1993). Secretogranin II: regulation of Synthesis and Post-Translational Proteolysis in Bovine Adrenal Chromaffin Cells. *Journal of Neuroendocrinology* **5,** 655-662.

Spaulding, S. W. (1993). The ways in which hormones change cyclic adenosine 3', 5'-monophosphate-dependent protein kinase subunits, and how such changes affect cell behavior. *Endocrine Reviews* **14,** 632-650.

Stewart, F. & Allen, W. R. (1981). Biological functions and receptor binding activities of equine chorionc gonadotrophins. *Journal of Reprod.uction and Fertility* **62,** 527-536.

Steyer, J. A., Horstmann, H. & Almers, W. (1997). Transport, docking and exocytosis of single secretory granules in live chromaffin cells. *Science* **388,** 474-478.

Strahl, B. D., Huang, H. J., Pedersen, N. R., Wu, J. C., Ghosh, B. R. & Miller, W. L. (1997). Two proximal activating protein-1-binding sites are sufficient to stimulate transcription of the ovine follicle-stimulating hormone-beta gene. *Endocrinology* **138,** 2621-2631.

Strub, J. M., Goumon, Y., Lugardon, K., Capon, C., Lopez, M., Moniatte, M., Vandorsselaer, A., Aunis, D. & Metzboutigue, M. H. (1996). Antibacterial Activity Of Glycosylated and Phosphorylated Chromogranin-A-Derived Peptide-173-194 From Bovine Adrenal-Medullary Chromaffin Granules. *Journal of Biological Chemistry* **271,** 28533-28540.

Strub, J. M., Sorokine, O., VanDorsselaer, A., Aunis, D. & MetzBoutigue, M. H. (1997). Phosphorylation and O-Glycosylation sites of bovine Chromogranin A from adrenal medullary chromaffin granules and their relationship with biological activities. *Journal of Biological Chemistry* **272,** 11928-11936.

Suemizu, H., Osamura, Y. & Watanabe, K. (1988). Ultrastructural localization of hCG and subunits in the human placenta and choriocarcinoma cell lines - morphological approach to secretory pathway. *Acta Histochem Cytochem* **21,** 265-271.

Syversen, U., Jacobsen, M. B., O'Connor, D. T., Ronning, K. & Waldum, H. L. (1994). Immunoassays For Measurement of Chromogranin-A and Pancreastatin-Like Immunoreactivity in Humans - Correspondence in Patients With Neuroendocrine Neoplasia. *Neuropeptides* **26,** 201-206.

Takiyyuddin, M. A., Parmer, R. J., Kailasam, M. T., Cervenka, J. H., Kennedy, B., Ziegler, M. G., Lin, M. C., Li, J., Grim, C. E., Wright, F. A. & O'Connor, D. T. (1995). Chromogranin-A in Human Hypertension - Influence of Heredity. *Hypertension* **26,** 213-220.

Talmadge, K., Vamvakopolous, N. C. & Fiddes, J. C. (1984). Evolution of the genes for the beta subunits of the human chorionic gonadotrophin and luteinising hormone. *Nature* **307,** 37-40.

Tasaka, K., Masumoto, N., Mizuki, J., Ikebuchi, Y., Ohmichi, M., Kurachi, H., Miyake, A. & Murata, Y. (1998). Rab3B is essential for GnRH-induced gonadotrophin release from anterior pituitary cells. *Journal of Endocrinology* **157,** 267-274.

Tashjian, A. H. J., Yasumura, Y., Levine, L., Sato, G. H. & Parker, M. L. (1968). Establishment of clonal strains of rat pituitary tumor cells that secrete growth hormone. *Endocrinology* **82,** 342-352.

Tatemoto, K., Efendic, S., Mutt, V., Makk, G., Feistner, G. J. & Barchas, J. D. (1986). Pancreastatin, a novel pancreatic peptide that inhibits insulin secretion. *Nature* **324,** 476-478.

Thiny, M. T., Antczak, C., Fields, K., Jin, L. & Lloyd, R. V. (1994). Effects of Estrogen and Dexamethasone On a Transgenic Pituitary Cell- Line. *Laboratory Investigation* **70,** 899-906.

Thomas, G. B., Oldham, C. M., Hoskinson, R. M., Scaramuzzi, R. J. & Martin, G. B. (1987). Effect of immunisation against progesterone on oestrus, cycle length, ovulation rate, luteal regression and LH secretion in the ewe. *Australian Journal of Biological Science* **40,** 307-313.

Thomas, P., Mellon, P. L., Turgeon, J. L. & Waring, D. W. (1996). The LβT2 Clonal Gonadotrope - a Model For Single-Cell Studies of Endocrine Cell Secretion. *Endocrinology* **137,** 2979-2989.

Thomas, S. G. & Clarke, I. J. (1997). The positive feedback action of estrogen mobilizes LH-containing, but not FSH-containing secretory granules in ovine gonadotropes. *Endocrinology* **138,** 1347-1350.

Thomas, S. G., Takahashi, M., Neill, J. D. & Clarke, I. J. (1998). Components of the neuronal exocytotic machinery in the anterior pituitary of the ovariectomised ewe and the effects of oestrogen in gonadotropes as studied with confocal microscopy. *Neuroendocrinology* **67,** 244-259.

Thompson, M. E., Valentine, D. L., Strada, S. J., Wagner, J. A. & Scammell, J. G. (1994). Transcriptional Regulation Of Secretogranin-II and Chromogranin-B by Cyclic-AMP In a Rat Pheochromocytoma Cell-Line. *Molecular Pharmacology* **46,** 880-889.

Thorn, P. (1996). Spatial domains of Ca^{2+} signaling in secretory epithelial cells. *Cell Calcium* **20,** 203-214.

Thotakura, N. R. & Blithe, D. L. (1995). Glycoprotein Hormones - Glycobiology Of Gonadotropins, Thyrotropin and Free Alpha-Subunit. *Glycobiology* **5,** 3-10.

Tooze, S. A., Flatmark, T., Tooze, J. & Huttner, W. B. (1991). Characterisation of the immature secretory granule, an intermediate in granule biogenesis. *Journal of Cell Biology* **115,** 1491-1503.

Tse, A., Tse, F. W., Almers, W. & Hille, B. (1993). Rhythmic Exocytosis Stimulated by GnRH-Induced Calcium Oscillations in Rat Gonadotropes. *Science* **260,** 82-84.

Tsunasawa, S., Liu, W.-K., Burleigh, B. D. & Ward, D. N. (1977). Studies of disulfide bond location in ovine lutropin beta subunit. *Biochim Biophys Acta* **492,** 340-356.

Tsutsumi, M., Zhou, W., Millar, R. P., Mellon, P. L., Roberts, J. L., Flanagan, C. A., Dong, K., Gillo, B. & Sealfon, S. C. (1992). Cloning and Functional Expression of a Mouse Gonadotropin-Releasing- Hormone Receptor. *Molecular Endocrinology* **6,** 1163-1169.

Turgeon, J. L., Kimura, Y., Waring, D. W. & Mellon, P. L. (1996). Steroid and Pulsatile Gonadotropin-Releasing-Hormone (GnRH) Regulation Of Luteinizing-Hormone and GnRH Receptor In a Novel Gonadotrope Cell-Line. *Molecular Endocrinology* **10,** 439-450.

Urbe, S., Dittie, A. S. & Tooze, S. A. (1997). pH-dependent processing of secretogranin II by the endopeptidase PC2 in isolated immature secretory granules. *Biochemical Journal* **321,** 65-74.

Vankammen, D. P., Peters, J., Yao, J., Neylan, T., Beuger, M., Pontius, E. & O'Connor, D. T. (1991). CSF Chromogranin-A-Like Immunoreactivity in Schizophrenia - Assessment of Clinical and Biochemical Relationships. *Schizophrenia Research* **6,** 31-39.

Vugt, D. A. V., Bakst, G., Dyrenfurth, I. & Ferin, M. (1983). Naloxone stimulation of LH secretion in the female monkey: influence of endocrine and experimental conditions. *Endocrinology* **113,** 1858-1864.

Wacker, I., Kaether, C., Kromer, A., Migala, A., Almers, W. & Gerdes, H. H. (1997). Microtubule-dependent transport of secretory vesicles visualized in real time with a GFP-tagged secretory protein. *Journal of Cell Science* **110,** 1453-1463.

Wallace, J. M. & McNeilly, A. S. (1986). Changes in FSH and the pulsatile secretion of LH during treatment of ewes with bovine follicular fluid throughout the luteal phase of the oestrous cycle. *Journal of Endocrinology* **111,** 317-327.

Wand, G. S., Takiyyuddin, M., O'Connor, D. T. & Levine, M. A. (1991). A Proposed Role For Chromogranin-A as a Glucocorticoid-Responsive Autocrine Inhibitor of Proopiomelanocortin Secretion. *Endocrinology* **128,** 1345-1351.

Ward, D. N., Fujino, M., Lamkin, W.M. (1966). Evidence for two carbohydrate moieties in ovine luteinizing hormone (LH). *Federation Proceedings* **25,** 348-351.

Watanabe, T., Azuma, T., Banno, T., Jeziorowski, T., Ohsawa, Y., Waguri, S., Grube, D. & Uchiyama, Y. (1998a). Immunocytochemical localization of chromogranin A and secretogranin II in female rat gonadotropes. *Archives of Histology and Cytology* **61,** 99-113.

Watanabe, T., Banno, T., Jeziorowski, T., Ohsawa, Y., Waguri, S., Grube, D. & Uchiyama, Y. (1998b). Effects of sex steroids on secretory granule formation in gonadotropes of castrated male rats with respect to granin expression. *Endocrinology* **139,** 2765-2773.

Watanabe, T., Uchiyama, Y. & Grube, D. (1991). Topology of chromogranin A and secretogranin II in the rat anterior pituitary: potential marker proteins for distinct secretory pathways in gonadotrophs. *Histochemistry* **96,** 285-293.

Webb, R. & England, B. G. (1982). Relationship between LH receptor concentrations in thecal and granulosa cells and in-vivo and in-vitro steroid secretion by ovine follicles during the preovulatory period. *Journal of Reproduction and Fertility* **66,** 169-180.

Weiland, F. T., Gleason, M. L., Serafini, T. A. & Rothman, J. E. (1987). The Rate of Bulk Flow from the Endoplasmic Reticulum to the Cell Surface. *Cell* **50,** 289-300.

Weiss, J., Guendner, M. J., Halvorson, L. M. & Jameson, J. L. (1995). Transcriptional activation of the follicle-stimulating hormone beta-subunit gene by activin. *Endocrinology* **136,** 1885-1891.

Weiss, J., Harris, P. E., Halvorson, L. M., Crowley Jr, W. F. & Jameson, J. L. (1993). Perfusion of rat pituitary cells with gonadotrophin-releasing hormone, activin, and inhibin reveals distinct effects on gonadotrophin gene expression and secretion. *Endocrinology* **132,** 2307-2011.

Wide, L. & Hobson, B. M. (1983). Qualitative differences in follicle-stimulating hormone activity in the pituitaries of young women compared to that ofmen and elderly women. *Journal of Clinical Endocrinology and Metabolism* **56,** 371-375.

Windle, J. J., Weiner, R. I. & Mellon, P. L. (1990). Cell-Lines of the Pituitary Gonadotrope Lineage Derived By Targeted Oncogenesis in Transgenic Mice. *Molecular Endocrinology* **4,** 597-603.

Winkler, H. & Fischer-Colbrie, R. (1992). The Chromogranins A and B - the First 25 Years and Future Perspectives. *Neuroscience* **49,** 497-528.

Witkin, J., Paden, C. & Silverman, A. J. (1982). The luteinizing hormone-releasing hormone (LHRH) systems in the rat brain. *Neuroendocrinology* **35,** 429-438.

Wooge, C. H. & Conn, P. M. (1987). Measurement of Synergistic Effects of Protein Kinase-C Activators and Calcium Ionophore in Pituitary Cell-Cultures. *Methods in Enzymology* **141,** 429-435.

Wu, H. J., Rozansky, D. J., Parmer, R. J., Gill, B. M. & O'Connor, D. T. (1991). Structure and Function of the Chromogranin-A Gene - Clues to Evolution and Tissue-Specific Expression. *Journal of Biological Chemistry* **266,** 13130-13134.

Yanisch-Perron, C., Vieira, J. & Messing, J. (1985). Improved M13 phage cloning vectors and host strains: Nucleotide sequences of the M13mp18 and pUC19 vectors. *Gene* **33,** 103.

Yoo, S. H. (1992). Identification of the Ca^{2+}-Dependent Calmodulin-Binding Region of Chromogranin-A. *Biochemistry* **31,** 6134-6140.

Yoo, S. H. (1994). pH-Dependent Interaction of Chromogranin-A With Integral Membrane- Proteins of the Secretory Vesicle Including a 260 kDa Protein Reactive to the Inositol 1,4,5-Trisphosphate Receptor Antibody. *Biophysical Journal* **66,** A 384-a 384.

Yoo, S. H. (1995). pH-Induced and Ca^{2+}-Induced Conformational Change and Aggregation of Chromogranin-B - Comparison With Chromogranin-A and Implication in Secretory Vesicle Biogenesis. *Journal of Biological Chemistry* **270,** 12578-12583.

Yoo, S. H. & Albanesi, J. P. (1990a). Ca^{2+}-Induced Conformational Change and Aggregation of Chromogranin-A. *Journal of Biological Chemistry* **265,** 14414-14421.

Yoo, S. H. & Albanesi, J. P. (1990b). Inositol 1,4,5-Trisphosphate-Triggered Ca^{2+} Release From Bovine Adrenal-Medullary Secretory Vesicles. *Journal of Biological Chemistry* **265,** 13446-13448.

Yoo, S. H. & Albanesi, J. P. (1991). High-Capacity, Low Affinity Ca^{2+} Binding of Chromogranin-A - Relationship Between the pH-Induced Conformational Change and Ca^{2+} Binding Property. *Journal of Biological Chemistry* **266,** 7740-7745.

Yoo, S. H. & Kang, Y. K. (1997). Identification of the secretory vesicle membrane binding region of chromogranin B. *FEBS Letters* **406,** 259-262.

Yoo, S. H. & Lewis, M. S. (1992). Effects of pH and Ca^{2+} On Monomer-Dimer and Monomer-Tetramer Equilibria of Chromogranin-A. *Journal of Biological Chemistry* **267,** 11236-11241.

Yoo, S. H. & Lewis, M. S. (1993). Dimerization and Tetramerization Properties of the C-Terminal Region of Chromogranin-A - a Thermodynamic Analysis. *Biochemistry* **32,** 8816-8822.

Yoo, S. H. & Lewis, M. S. (1994). pH-Dependent Interaction of an Intraluminal Loop of Inositol 1,4,5- Trisphosphate Receptor With Chromogranin-A. *FEBS Letters* **341,** 28-32.

You, Z. B., Saria, A., Fischer-Colbrie, R., Terenius, L., Goiny, M. & Herreramarschitz, M. (1996). Effects of Secretogranin II-Derived Peptides On the Release of Neurotransmitters Monitored in the Basal Ganglia of the Rat with in-vivo Microdialysis. *Naunyn-Schmiedebergs Archives of Pharmacology* **354,** 717-724.

Zeng, H., Ji, I. & Ji, T. H. (1995). Lys-91 and His-90 of the alpha-subunit are crucial for receptor binding and hormone action of follicle-stimulating hormone (FSH) and play hormone-specific roles in FSH and human chorionic gonadotrophin. *Endocrinology* **136,** 2498-2953.

Zhang, J. X., Fasciotto, B. H., Darling, D. S. & Cohn, D. V. (1994). Pancreastatin, a Chromogranin A-Derived Peptide, Inhibits Transcription Of the Parathyroid-Hormone and Chromogranin-A Genes and Decreases the Stability Of the Respective Messenger Ribonucleic-Acids In Parathyroid Cells In Culture. *Endocrinology* **134,** 1310-1316.

Zhang, L., Marcu, M. G., Nau-Staudt, K. & Trifaro, J.-M. (1996). Recombinant scinderin enhances exocytosis an effect blocked by two scinderin-derived actin binding peptides and PIP2. *Neuron* **17,** 287-296.